FUNCTIONAL MEMBRANES FOR LIMITED PROTEIN DIGESTION AND PHOSPHOPEPTIDE ENRICHMENT PRIOR TO MASS SPECTROMETRY

By

Yujing Tan

A DISSERTATION

Submitted to
Michigan State University
in partial fulfillment of the requirements
for the degree of

DOCTOR OF PHILOSOPHY

Chemistry

2012

ABSTRACT

FUNCTIONAL MEMBRANES FOR LIMITED PROTEIN DIGESTION AND PHOSPHOPEPTIDE ENRICHMENT PRIOR TO MASS SPECTROMETRY

By

Yujing Tan

Mass spectrometry (MS) is the leading technique for rapid identification of proteins and characterization of their posttranslational modifications. However, as with most analyses, the success of MS methods depends critically on sample purification and pretreatment. Microporous membranes are attractive as a platform for enrichment and modification of proteins and peptides because convection and short radial diffusion distances in pores provide rapid analyte mass transport to binding or catalytic sites. Additionally, variation of the transmembrane flow rate can control the extent of reactions such as digestion. This research exploits facile layer-by-layer adsorption to incorporate nanoparticles or enzymes in micropores and create functional membranes. As tools for sample preparation prior to MS analysis, TiO_2-modified membranes enrich phosphopeptides and protease-containing membranes afford control over protein digestion.

Posttranslational protein phosphorylation is one of the most important mechanisms for creating protein diversity in eukaryotic cells. However due to the relatively low abundance of most phosphopeptides in proteolytic digests, phosphopeptide enrichment is a prerequisite step for effective and efficient MS analysis of phosphorylation. Alternating adsorption of poly(styrene sulfonate) (PSS) and TiO_2 nanoparticles in porous nylon substrates creates TiO_2-modified membranes for rapid enriching of phosphopeptides from small-volume (10's of μL) samples. These TiO_2-modified membranes bind 540 nmols of phosphopeptides in a 22-mm diameter disc and selectively isolate the phosphopeptides from α-casein, β-casein and ovalbumin digests even

in a 100-fold excess of non-phosphorylated BSA digests if 2 % TFA is the loading and washing buffer. The combination of membrane enrichment and tandem MS reveals seven phosphorylation sites from *in vivo* phosphorylated tau protein, which is associated with Alzheimer's disease, and identification of such sites might aid the design of therapeutic drugs that inhibit phosphorylation.

Using a similar approach to membrane modification, sequential adsorption of PSS and proteases in porous nylon substrates yields enzymatic membrane reactors for limited protein digestion. Although a high local enzyme density (~30 mg/cm^3) and small pore diameters in the membrane lead to digestion in < 1 s, the low membrane thickness (170 μm) affords control over residence times at the ms level to limit digestion. Most importantly, pepsin-containing membranes afford control of peptides sizes by altering the flow rate. Apomyoglobin digestion demonstrates that peptide lengths increase as the residence time in the membrane decreases. Under denaturing conditions, limited membrane digestion of bovine serum albumin and subsequent ESI-Orbitrap MS analysis reveal large peptides (3-10 kD) that increase the sequence coverage from 53 % (2-s digestion) to 82 % (0.05-s digestion). Moreover, electron transfer dissociation tandem MS on a large myoglobin proteolytic peptide (8 kD) provides a resolution of 1-2 amino acids, which suggests that this protease-modified membrane might find applications in hydrogen-deuterium exchange or middle-down proteomics studies. In addition, using trypsin- and α-chymotrypsin-modified membranes, a limited proteolysis study of a large Arabidopsis GTPase, ROOT HAIR DEFECTIVE 3, shows suitable probing for labile regions near the C-terminus to suggest what protein reconstruction might make RHD3 more suitable for crystallization. These studies clearly demonstrate the potential of functional membranes for rapid and controlled purification or pretreatment prior to MS analysis.

I dedicate this dissertation to my parents, Guisheng Tan and Linghua Wu,

for their love and support.

ACKNOWLEDGEMENT

First I would like to thank my advisor Prof. Merlin Bruening for his guidance and support over the past five years. More than an advisor, he is a mentor, collaborator and friend. He has taught me to be a scientist and to seriously do things the right way. His attitude and professional conduct inspired me to pursue the honor of this degree. Despite numerous failures and disappointments along the way, his patience and trust encouraged me to continue and eventually make it to the finish line. Though seemingly infrequent, the moments we achieved exciting results and success together helped me work through the hard times.

I want to give special thanks to my second reader, Prof. Gavin Reid, who served as the advisor in the mass spectrometry portion of this work. His knowledge, enthusiasm and exactness prompted my progress in mass spectrometry step by step. I am grateful for all his helpful suggestions and input on my work in this dissertation. I also wish to thank Prof. Gary Blanchard and Prof. Dana Spence for being my committee members and for their suggestions on this project.

I also would like to thank Profs. Min-Hao Kuo, Michael Garavito, Federica Brandizzi, Jetze Tepe, Narayanan Parameswaran and Daniel Jones for collaborations and kind help on this dissertation work. Similarly, I would like to acknowledge Drs. Yi Zheng, Dexin Sui, Xiao Zhou, Amanda Palumbo, Teri Lansdell, Li Cui , Jinlan Dong and Wen Qin for their help and contributions to this dissertation.

I am also very grateful to all my fellow group members, those who graduated before me, who are fighting hard now and those who just started, for their sincere support and help. Especially, Drs. Lu Ouyang, David Dotzauer and Weihan Wang helped me in the early stages and brought me up to speed with my lab-work. As a longtime friend and roommate, Weihan is

like a big brother to me. His hard work and interest in science have always set a good example for me.

Lastly I wish to express my deepest appreciation to my family and friends for their love and support. As the only child, I am sorry for not being home for every Chinese traditional holiday and family reunion in the past five years. Their understanding and support sustained me so I could accomplish my goal: being a doctor. Thanks to the internet, we could "see" and talk with each other weekly. For the friends in both China and the U.S., whenever outside school, I appreciate that they stayed with me through the good times and put up with my complaints and mood in the bad times.

Because of the people and stories involved, writing this acknowledgement is like traveling back through the days I spent chasing this degree. Without the help and support from the people mentioned and countless more, I could not finish this dissertation. Finally, allow me to thank them all again with my sincerest gratitude.

TABLE OF CONTENT

LIST OF TABLES

LIST OF FIGURES

LIST OF SCHEMES

LIST OF ABBREVIATIONS

MS	Mass spectrometry
HDX	Hydrogen-deuterium exchange
MALDI	Matrix-assisted laser desorption/ionization
ESI	Electrospray ionization
DHB	2,5-Dihydroxy benzoic acid
HPLC	High-performance liquid chromatography
DESI	Desorption electrospray ionization
DART	Direct analysis in real time
m/z	Mass-to-charge
FT-ICR	Fourier transfer ion cyclotron resonance
RF	Radio frequency
TOF	Time of flight
LTQ	Linear trap quadrupoles
CID	Collision induced dissociation
CAD	Collision activated dissociation
ACS	American Chemical Society
PMF	Peptide mass fingerprinting
RP-HPLC	Reverse-phase high performance liquid chromatography
PTMs	Posttranslational modifications
ECD	Electron capture dissociation
ETD	Electron transfer dissociation
ATP	Adenosine-5'-triphosphate

Ser	Serine
Thr	Threonine
Tyr	Tyrosine
Arg	Arginine
SDS-PAGE	Sodium dodecyl sulfate polyacrylamide gel electrophoresis
WB	Western blotting
Lys	Lysine
His	Histidine
IMAC	Immobilized metal affinity chromatography
NTA	Nitrilotriacetate acid
TiO_2	Titanium dioxide
MOAC	Metal oxide affinity chromatography
TFA	Trifluoroacetic acid
ASBMB	American Society for Biochemistry and Molecular Biology
SIMAC	Sequential elution from IMAC
SCX	Strong cation exchange
ACN	Acetonitrile
HCD	High-energy collision-induced dissociation
IMERs	Immobilized enzyme reactors
PLGA	Poly(L-glutamic acid)
PLL	Poly(L-lysine)
PAH	Poly(allylamine)
PSS	Poly(styrene sulfonate)

DSC	N,N’-disuccinimidyl carbonate
DSS	N,N’- disuccinimidyl suberate
PMO	Periodic mesoporous organosilica
Leu	Leucine
Phe	Phenylalanine
Ile	Isoleucine
Trp	Tryptophan
NMR	Nuclear magnetic resonance
UPLC	Ultra-performance liquid chromatography
bANc1p	Bovine mitochondrial ADP/ATP carrier isoform 1
CATR	Carboxyatractyloside
BA	Bongkrekic acid
BSA	Bovine serum albumin
ICP-OES	Inductively coupled plasma-optical emission spectroscopy
EDX	Energy-dispersive X-ray spectroscopy
GSK-3β	Glycogen synthase kinase-3β
TNF-α	Tumor necrosis factor
THP-1	Human acute monocytic leukemia
IκBα	Inhibitor of kappa-B-alpha
IKKβ	Inhibitor of kappa-B kinase beta
GRK5	G-protein coupled receptor kinase-5
FPLC	Fast protein liquid chromatography
Met	Methionine

cam	Carbamidomethyl
DTT	1,4-dithio-DL-threitol
TCEP	Tris(2-carboxyethyl) phosphine hydrochloride
NALS	Non-ionic acid labile surfactant
FA	Formic acid
RHD3	Root hair defective 3
SUMO	Small ubiquitin-like modifier
SEC	Size exclusion chromatography
His-tag	Polyhistidine-tag

Chapter 1. Introduction

This dissertation describes the fabrication and use of functionalized porous membranes for protein digestion and phosphopeptide isolation prior to mass spectrometry (MS) analysis. More specifically, the research focuses mainly on TiO_2-modifed membranes for phosphopeptide enrichment and phosphoprotein characterization, and protease-modified membranes for limited protein digestion. To provide context for the work, this chapter starts with an overview of MS-based proteomics and then reviews the importance of phosphoproteomics along with current phosphopeptide enrichment and MS-based detection and characterization methods. With respect to protease-modified membranes, a subset of enzymatic membrane reactors, this introduction reviews the development of immobilized enzyme reactors in terms of immobilization methods, available supports and applications. Additionally, this chapter describes two current MS-based methods for studying protein structure, e.g., hydrogen-deuterium exchange (HDX) and limited proteolysis, as these methods may benefit from the new protease-modified membranes. Finally, the last section of this chapter outlines the dissertation.

1.1 Mass spectrometry for proteomics

With the completion of genome sequences for many plant and animal species, the focus of much biochemical research has shifted to comprehensive studies of the proteins expressed by these genes, i.e. proteomics. As proteins function like the building blocks of life, proteomics research is vital to understand many life processes.[1] MS uses protein and peptide masses to identify proteins and characterize their modifications, and because it is rapid, versatile and potentially comprehensive, MS has become the most powerful tool in the proteomics area.[2] Nevertheless, the complexity of the proteome makes comprehensive protein characterization a

daunting and as yet unfulfilled task. The desire to fully understand the proteome is continually pushing the boundaries of instrumentation and methodologies, and new MS-based tools and approaches appear regularly to extend the scope of proteomics applications.[3]

MS includes ionization, mass analysis, and complex data processing. This section briefly describes basic concepts and new features in each of these areas. This knowledge is vital to the later chapters in this dissertation, as MS-based analysis is the endpoint for the functional membranes developed in this dissertation.

1.1.1 Ionization techniques

Since the invention of matrix-assisted laser desorption/ionization (MALDI)[4] and electrospray ionization (ESI)[5] more than two decades ago, MS-based proteomics has improved tremendously.[3, 6-7] Before MALDI and ESI, ionization of large peptides or proteins was extremely challenging due to their thermal instability or low volatility. These two so-called "soft" ionization techniques successfully ionize large species and turn them into gas phase ions without significant degradation. The awarding of the 2002 Nobel Prize in Chemistry to the inventors of ESI and MALDI in part reflects the impact of these innovations on MS-based proteomics.[8]

1.1.1.1 MALDI

The MALDI ionization process involves two steps. In the first step, the matrix, such as 2,5-dihydroxy benzoic acid (DHB) or α-cyano-4-hydroxycinnamic acid, absorbs the laser energy (typically at a wavelength of 337 or 355 nm). The ideal matrix will have good solubility in water, strong optical absorption, a low molecular weight and facile vaporization, and additionally act as a proton source. In the second step, the matrix transfers adequate energy to ionize the acidified peptide or protein analytes and send them into the gas phase. The predominant ions are singly

charged, $[M+H]^+$. The MALDI mass spectrum is generated after one or a few laser shots, and these spectra differ somewhat from shot to shot. In practice, a reliable spectrum with a sufficient signal to noise ratio is the average of tens or hundreds of spectra.[9]

1.1.1.2 ESI

Unlike MALDI, the ESI ionization process generates ions from the solution containing the analytes of interests. The liquid is dispersed into a fine aerosol and driven by the voltage (2-6 kV) between the capillary nozzle and mass spectrometer inlet. At the capillary tip, droplets emerge from a Taylor cone in a well-defined physicochemical process.[10] In the subsequent transition process, the solvent–analyte droplets gradually shrink due to the evaporation of solvent, and when the charge repulsion force exceeds the surface tension the droplets split and reform new ones in a process known as Coulomb fission. The analytes will have various charge states when they reach the inlet of the mass analyzer.[11] Compared to MALDI, an obvious advantage is that high charge states enable detection of larger molecular weight species under the same analyzer m/z range. The continuous electrospray also makes on-line analysis achievable, so ESI couples well to separation techniques like high-performance liquid chromatography (HPLC). This coupling dramatically increases the throughput and sensitivity of detection. Furthermore, improvement in Nano-HPLC or Micro-ESI are making the ESI ionization process even more useful and practical.[12]

1.1.1.3 DESI and DART

Desorption electrospray ionization (DESI)[13] and direct analysis in real time (DART)[14] are examples of emerging ionization methods. These techniques require little sample preparation and can directly analyze gas, liquid and solid phase samples under ambient

conditions (Figure 1.1). The ionization takes place directly at the surface of samples ranging from fruits, vegetables, blood, urine, and tissues.[13] The unique ambient properties of these techniques may enlarge MS applications in proteomics, and I expect more application using these methods in the future.

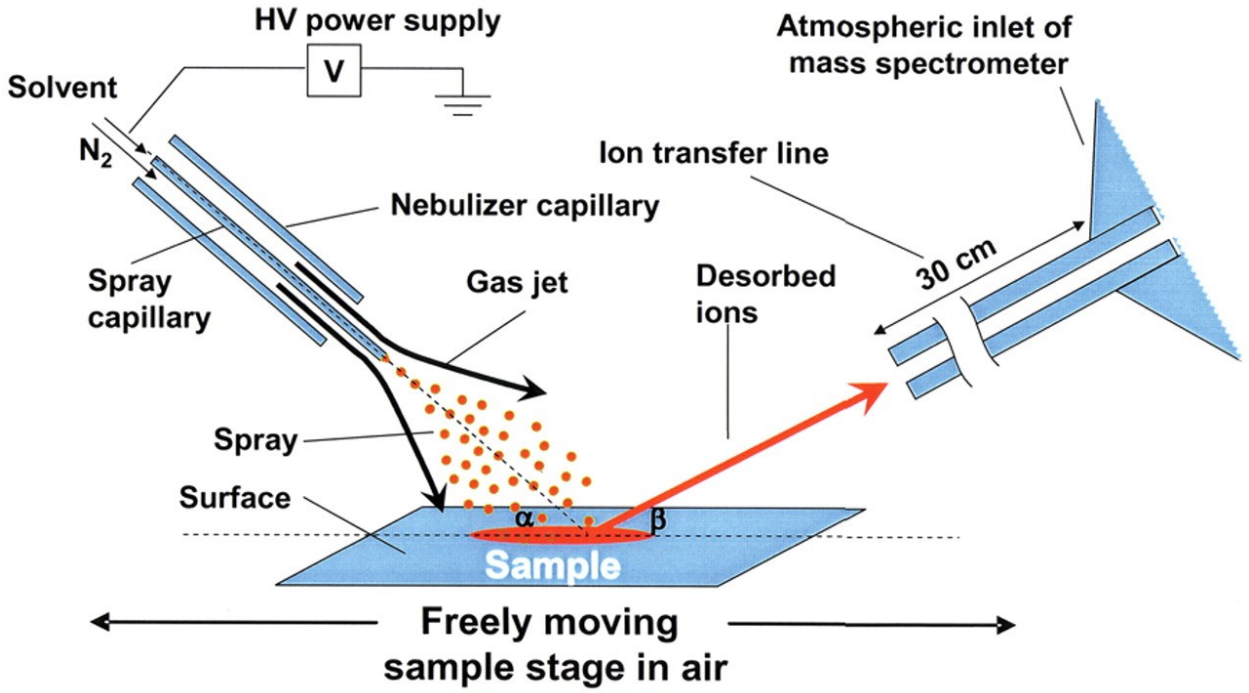

Figure 1.1. Schematic diagram of DESI. The solvent is influenced by high voltage and the sheath gas direct sprays onto the sample surface. Desorbed ions are ejected into the ion transfer line, with variation of angles α and β to optimize collection. The figure is reprinted from reference [13] with permission from the American Association for the Advancement of Science. For interpretation of the references to color in this and all other figures, the reader is referred to the electronic version of this dissertation.

1.1.2 Mass analyzers

A typical mass spectrometer contains a sample introduction and ionization source, a mass analyzer, an ion detector and data processing electronics, but the mass analyzer is the core component. The basic functions of the analyzer include storing or scanning ions and separating them according to their mass-to-charge (m/z) ratios. There are four common strategies to separate or store ions.[3] The first is frequency based analysis, e.g. Fourier transfer ion cyclotron resonance (FT-ICR) and Orbitrap methods; the second is the stable trajectory of ions by specific alternating and constant electric fields, and the representative analyzers contain quadrupoles; the third combines the stabilizer principle and radio frequency (RF) and applies to ion traps; the last principle is the travelling time of ions between the ion source and ion detector, and hence it is termed as time of flight (TOF). The ion trap and Orbitrap deserve further details here, as they are the two mass analyzers employed for all the results in this dissertation.

1.1.2.1 Linear ion trap

Thermo Scientific specifically terms the linear ion trap as the LTQ, or linear trap quadrupoles. Compared to the traditional 3-D ion trap, one major advantage of the LTQ is that the longer dimension of the ions' traveling axis allows storage of more ions. The workflow and mechanisms are almost the same for all ion traps. In detail, the ions created at the ion source travel through a few sets of lenses and quadru/octopoles that help to concentrate and align the ion beams. After ions enter the LTQ, they are stabilized through collision with a noble gas and trapped at the center of the chamber by the trapping potential at both ends of the traveling axis. Finally by increasing the amplitude of the RF field, the ions become unstable according to their m/z value (low m/z first) and are ejected from the LTQ.[15] The LTQ has the advantages of easy

operation, low detection limits, rapid analysis, low maintenance, and variable resolution at a low cost, so it is the most common mass analyzer.

The ion trap can also perform MS/MS analysis. The ions with specific m/z are first selected from all ions trapped in the LTQ. Subsequently, the selected ions are excited to undergo collisions with N_2 or Ar gas. The collisions convert kinetic energy into internal energy that is distributed to chemical bonds. Bond dissociation occurs when the distributed internal energy exceeds the bond energy in a process known as collision induced dissociation (CID) or collision activated dissociation (CAD).[16] The spectrum of fragment ions provides structural and sequence information about the selected targets.

1.1.2.2 Orbitrap

Invented by Makarov in 2000 and commercially available from Thermo in 2005, the LTQ-Orbitrap hybrid mass analyzer is gradually maturing as one of the leading analyzers for proteomics research.[17-18] This hybrid mass analyzer retains the advantage of the LTQ and is capable of high mass accuracy (1-10 ppm) and high mass resolution (up to 150,000).[18] The ions trapped in the LTQ can transfer into the Orbitrap and are stabilized without magnetic or RF fields. The ions are trapped in a quadru-logarithmic field, and both orbit radially around the axial electrode (z) and oscillate along the axial electrode at different frequencies (ω), and the ω is proportional to $(m/z)^{-1/2}$ (Figure 1.2). Similar to the FT-ICR, the analyzer measures the imaging current induced by the oscillation and then transforms this current into a mass spectrum using a fast FT.[17]

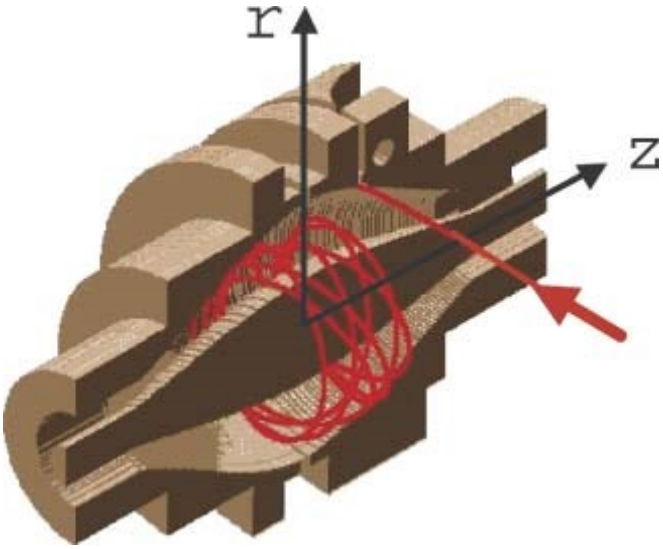

Figure 1.2. The cross section of the Orbitrap analyzer where the red line is ion trajectory. The Figure is reprinted from reference [17] with permission of the American Chemical Society (ACS).

Compared to the FT-ICR, the Orbitrap offers similar mass resolution and mass accuracy at a lower price and maintenance cost, thus providing an alternative for analysis of intact proteins or complex samples. However, the FT-ICR still has its unique properties of high mass range and the capability to perform ion reactions in the ICR cell. In contrast, the Orbitrap works only as an analyzer and needs the LTQ to perform the ion trapping and fragmentation or reaction.[2] In conclusion, thanks to the Orbitrap, high mass accuracy and resolution facilitate the data analysis process in peptide mass fingerprinting (PMF) and *de novo* peptide sequencing.

1.1.3 Proteomics approaches

With the availability of various advanced instruments, procedures to analyze proteins are undergoing continuous refinements. However, all methods start with sample preparation aiming to reduce complexity and to make the buffer compatible with the instrument. Chromatography and two-dimensional gel electrophoresis are the most effective and widely used separation methods prior to the MS analysis. In the instrument, MS data acquisitions have two major modes. The first is the full-scan MS which detects and records a full spectrum at a given time, and the

other is a MS/MS (tandem MS) or MS^n scan, which analyzes the fragments (product ions) from isolated ions (precursor ions). Known as data-dependent acquisition, the parameters (e.g. the signal threshold, the number of selected ions and the selection criteria) used for a tandem MS or MS^n scan usually depend on the results of full-scan MS.

Figure 1.3 shows the systematic labeling of the product ions that result from fragmentation of a peptide. Cleavage of the amide bond will generate b ions (charge retained at N-terminus side) and y ions (charge retained at C-terminus side). Similarly the a-x pair results from cleavage of the C_α-C bond and the c-z pair stems from breaking of the N- C_α bond.[19] The product ions provide information on the peptide sequence. The analysis can occur with proteolytic peptides, a bottom-up approach, or direct analysis of an intact protein, a top-down approach (Figure 1.4).

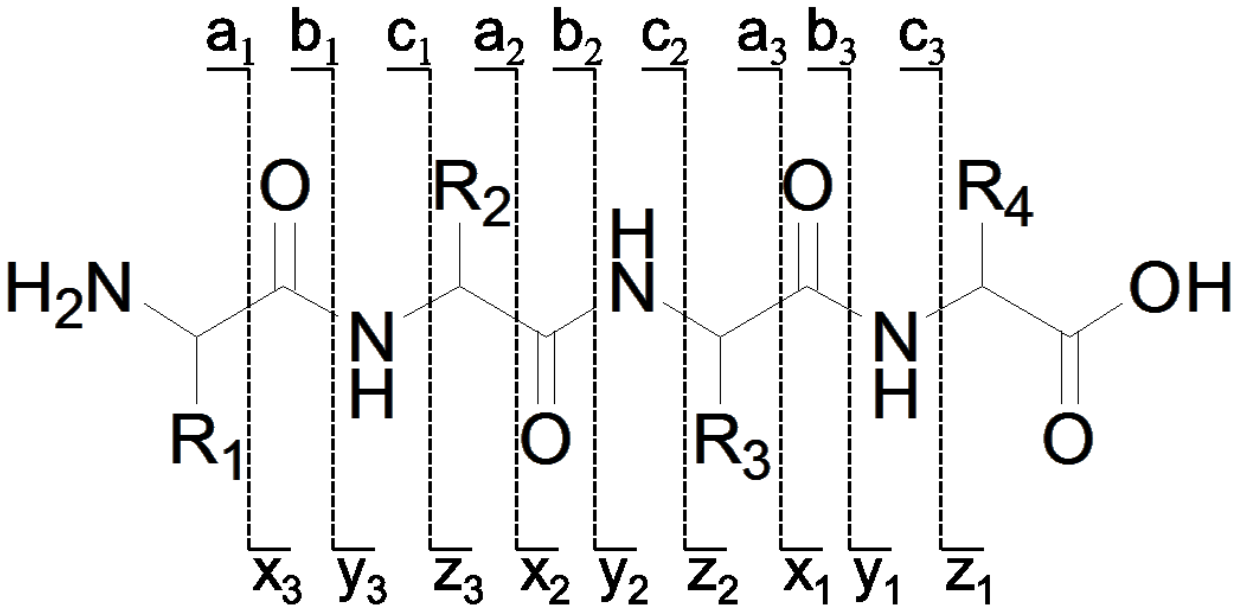

Figure 1.3. Peptide fragmentation notation based on the scheme created by Roepstorff and Fohlman.[19]

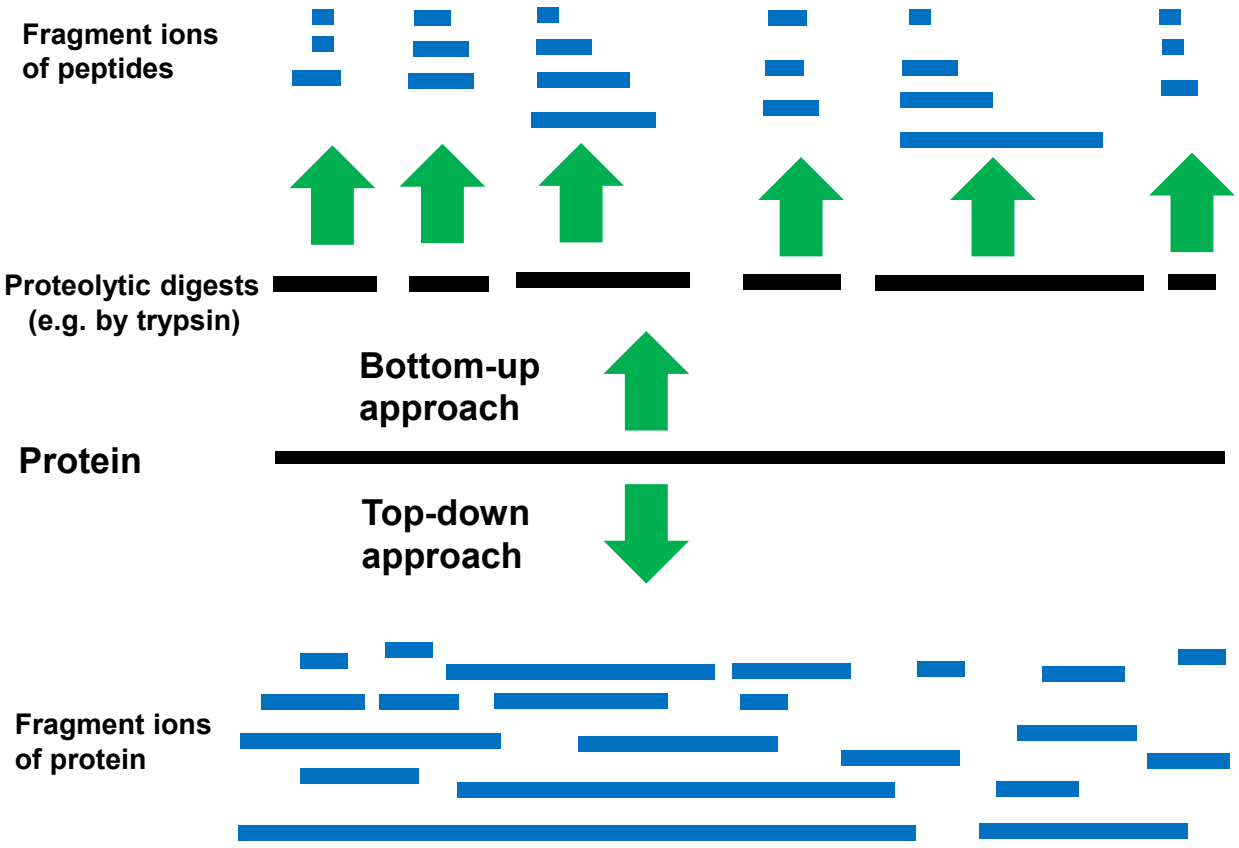

Figure 1.4. Simple representation of the bottom-up and top-down approaches to protein analysis by MS. The bottom-up approach examines proteolytic digests and the fragmentation of the digested peptides, whereas the top-down approach employs direct fragmentations of the intact protein.

1.1.3.1 Bottom-up approach

To date, the bottom-up strategy is the most widely used method to analyze proteins in complex mixtures.[20] This approach starts with digestion of the proteins. In the traditional method, the proteins are first separated through two-dimensional gel electrophoresis, and the proteolysis takes place in the gel prior to peptide extraction. The digests are then submitted for MS analysis. Currently, most protein mixtures undergo in-solution digestion, the proteolytic peptide mixture is separated through reverse-phase high performance liquid chromatography (RP-HPLC), and the eluent is analyzed by ESI-MS on-line. This method greatly increases the throughput of the process. For MS analysis, the full scan MS is first applied, and data-dependent acquisition is triggered to obtain tandem mass spectra according to different settings. In the data interpretation, both manual *de novo* peptide sequencing or database searching using algorithms such as SEQUEST[21] can extract information from the tandem MS spectra. In database searching, the actual tandem spectrum are compared with the predicted *in silico* fragmentation results of peptides from the chosen set of proteins. Then the identified peptides will be used to map the original proteins. Although this approach is effective, it has several drawbacks: the loss of peptides during separation and ionization will decrease the probability of protein identification and characterization; the peptide-protein mapping method will ambiguously assign peptides to various isoforms; the proteolytic peptides cannot provide comprehensively identify posttranslational modifications (PTMs). Ideally, analysis of the intact protein will solve these potential problems, and I discuss that approach below.

1.1.3.2 Top-down approach

The top-down approach directly ionizes and fragments intact proteins instead of proteolytic peptides.[20] Although the bottom-up approach remains the main tool for proteomics analysis, the top-down approach is gathering more and more interest to obtain protein mass information, differentiate isoforms, and characterize all PTMs at once.[22-25] Powerful mass analyzers such as FT-ICR or Orbitrap instruments coupled with electron capture dissociation (ECD)[26] or electron transfer dissociation (ETD)[27] make this approach feasible, as these fragmentation methods efficiently break the peptide bonds and generate sufficient fragment ions to provide sequence information. Nevertheless, for whole proteomics studies, the top-down approach requires more material than the bottom-up approach and throughput of the top-down method is still low.[28] Although the high mass accuracy and resolution in modern MS can handle single protein or simple protein mixtures, the front-end chromatographic separation of proteins is far behind RP-HPLC peptide separations, and this shortcoming limits the broad replacement of the bottom-up approach for large-scale proteomics.[29]

1.1.3.3 Middle-down approach

In an effort to combine some of the assets of the above two approaches, middle-down proteomics has emerged as a new way to examine multiple PTMs in a single long peptide (3 kD-10 kD).[30-31] This method keeps the digestion from the bottom-up approach but attempts to obtain large peptides through limited proteolysis. In particular, this approach was applied to examine PTMs in Histones.[28, 32] In one histone H3 study, Kelleher and coworkers used the endoproteinase Glu-C to release the tail peptide (residues 1-50) from the protein and performed ECD fragmentation to obtain information on PTMs. The rationale is to efficiently fragment the

large peptide and get high sequence resolution from the fragments, as almost all methylation and acetylation occur in the first 50 amino acid.[30]

So far this section has described some concepts and usage of MS in proteomics. Notably the sample preparation is vital to achieve the desired results. My focus is to simplify the sample preparation to facilitate the MS detection. Sample preparation is also vital in the development of phosphoproteomics.

1.2 Phosphorylation: a key to protein function

PTMs significantly increase the proteome complexity and function in human cells, and they also make the proteome a more challenging research area.[33-34] One category of the PTMs is covalent modification with functional groups including phosphorylation, glycosylation, methylation and acetylation. The second category of PTMs is the cleavage of one or more amino acids from the original protein. Among the first category, protein phosphorylation is the most common PTM and the most widely studied.[34] Around 500 protein kinases catalyze the transfer of the phosphate group from adenosine-5'-triphosphate (ATP) to one or more substrate proteins , although ideally these protein kinases are chemo-specific.[35] The γ-position phosphate group is the most common donor, and this covalent addition is reversible with the help of a phosphatase. Reversible phosphorylation controls cell functions such as differentiation, apoptosis, and signal transduction, consequently this phenomenon is involved in cell division, cell growth, and gene expression.[33, 36-37]

In eukaryotic cells, phosphorylation occurs on serine (Ser), threonine (Thr) and tyrosine (Tyr) residues, and early studies suggest that the ratio of modifications on these three sites is 1800:200:1.[38] In 2006, Mann and coworkers studied the phosphorylation events on Hela cells stimulated with epidermal growth factor and revealed 6,600 phosphorylations on 2,244 proteins.

Their statistical results show that the relative percentages of phosphorylation on Ser, Thr and Tyr are 86.4%, 11. 8% and 1.8%, respectively.[39] Thus, phosphorylation of serine is the dominant modification. Figure 1.5 demonstrates the kinase-catalyzed mechanism in which serine takes a γ-position phosphate from ATP to form phosphorylated serine. Thr and Tyr share the same mechanism but with different kinases.

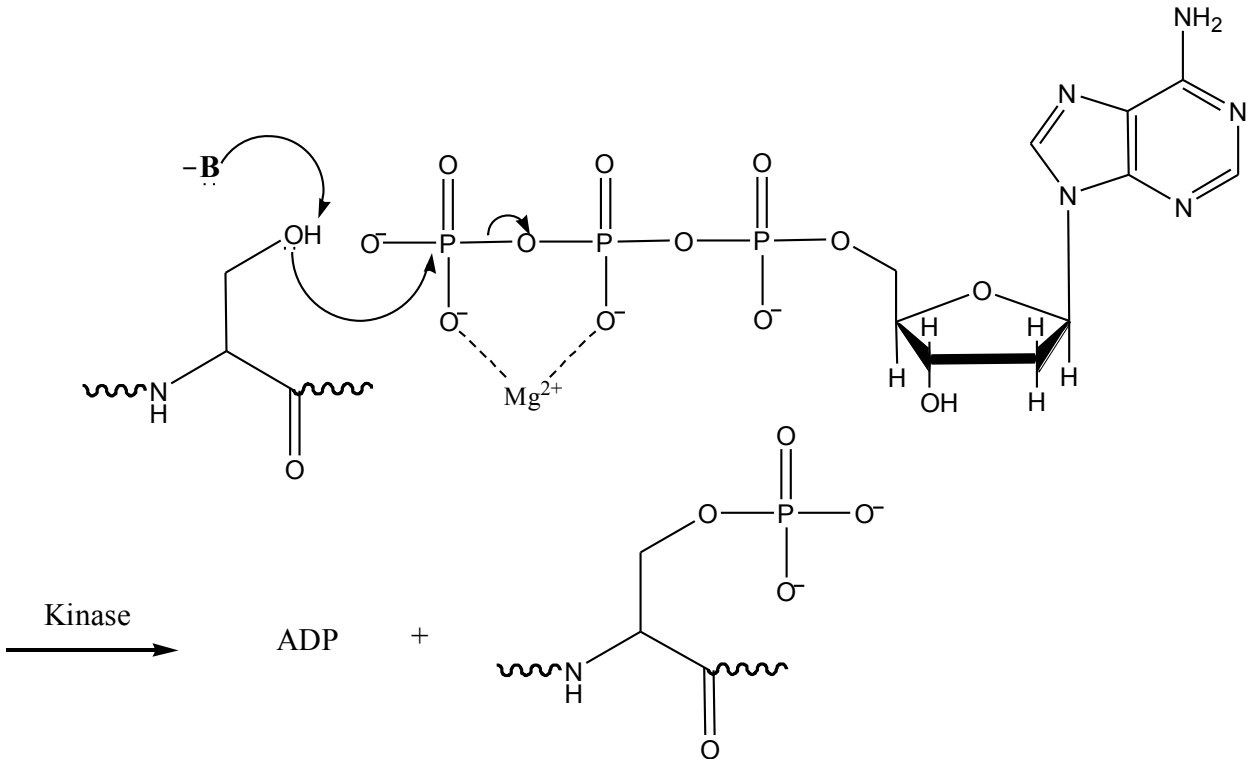

Figure 1.5. Mechanism for kinase-catalyzed phosphorylation of serine. The figure is adapted from reference [43].

Given that the tertiary structure of proteins provides their unique properties, conformational changes after phosphorylation are vital to mediate protein activity. Interestingly, phosphorylation typically gives rise to changes from an inactive to an active protein mode, and the opposite case is rare.[40] In the perspective of mechanisms, addition of phosphate will alter not only the conformation in the region but also the local charge density, consequently both factors will alter the protein microenvironment. As an example, the phosphorylated Ser_{14} of glycogen phosphorylase charge-pairs intramolecularly with arginine ($Arg_{69)}$ and intermolecularly with Arg_{43}. The interaction of two subunits drives an allosteric conformational change to activate the enzymatic function of cleaving glucose-1-phosphate from glycogen.[40]

About one third of the proteins in humans are substrates for phosphorylation at some stage in their life cycle,[41] but at any given time, the absolute amount of phosphorylated proteins is much less than that of regular proteins. Moreover, for a certain protein, the amount of the phosphorylated form may be lower than that of its unphosphorylated counterpart (low stoichiometry), and different sites on a protein may be phosphorylated to different degrees. On top of the above factors that complicate analysis of phosphorylation, because kinases and phosphatases play their roles at the same time, phosphorylation is intrinsically dynamic and transient.[42] The importance of phosphorylation and challenges in its detection are driving continuous improvements in detection methods and instrumentation.[43]

1.3 Phosphoproteomics: detection of protein phosphorylation, enrichment techniques and analysis strategy

As mentioned in the previous section, phosphorylation of protein side chains is one of the most important PTMs and serves as a crucial mechanism for creating diversity in eukaryotic cells. A fundamental understanding of regulatory pathways at the molecular level requires the identification of the phosphorylation states in specific proteins. The following subsection describes the historical methods for phosphorylation detection and the current leading MS-based method. A subsequent subsection introduces several phosphopeptide enrichment strategies employed prior to the MS analysis to facilitate detection, and the last subsection discusses MS fragmentation methods.

1.3.1 Detection of protein phosphorylation

Initially, detection of the γ–[^{32}P] phosphate transfer from ATP to the protein side chain served as the primary method for examining phosphorylation.[44] In this technique, precipitation of phosphorylated proteins using trichloroacetic acid separates them from a protein mixture, and proves that the phosphorylations on Ser, Thr and Tyr are acid stable. After the protein washing, a scintillation counter detects the ^{32}P if phosphorylation occurs. However, the localization of the phosphorylation sites and determination of the stoichiometry are a challenge for this traditional method. Moreover, this technique is more suitable for studying a targeted known protein than for detection of global protein phosphorylation.

Based on sodium dodecyl sulfate polyacrylamide gel electrophoresis (SDS-PAGE), Western blotting (WB) is the most widely used analytical technique to detect proteins in a given

biological sample.[45] With appropriate phosphor-antibodies, WB is also the most common approach to detect specific phosphorylation events.[46] Phosphotyrosine antibodies show the most specificity for the phosphorylated residues, and binding of these antibodies does not depend greatly on the surrounding amino acid sequence. Thus, antibody methods for detection of phosphorylated tyrosine are highly developed.[47] However due to much less specific binding, detection of phosphoserine and phosphotheronine with WB has developed more slowly. The available phosphoserine and phosphothreonine antibodies rely on motif-based selectivity (e.g. affinity to the RXRXXpT or pSXR sequence, where X is any amino acid).[46] In other words, the antibodies will reveal phosphoserine or phosphotheronine only if they are present in select sequences. Because of insufficient specificity, the antibodies for probing phosphoserine and phosphotheronine are not widely used. Moreover, the success of this method depends on the availability of the various phosphor-antibodies. This method is often a way to confirm a known phosphorylation event rather than a discovery path to reveal new phosphorylation events.

Both ^{32}P detection and WB are not high throughput techniques. From the perspective of systems biology or global protein phosphorylation studies under a certain stimulus, the protein complexity and abundance overwhelm the capabilities of these two detection methods. Currently, MS is the leading technology for evaluation of the phosphoproteome [6, 38-39, 48-49] due to its high sensitivity and throughput, and the capability to localize the phosphorylation site at specific amino acids using tandem MS.[39]

The major goal of phosphoproteomics is to identify and quantify phosphorylated proteins, and further to determine the location of the phosphorylated sites. This goal is normally realized by examining the proteolytic peptides generated from a pure protein or a protein mixture. Addition of 79.966 Da (phosphate group) to the known peptide mass is evidence for

phosphorylation. For an unknown sample, the signature indication is the loss of 97.995 Da (trihydrogen phosphate) from Ser and Thr, or 79.966 Da (phosphate) from Tyr during a CID process. The next step is to determine the peptide sequence and localize the phosphate groups at certain amino acids. Localization relies on the product ions in the tandem MS or MS^n spectra, where the product ions refer to the CID fragments of the selected peptides. The workflow is straightforward, but there are many practical issues associated with the entire analysis such as sample preparation (including phosphopeptide enrichment), peptide fragmentation and data interpretation. Each step needs careful refinement to get accurate and reliable results for protein phosphorylation.

1.3.2 Enrichment of phosphopeptides

Although reversible phosphorylation is ubiquitous in cells, the phosphoproteins are generally present at relatively low abundance compared to the non-phosphorylated proteins because of the intrinsically dynamic and transient nature of phosphorylation.[42] This low abundance makes detection of phosphorylation extremely difficult in conventional MS analysis, especially in complex mixtures. Additionally, two papers suggest that the non-phosphorylated peptides have a higher ionization efficiency than their phosphorylated analogues.[50-51] Based on the study of many synthetic phosphopeptides, Steen and coworkers disagree with the statement that phosphopeptides have low ionization efficiencies.[52] However, this contradiction may be due to the presence of lysine (Lys), Arg and histidine (His) in Steen's analyzed phosphopeptides. These basic residues will increase the ionization efficiency when using ESI.[53-54] Efforts have been made to enhance the signal intensity in MALDI-MS by adding

matrix additives like ammonium citrate[55] or phosphoric acid[56]. Nevertheless in complex mixtures, phosphopeptide enrichment is a prerequisite for MS analysis.[57-58]

For decades, many strategies have been developed to carry out phosphopeptide enrichment. The traditional biological process is immunoprecipitation, in which specific antibodies capture phosphorylated species in a protein mixture. The most reliable antibodies are only suitable for pTyr, so there are intensive studies of Tyr phosphorylation.[59-60] In contrast the motif-based anti-pSer and anti-pThr antibodies limit studies of Ser and Thr phosphorylation.[61-62]

Chemical derivatization is another important strategy for enriching phosphoproteins and phosphopeptides. For example, β-elimination of the phosphate groups present at Ser or Thr residues followed by a Michael addition reaction can link a biotin-tag to the peptides or proteins that originally contained the phosphate group.[63] Later, Zhou and co-workers introduced a multi-step chemical modification using phosphoramidate chemistry for all phosphorylated residues.[64] Unfortunately, the general drawback of chemical derivatization is that potential side reactions and conversion yields below 100 % result in both sample loss and increased complexity.[65]

The most common phosphopeptide enrichment strategy is affinity chromatography. First introduced in 1975, immobilized metal affinity chromatography (IMAC) initially aimed to fractionate proteins based on the coordination interaction between a metal ion and the imidazole group on histidine.[66] Metal chelators such as iminodiacetic acid and nitrilotriacetate acid (NTA) link the affinity metal ions to the chromatographic support.[67] Today, IMAC columns are one of the primary tools for purifying tagged recombinant proteins. Introduced by Andersson and Porath in 1986,[68] IMAC using Fe^{3+} complexes (IMAC-Fe) has been the most common

method to enrich phosphopeptides. IMAC-Fe relies on hard acid-hard base interactions between positively charged metal-ligand complexes and specific negative functional group such as phosphates. Other candidate metal ions include Al^{3+},Ga^{3+},Co^{3+} and Ti^{4+},[69] and this technique is widely used in silica column[70], magnetic beads[71] and modified MALDI plates.[72]

In the past, titanium dioxide (TiO_2) served as a stationary phase to adsorb organic phosphate or phospholipids.[73-74] More recently, TiO_2 has been widely used as an alternative to IMAC for phosphopeptide enrichment.[73-76] At acidic pH, TiO_2 has a positively charged surface that selectively adsorbs phosphorylated species,[77] and the adsorbed phosphopeptides can be easily eluted at basic conditions.[78] This technique belongs to the large category of metal oxide affinity chromatography (MOAC).[79-80] Unlike IMAC, which requires frequent recharging (loading of the metal ion) before use, the MOAC material themselves (TiO_2 or ZrO_2 beads) can be the packing material for a column.[2] Moreover TiO_2 has been reported to be more effective than IMAC in the specific enrichment of phosphopeptides.[80-88] Furthermore TiO_2 columns already have a number of online applications in phosphopeptide enrichment, and this online approach greatly improves throughput and enhances global phosphorylation studies.[80, 85, 89]

Unfortunately, both IMAC and MOAC suffer from unwanted binding of highly acidic peptides. Thus peptides containing multiple glutamic acid and aspartic acid residues frequently co-purify with phosphopeptides.[79] O-methyl esterification can block the acidic residues and enhance the specific phosphopeptide binding.[34] However, incomplete esterification complicates MS analysis.[90] More recent studies suggest that excluders such as DHB[79, 81,

91-92] can block the non-specific binding sites without influencing the phosphopeptide binding.[93-94] Jenson and Larsen suggest that compounds with different coordination geometries have affinity towards different sites on TiO_2. Figure 1.6 shows the coordination modes between TiO_2 or salicylic acid and phosphate. The bridging-bidentate binding between phosphate and TiO_2 does not compete with sites for the chelating-bidentate binding between substituted carboxylic acid and TiO_2. However, the chelate-bidentate binding does affect adsorption of acidic peptides. A list of excluders in order of inhibiting efficiency includes: DHB ~ salicylic acid ~ phthalic acid > benzoic acid ~ cyclohexane carboxylic acid > phosphoric acid > trifluoroacetic acid (TFA) >acetic acid.[79] Careful selection of loading, washing and elution buffer will improve the selectivity and efficiency of phosphopeptide binding.[81, 89]

Another empirical rule is that TiO_2 prefers mono-phosphopeptides over multi-phosphopeptides, whereas IMAC selectively enriches multi-phosphopeptides.[95-96] I presume that this phenomenon reflects incomplete elution of multi-phosphopeptides from TiO_2 rather than a lack of binding of these species. In addition IMAC sometimes suffers from insufficient binding capacity, and the multi-phosphopeptides likely occupy binding sites rather than mono-phosphopeptides. Multi-phosphopeptides readily elute from IMAC resins, and TiO_2 usually has no binding capacity problem. Liang et al. showed a binging capacity of 300 μmol of phenyl phosphate per gram of cross-linked TiO_2 nanoparticles.[97]

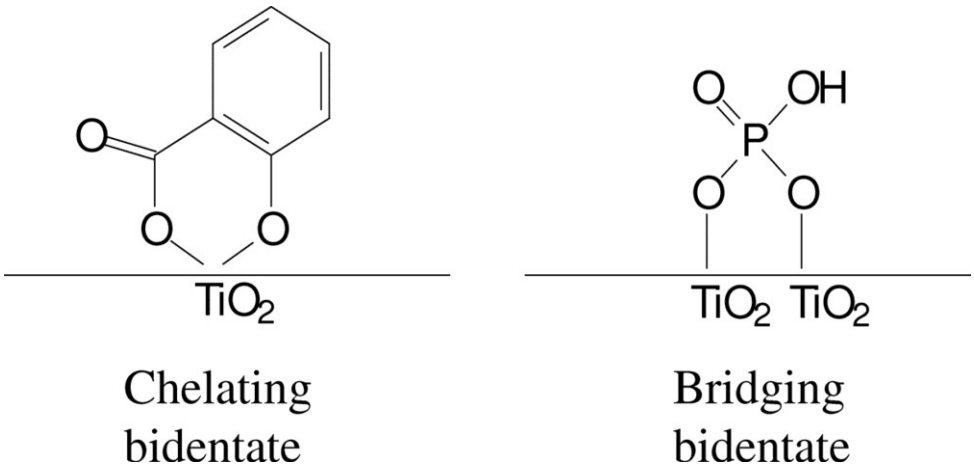

Figure 1.6. The left drawing represents the chelating bidentate binding mode between TiO_2 and salicylic acid, while the right drawing represents the bridging bidentate mode between TiO_2 and phosphate. The figure is reprinted from reference [79] with permission from the American Society for Biochemistry and Molecular Biology (ASBMB).

Due to their intrinsic selectivities for mono-phosphorylated and multi-phosphorylated peptides, respectively, TiO_2 and IMAC are sometimes used together to achieve complementary information.[95-96] Thingholm and coworkers developed a sequential elution from IMAC (SIMAC) strategy to increase the comprehensiveness of phosphopeptide enrichment. Scheme 1.1 illustrates their SIMAC workflow to enrich phosphorylated peptides. They first employ IMAC beads in GELoader tips to enrich phosphorylated peptides. After incubation for 30 min and washing, acid elution (1 % TFA, pH 1.0) is applied to elute the mono-phosphopeptides. Peptides that passed through the column in the loading, wash and acid elution are enriched by adsorption on TiO_2. The eluent from TiO_2 (primarily mono-phosphopeptides) and a basic eluent (NH_4OH, pH 11.3) that removed phosphopeptides remaining on the IMAC resin (primarily multi-phosphopeptides) are analyzed by MALDI MS or LC-ESI MS/MS. In a phosphoproteome study

of 120 μg of protein from human mesenchymal stem cells, compared to an optimized TiO_2 enrichment method, the SIMAC identified two-fold more total phosphopeptides, including a three-fold increase in multi-phosphopeptides.

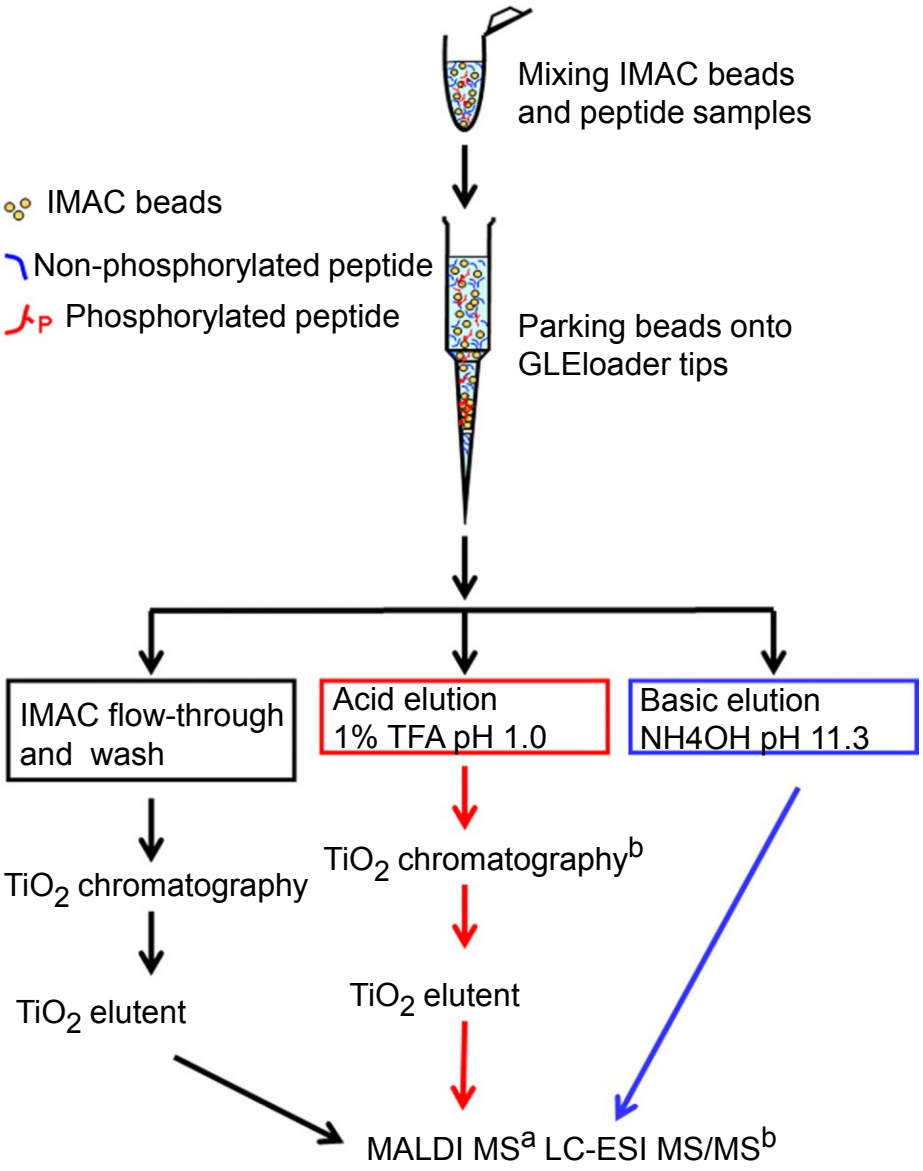

Scheme 1.1. The workflow of the SIMAC strategy to enrich phosphorylated peptides. [a]Step is performed only in a simple peptide mixture and [b]Steps are performed only in the complex peptide mixture. The figure is reprinted from reference [95] with permission from the ASBMB.

For even larger scale phosphorylation studies (e.g. over five thousand phosphorylation events), the IMAC and/or MOAC enrichment are not adequate to reduce the sample complexity while maintaining all valuable information. Similar to RP-HPLC, strong cation exchange (SCX) chromatography fractionates the complex sample and alleviates the workload for later enrichment steps. At pH 2.7, the phosphate group will bring a negative charge to modified peptides, so compared to non-phosphorylated peptides, phosphopeptides should elute in early fractions of the SCX eluate. The SCX approach divides one extremely complex sample into tens of moderately complex samples, on which either IMAC or MOAC have reasonable enrichment performance. Scheme 1.2 demonstrates the procedure for phosphopeptide enrichment and analysis from a yeast lysate. In the protocol, the protein extracts from yeast cells are first reduced, alkylated and digested with trypsin in solution. The SCX fractionates the peptides mixture into 12 tubes. Each fraction undergoes desalting and enrichment by IMAC and eventually analysis by LC-MS/MS.[98] With this SCX/IMAC enrichment protocol to explore the phosphoproteome in several systems, Gygi and Villén found 5,500 and 13,000 phosphorylation events in mouse and Drosophila embryo characterizations, respectively.[99-100]

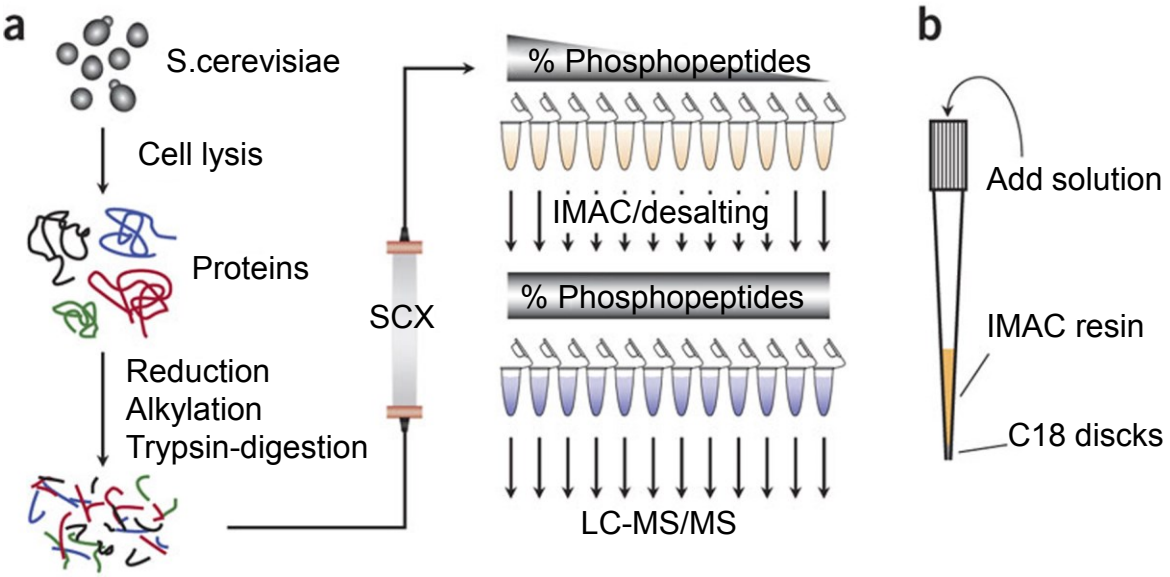

Scheme 1.2. (a) A procedure for phosphopeptides enrichment from cells prior to LC-MS/MS. Extracts for yeast are reduced, alkylated and digested with trypsin in solution. The SCX fractionates the peptide mixture into 12 tubes. Each fraction undergoes desalting and enrichment by IMAC and eventually analysis by LC-MS/MS. (b) The IMAC tip used for enrichment after the SCX in procedure (a). The phosphopeptides trapped on the IMAC resin will be first eluted onto the C18 disks without acetonitrile (ACN), next rinsing will desalt the sample, and finally phosphopeptides are eluted by organic solvent. The figure is reprinted from reference [98] with permission from the Nature Publishing Group.

1.3.3 MS Analysis Strategy

Both fragmentation methods and gas phase ion chemistry play a vital role in the characterization of phosphopeptides.[101] In the conventional bottom-up approach, the phosphopeptides are traditionally fragmented by CID. The tandem MS identifies certain species as phosphopeptides based on the neutral loss of 98 Da or 80 Da. However these particularly neutral loss fragments dominate the tandem mass spectrum so little sequence information is

available. A data-dependent acquisition mode supplements this incomplete information, as MS^3 is triggered at the dominant peak in tandem MS. The MS^3 spectrum contains the sequence information for the peptide.[2, 101]

Although this is a universal approach, some gas phase ion chemistry will influence the results under certain circumstance. When using MALDI as the ion source and an ion trap as the analyzer, Palumbo et al. observed phosphate rearrangement and competing loss phenomena in some cases. From studies on synthetic phosphopeptides, they conclude that phosphate rearrangement happens at a high probability when the number of basic residuals (Lys, Arg and His) is larger than the peptide charge (usually one in MALDI ionization). There is also a potential for competing losses of 98 Da from either the precursor ion or from the b- and y-type product ions. (either directly as 98 Da (H_3PO_4) from a phosphorylated Ser or Thr residue, or as the combined losses of 80 Da (HPO_3) from a phosphorylated Serine or Threonine residue and 18 Da (H_2O) from a non-phosphorylated Ser or Thr residue). Both events result in ambiguity in assigning the sites of phosphorylation within the peptide sequence.[102]

As an alternative fragmentation method to characterize the phosphorylation sites and peptide sequence, high-energy collision-induced dissociation (HCD) is carried out exclusively in another cell provided with the LTQ-Orbitrap instrument.[103] Based on the same collision mechanism as CID, the HCD uses increased radio frequency voltage (2500 V compared to 1500 V) for containing more ions in the trap. This modification leads to more fragmentation in the cell, and production of more b- and y-type product ions in addition to immonium ions. The more comprehensive fragmentations facilitate the *de novo* sequencing and localization of phosphorylation.

Different from the collision of positively charged peptides with a noble gas, gas-phase ion/ion chemistry is another path to induce fragmentation.[26-27] In the ETD process, an anion with low electron affinity, such as fluoranthene ion, donates an electron to the multi-charged peptide cation to generate one hydrogen radical that initiates peptides fragmentation. The largest difference is the fragmentation pathway, where the CID fragments first at the lowest energy bond and then the amide bonds, ETD favors cleavage of the C_α-N bond and the labile modification will remain on its residue.[104] As a result, the localization of phosphorylation is straightforward and clear. Figure 1.7 is an analogy of the outcome of the dissociation from CID (CAD) or ETD for short peptides, peptides with PTMs and large peptides.

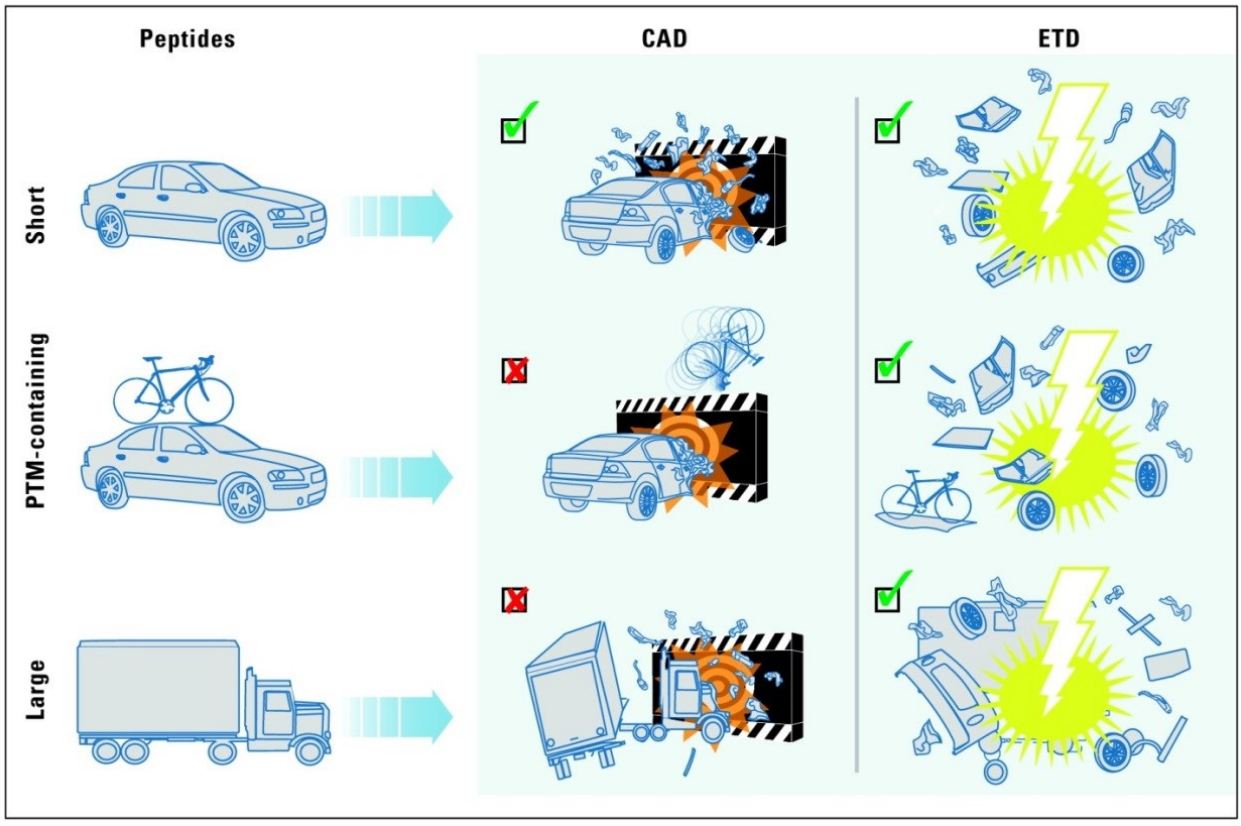

Figure 1.7. Illustration of outcomes from ETD or CID (CAD) dissociation for short peptides, peptides containing PTMs and large peptides. ETD is effective for the three types of peptides,

while CID works well for short peptides but less effectively for peptides containing PTMs and large peptides. The Figure is reprinted from reference [104] with permission from the ACS.

One of the inventors of the ETD technique, Coon, and his coworkers recently conducted a phosphoproteome study on the human embryonic stem cell and revealed 8087 unique phosphopeptides by ETD and 3868 unique phosphopeptides by CID.[105] Although the ETD approach is superior to the CID method in terms of peptide identification efficiency and phosphorylation assignment, many factors such as precursor ion charge, precursor ion mass/charge ratio and identity of peptides will great influence the results in both methods.[106] Phosphoproteome studies should employ both fragmentation methods if possible.

Inspired by these pioneering studies, this dissertation (chapters 2 and 3) introduces a membrane-based TiO_2 enrichment technique and its investigation of the phosphorylation of tau protein.

1.4 Immobilized enzyme reactors

Immobilization of enzymes on a support already has a history of almost 100 years.[107] In recent developments, immobilized enzyme reactors (IMERs) have found applications in the areas of digestion, catalysis of small-molecule reactions (e.g. glucose oxidase) and enzyme inhibitor screening.[108-109] This section will focus on the contribution of IMERs to proteomics, specifically the usage of immobilized proteases such as trypsin and pepsin to digest proteins prior to their MS analysis, as this is related to the work in chapters 4 and 5.

As emphasized above, sample preparation is a vital step in MS-based proteomics. For a bottom-up approach, an efficient and effective proteolysis will yield high quality peptide-containing samples for successful protein identification and characterization.[108, 110] IMERs

containing proteases usually contain a high enzyme density to catalyze digestion in a few seconds, and this fast digestion greatly increases the throughput for proteomics studies compared to the traditional 16-h in-solution digestion. Other assets of digestion in IMERs include minimal autolysis of the protease, reusability and on-line automation.[108, 110] The immobilization process stabilizes the proteases and enhances their tolerance to high temperatures, pH variations and organic buffer.[109] Most column-based IMERs can directly couple to HPLC-MS instruments to reduce sample handling, increase sensitivity and decrease analysis time.[111] The choice of immobilization methods, supports and enzymes plays an important role in tailoring IMERs for a particular purpose, and the following subsections discuss these three variables. Unfortunately, there is no universal protocol for creating effective IMERs.

1.4.1 Immobilization methods

The major techniques to immobilize enzymes are either chemical linkage with covalent bonds or physical adsorption that relies on hydrogen bonds and hydrophobic or ionic interactions. The main goal is to trap the enzymes on the support while retaining their activity. Among the available anchoring methods, hydrophobic adsorption to the support is the simplest but also the least robust. Lee et al. immobilize trypsin onto a polyvinylidene fluoride membrane via hydrophobic interactions.[112] They successfully incorporate the miniaturized trypsin-modified membrane in a common capillary fitting and perform digestion prior to online nano-ESI-MS. The method requires very little sample consumption (<5 fmol) and achieves low detection limits (10^{-8} M). However replacement of the protease by hydrophobic proteins or leaching of protease in the presence of surfactants used to increase the protein solubility will limit the lifetime of the IMER.[111]

Proteins adsorption via electrostatic interaction is another versatile method suitable for enzyme immobilization on charged substrates.[113-117] Moreover the bound enzymes demonstrate similar or higher activity compared to the free enzyme in solution.[113-115] Bhattacharyya and coworkers use layer-by-layer-assembled films to capture enzymes in membranes. They first covalent attach either poly(L-glutamic acid) (PLGA) or poly(L-lysine) (PLL) to the surface and pores of the membrane substrate.[113] Then they electrostatically adsorb poly(allylamine) hydrochloride (PAH) and poly(styrene sulfonate) (PSS) to create PLL-PSS-PAH or PLGA-PAH-PSS assemblies, which have positive and negative surface charges, respectively. Figure 1.8 shows the three steps to create a negatively charged PLGA-PAH-PSS assembly. As expected, the adsorption is much greater when the protein charge is opposite to the charge on the substrate than when the two charges have the same sign. Although this electrostatic immobilization method is facile and versatile, leaching or replacement of the enzyme is possible when the buffer has a high ionic strength or incoming proteins are highly charged.

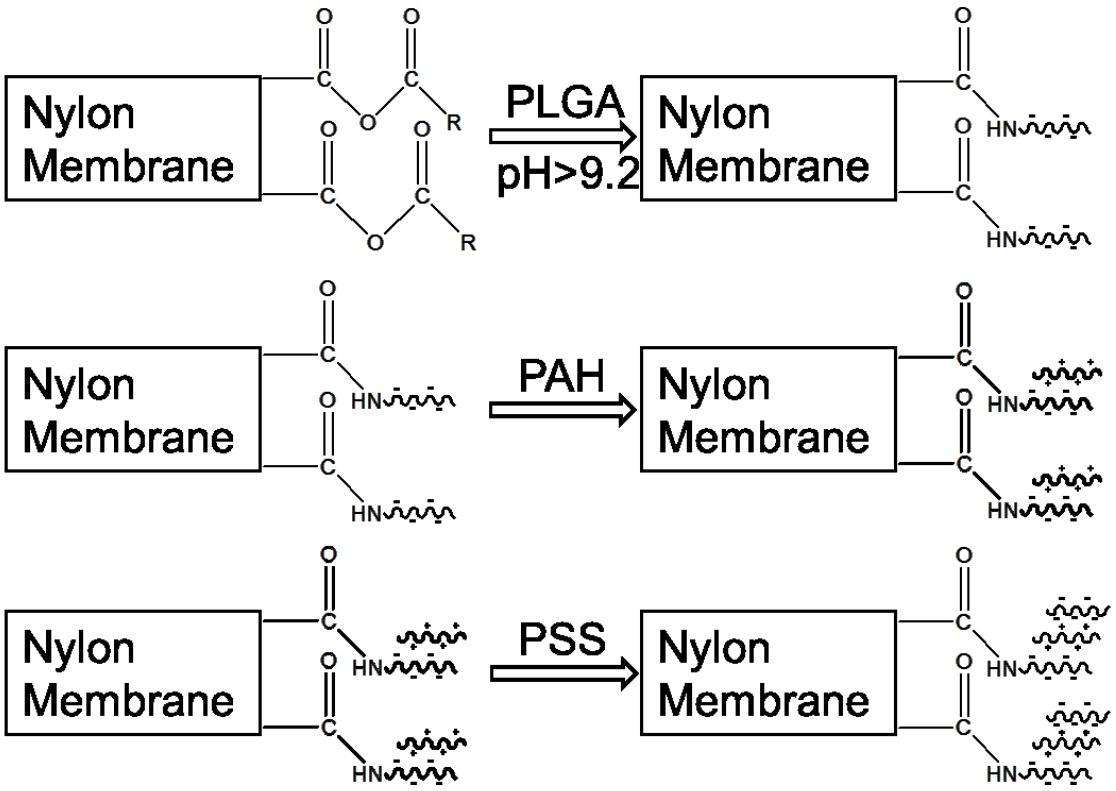

Figure 1.8. The procedure to create a PLGA-PAH-PSS assembly on a nylon membrane. The PLGA is first covalently attached to the nylon membrane, and positively charged PAH absorbs to the negatively charged PLGA through electrostatic interactions. Similarly, the PSS attaches to the PAH and leaves the surface negatively charged. This Figure is redrawn according to reference [113] with permission of the ACS.

Compared to adsorption, covalent binding of enzymes to a substrate will provide more robust attachment. The most common covalent binding method includes activation of supports containing amino group with glutaraldehyde, a homo-functional cross-linker (Figure 1.9a).[109] The glutaraldehyde reacts with the amine on the support via one aldehyde and leaves the other aldehyde ready to connect to the protein N-terminus or a free amine of a lysine residue. To prevent potential hydrolysis, the labile Schiff base is further reduced by sodium borohydride in some cases.[118] Other strategies employ N,N'-disuccinimidyl carbonate (DSC, Figure 1.9b) or

N,N'- disuccinimidyl suberate (DSS) as a linker (Figure 1.9c). With DSS a six-carbon chain spaces the enzyme from the surface, and the enzyme linking occurs via an amide bond.[119] The covalent method provides stable immobilization, but the enzyme concentration in the immobilization solution must be high, and the reaction may require many hours.[118, 120-121] Moreover, a recent review also discusses the concern of enzyme-activity loss during the covalent immobilization reaction.[122] A number of other reactions are also available for covalent immobilization. [109]

In summary, all enzyme-immobilization methods developed so far are effective but have some drawbacks. The choice of a specific method may need to balance the project goals with aspects that can be sacrificed, such as short reaction time, low starting material concentrations or partial loss of enzyme activity.

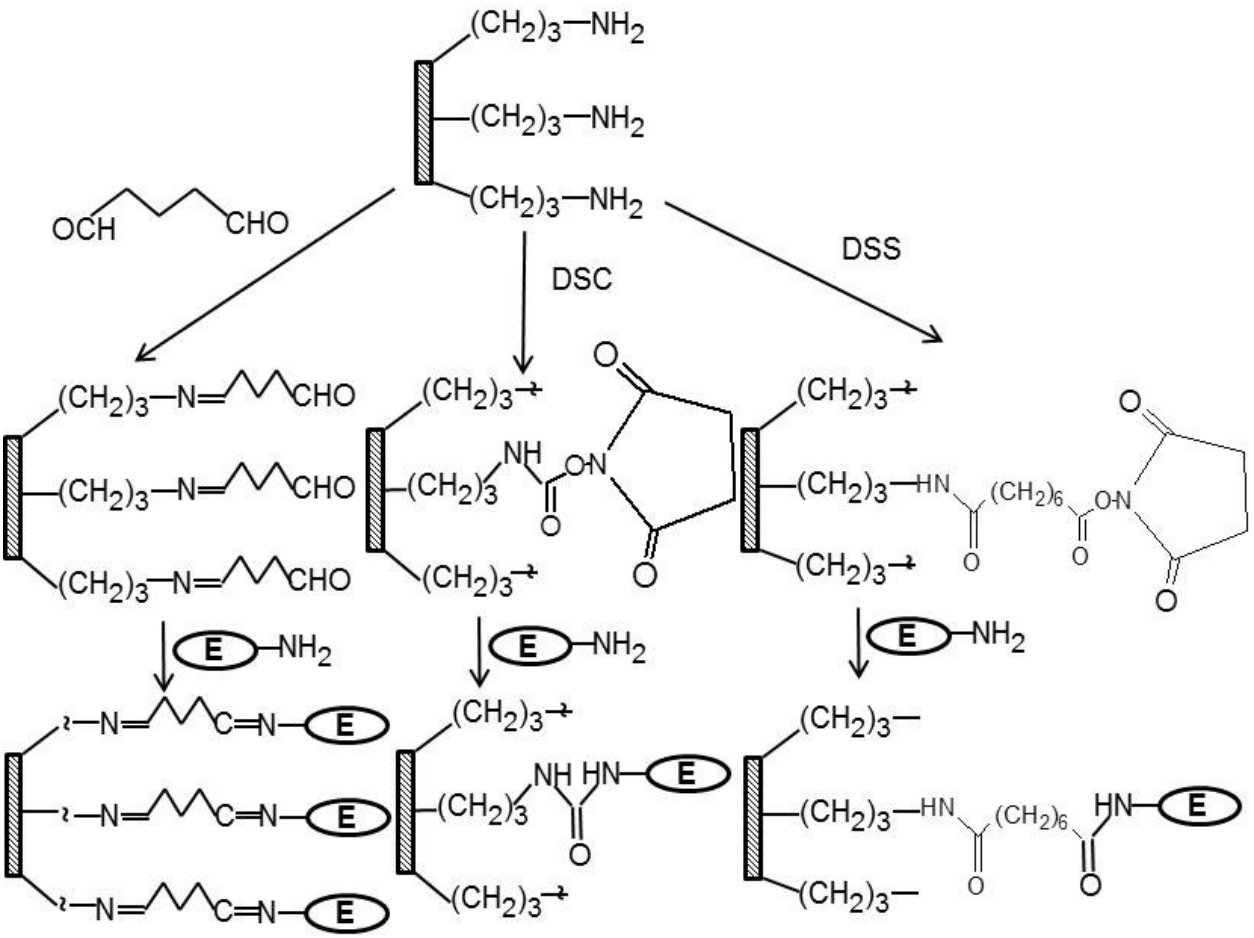

Figure 1.9. Three procedures to covalently link enzymes to an amine-containing surface via different cross-linkers (a) glutaraldehyde, (b) DSC and (c) DSS. The figure is reprinted from reference [109] with permission from the Elsevier .

1.4.2 Immobilization supports

The basic criteria to choose the support are high surface area, good mechanical strength and stability over the necessary range of pH values and temperature. For most applications both polymeric and inorganic materials are acceptable. Supports are already available in a wide range of geometries including beads, monoliths, nano/micro particles, microfluidic channels and membranes. Below I describe a few examples of specific supports for enzyme immobilization.

Magnetic microspheres are attractive supports because they can be readily recovered from complex mixtures using a magnetic field. Zhang and coworkers employ a one-step reaction to bind trypsin to silica-coated magnetic microspheres via a 3-glycidoxypropyltrimethoxysilane linker.[123-124] In addition to their magnetic properties, these microspheres adsorb microwave radiation to promote digestion in solutions containing the trypsin-modified beads. A 15-s microwave-enhanced digestion was equivalent to or better than the traditional 16-h digestion with free trypsin.[123]

Monoliths have emerged as attractive enzyme supports in recent years. Both silica and organic polymers can form monolithic disks, columns and capillaries.[111] In addition to chemical and physical stability, the high surface area and low backpressure of such porous monoliths make them attractive for diverse enzyme-based applications, including coupling to HPLC-MS for online reactions.[120] Svec and coworkers successfully immobilized trypsin and endoproteinase LysC onto a poly-(glycidyl methacrylate-co-ethylene dimethacrylate) monolith. They demonstrate that hydrophilization via photografting of poly(ethylene glycol) methacrylate greatly reduces nonspecific adsorption of hydrophobic proteins and peptides, and later they apply this enzyme reactor to the digestion of immunoglobulin G. A 6-min digestion is similar to in-solution digestion for 24 h.[120]

Microfluidic devices are appealing for online biological and chemical analyses with minimal sample consumption.[125] Liu et al. incorporate proteases and charged polysaccharides into a microchip using layer-by-layer assembly. They achieve a detection limit as low as 0.1 ng/μL with cytochrome c digests, and the microchip rector digests femtomoles of protein per analysis within seconds.[115] They conclude that the high enzyme density in the micro-channel increases digestion rates three orders of magnitude relative to in-solution digestion.

Commercial polymer membranes serve as filters in many applications, but they are also excellent supports for enzymes.[126] Their large surface area to volume ratio leads to a high density of immobilized enzymes, and short radial diffusion distance in pores will allow enzyme-substrate reactions without diffusion limitations. Furthermore, the small membrane thickness (~100 μm) enables convective transport with a simple syringe pump. Our previous group members, Xu and Wang developed membrane-based digestion in which a 6-s digestion of BSA leads to 84 % sequence coverage in MALDI-MS. This sequence coverage is significantly higher than the 71 % obtained after in-solution digestion for 16 h.[114] Moreover trypsin-modified membranes still function in the presence of 0.05 wt% SDS, whereas trypsin in solution does not catalyze digestion under similar conditions. This is another evidence that immobilization enhances enzyme stability. In summary enzyme immobilization on a variety of supports is creating exciting opportunities for IMERs in proteomics.

1.4.3 Immobilized trypsin and pepsin, reactors for protein digestion

Although there are a number of proteases applicable to digestion for proteomics, trypsin and pepsin are the most readily available. In the bottom-up approach, trypsin is the protease of choice due to its low cost, predictable selectivity, and efficient performance.[127] Trypsin catalyzes protein cleavage at the C-terminus of Lys and Arg residues, unless the following amino acid is proline. Usually, new digestion methods pursue rapid and complete digestion, and the studies described in the previous subsection all achieved this goal. However, the digestion mechanism is also important for controlling the process.

Liu and coworkers use a nanoporous material to confine the protease-substrate reaction and find that confinement increases the digestion efficiency. BSA and myoglobin digestion with such trapping materials yield more peptides than traditional in-solution digestion. Using MS

fingerprinting, they identify 293 proteins after nanopore digestion of a normal human liver cytoplasm sample, whereas analysis of an in-solution digest leads to identification of only 100 proteins.[128] In a subsequent study, they propose that in a confined environment partially digested peptides compete with the intact protein for digestion sites. Cleavage of the peptides is more likely than proteolysis of the intact protein, so complete digestion occurs more readily than digestion of a protein into a few pieces.[129] Very recently, Liu's group invented a periodic mesoporous organosilica (PMO) material for membrane protein digestion.[130] Due to the hydrophobicity and structure rigidity, membrane proteins resist proteolysis. Scheme 1.3 describes the strategy for using the PMO to digest bacteriorhodopsin. This amphiphilic PMO can adsorb and trap hydrophobic membrane proteins into its pores and later concentrate trypsin from aqueous solution into pores and promote proteolysis. To prove the general utility, they successfully apply this material for identification of membrane protein extracted from mouse liver. [130]

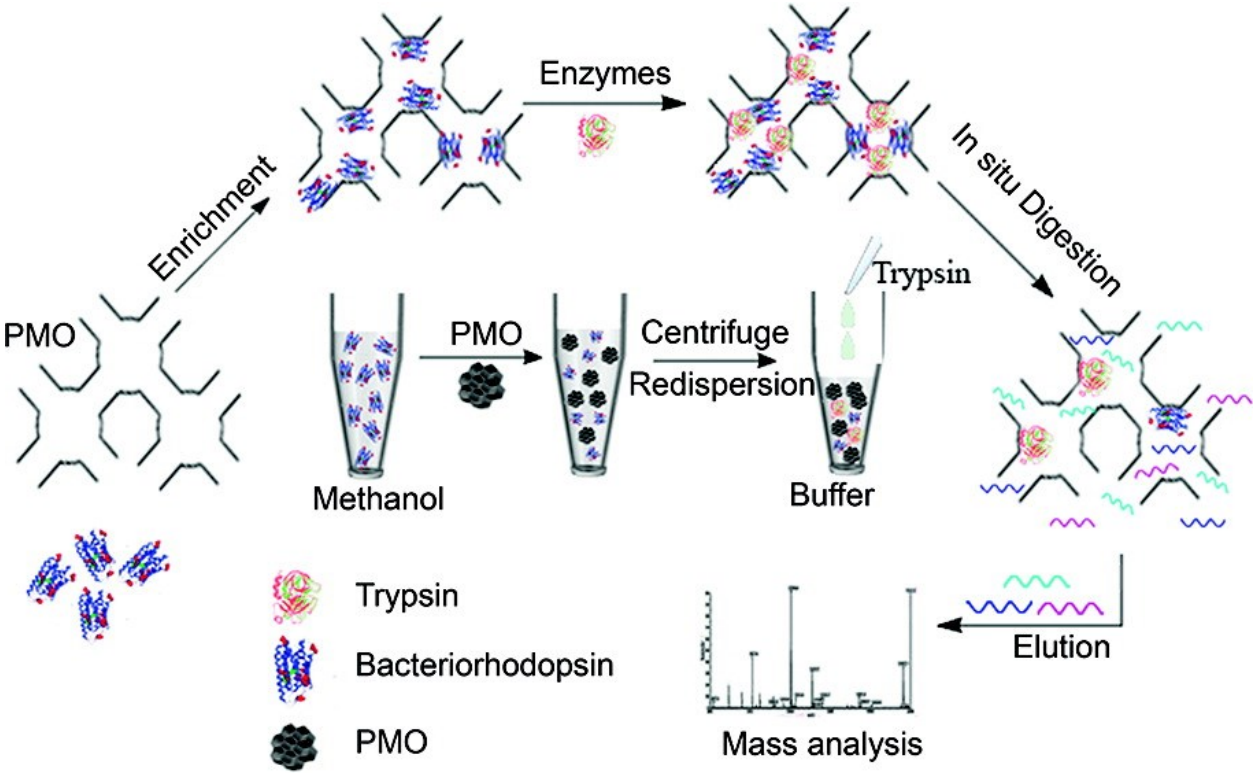

Scheme 1.3. The strategy for using PMO in the digestion of bacteriorhodopsin. The PMO first extracts the membrane protein from methanol into its pores, and after centrifugation the PMO is immersed into a trypsin-containing solution to adsorb trypsin for confined digestion. Finally, the peptides are eluted for MS analysis. The figure is reprinted from reference [130] with permission from the ACS.

Pepsin is also a relatively inexpensive protease, but it is less specific than trypsin. Because pepsin shows a preference for cleavage after most hydrophobic amino acid, many amide bonds are potential cleavage sites.[131] A statistical analysis from 39 peptic protein digestions demonstrates that the probability of N-terminus cleavage after leucine (Leu) and phenylalanine (Phe) is greater than 40 %, whereas other residues such as isoleucine (Ile), Tyr and tryptophan (Trp) are less vulnerable.[132] Unlike trypsin, pepsin shows optimal activity under acidic conditions (pH 1-2) that may partially denature proteins and, in particular, help to solubilize

membrane proteins. Zhang et al. couple a pepsin-modified column to a SCX-RPLC-ESI-MS/MS system to improve the digestion and identification of membrane proteins. In their study they annotate 91 out 235 identified proteins as membrane proteins with transmembrane domains.[133] Wilson and coworkers also immobilize pepsin in a microfluidic reactor to perform digestion and on-chip electrospray ionization. They achieve high sequence coverage with peptic digests of myoglobin, ubiquitin and bovine serum albumin using a digestion time of 4 s.[134] The Forest group finds that apomyoglobin digestion with a pepsin/rhizopuspepsin-containing column gives more complete proteolysis than conventional solution-phase digestion.[135] These studies are particularly relevant to the use of pepsin for digestion in HDX studies, which I describe in the next section.

1.5 Hydrogen-deuterium exchange and limited proteolysis for MS

As mentioned in the protein phosphorylation discussion, changes in protein structure or conformation and protein-protein interactions are key factors controlling protein function. X-ray crystallography and high-resolution nuclear magnetic resonance (NMR) remain the dominant tools for studying protein structure and dynamics.[136] However, these techniques are time-consuming and require either protein crystals, which are often not available, or highly pure protein.[137]

In the 1950s, Kaj Ulrik Linderstrøm-Lang first explored the deuterium exchange phenomenon in proteins.[138] Remarkably, under physiological conditions the hydrogen on the amide bond (except Proline) rapidly exchanges with deuterium when an unfolded region is exposed to D_2O, but in a folded region or areas with strong hydrogen-bonding, the hydrogen on the amide bond exchanges at a much slower rate or even not at all (Figure 1.10).[139] By

investigating which areas of a protein undergo deuterium exchange, one can generate low-resolution structural information. MS is the natural tool to analyze the mass increases due to HDX, and the first HDX-MS studies on proteins appeared in 1991.[140] HDX-MS research is now an important tool for exploring regional protein structure and dynamics, with expanding applications.[137, 139, 141] The following subsections describe HDX-MS applications using top-down and bottom-up approaches for analysis.

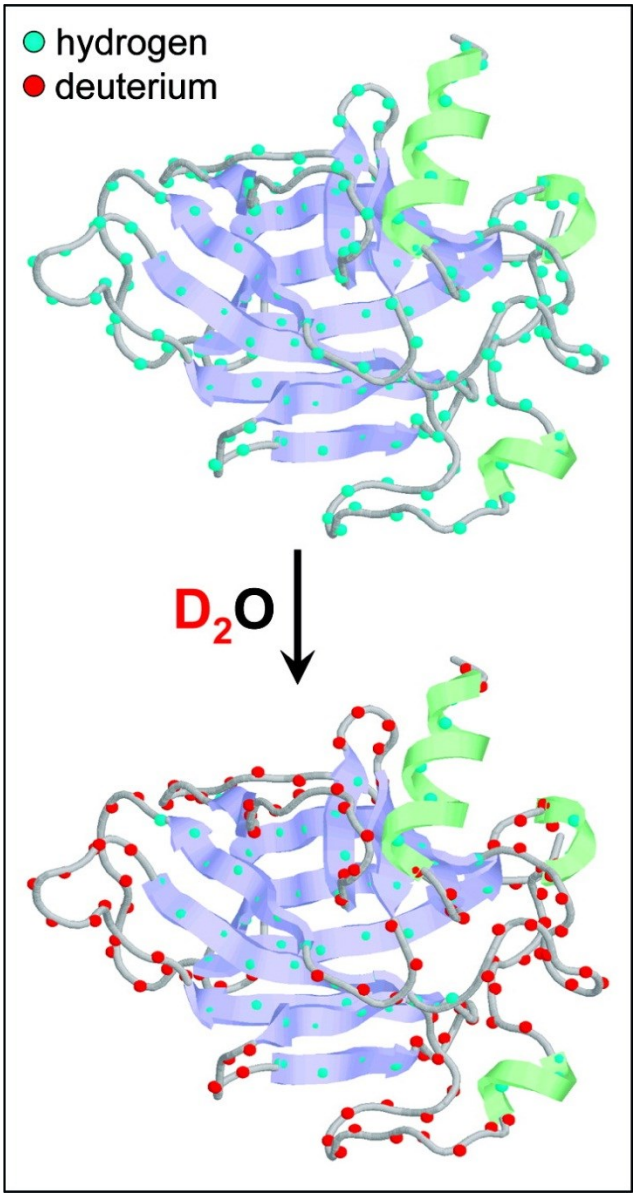

Figure 1.10. Conceptual drawing of HDX on a protein. The green balls represent the amide hydrogens, and the red balls stand for the exchanged deuterium after the protein is exposed to D_2O. The hydrogens on the loops and some unfolded helices exchange with deuterium rapidly. The hydrogen in the folded or protected areas has very slow or negligible exchange rates. The figure is reprinted from reference [136] with permission of the ACS.

1.5.1 HDX-MS using the top-down approach

After allowing HDX for a given time, the protein can directly undergo electrospray ionization and fragmentation by ECD. Konermann and coworkers demonstrate the success of this approach on a small protein, horse myoglobin.[142] They compare the deuterium exchange state (where and how many deuterium are in the amide bonds) between the native holomyoglobin and the apomyoglobin without the prosthetic heme group. ECD fragmentation gives a resolution of less than two amino acids and result shows that the F-helix is unfolded in the apomyoglobin and the G- and H-helix are also partially denatured. The conclusion is based on greater deuterium exchange in those region in the apo-form compared to the native form, and the result is consistent with previous NMR data.[143] The ECD fragmentation greatly reduces the H/D scrambling that may occur during the CID process. In CID, intermolecular proton migration results in ambiguous assignments of H/D on the amide bonds.[144] Another common concern is back-exchange, where the exchanged deuterium will return to hydrogen if the solvent changes back to H_2O, but that issue does not exist in this study due to the on-line procedure that requires no buffer exchange. However, this method only applies to proteins with a limited size. Larger proteins do not undergo efficient fragmentation, so the amino acid resolution will be very low.

1.5.2 HDX-MS using the bottom-up approach

Most HDX studies employ a bottom-up approach, in which the HDX is first quenched by lowering the pH to 2.5 and the temperature to 0 ºC. In this environment, the exchange rate is five orders of magnitude slower than that at physiological conditions.[137] John Engen employs an effective protocol for analysis of HDX: After HDX and quenching, the protein undergoes rapid

peptic digestion followed by ultra-performance liquid chromatography (UPLC) and ESI-MS or ESI-MS/MS by ETD (Figure 1.11). The main goal is to shorten the time between the quenching and MS analysis to reduce the chance of back exchange and reflect only the exchange in the native state. High amino acid resolution in ESI-MS relies on the overlap of peptides generated from peptic digestion.[137, 145] Pepsin is the enzyme of choice for the low pH condition, and immobilized-pepsin reactors enhance the digestion efficiency and shorten the digestion time to enhance amino acid resolution and prevent back-exchange. Thus, further improvement in on-line immobilized-pepsin reactors is important to facilitate HDX studies.[135, 146]

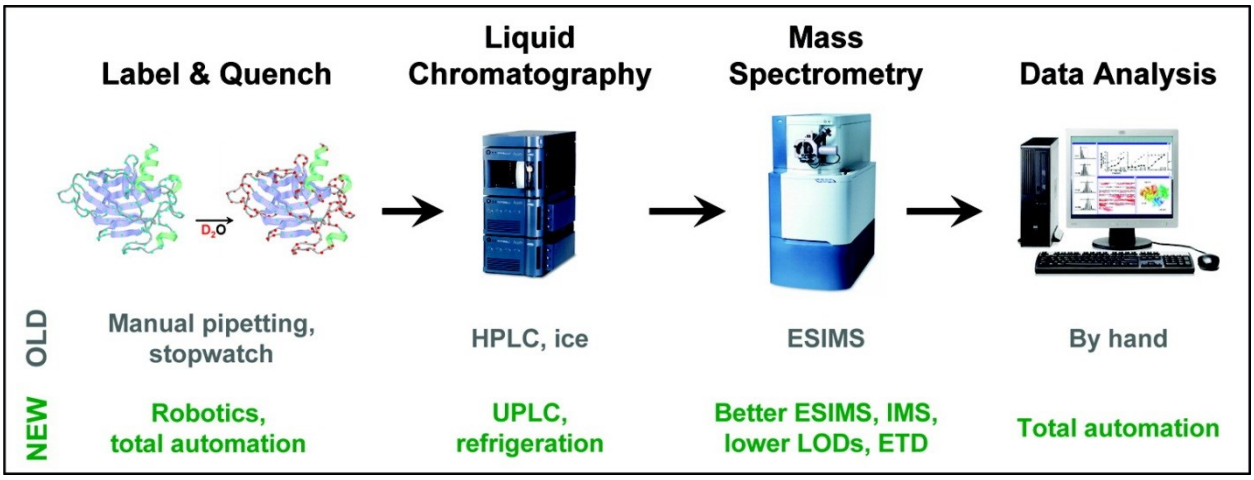

Figure 1.11. The workflow for obtaining protein structure information using HDX-MS. In the old pathway, the protein is labeled in D_2O and quenched by acid manually, the digested peptides are separate by HPLC on ice and analyzed by ESI-MS, and data is interpreted by hand. In the new protocol, the robotic automation precisely controls the labeling and quenching, and UPLC with refrigeration reduces the back exchange during peptide separation. Multiple MS analysis tools are available for different purposes, and the data processing is achieved with automated algorithms. The figure is reprinted from reference [136] with permission of the ACS.

1.5.3 HDX-MS using multiple acidic proteases

In the bottom-up approach, the spatial resolution for a high quality deuterium-exchange determination depends on a nearly complete, but overlapped digestion. Forest and coworkers employ both pepsin and rhizopuspepsin to improve the digestion[135] and study the bovine mitochondrial ADP/ATP carrier isoform 1 (bANc1p), which plays an important role of catalyzing the transport of ADP/ATP across the mitochondrial inner membrane in energy metabolism. In a conformational dynamics study of this protein, they discover that two toxin blockers (carboxyatractyloside or CATR, and bongkrekic acid or BA) induce different conformational changes when they form CATR-bANc1p and BA-bANc1p. The CATR-bANc1p complex result from HDX-MS agrees with their three-dimensional structure of CATR- bANc1p, and this agreement validates their method. The structure of BA-bANc1p is unknown, so the findings about BA- bANc1p from HDX-MS provide important information for the structure and mechanism.[147]

1.5.4 Limited proteolysis for protein structure elucidation

Limited proteolysis, incomplete digestion of a non-denatured protein, is another traditional method to probe protein structure, but it is not often combined with MS. This technique is particularly useful for identifying disordered regions of a protein, removing the loose and flexible regions from a protein or cutting the unstable hinge between domains.[148] The rationale is that compared to the global, stable and protected region, the other parts of the protein are more accessible to the protease, so they have a higher possibility for the initial cleavage. A few studies combined limited proteolysis and MS for studying protein

structure,[149-150] but limited proteolysis usually serves as a supplement to traditional x-ray crystallography and two-dimensional NMR analysis.

Burley's group recently employs a high-throughput protocol for protein domain elucidation. They apply 96-well arrays for limited digestion in orthogonal conditions (four proteases and six reaction times). From an experiment with 400 target proteins, they draw statistical conclusions, most notably that proteins digested to contain only stable globular domains have the highest probability for crystallization (and subsequent structure determination). In conclusion, they believe the high throughput limited digestion process can effectively gather the domain information for the protein and determine the optimal construct selection to facilitate crystallization and protein structure determination.[151]

Sharing the same concept that stable and globular proteins have a high tendency to crystallize, Edwards and coworkers add trace amounts of protease (enzyme/substrate ratio from 1:10000 to 1:100 wt/wt) into protein crystallization solutions, and find that *in situ* limited proteolysis promotes the crystallization of 55 bacterial and 14 human proteins.[152] Although the crystals are sometimes difficult to reproduce, the idea of using limited proteolysis to improve crystallization is worth considering along with systematic methods for limited digestion.

Yamaguchi, Miyazaki and Maeda mention limited proteolysis with respect to proteomics. [153] They integrate protease-containing microreactors into the digestion prior to MS analysis, and decrease the in-solution reaction from 16-h to a few minutes. However, the "limited proteolysis" in their study refers more to rapid and efficient digestion than its traditional definition.

The innovative and excellent work described above serves as an inspiration to utilize the unique property of protease-containing membranes for limited digestion in proteomics research.

The dissertation (chapter 4 and 5) describes limited proteolysis via msec-digestion in a protease-containing membrane and the potential application of this technique in middle-down proteomics and low resolution probing of protein structure.

1.6 Outline of Dissertation

The following dissertation contains five chapters. The basic structure is a fundamental study followed by a chapter with one or more biological applications. Thus, chapters 2 and 3 describe the development and characterization of TiO_2-modified membranes, and an investigation primarily of tau phosphorylation, respectively. Similarly, chapter 4 discusses the limited proteolysis of model proteins, bovine serum albumin and apomyoglobin, in a protease-modified membrane, and the subsequent chapter explores limited proteolysis for probing the structure of a root hair defective protein. Finally, chapter 6 summarizes the above work and provides some future research directions. Specifically, the next five chapter titles are:

Chapter 2: Phosphopeptide Enrichment with TiO_2-Modified Membranes

Chapter 3: Investigation of Phosphorylation in Tau Protein and the Nuclear Factor Kappa B (NF-κB) Pathway using Phosphopeptide Enrichment with TiO_2-modified Membranes

Chapter 4: Limited Proteolysis Via msec-Digestions in Protease-Modified Membranes

Chapter 5: Protease-Modified Membranes for Studies of Protein Structure: Limited Proteolysis and Rapid Digestion for HDX

Chapter 6: Summary and Future Work

REFERENCES

1.7 References

1. Yarmush, M. L.; Jayaraman, A., Advances in Proteomic Technologies. *Annu. Rev. Biomed. Eng.* **2002,** *4* (1), 349-373.

2. Yates, J. R.; Ruse, C. I.; Nakorchevsky, A., Proteomics by Mass Spectrometry: Approaches, Advances, and Applications. *Annu. Rev. Biomed. Eng.* **2009,** *11* (1), 49-79.

3. Han, X.; Aslanian, A.; Yates Iii, J. R., Mass Spectrometry for Proteomics. *Curr. Opin. Chem. Biol.* **2008,** *12* (5), 483-490.

4. Karas, M.; Bachmann, D.; Hillenkamp, F., Influence of the Wavelength in High-Irradiance Ultraviolet Laser Desorption Mass Spectrometry of Organic Molecules. *Anal. Chem.* **1985,** *57* (14), 2935-2939.

5. Yamashita, M.; Fenn, J. B., Electrospray Ion Source. Another Variation on the Free-Jet Theme. *J. Phys. Chem.* **1984,** *88* (20), 4451-4459.

6. Aebersold, R.; Mann, M., Mass Spectrometry-Based Proteomics. *Nature* **2003,** *422* (6928), 198-207.

7. Domon, B.; Aebersold, R., Mass Spectrometry and Protein Analysis. *Science* **2006,** *312* (5771), 212-217.

8. Tanaka, K., The Origin of Macromolecule Ionization by Laser Irradiation (Nobel Lecture). *Angew. Chem. Int. Ed.* **2003,** *42* (33), 3860-3870.

9. Liao, P.-C.; Allison, J., Dissecting Matrix-Assisted Laser Desorption/Ionization Mass Spectra. *J. Mass Spectrom.* **1995,** *30* (5), 763-766.

10. Taylor, G., Disintegration of Water Drops in an Electric Field. *Proc. R. Soc. Lond. A, Math. Phys. Sci.* **1964,** *280* (1382), 383-397.

11. Felitsyn, N.; Peschke, M.; Kebarle, P., Origin and Number of Charges Observed on Multiply-Protonated Native Proteins Produced by ESI. *Int. J. Mass spectrom.* **2002,** *219* (1), 39-62.

12. Martin, S. E.; Shabanowitz, J.; Hunt, D. F.; Marto, J. A., Subfemtomole MS and MS/MS Peptide Sequence Analysis Using Nano-HPLC Micro-ESI Fourier Transform Ion Cyclotron Resonance Mass Spectrometry. *Anal. Chem.* **2000,** *72* (18), 4266-4274.

13. Takáts, Z.; Wiseman, J. M.; Gologan, B.; Cooks, R. G., Mass Spectrometry Sampling under Ambient Conditions with Desorption Electrospray Ionization. *Science* **2004,** *306* (5695), 471-473.

14. Cody, R. B.; Laramée, J. A.; Durst, H. D., Versatile New Ion Source for the Analysis of Materials in Open Air under Ambient Conditions. *Anal. Chem.* **2005,** *77* (8), 2297-2302.

15. Douglas, D. J.; Frank, A. J.; Mao, D., Linear Ion Traps in Mass Spectrometry. *Mass Spectrom. Rev.* **2005,** *24* (1), 1-29.

16. Papayannopoulos, I. A., The Interpretation of Collision-Induced Dissociation Tandem Mass Spectra of Peptides. *Mass Spectrom. Rev.* **1995,** *14* (1), 49-73.

17. Makarov, A., Electrostatic Axially Harmonic Orbital Trapping: A High-Performance Technique of Mass Analysis. *Anal. Chem.* **2000,** *72* (6), 1156-1162.

18. Hu, Q.; Noll, R. J.; Li, H.; Makarov, A.; Hardman, M.; Graham Cooks, R., The Orbitrap: A New Mass Spectrometer. *J. Mass Spectrom.* **2005,** *40* (4), 430-443.

19. Roepstorff, P.; Fohlman, J., Letter to the Editors. *Biol. Mass Spectrom.* **1984,** *11* (11), 601-601.

20. Kelleher, N. L.; Lin, H. Y.; Valaskovic, G. A.; Aaserud, D. J.; Fridriksson, E. K.; McLafferty, F. W., Top Down Versus Bottom up Protein Characterization by Tandem High-Resolution Mass Spectrometry. *J. Am. Chem. Soc.* **1999,** *121* (4), 806-812.

21. Eng, J.; McCormack, A.; Yates, J., An Approach to Correlate Tandem Mass Spectral Data of Peptides with Amino Acid Sequences in a Protein Database. *J. Am. Soc. Mass Spectrom.* **1994,** *5* (11), 976-989.

22. Reid, G. E.; McLuckey, S. A., 'Top Down' Protein Characterization Via Tandem Mass Spectrometry. *J. Mass Spectrom.* **2002,** *37* (7), 663-675.

23. McLafferty, F. W.; Breuker, K.; Jin, M.; Han, X.; Infusini, G.; Jiang, H.; Kong, X.; Begley, T. P., Top-Down MS, a Powerful Complement to the High Capabilities of Proteolysis Proteomics. *FEBS J.* **2007,** *274* (24), 6256-6268.

24. Kellie, J. F.; Tran, J. C.; Lee, J. E.; Ahlf, D. R.; Thomas, H. M.; Ntai, I.; Catherman, A. D.; Durbin, K. R.; Zamdborg, L.; Vellaichamy, A.; Thomas, P. M.; Kelleher, N. L., The Emerging Process of Top Down Mass Spectrometry for Protein Analysis: Biomarkers, Protein-Therapeutics, and Achieving High Throughput. *Mol. Biosyst.* **2010,** *6* (9), 1532-1539.

25. Liu, J.; Huang, T.-Y.; McLuckey, S. A., Top-Down Protein Identification/Characterization of a Priori Unknown Proteins Via Ion Trap Collision-Induced Dissociation and Ion/Ion Reactions in a Quadrupole/Time-of-Flight Tandem Mass Spectrometer. *Anal. Chem.* **2009,** *81* (4), 1433-1441.

26. Zubarev, R. A.; Kelleher, N. L.; McLafferty, F. W., Electron Capture Dissociation of Multiply Charged Protein Cations. A Nonergodic Process. *J. Am. Chem. Soc.* **1998,** *120* (13), 3265-3266.

27. Syka, J. E. P.; Coon, J. J.; Schroeder, M. J.; Shabanowitz, J.; Hunt, D. F., Peptide and Protein Sequence Analysis by Electron Transfer Dissociation Mass Spectrometry. *Proc. Natl. Acad. Sci. U. S. A.* **2004,** *101* (26), 9528-9533.

28. Siuti, N.; Kelleher, N. L., Decoding Protein Modifications Using Top-Down Mass Spectrometry. *Nat. Methods* **2007,** *4* (10), 817-821.

29. Armirotti, A.; Damonte, G., Achievements and Perspectives of Top-Down Proteomics. *Proteomics* **2010,** *10* (20), 3566-3576.

30. Garcia, B. A.; Siuti, N.; Thomas, C. E.; Mizzen, C. A.; Kelleher, N. L., Characterization of Neurohistone Variants and Post-Translational Modifications by Electron Capture Dissociation Mass Spectrometry. *Int. J. Mass spectrom.* **2007,** *259* (1–3), 184-196.

31. Cannon, J.; Lohnes, K.; Wynne, C.; Wang, Y.; Edwards, N.; Fenselau, C., High-Throughput Middle-Down Analysis Using an Orbitrap. *J. Proteome Res.* **2010,** *9* (8), 3886-3890.

32. Garcia, B. A.; Shabanowitz, J.; Hunt, D. F., Characterization of Histones and Their Post-Translational Modifications by Mass Spectrometry. *Curr. Opin. Chem. Biol.* **2007,** *11* (1), 66-73.

33. Lee, M.; Goodbourn, S., Signalling from the Cell Surface to the Nucleus. *Regulation of Gene Expression* **2001,** *37*, 71-85.

34. Ficarro, S. B.; McCleland, M. L.; Stukenberg, P. T.; Burke, D. J.; Ross, M. M.; Shabanowitz, J.; Hunt, D. F.; White, F. M., Phosphoproteome Analysis by Mass Spectrometry and Its Application to Saccharomyces Cerevisiae. *Nat. Biotechnol.* **2002,** *20* (3), 301-305.

35. Manning, G.; Whyte, D. B.; Martinez, R.; Hunter, T.; Sudarsanam, S., The Protein Kinase Complement of the Human Genome. *Science* **2002,** *298* (5600), 1912-1934.

36. Hunter, T., Signaling - 2000 and Beyond. *Cell* **2000,** *100* (1), 113-127.

37. Graves, J. D.; Krebs, E. G., Protein Phosphorylation and Signal Transduction. *Pharmacol. Ther.* **1999,** *82* (2-3), 111-121.

38. Mann, M.; Ong, S. E.; Gronborg, M.; Steen, H.; Jensen, O. N.; Pandey, A., Analysis of Protein Phosphorylation Using Mass Spectrometry: Deciphering the Phosphoproteome. *Trends Biotechnol.* **2002,** *20* (6), 261-268.

39. Olsen, J. V.; Blagoev, B.; Gnad, F.; Macek, B.; Kumar, C.; Mortensen, P.; Mann, M., Global, in vivo, and Site-Specific Phosphorylation Dynamics in Signaling Networks. *Cell* **2006,** *127* (3), 635-648.

40. Johnson, L.; Lewis, R., Structural Basis for Control by Phosphorylation. *Chem. Rev.* **2001,** *101*, 2209-2242.

41. Cohen, P., The Regulation of Protein Function by Multisite Phosphorylation - a 25 Year Update. *Trends Biochem. Sci* **2000,** *25* (12), 596-601.

42. Thingholm, T. E.; Jensen, O. N.; Larsen, M. R., Analytical Strategies for Phosphoproteomics. *Proteomics* **2009,** *9* (6), 1451-1468.

43. Walsh, C. T., *Posttranslational Modification of Proteins: Expending Nature's Inventory*. Roberts and Company Publishers: Englewood, Colorado, USA, 2006.

44. Cohen, P., The Origins of Protein Phosphorylation. *Nat. Cell Biol.* **2002,** *4* (5), E127-E130.

45. Towbin, H.; Staehelin, T.; Gordon, J., Electrophoretic Transfer of Proteins from Polyacrylamide Gels to Nitrocellulose Sheets: Procedure and Some Applications. *Proc. Natl. Acad. Sci. U. S. A.* **1979,** *76* (9), 4350-4354.

46. Zhang, H.; Zha, X.; Tan, Y.; Hornbeck, P. V.; Mastrangelo, A. J.; Alessi, D. R.; Polakiewicz, R. D.; Comb, M. J., Phosphoprotein Analysis Using Antibodies Broadly Reactive against Phosphorylated Motifs. *J. Biol. Chem.* **2002,** *277* (42), 39379-39387.

47. Izaguirre, G.; Aguirre, L.; Ji, P.; Aneskievich, B.; Haimovich, B., Tyrosine Phosphorylation of A-Actinin in Activated Platelets. *J. Biol. Chem.* **1999,** *274* (52), 37012-37020.

48. Zhou, H.; Watts, J. D.; Aebersold, R., A Systematic Approach to the Analysis of Protein Phosphorylation. *Nat. Biotechnol.* **2001,** *19* (4), 375-378.

49. Kalume, D. E.; Molina, H.; Pandey, A., Tackling the Phosphoproteome: Tools and Strategies. *Curr. Opin. Chem. Biol.* **2003,** *7* (1), 64-69.

50. Craig, A. G.; Hoeger, C. A.; Miller, C. L.; Goedken, T.; Rivier, J. E.; Fischer, W. H., Monitoring Protein-Kinase and Phosphatase Reactions with Matrix-Assisted Laser-Desorption Ionization Mass-Spectrometry and Capillary Zone Electrophoresis - Comparison of the Detection Efficiency of Peptide-Phosphopeptide Mixtures. *Biol. Mass Spectrom.* **1994,** *23* (8), 519-528.

51. Liao, P. C.; Leykam, J.; Andrews, P. C.; Gage, D. A.; Allison, J., An Approach to Locate Phosphorylation Sites in a Phosphoprotein - Mass Mapping by Combining Specific Enzymatic Degradation with Matrix-Assisted Laser-Desorption Ionization Mass-Spectrometry. *Anal. Biochem.* **1994,** *219* (1), 9-20.

52. Steen, H.; Jebanathirajah, J. A.; Rush, J.; Morrice, N.; Kirschner, M. W., Phosphorylation Analysis by Mass Spectrometry. *Mol. Cell. Proteomics* **2006,** *5* (1), 172-181.

53. Krause, E.; Wenschuh, H.; Jungblut, P. R., The Dominance of Arginine-Containing Peptides in MALDI-Derived Tryptic Mass Fingerprints of Proteins. *Anal. Chem.* **1999,** *71* (19), 4160-4165.

54. Clipston, N. L.; Jai-nhuknan, J.; Cassady, C. J., A Comparison of Negative and Positive Ion Time-of-Flight Post-Source Decay Mass Spectrometry for Peptides Containing Basic Residues. *Int. J. Mass spectrom.* **2003,** *222* (1), 363-381.

55. Asara, J. M.; Allison, J., Enhanced Detection of Phosphopeptides in Matrix-Assisted Laser Desorption/Ionization Mass Spectrometry Using Ammonium Salts. *J. Am. Soc. Mass Spectrom.* **1999,** *10* (1), 35-44.

56. Kjellstrom, S.; Jensen, O. N., Phosphoric Acid as a Matrix Additive for MALDI MS Analysis of Phosphopeptides and Phosphoproteins. *Anal. Chem.* **2004,** *76* (17), 5109-5117.

57. Paradela, A.; Albar, J. P., Advances in the Analysis of Protein Phosphorylation. *J. Proteome Res.* **2008,** *7* (5), 1809-1818.

58. Reinders, J.; Sickmann, A., State-of-the-Art in Phosphoproteomics. *Proteomics* **2005,** *5* (16), 4052-4061.

59. Pandey, A.; Fernandez, M. M.; Steen, H.; Blagoev, B.; Nielsen, M. M.; Roche, S.; Mann, M.; Lodish, H. F., Identification of a Novel Immunoreceptor Tyrosine-Based Activation Motif-Containing Molecule, Stam2, by Mass Spectrometry and Its Involvement in Growth Factor and Cytokine Receptor Signaling Pathways. *J. Biol. Chem.* **2000,** *275* (49), 38633-38639.

60. Steen, H.; Kuster, B.; Fernandez, M.; Pandey, A.; Mann, M., Tyrosine Phosphorylation Mapping of the Epidermal Growth Factor Receptor Signaling Pathway. *J. Biol. Chem.* **2002,** *277* (2), 1031-1039.

61. Collins, M. O.; Yu, L.; Choudhary, J. S., Analysis of Protein Phosphorylation on a Proteome-Scale. *Proteomics* **2007,** *7* (16), 2751-2768.

62. Gronborg, M.; Kristiansen, T. Z.; Stensballe, A.; Andersen, J. S.; Ohara, O.; Mann, M.; Jensen, O. N.; Pandey, A., A Mass Spectrometry-Based Proteomic Approach for Identification of Serine/Threonine-Phosphorylated Proteins by Enrichment with Phospho-Specific Antibodies - Identification of a Novel Protein, Frigg, as a Protein Kinase a Substrate. *Mol. Cell. Proteomics* **2002,** *1* (7), 517-527.

63. Oda, Y.; Nagasu, T.; Chait, B. T., Enrichment Analysis of Phosphorylated Proteins as a Tool for Probing the Phosphoproteome. *Nat. Biotechnol.* **2001,** *19* (4), 379-382.

64. Zhou, H. L.; Watts, J. D.; Aebersold, R., A Systematic Approach to the Analysis of Protein Phosphorylation. *Nat. Biotechnol.* **2001,** *19* (4), 375-378.

65. McLachlin, D. T.; Chait, B. T., Improved Beta-Elimination-Based Affinity Purification Strategy for Enrichment of Phosphopeptides. *Anal. Chem.* **2003,** *75* (24), 6826-6836.

66. Porath, J.; Carlsson, J. A. N.; Olsson, I.; Belfrage, G., Metal Chelate Affinity Chromatography, a New Approach to Protein Fractionation. *Nature* **1975,** *258* (5536), 598-599.

67. Hochuli, E.; Döbeli, H.; Schacher, A., New Metal Chelate Adsorbent Selective for Proteins and Peptides Containing Neighbouring Histidine Residues. *J. Chromatogr.* **1987,** *411* (0), 177-184.

68. Andersson, L.; Porath, J., Isolation of Phosphoproteins by Immobilized Metal (Fe-3+) Affinity-Chromatography. *Anal. Biochem.* **1986,** *154* (1), 250-254.

69. Han, G. H.; Ye, M. L.; Zou, H. F., Development of Phosphopeptide Enrichment Techniques for Phosphoproteome Analysis. *Analyst* **2008,** *133* (9), 1128-1138.

70. Feng, S.; Pan, C. S.; Jiang, X. G.; Xu, S. Y.; Zhou, H. J.; Ye, M. L.; Zou, H. F., Fe3+ Immobilized Metal Affinity Chromatography with Silica Monolithic Capillary Column for Phosphoproteome Analysis. *Proteomics* **2007,** *7* (3), 351-360.

71. Xu, X. Q.; Deng, C. H.; Gao, M. X.; Yu, W. J.; Yang, P. Y.; Zhang, X. M., Synthesis of Magnetic Microspheres with Immobilized Metal Ions for Enrichment and Direct Determination of Phosphopeptides by Matrix-Assisted Laser Desorption Ionization Mass Spectrometry. *Adv. Mater.* **2006,** *18* (24), 3289-+.

72. Dunn, J. D.; Igrisan, E. A.; Palumbo, A. M.; Reid, G. E.; Bruening, M. L., Phosphopeptide Enrichment Using MALDI Plates Modified with High-Capacity Polymer Brushes. *Anal. Chem.* **2008,** *80* (15), 5727-5735.

73. Ikeguchi, Y.; Nakamura, H., Determination of Organic Phosphates by Column-Switching High Performance Anion-Exchange Chromatography Using on-Line Preconcentration on Titania. *Anal. Sci.* **1997,** *13* (3), 479-483.

74. Ikeguchi, Y.; Nakamura, H., Selective Enrichment of Phospholipids by Titania. *Anal. Sci.* **2000,** *16* (5), 541-543.

75. Kawahara, M.; Nakamura, H.; Nakajima, T., Group Separation of Ribonucleosides and Deoxyribonucleosides on a New Ceramic Titania Column. *Anal. Sci.* **1989,** *5* (6), 763-764.

76. Matsuda, H.; Nakamura, H.; Nakajima, T., New Ceramic Titania - Selective Adsorbent for Organic-Phosphates. *Anal. Sci.* **1990,** *6* (6), 911-912.

77. Kosmulski, M., The Significance of the Difference in the Point of Zero Charge between Rutile and Anatase. *Adv. Colloid Interface Sci.* **2002,** *99* (3), 255-264.

78. Connor, P. A.; McQuillan, A. J., Phosphate Adsorption onto TiO2 from Aqueous Solutions: An in Situ Internal Reflection Infrared Spectroscopic Study. *Langmuir* **1999,** *15* (8), 2916-2921.

79. Larsen, M. R.; Thingholm, T. E.; Jensen, O. N.; Roepstorff, P.; Jorgensen, T. J. D., Highly Selective Enrichment of Phosphorylated Peptides from Peptide Mixtures Using Titanium Dioxide Microcolumns. *Mol. Cell. Proteomics* **2005,** *4* (7), 873-886.

80. Pinkse, M. W. H.; Uitto, P. M.; Hilhorst, M. J.; Ooms, B.; Heck, A. J. R., Selective Isolation at the Femtomole Level of Phosphopeptides from Proteolytic Digests Using 2d-NanoLC-ESI-MS/MS and Titanium Oxide Precolumns. *Anal. Chem.* **2004,** *76* (14), 3935-3943.

81. Jensen, S. S.; Larsen, M. R., Evaluation of the Impact of Some Experimental Procedures on Different Phosphopeptide Enrichment Techniques. *Rapid Commun. Mass Spectrom.* **2007,** *21* (22), 3635-3645.

82. Thingholm, T. E.; Jorgensen, T. J. D.; Jensen, O. N.; Larsen, M. R., Highly Selective Enrichment of Phosphorylated Peptides Using Titanium Dioxide. *Nat. Protoc.* **2006,** *1* (4), 1929-1935.

83. Hata, K.; Morisaka, H.; Hara, K.; Mima, J.; Yumoto, N.; Tatsu, Y.; Furuno, M.; Ishizuka, N.; Ueda, M., Two-Dimensional HPLC on-Line Analysis of Phosphopeptides Using Titania and Monolithic Columns. *Anal. Biochem.* **2006,** *350* (2), 292-297.

84. Li, Y.; Xu, X. Q.; Qi, D. W.; Deng, C. H.; Yang, P. Y.; Zhang, X. M., Novel Fe3O4@TiO2 Core-Shell Microspheres for Selective Enrichment of Phosphopeptides in Phosphoproteome Analysis. *J. Proteome Res.* **2008,** *7* (6), 2526-2538.

85. Pinkse, M. W. H.; Mohammed, S.; Gouw, L. W.; van Breukelen, B.; Vos, H. R.; Heck, A. J. R., Highly Robust, Automated, and Sensitive on Line TiO2-Based Phosphoproteomics Applied to Study Endogenous Phosphorylation in Drosophila Melanogaster. *J. Proteome Res.* **2008,** *7* (2), 687-697.

86. Thingholm, T. E.; Larsen, M. R.; Ingrell, C. R.; Kassem, M.; Jensen, O. N., TiO2-Based Phosphoproteomic Analysis of the Plasma Membrane and the Effects of Phosphatase Inhibitor Treatment. *J. Proteome Res.* **2008,** *7* (8), 3304-3313.

87. Yu, L. R.; Zhu, Z. Y.; Chan, K. C.; Issaq, H. J.; Dimitrov, D. S.; Veenstra, T. D., Improved Titanium Dioxide Enrichment of Phosphopeptides from Hela Cells and High Confident Phosphopeptide Identification by Cross-Validation of MS/MS and MS/MS/MS Spectra. *J. Proteome Res.* **2007,** *6* (11), 4150-4162.

88. Rainer, M.; Sonderegger, H.; Bakry, R.; Huck, C. W.; Morandell, S.; Huber, L. A.; Gjerde, D. T.; Bonn, G. K., Analysis of Protein Phosphorylation by Monolithic Extraction Columns Based on Poly(Divinylbenzene) Containing Embedded Titanium Dioxide and Zirconium Dioxide Nano-Powders. *Proteomics* **2008,** *8* (21), 4593-4602.

89. Cantin, G. T.; Shock, T. R.; Park, S. K.; Madhani, H. D.; Yates, J. R., Optimizing TiO2-Based Phosphopeptide Enrichment for Automated Multidimensional Liquid Chromatography Coupled to Tandem Mass Spectrometry. *Anal. Chem.* **2007,** *79* (12), 4666-4673.

90. Trinidad, J. C.; Specht, C. G.; Thalhammer, A.; Schoepfer, R.; Burlingame, A. L., Comprehensive Identification of Phosphorylation Sites in Postsynaptic Density Preparations. *Mol. Cell. Proteomics* **2006,** *5* (5), 914-922.

91. Sugiyama, N.; Masuda, T.; Shinoda, K.; Nakamura, A.; Tomita, M.; Ishihama, Y., Phosphopeptide Enrichment by Aliphatic Hydroxy Acid-Modified Metal Oxide Chromatography for Nano-LC-MS/MS in Proteomics Applications. *Mol. Cell. Proteomics* **2007,** *6* (6), 1103-1109.

92. Yu, L.-R.; Zhu, Z.; Chan, K. C.; Issaq, H. J.; Dimitrov, D. S.; Veenstra, T. D., Improved Titanium Dioxide Enrichment of Phosphopeptides from Hela Cells and High Confident Phosphopeptide Identification by Cross-Validation of MS/MS and MS/MS/MS Spectra. *J. Proteome Res.* **2007,** *6* (11), 4150-4162.

93. Simon, E. S.; Young, M.; Chan, A.; Bao, Z. Q.; Andrews, P. C., Improved Enrichment Strategies for Phosphorylated Peptides on Titanium Dioxide Using Methyl Esterification and pH Gradient Elution. *Anal. Biochem.* **2008,** *377* (2), 234-242.

94. Tsai, C. F.; Wang, Y. T.; Chen, Y. R.; Lai, C. Y.; Lin, P. Y.; Pan, K. T.; Chen, J. Y.; Khoo, K. H.; Chen, Y. J., Immobilized Metal Affinity Chromatography Revisited: pH/Acid Control toward High Selectivity in Phosphoproteomics. *J. Proteome Res.* **2008,** *7* (9), 4058-4069.

95. Thingholm, T. E.; Jensen, O. N.; Robinson, P. J.; Larsen, M. R., Simac (Sequential Elution from IMAC), a Phosphoproteomics Strategy for the Rapid Separation of Monophosphorylated from Multiply Phosphorylated Peptides. *Mol. Cell. Proteomics* **2008,** *7* (4), 661-671.

96. Bodenmiller, B.; Mueller, L. N.; Mueller, M.; Domon, B.; Aebersold, R., Reproducible Isolation of Distinct, Overlapping Segments of the Phosphoproteome. *Nat. Methods* **2007,** *4* (3), 231-237.

97. Liang, S. S.; Makamba, H.; Huang, S. Y.; Chen, S. H., Nano-Titanium Dioxide Composites for the Enrichment of Phosphopeptides. *J. Chromatogr.* **2006,** *1116* (1-2), 38-45.

98. Villén, J.; Gygi, S. P., The Scx/IMAC Enrichment Approach for Global Phosphorylation Analysis by Mass Spectrometry. *Nat. Protoc.* **2008,** *3* (10), 1630-1638.

99. Villén, J.; Beausoleil, S. A.; Gerber, S. A.; Gygi, S. P., Large-Scale Phosphorylation Analysis of Mouse Liver. *Proc. Natl. Acad. Sci. U. S. A.* **2007,** *104* (5), 1488-1493.

100. Zhai, B.; Villén, J.; Beausoleil, S. A.; Mintseris, J.; Gygi, S. P., Phosphoproteome Analysis of Drosophila Melanogaster Embryos. *J. Proteome Res.* **2008,** *7* (4), 1675-1682.

101. Palumbo, A. M.; Smith, S. A.; Kalcic, C. L.; Dantus, M.; Stemmer, P. M.; Reid, G. E., Tandem Mass Spectrometry Strategies for Phosphoproteome Analysis. *Mass Spectrom. Rev.* **2011,** *30* (4), 600-625.

102. Palumbo, A. M.; Reid, G. E., Evaluation of Gas-Phase Rearrangement and Competing Fragmentation Reactions on Protein Phosphorylation Site Assignment Using Collision Induced Dissociation-MS/MS and MS(3). *Anal. Chem.* **2008,** *80* (24), 9735-9747.

103. Olsen, J. V.; Macek, B.; Lange, O.; Makarov, A.; Horning, S.; Mann, M., Higher-Energy C-Trap Dissociation for Peptide Modification Analysis. *Nat. Methods* **2007,** *4* (9), 709-712.

104. Coon, J. J., Collisions or Electrons? Protein Sequence Analysis in the 21st Century. *Anal. Chem.* **2009,** *81* (9), 3208-3215.

105. Swaney, D. L.; Wenger, C. D.; Thomson, J. A.; Coon, J. J., Human Embryonic Stem Cell Phosphoproteome Revealed by Electron Transfer Dissociation Tandem Mass Spectrometry. *Proc. Natl. Acad. Sci. U. S. A.* **2009,** *106* (4), 995-1000.

106. Good, D. M.; Wirtala, M.; McAlister, G. C.; Coon, J. J., Performance Characteristics of Electron Transfer Dissociation Mass Spectrometry. *Mol. Cell. Proteomics* **2007,** *6* (11), 1942-1951.

107. Nelson, J. M.; Griffin, E. G., Adsorption of Invertase. *J. Am. Chem. Soc.* **1916,** *38* (5), 1109-1115.

108. Ma, J.; Zhang, L.; Liang, Z.; Shan, Y.; Zhang, Y., Immobilized Enzyme Reactors in Proteomics. *TrAC, Trends Anal. Chem.* **2011,** *30* (5), 691-702.

109. Girelli, A. M.; Mattei, E., Application of Immobilized Enzyme Reactor in on-Line High Performance Liquid Chromatography: A Review. *J. Chromatogr. B* **2005,** *819* (1), 3-16.

110. Kim, J.; Kim, B. C.; Lopez-Ferrer, D.; Petritis, K.; Smith, R. D., Nanobiocatalysis for Protein Digestion in Proteomic Analysis. *Proteomics* **2010,** *10* (4), 687-699.

111. Krenkova, J.; Svec, F., Less Common Applications of Monoliths: Iv. Recent Developments in Immobilized Enzyme Reactors for Proteomics and Biotechnology. *J. Sep. Sci.* **2009,** *32* (5-6), 706-718.

112. Cooper, J. W.; Chen, J.; Li, Y.; Lee, C. S., Membrane-Based Nanoscale Proteolytic Reactor Enabling Protein Digestion, Peptide Separation, and Protein Identification Using Mass Spectrometry. *Anal. Chem.* **2003,** *75* (5), 1067-1074.

113. Smuleac, V.; Butterfield, D. A.; Bhattacharyya, D., Layer-by-Layer-Assembled Microfiltration Membranes for Biomolecule Immobilization and Enzymatic Catalysis. *Langmuir* **2006,** *22* (24), 10118-10124.

114. Xu, F.; Wang, W. H.; Tan, Y. J.; Bruening, M. L., Facile Trypsin Immobilization in Polymeric Membranes for Rapid, Efficient Protein Digestion. *Anal. Chem.* **2010,** *82* (24), 10045-10051.

115. Liu, Y.; Zhong, W.; Meng, S.; Kong, J.; Lu, H.; Yang, P.; Girault, H. H.; Liu, B., Assembly-Controlled Biocompatible Interface on a Microchip: Strategy to Highly Efficient Proteolysis. *Chemistry – A European Journal* **2006,** *12* (25), 6585-6591.

116. Bhattacharjee, S.; Dong, J.; Ma, Y.; Hovde, S.; Geiger, J. H.; Baker, G. L.; Bruening, M. L., Formation of High-Capacity Protein-Adsorbing Membranes through Simple Adsorption of Poly(Acrylic Acid)-Containing Films at Low pH. *Langmuir* **2012,** *28* (17), 6885-6892.

117. Liu, G.; Dotzauer, D. M.; Bruening, M. L., Ion-Exchange Membranes Prepared Using Layer-by-Layer Polyelectrolyte Deposition. *J. Membr. Sci.* **2010,** *354* (1–2), 198-205.

118. Sproß, J.; Sinz, A., A Capillary Monolithic Trypsin Reactor for Efficient Protein Digestion in Online and Offline Coupling to ESI and MALDI Mass Spectrometry. *Anal. Chem.* **2010,** *82* (4), 1434-1443.

119. Calleri, E.; Temporini, C.; Furlanetto, S.; Loiodice, F.; Fracchiolla, G.; Massolini, G., Lipases for Biocatalysis: Development of a Chromatographic Bioreactor. *J. Pharm. Biomed. Anal.* **2003,** *32* (4–5), 715-724.

120. Krenkova, J.; Lacher, N. A.; Svec, F., Highly Efficient Enzyme Reactors Containing Trypsin and Endoproteinase Lysc Immobilized on Porous Polymer Monolith Coupled to MS Suitable for Analysis of Antibodies. *Anal. Chem.* **2009,** *81* (5), 2004-2012.

121. Dulay, M. T.; Baca, Q. J.; Zare, R. N., Enhanced Proteolytic Activity of Covalently Bound Enzymes in Photopolymerized Sol Gel. *Anal. Chem.* **2005,** *77* (14), 4604-4610.

122. Brady, D.; Jordaan, J., Advances in Enzyme Immobilisation. *Biotechnol. Lett* **2009,** *31* (11), 1639-1650.

123. Lin, S.; Yao, G.; Qi, D.; Li, Y.; Deng, C.; Yang, P.; Zhang, X., Fast and Efficient Proteolysis by Microwave-Assisted Protein Digestion Using Trypsin-Immobilized Magnetic Silica Microspheres. *Anal. Chem.* **2008,** *80* (10), 3655-3665.

124. Lin, S.; Yun, D.; Qi, D.; Deng, C.; Li, Y.; Zhang, X., Novel Microwave-Assisted Digestion by Trypsin-Immobilized Magnetic Nanoparticles for Proteomic Analysis. *J. Proteome Res.* **2008,** *7* (3), 1297-1307.

125. Xu, F.; Zhen, G.; Yu, F.; Kuennemann, E.; Textor, M.; Knoll, W., Combined Affinity and Catalytic Biosensor: In Situ Enzymatic Activity Monitoring of Surface-Bound Enzymes. *J. Am. Chem. Soc.* **2005,** *127* (38), 13084-13085.

126. Bruening, M. L.; Dotzauer, D. M.; Jain, P.; Ouyang, L.; Baker, G. L., Creation of Functional Membranes Using Polyelectrolyte Multilayers and Polymer Brushes. *Langmuir* **2008,** *24* (15), 7663-7673.

127. Lee, T. D.; Shively, J. E., [19] Enzymatic and Chemical Digestion of Proteins for Mass Spectrometry. In *Methods Enzymol.*, James, A. M., Ed. Academic Press: 1990; Vol. Volume 193, pp 361-374.

128. Qian, K.; Wan, J.; Qiao, L.; Huang, X.; Tang, J.; Wang, Y.; Kong, J.; Yang, P.; Yu, C.; Liu, B., Macroporous Materials as Novel Catalysts for Efficient and Controllable Proteolysis. *Anal. Chem.* **2009,** *81* (14), 5749-5756.

129. Bi, H.; Qiao, L.; Busnel, J.-M.; Liu, B.; Girault, H. H., Kinetics of Proteolytic Reactions in Nanoporous Materials. *J. Proteome Res.* **2009,** *8* (10), 4685-4692.

130. Gan, J.; Zhu, J.; Yan, G.; Liu, Y.; Yang, P.; Liu, B., Periodic Mesoporous Organosilica as a Multifunctional Nanodevice for Large-Scale Characterization of Membrane Proteins. *Anal. Chem.* **2012,** *84* (13), 5809-5815.

131. Nelson, D. L.; Lehninger, A. L.; Cox, M. M., *Lehninger Principles of Biochemistry*. W.H. Freeman: New York, 2008.

132. Hamuro, Y.; Coales, S. J.; Molnar, K. S.; Tuske, S. J.; Morrow, J. A., Specificity of Immobilized Porcine Pepsin in H/D Exchange Compatible Conditions. *Rapid Commun. Mass Spectrom.* **2008,** *22* (7), 1041-1046.

133. Ma, J.; Hou, C.; Sun, L.; Tao, D.; Zhang, Y.; Shan, Y.; Liang, Z.; Zhang, L.; Yang, L.; Zhang, Y., Coupling Formic Acid Assisted Solubilization and Online Immobilized Pepsin Digestion with Strong Cation Exchange and Microflow Reversed-Phase Liquid Chromatography with Electrospray Ionization Tandem Mass Spectrometry for Integral Membrane Proteome Analysis. *Anal. Chem.* **2010,** *82* (23), 9622-9625.

134. Liuni, P.; Rob, T.; Wilson, D. J., A Microfluidic Reactor for Rapid, Low-Pressure Proteolysis with on-Chip Electrospray Ionization. *Rapid Commun. Mass Spectrom.* **2010,** *24* (3), 315-320.

135. Rey, M.; Man, P.; Brandolin, G.; Forest, E.; Pelosi, L., Recombinant Immobilized Rhizopuspepsin as a New Tool for Protein Digestion in Hydrogen/Deuterium Exchange Mass Spectrometry. *Rapid Commun. Mass Spectrom.* **2009,** *23* (21), 3431-3438.

136. Engen, J. R.; Smith, D. L., Peer Reviewed: Investigating Protein Structure and Dynamics by Hydrogen Exchange MS. *Anal. Chem.* **2001,** *73* (9), 256 A-265 A.

137. Engen, J. R., Analysis of Protein Conformation and Dynamics by Hydrogen/Deuterium Exchange MS. *Anal. Chem.* **2009,** *81* (19), 7870-7875.

138. Englander, S. W.; Mayne, L.; Bai, Y.; Sosnick, T. R., Hydrogen Exchange: The Modern Legacy of Linderstrøm-Lang. *Protein Sci.* **1997,** *6* (5), 1101-1109.

139. Konermann, L.; Pan, J.; Liu, Y.-H., Hydrogen Exchange Mass Spectrometry for Studying Protein Structure and Dynamics. *Chem. Soc. Rev.* **2011,** *40* (3), 1224-1234.

140. Katta, V.; Chait, B. T.; Carr, S., Conformational Changes in Proteins Probed by Hydrogen-Exchange Electrospray-Ionization Mass Spectrometry. *Rapid Commun. Mass Spectrom.* **1991,** *5* (4), 214-217.

141. Kaltashov, I. A.; Bobst, C. E.; Abzalimov, R. R., H/D Exchange and Mass Spectrometry in the Studies of Protein Conformation and Dynamics: Is There a Need for a Top-Down Approach? *Anal. Chem.* **2009,** *81* (19), 7892-7899.

142. Pan, J.; Han, J.; Borchers, C. H.; Konermann, L., Hydrogen/Deuterium Exchange Mass Spectrometry with Top-Down Electron Capture Dissociation for Characterizing Structural Transitions of a 17 Kda Protein. *J. Am. Chem. Soc.* **2009,** *131* (35), 12801-12808.

143. Eliezer, D.; Yao, J.; Dyson, H. J.; Wright, P. E., Structural and Dynamic Characterization of Partially Folded States of Apomyoglobin and Implications for Protein Folding. *Nat. Struct. Biol.* **1998,** *18* (2), 148-155.

144. Jørgensen, T. J. D.; Gårdsvoll, H.; Ploug, M.; Roepstorff, P., Intramolecular Migration of Amide Hydrogens in Protonated Peptides Upon Collisional Activation. *J. Am. Chem. Soc.* **2005,** *127* (8), 2785-2793.

145. Morgan, C. R.; Engen, J. R., Investigating Solution-Phase Protein Structure and Dynamics by Hydrogen Exchange Mass Spectrometry. In *Current Protocols in Protein Science*, John Wiley & Sons, Inc.: 2009.

146. Rob, T.; Liuni, P.; Gill, P. K.; Zhu, S.; Balachandran, N.; Berti, P. J.; Wilson, D. J., Measuring Dynamics in Weakly Structured Regions of Proteins Using Microfluidics-Enabled Subsecond H/D Exchange Mass Spectrometry. *Anal. Chem.* **2012,** *84* (8), 3771-3779.

147. Rey, M.; Man, P.; Clémençon, B.; Trézéguet, V.; Brandolin, G.; Forest, E.; Pelosi, L., Conformational Dynamics of the Bovine Mitochondrial Adp/Atp Carrier Isoform 1 Revealed by Hydrogen/Deuterium Exchange Coupled to Mass Spectrometry. *J. Biol. Chem.* **2010,** *285* (45), 34981-34990.

148. Fontana, A.; Polverino de Laureto, P.; Spolaore, B.; Frare, E.; Zambonin, M., Detecting Disordered Regions in Proteins by Limited Proteolysis. In *Instrumental Analysis of Intrinsically Disordered Proteins*, John Wiley & Sons, Inc.: 2010; pp 569-626.

149. Cohen, S. L.; Chait, B. T., Mass Spectrometry as a Tool for Protein Crystallography. *Annu. Rev. Biophys. Biomol. Struct.* **2001,** *30* (1), 67-85.

150. Cohen, S. L.; Chait, B. T.; Ferré-D'Amaré, A. R.; Burley, S. K., Probing the Solution Structure of the DNA-Binding Protein Max by a Combination of Proteolysis and Mass Spectrometry. *Protein Sci.* **1995,** *4* (6), 1088-1099.

151. Gao, X.; Bain, K.; Bonanno, J.; Buchanan, M.; Henderson, D.; Lorimer, D.; Marsh, C.; Reynes, J.; Sauder, J.; Schwinn, K.; Thai, C.; Burley, S., High-Throughput Limited Proteolysis/Mass Spectrometry for Protein Domain Elucidation. *J. Struct. Funct. Genomics.* **2005,** *6* (2), 129-134.

152. Dong, A.; Xu, X.; Edwards, A. M., In Situ Proteolysis for Protein Crystallization and Structure Determination. *Nat. Methods* **2007,** *4* (12), 1019-1021.

153. Yamaguchi, H.; Miyazaki, M.; Maeda, H., Limited Proteolysis in Proteomics Using Protease-Immobilized Microreactors. Functional Genomics. Kaufmann, M.; Klinger, C., Eds. Springer New York: 2012; Vol. 815, pp 187-198.

Chapter 2. Phosphopeptide Enrichment with TiO_2-Modified Membranes

(This chapter was submitted for publication as part of an article in *Analytical Chemistry*)

Selective enrichment of phosphopeptides prior to their analysis by mass spectrometry (MS) is vital for identifying protein phosphorylation sites involved in cellular regulation. This chapter describes modification of porous nylon substrates with TiO_2 nanoparticles to create membranes that rapidly enrich phosphopeptides from small-volume samples. Membranes with a 22-mm diameter bind 540 nmol of phosphoangiotensin and recover 70% of the phosphopeptides in mixtures with a 15-fold excess of unphosphorylated protein digests. Recovery is 90 % for a pure phosphopeptide. Insertion of small membrane disks into HPLC fittings allows enrichment of small-volume (10's of μL) samples. Using 2 % TFA as the loading and washing buffer, the TiO_2-modified membranes selectively bind phosphopeptides in a 100-fold excess of unphosphorylated protein digests.

2.1 Introduction

Phosphorylation of serine, threonine, or tyrosine residues is one of the most important mechanisms for creating protein diversity in eukaryotic cells.[1] Remarkably, about one-third of human proteins are substrates for phosphorylation at some stage in their life cycle,[2] and reversible phosphorylation plays a key role in regulating cell processes such as signal transduction and metabolism.[3-4] Thus, a fundamental understanding of regulatory pathways requires identification of protein phosphorylation states. Currently, the leading technology for evaluating protein phosphorylation is MS,[5] due to its high speed and sensitivity, and the ability

in some cases to determine the location of the phosphorylation site by tandem mass spectrometry (MS/MS) methods.[6] However, although reversible phosphorylation is ubiquitous in cells, phosphorylation is intrinsically a dynamic and transient property,[7] so phosphoproteins are generally present at relatively low abundances and low stoichiometries compared to unphosphorylated proteins.[8] To partially overcome the low abundance, a number of groups developed methods to enrich phosphopeptides from digested protein mixtures.[9-14] Most current phosphoprotein characterization occurs by electrospray ionization (ESI) or matrix assisted laser desorption/ionization (MALDI) MS following an initial phosphoprotein or phosphopeptide enrichment procedure.[15-17]

Phosphopeptide enrichment methods include immunoprecipitation, covalent immobilization, and adsorption to metal oxide resins or immobilized metal-ion complexes.[7, 18-20] All of these methods are useful, and they often provide complementary subsets of phosphopeptides.[21] Studies with adsorption to metal oxides suggest that this technique is particularly attractive for rapid and highly specific enrichment if binding conditions are carefully controlled.[17, 22] At low pH, TiO_2, the metal oxide most commonly used for phosphopeptide enrichment, has a positively charged surface that selectively adsorbs phosphorylated species, and the adsorbed species subsequently elute under basic conditions.[23] Addition of excluders and low-pH buffer to the phosphopeptide solution helps to alleviate nonspecific binding of acidic peptides to TiO_2.[24-25]

This chapter describes the functionalization of porous nylon substrates with a thin layer of TiO_2 nanoparticles to create membranes for phosphopeptide enrichment.[26] Adsorption of phosphopeptides from solutions passing through the membrane (Figure 2.1) followed by rinsing and elution yields concentrated solutions of isolated phosphopeptides. The sub-micron pore size

in the nylon allows phosphopeptide adsorption without mass transfer limitations, and the high surface areas of both the nylon substrate and the nanoparticles give materials with a high phosphopeptide binding capacity.[25] Moreover, because of the minimal membrane thickness and relatively large pore size, a syringe is sufficient to push solutions through the membrane (Figure 2.1).

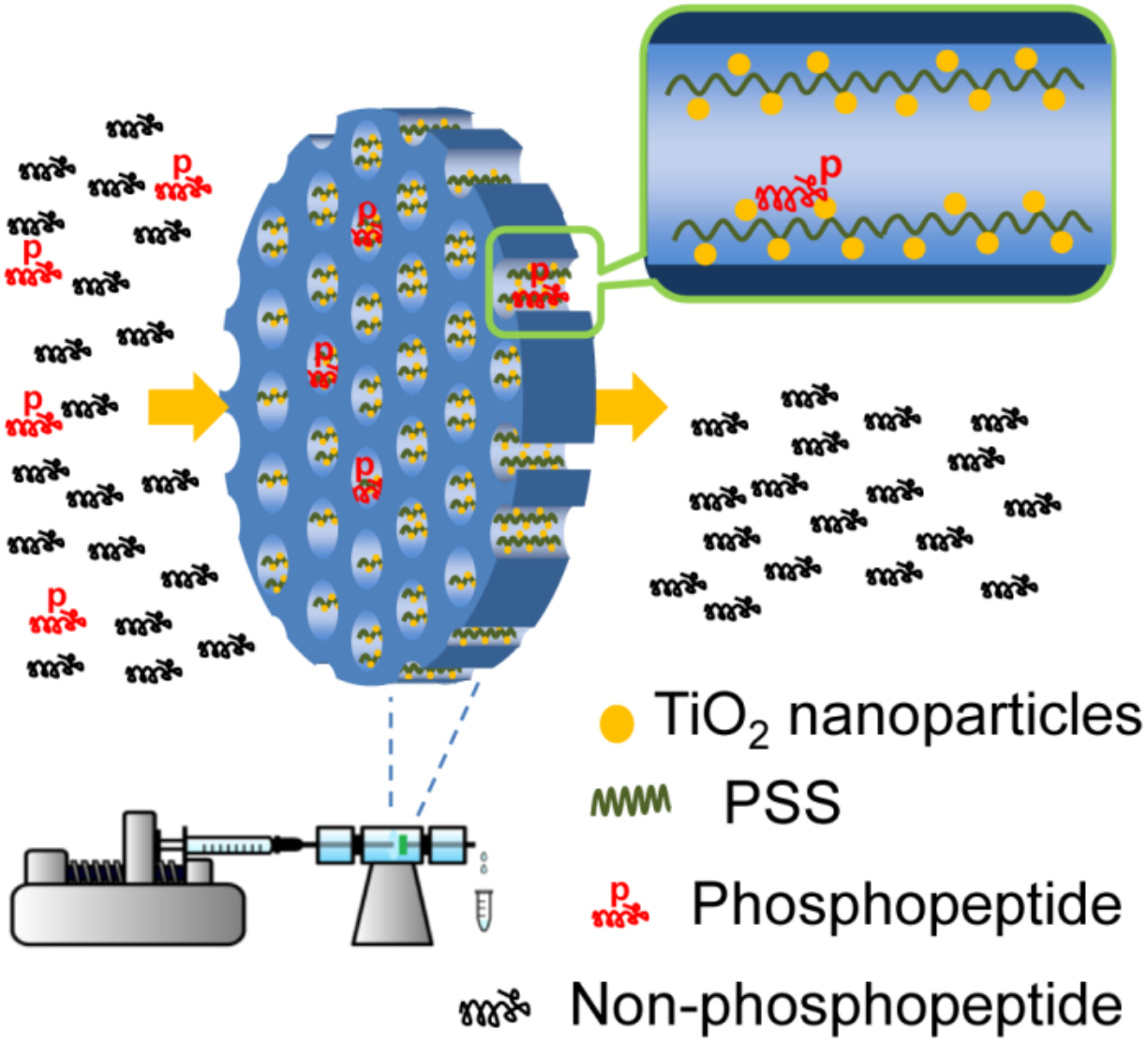

Figure 2.1. Cartoon of a membrane containing TiO_2 for phosphopeptide enrichment and a miniaturized membrane holder with a syringe pump. PSS=poly(styrene sulfonate).

2.2 Experimental

2.2.1 Materials and solutions

Titanium isopropoxide, poly(sodium 4-styrene-sulfonate) (PSS), bovine β-casein, bovine α-casein, chicken egg ovalbumin, and bovine serum albumin (BSA) were purchased from Sigma-Aldrich. BSA was digested using sequencing grade modified porcine trypsin treated with L-1-tosylamide-2-phenylethyl chloromethyl ketone (Sigma-Aldrich), whereas other proteins were digested using sequencing grade modified trypsin from Promega. Other reagents employed in the digestion include Tris-HCl (Invitrogen), urea (J.T.Baker), 1,4-dithio-DL-threitol (BioChemika), iodoacetamide (Sigma), and ammonium bicarbonate (Columbus Chemical). 2,5-dihydroxybenzoic acid (DHB) was purchased from Sigma. Human angiotensin II (DRVYIHPF) and phosphorylated angiotensin II (DRVpYIHPF) were acquired from Calbiochem. CH_3CH_2CO-LFTGHPEpSLEK (H_5 peptide) and CD_3CD_2CO- LFTGHPEpSLEK (D_5 peptide) were synthesized by Dr. Amanda Palumbo from Prof. Gavin E. Reid's group using manual stepwise Fmoc-based solid-phase peptide synthesis as described previously.[27]

Enrichment employed loading buffers containing 0.1 vol % trifluoroacetic acid (TFA), 49.9 vol % deionized water and 50 vol % acetonitrile (loading buffer I) or 2 vol % TFA, 48 vol % deionized water and 50 vol % acetonitrile (loading buffer II). Washing buffer I and II had the same compositions as loading buffers I and II, respectively. The elution buffer contained 1 vol % ammonium hydroxide (NH_4OH), 49 vol % deionized water and 50 vol % acetonitrile, and had a pH of 10.9.

2.2.2 Membranes and holders

Membrane modification and binding capacity studies employed an Amicon cell (model 8010, Millipore) that exposed a membrane area of 3.8 cm^2. A peristaltic pump pulled solutions through the membrane. The unmodified nylon membranes (25 mm-diameter, nominal pore size of 0.45 μm) were obtained from Millipore (HNWP02500). For experiments with small sample volumes (<1 mL), a 6 mm-diameter piece of membrane was placed in a flangeless fitting system (A-424, Upchurch Scientific) connected to 1/16 inch OD tubing via ferrules. The membrane was supported by a frit in the holder. The membrane area exposed to sample (0.02 cm^2) was determined by passing a dye solution through the apparatus and measuring the diameter of the colored membrane area with calipers. Sample injection occurred via a syringe pump using a 1-mL or 100-μL syringe (Figure 2.1).

2.2.3 Synthesis of titania nanoparticles

TiO_2 nanoparticles were prepared by the controlled hydrolysis of titanium isopropoxide.[28] $Ti(OCH(CH_3)_2)_4$ (1.25 mL) was dissolved in 25 mL of absolute ethanol, and this solution was added dropwise under vigorous stirring to 250 mL of water previously adjusted to pH 1.5 with nitric acid. The resulting transparent colloidal suspension was stirred overnight, and then stored in a refrigerator prior to use.

2.2.4 Membrane modification

Modification of UV/ozone-cleaned (10 min) nylon membranes with titania nanoparticles occurred through consecutive adsorption of PSS and titania. Ten mL of a 0.02 M PSS, 0.5 M

NaCl solution was first passed through the membrane at 2 mL/min, followed by 30 mL of deionized water at the same flow rate. Subsequently, a 10 mL aliquot of the titania suspension was circulated through the membrane at 1 mL/min for 30 minutes. Prior to passing through the membrane, the titania suspension was centrifuged for 5 min at 1300 g to remove large particles. After TiO_2 deposition, the membrane was rinsed with 30 mL of deionized water at 2 mL/min. A second PSS/TiO_2 bilayer was deposited similarly. The amount of TiO_2 in the membrane was determined by inductively coupled plasma-optical emission spectroscopy (ICP-OES) analysis of TiO_2-nanoparticle suspensions before and after passing them through the membrane. A calibration curve was prepared using a 2 % nitric acid solution containing Ti concentrations from 0.5 to 6 ppm. (Standards were prepared from 998 ppm Ti calibration solution from Sigma) The suspensions were diluted by a factor of 200 in 2% nitric acid prior to analysis.

2.2.5 Breakthrough curves and determination of binding capacity

In the breakthrough experiments, 50 mL of 20 μM phosphoangiotensin in loading buffer I was passed through a nylon membrane modified with a $(PSS/TiO_2)_2$ film, and the effluent was collected in 2.5-mL aliquots. The flow rate was 2 mL/min. Phosphoangiotensin concentrations in each aliquot were determined by MALDI-MS using angiotensin as an internal standard. The amount of bound phosphoangiotensin was determined from the difference in feed and effluent concentrations in each aliquot.

2.2.6 Determination of phosphopeptide recovery using labeled peptides

Ten pmol of H_5 peptide (CH_3CH_2CO-LFTGHPEpSLEK) and 150 pmol of BSA digest were dissolved in 100 μL of loading buffer I and passed through the small (0.02 cm^2) membrane at 10 μL/min. The membrane was washed with 500 μL of washing buffer I at 50 μL/min, and peptides were eluted with 30 μL of elution buffer at 3 μL/min. One μL of eluate (333 fmol of H_5 peptide assuming 100% recovery) and 1 μL of internal standard (500 fmol of D_5 peptide/μL) were spotted on a MALDI plate followed by 1 μL of matrix solution (40 mg/mL of 2,5 DHB in 1% TFA, 49% H_2O, 50% ACN). The ratio of MALDI-MS signals from the H_5 and D_5 peptides was compared to a calibration curve to determine the concentration of the H_5 peptide in the eluate.

2.2.7 Protein digestion

Bovine α-casein, β-casein and chicken ovalbumin (100 μg each) were first dissolved separately in 20 μL of 6 M urea, 50 mM Tris-HCl. Five μL of 10 mM DTT was added to each protein solution, and the solutions were heated for 1 hour at 56 ºC to break disulfide bonds. After cooling, 160 μL of 50 mM NH_4HCO_3 and 10 μL of 100 mM iodoacetamide were added to the solution, which was then allowed to stand for 1 hour in the dark. Finally 10 μL of 0.5 μg/μL modified trypsin was added to each sample, and the solution was incubated for 16 hours at 37 ºC. The digestion was quenched by addition of 11 μL of acetic acid to lower the pH to about 3. For the unphosphorylated protein BSA, the digestion followed a similar procedure except the trypsin employed was sequencing grade modified porcine trypsin from Sigma instead of sequencing grade trypsin because of the large amount of trypsin required to digest 1 mg of BSA.

2.2.8 Phophopeptide enrichment from protein digests

For analysis of phosphopeptides in a large excess of non-phosphorylated peptide, 15 pmol of α-casein, β-casein, and ovalbumin digests and 1500 pmol of BSA digest were dissolved in 500 μL loading buffer II. This solution was passed through the small-scale TiO_2-modified nylon membrane at 50 μL/min, and the membrane was washed with 3 mL of washing buffer II at 100 μL/min. Finally the phosphopeptides were eluted from the membrane with 10 μL of elution buffer at 2 μL/min .

2.2.9 Mass spectrometry and data analysis

An LTQ XL ion trap mass spectrometer equipped with a vMALDI source (Thermo Fisher Scientific, San Jose, CA) was used to perform MALDI-MS and CID-MS/MS analyses. Typically, 1 μL of sample solution was spotted onto the stainless steel MALDI plate, followed by addition of 1 μL of matrix solution (40 mg/mL of 2.5 DHB in 1% TFA, 49% H_2O, 50% ACN) and drying. MALDI-MS spectra were acquired using a laser power of 10 μJ across the m/z range 300-2000 (normal mass range) or 800-4000 (high mass range). CID-MS/MS was performed on mass-selected precursor ions, using default activation parameters (q=0.25, activation time 30 msec), with an isolation width of 5 Da, and normalized collision energies from 30-40. Spectra were the average of 60-150 scans. Assignment of peptides resulting from protein digestion was performed manually by mass fingerprinting or by MS/MS. Phosphorylation sites were manually assigned by matching MS/MS product ions with *in silico* peptide fragments generated using ProteinProspector (http://prospector.ucsf.edu).

2.3 Results and discussion

2.3.1 Characterization of TiO_2-modified nylon membranes

Nanoparticles are attractive adsorbents for phosphopeptides because of their high surface area to volume ratio.[29-31] TEM images show that the TiO_2 particles in this study have an average diameter of 5 nm (Figure 2.2), but the particles aggregate into clusters with a diameter of 50 nm. Alternating adsorption of PSS and nanoparticles immobilizes the TiO_2 in the membrane, [26, 31-32] but SEM images of membrane cross-sections do not show the TiO_2 nanoparticles (Figure 2.3c), perhaps because of the rough texture of the nylon membrane and the small and polydisperse nanoparticle size. However, the Ti energy-dispersive X-ray spectroscopy (EDX) map in Figure 2.3d reveals the presence of Ti over the whole cross-section of a modified membrane. Notably, the layer-by-layer method allows modification of nylon membranes with a PSS/TiO_2 film in just 30 min. Moreover, stacking of membranes in the Amicon cell permits simultaneous modification of several membranes, and a single 25-mm membrane provides 8 membranes for small-scale analysis.

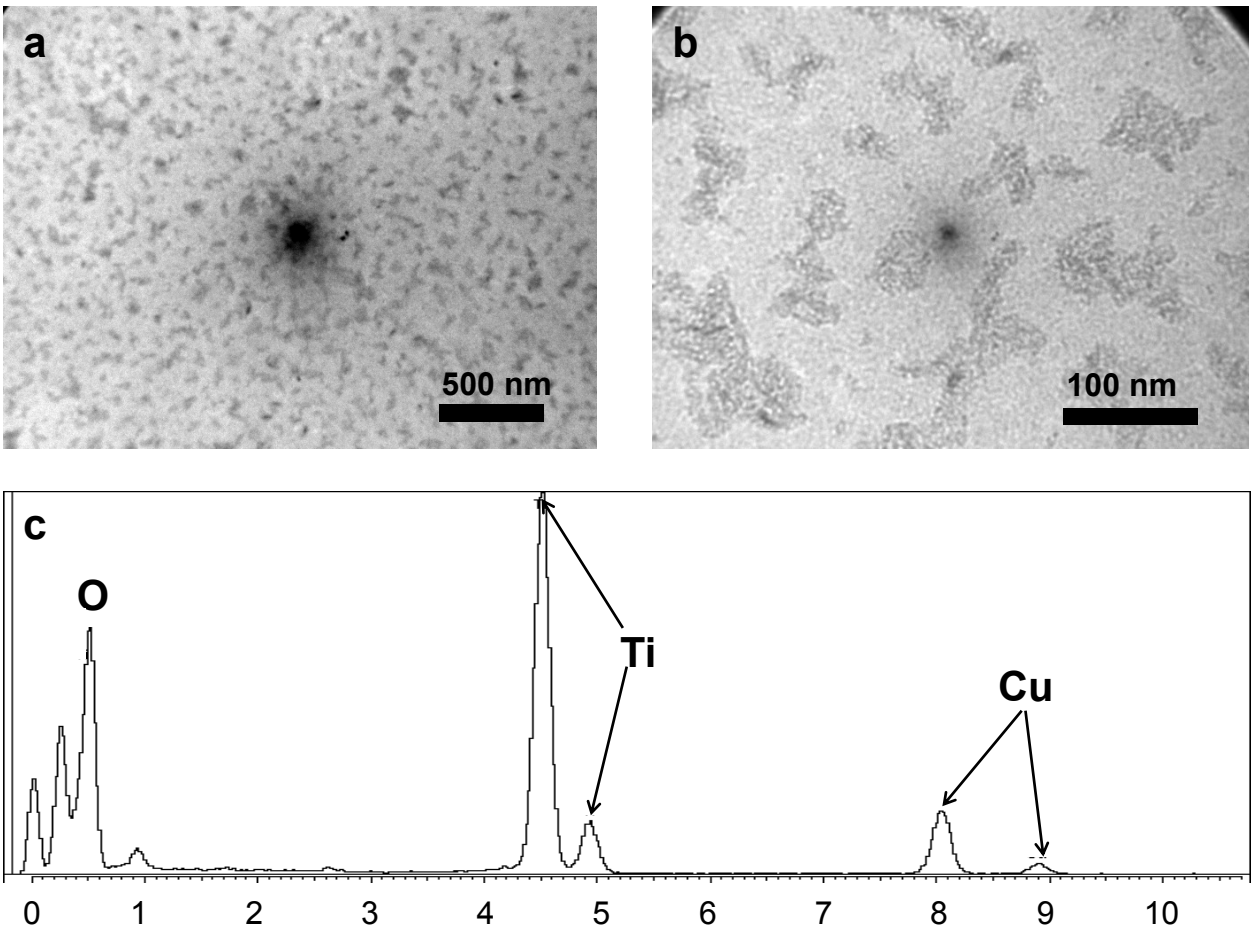

Figure 2.2. (a,b) TEM images showing the size distribution of TiO_2 nanoparticles at two different magnifications. (c) EDX analysis of the nanoparticles. The Cu signal arises from the supporting grid.

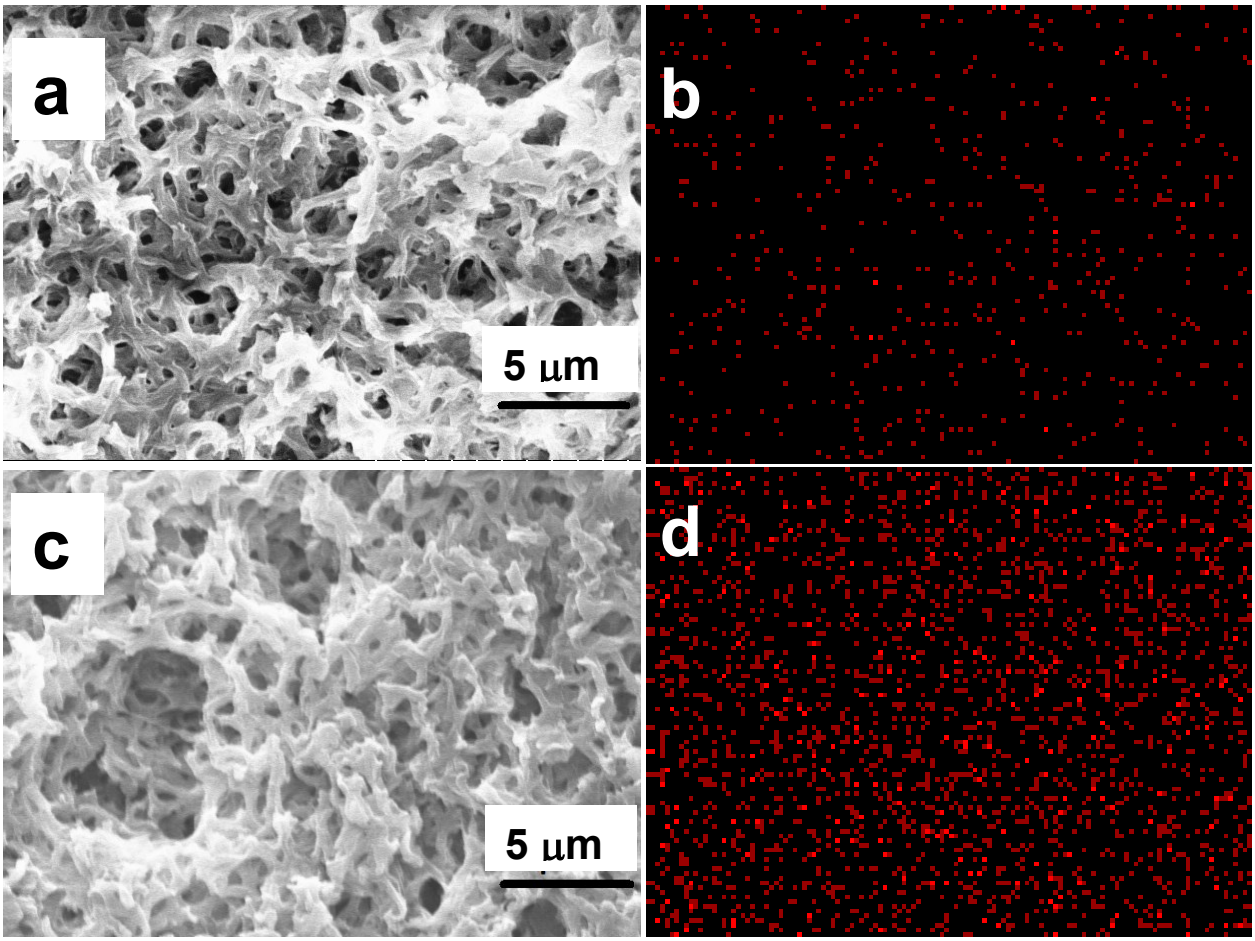

Figure 2.3. Cross-sectional SEM images of nylon membranes before (a) and after (c) coating with a PSS/TiO_2 nanoparticle film. Images b and d show the EDX Ti maps for the images in (a) and (c), respectively. In (b) and (d) Ti signals are proportional to the intensity of the red color, and image b indicates the noise of the measurement.

Nitrogen adsorption isotherms show that a porous nylon membrane (diameter of 25 mm and thickness of 170 μm) has a surface area of 3300 cm^2, which should facilitate the adsorption of large amounts of TiO_2 nanoparticles. Analysis of TiO_2 nanoparticle-containing solutions before and after passing them through the membrane shows that 30 μmol of TiO_2 adsorb to each

membrane (exposed membrane diameter of 22 mm) during deposition of a PSS/TiO_2 bilayer (Figure 2.4). Adsorption of a second PSS/TiO_2 bilayer approximately doubles the amount of TiO_2 (55 μmol) in the membrane, which should enhance phosphopeptide binding. For 50 nm particles, 55 μmol corresponds to 7 x 10^8 particles per cm^2 of internal membrane area, assuming a TiO_2 density of 4.2 g/cm^3.

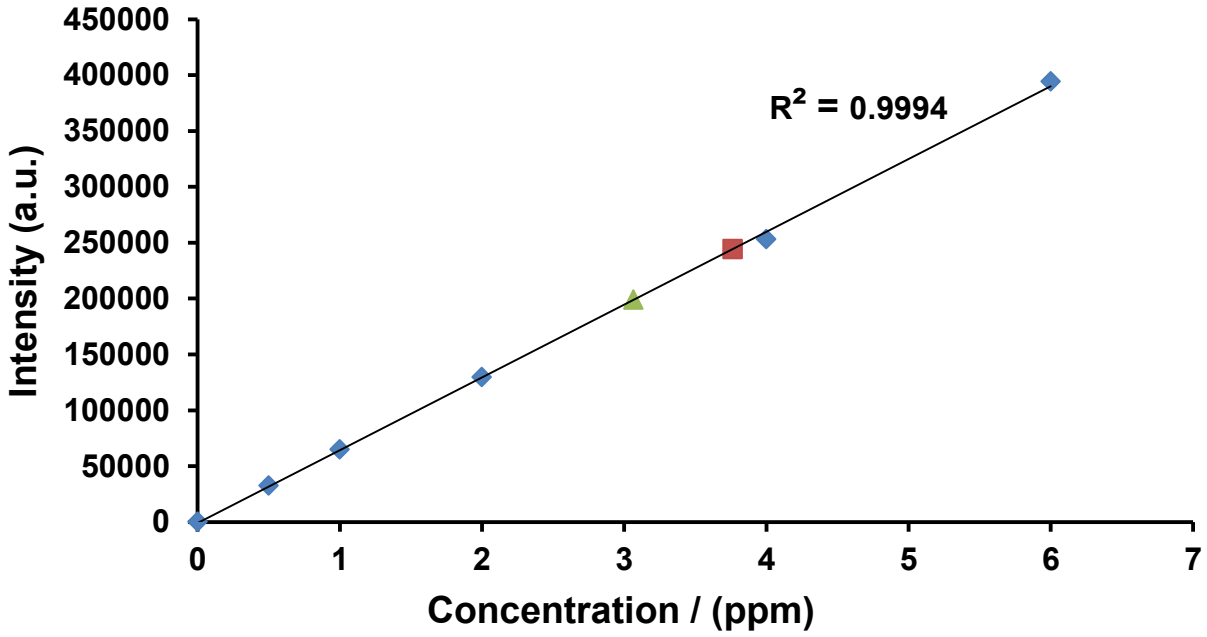

Figure 2.4. Calibration curve for the ICP-OES analysis of Ti. The square and triangle show the absorbance of the diluted Ti loading solution before and after passing through the nylon membrane.

2.3.2 Phosphopeptide binding capacity

Binding capacity is important in selectively capturing phosphopeptides because insufficient capacity may cause low sensitivity or selective detection of only strongly binding

phosphopeptides, whereas excess capacity may result in nonspecific binding. We employed classical breakthrough experiments to determine the amount of phosphopeptide, in this case phosphoangiotensin, that a $(PSS/TiO_2)_2$-modified membrane can capture. As Figure 2.5 shows, initially the membrane captures all the phosphopeptide in the loading solution, but as the membrane becomes saturated, phosphopeptides break through and eventually no phosphopeptides bind. Integrating the difference between the feed and permeate phosphopeptide concentrations in Figure 2.5 yields a binding capacity of 540 nmol of phosphoangiotensin/membrane (22 mm-diameter). Based on the 55 μmol of TiO_2 in the membrane, the binding capacity is 126 μmol phosphopeptides/gram of TiO_2. This result agrees reasonably well with a previous study that reported a binding capacity of 520 μmol phenyl phosphate/gram of 40 nm TiO_2.[30] Phenyl phosphate is much smaller than phosphoangiotensin and may give higher biding capacities

In most analytical applications, membrane loading is much less than saturation to avoid the loss of desired analytes in the permeate. Defining dynamic capacity as the amount of binding that occurs before the permeate concentration is 10 % of that in the feed; the dynamic phosphoangiotensin-binding capacity is 365 nmol phosphopeptides per membrane. Moreover, the dynamic capacity is the same at flow rates of 2 and 4 mL/min, suggesting kinetics and diffusion do not limit binding prior to approaching saturation

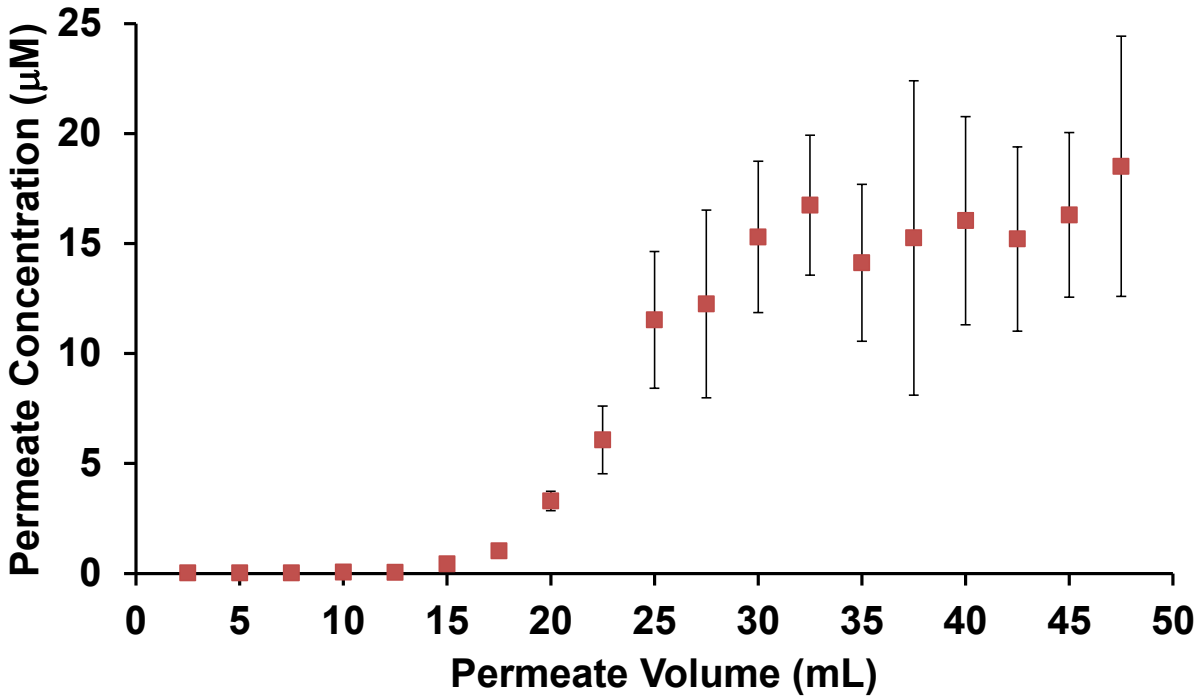

Figure 2.5. Breakthrough curve for the passage of 20 μM phosphoangiotensin (in loading buffer I, 0.1% TFA) through a 22 mm-diameter nylon membrane modified with a $(PSS/TiO_2)_2$ film. The flow rate through the membrane was 2 mL/min. Angiotensin served as an internal standard, and the large error bars (standard deviation of 40%), result from the uncertainty inherent in quantitative analysis based on MALDI-MS.

2.3.3 Phosphopeptide elution

In experiments that examined phosphopeptide elution and membrane reusability, 5 mL of 4 μM phosphoangiotensin in loading buffer I was passed through the membrane (2 mL/min) followed by 5 mL of washing buffer I and 5 mL of elution buffer at the same flow rate. Finally the membrane was reconditioned with 10 mL loading buffer I, and the same experiment was repeated nine times. The concentrations of phosphoangiotensin in the loading, rinsing and eluate

solutions were determined with MALDI-MS using angiotensin as an internal standard. (A calibration curve accounted for small differences in the ionization efficiencies of angiotensin and phosphoangiotensin). Comparison of the amount of phosphoangiotensin removed from the loading solution with the amount of phosphoangiotensin in the eluate gave an efficiency of phosphoangiotensin elution between 80 and 100%. Unfortunately, the limited accuracy of the MALDI-MS analyses does not allow us to know whether there is a small (10 to 20 %) phosphopeptide loss during elution. To examine the stability of membrane performance, we determined the elution efficiency over 10 experiments with the same membrane. Figure 2.6 shows that the fraction of phosphoangiotensin recovered in the eluate is stable at ~90%, which suggests that there is no significant loss of TiO_2 or buildup of phosphoangiotensin in the membrane during the experiment.

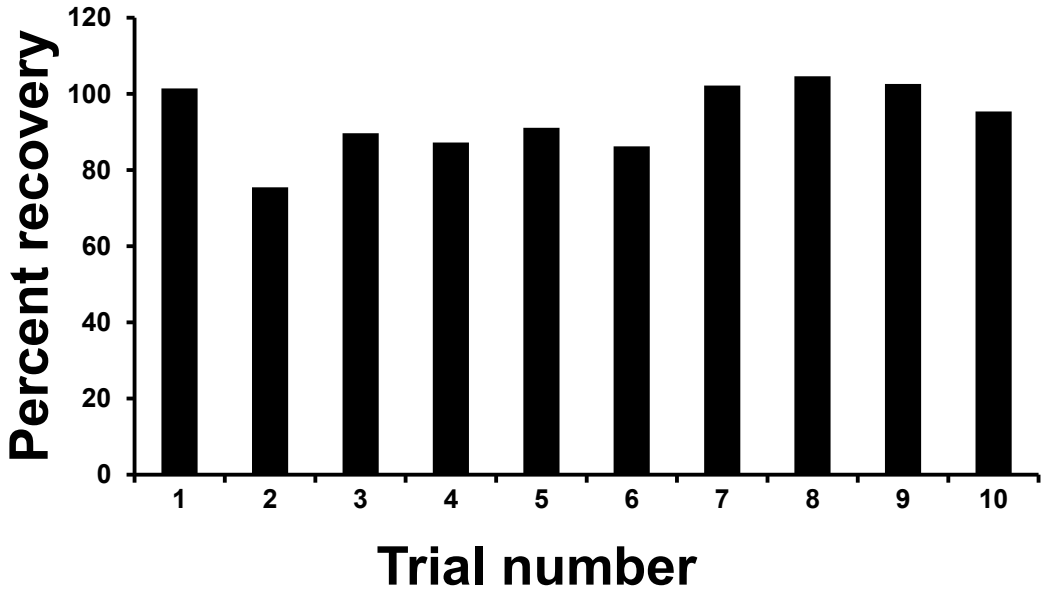

Figure 2.6. Fraction of the phosphoangiotensin recovered from a loading solution after binding and elution from a nylon membrane modified with a $(PSS/TiO_2)_2$ film. The same membrane was employed repeatedly.

2.3.4 Phosphopeptide recovery

Although phosphoangiotensin recovery from single-peptide solutions (amount in eluate/amount in loading solution) is around 90 %, recoveries from mixtures of digested proteins may be much less because nonspecific binding may block adsorption sites. To quantitatively examine recoveries in a more complex mixture, we employed H_5 (CH_3CH_2CO-LFTGHPEpSLEK) and D_5 (CD_3CD_2CO-LFTGHPEpSLEK) peptides, where the D_5 peptide spotted on the MALDI plate with the sample served as an internal standard (see Figure 2.7 for the calibration curve). We added 10 pmol of the target H_5 peptide (CH_3CH_2CO-LFTGHPEpSLEK) to a 150 pmol BSA digest in 100 μL of loading buffer I, passed this mixture through a nylon membrane modified with $(PSS/TiO_2)_2$ (Figure 2.8 shows mass spectra of the solution before and after passing through the membrane), rinsed the membrane to remove non-specifically bound peptides, and eluted the phosphopeptides with 30 μL of elution buffer. Comparison of the H_5/D_5 peptide signal intensity ratios for reference and eluate solutions (Figure 2.9) indicates an overall H_5 peptide recovery >70% in the eluate. The high recovery occurs despite a 15-fold excess of BSA.

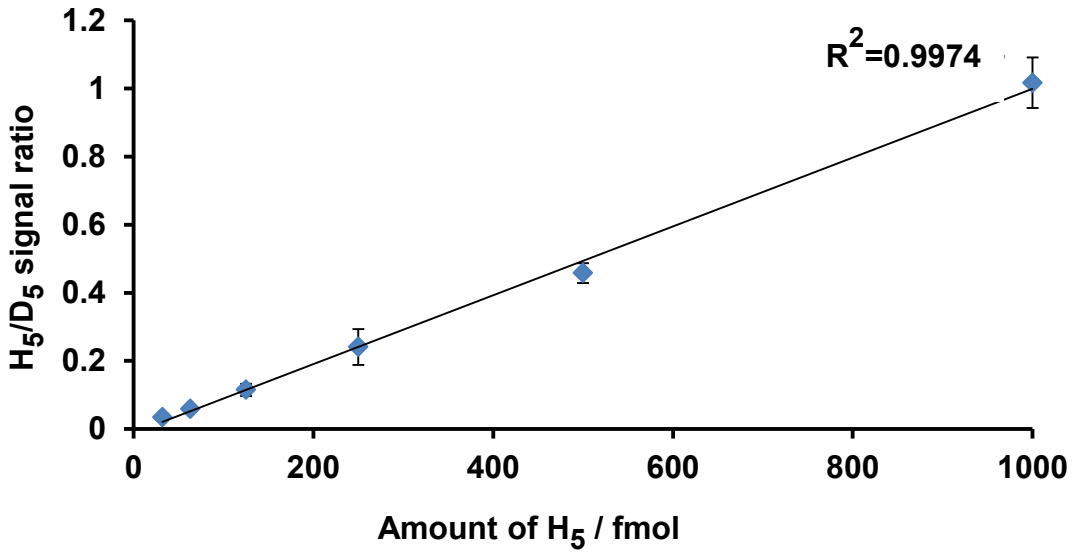

Figure 2.7. Calibration curve showing the ratio of H_5 to D_5 peptide signals from MALDI-MS analysis. The amount of D_5 peptide spotted in all analyses was 1000 fmol, and the amount of H_5 peptide varied.

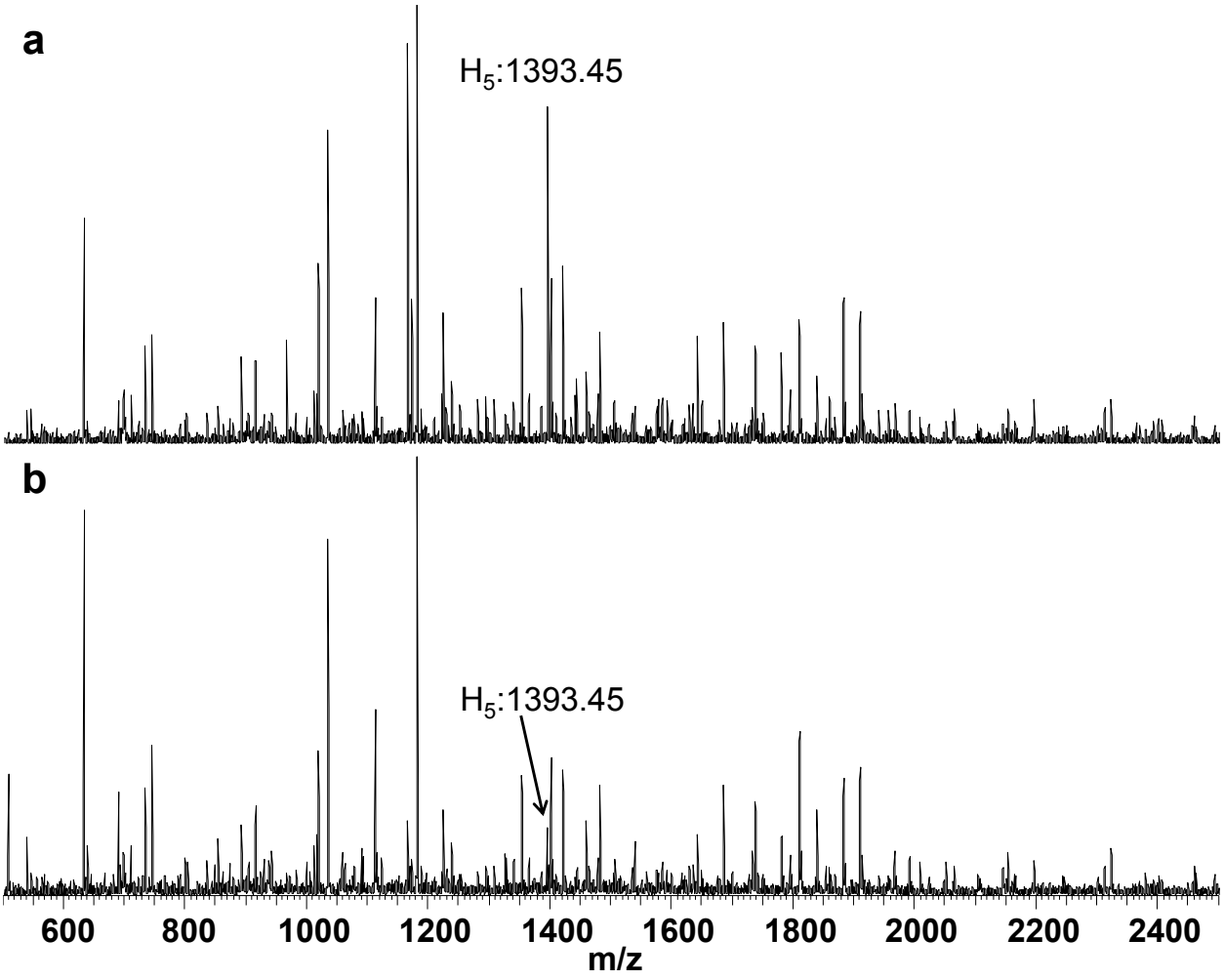

Figure 2.8. MALDI mass spectra of 1 μL of a solution containing 100 fmol H_5 peptide and 1.5 pmol digested BSA (a) before and (b) after passing through a small membrane (0.02 cm^2) modified with $(PSS/TiO_2)_2$.

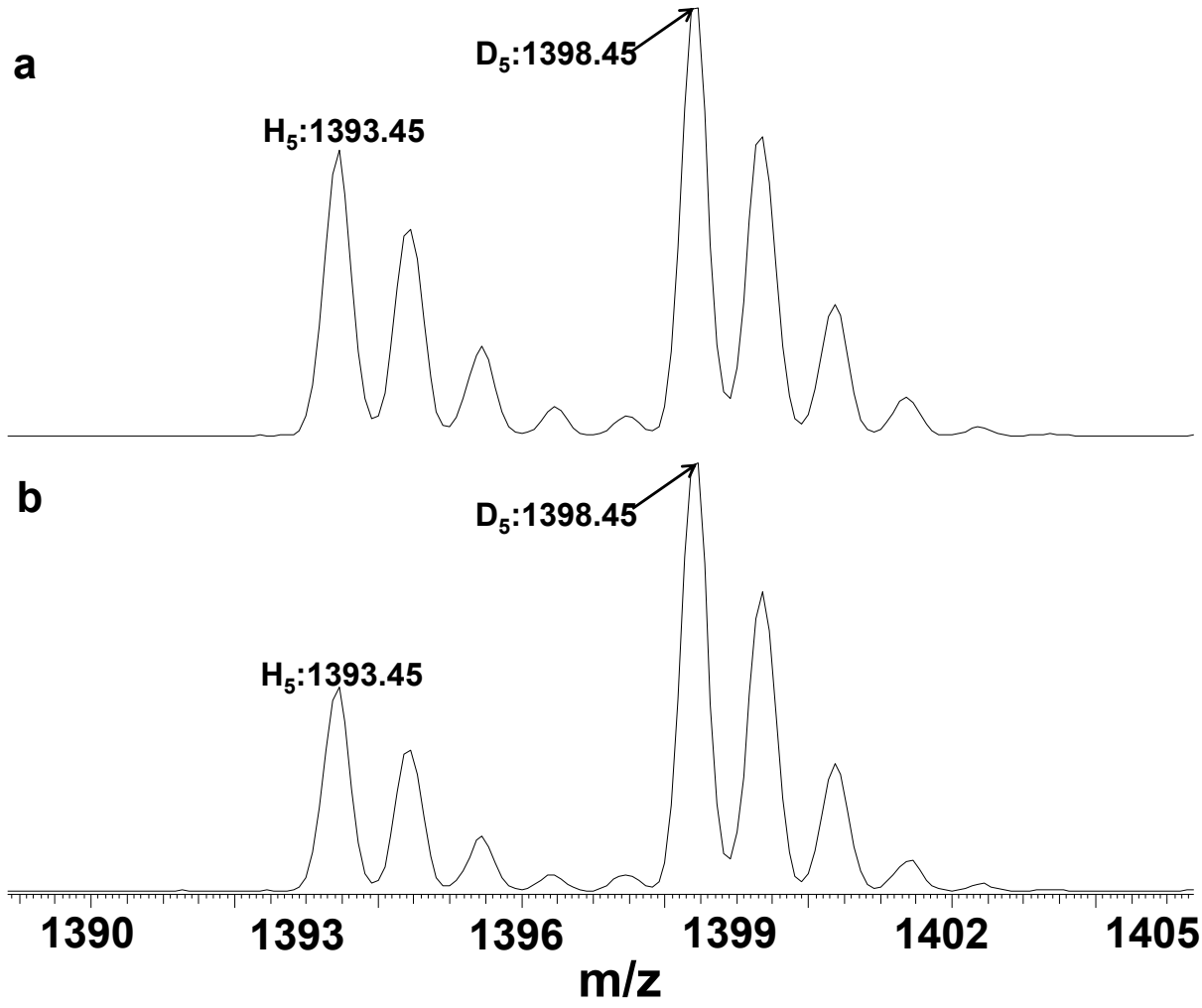

Figure 2.9. MALDI mass spectra of (a) 500 fmol of D_5 peptide internal standard with 333 fmol of H_5 peptide, and (b) 500 fmol of D_5 internal standard plus 1 μL of the eluate from enrichment of 10 pmol H_5 peptide into 30 μL of elution buffer. For spectrum (b), 100% recovery would correspond to spotting of 333 fmol, which should yield a spectrum similar to (a).

2.3.5 Phosphopeptide enrichment from a mixture of α-casein, β-casein, and ovalbumin digests

In a test of enrichment from digests on only phosphoproteins, fifteen pmol of three digested phosphoproteins were combined in 100 μL of loading buffer I. The conventional MALDI mass spectrum of 1 μL (150 fmol of each protein) of this solution has weak phosphopeptide signals compared to signals of non-phosphorylated peptides (Figure 2.10a). Passage of the same solution through a TiO_2-modified membrane both isolates and concentrates phosphopeptides because binding occurs from 100 μL of solution and elution requires only 10 μL of eluent. The mass spectrum of the enriched sample (Figure 2.10b) contains 15 signals due to phosphopeptides and in the few cases where the phosphopeptide signals are also present in the loading-solution MALDI mass spectrum, signal intensities are an order of magnitude stronger after enrichment. (The large number of peptides results from some missed and nonspecific cleavages and variable alkylation.) Moreover, the spectrum of the enriched sample has only a few weak signals (S/N <8) that stem from non-phosphorylated peptides.

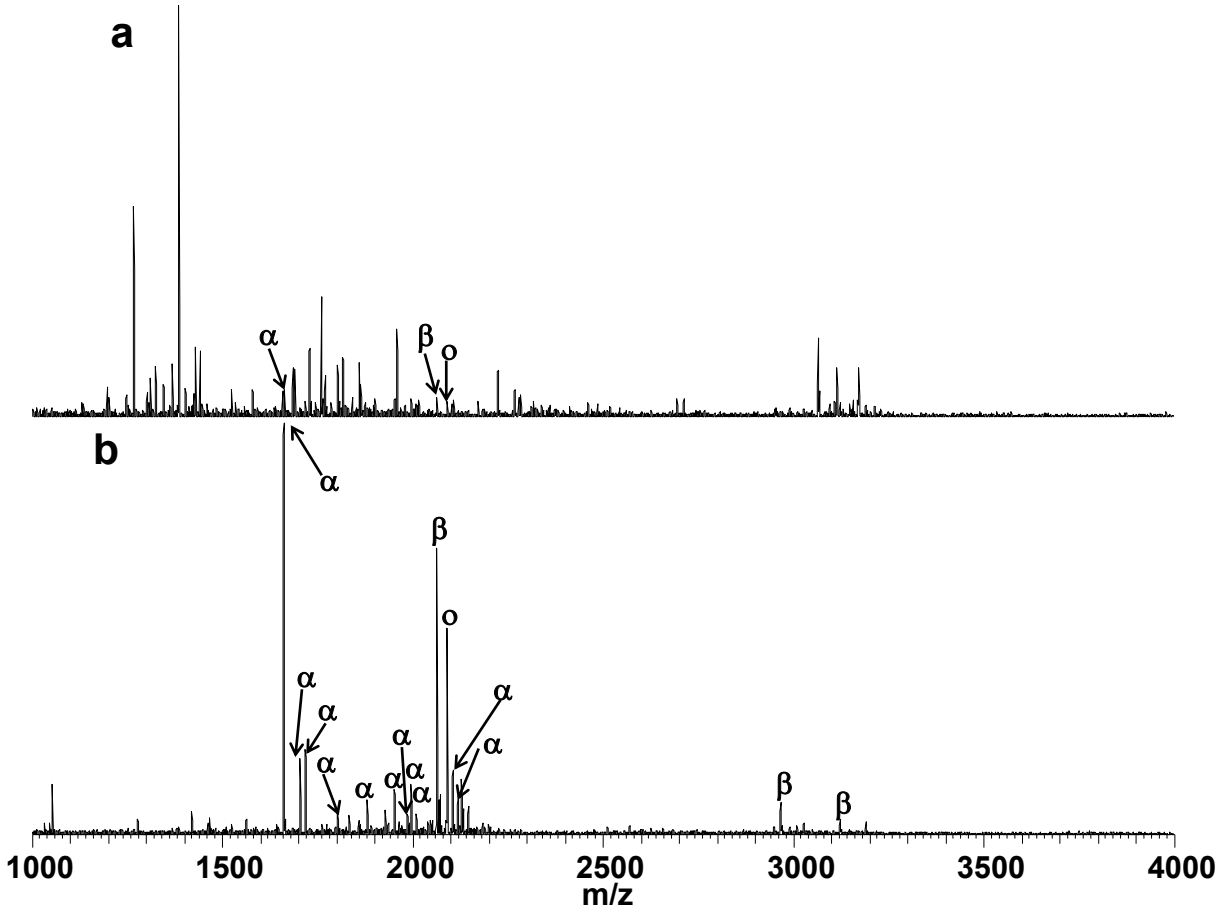

Figure 2.10. (a) MALDI mass spectrum of 1 μL of loading buffer I containing 150 fmol (each) of digested α-casein, β-casein and ovalbumin. This solution also contained 13 mM urea. (b) Mass spectrum of the peptides collected from 100 μL of the above solution by adsorption on a nylon membrane modified with $(PSS/TiO_2)_2$, rinsing of the membrane with 100 μL washing buffer I, and elution of the peptides with 10 μL of elution buffer. One μL of the eluate was spotted on the MALDI plate prior to addition of matrix.

2.3.6 Phosphopeptide enrichment from α-casein, β-casein, and ovalbumin digests in a 100-fold excess of digested BSA

To mimic a modestly complex biological sample, we examined enrichment from 500 μL of loading buffer I containing 15 pmol (each) of digested α-casein, β-casein, and ovalbumin along with 1500 pmol of digested BSA. In this case, to reduce non-specific binding we employed 2 % TFA in 1:1 water:ACN as the loading buffer.[33] The MALDI mass spectrum of the loading solution (1 μL of solution, 30 fmol of each phosphopeptide and 3 pmol of digested BSA) reveals only one small phosphopeptide signal, along with many signals from BSA peptides (Figure 2.11a). In contrast the mass spectrum of the enriched sample (Figure 2.11b) contains signals from 19 phosphopeptides and no non-phosphorylated peptide signals with S/N >3. The S/N for the phosphopeptides ranges from 3 to 50. Increases in the phosphopeptide S/N stem from a 50-fold pre-concentration (assuming full recovery) and a decrease in ion suppression. The S/N of the enriched sample is about half of that for enriched digests that do not contain BSA (Figure 2.10), presumably because the higher TFA concentration decreases the efficiency of phosphopeptide binding to the TiO_2. (Table 2.1 contains m/z values, S/N, and sequences for the peptides identified from Figure 2.11.)

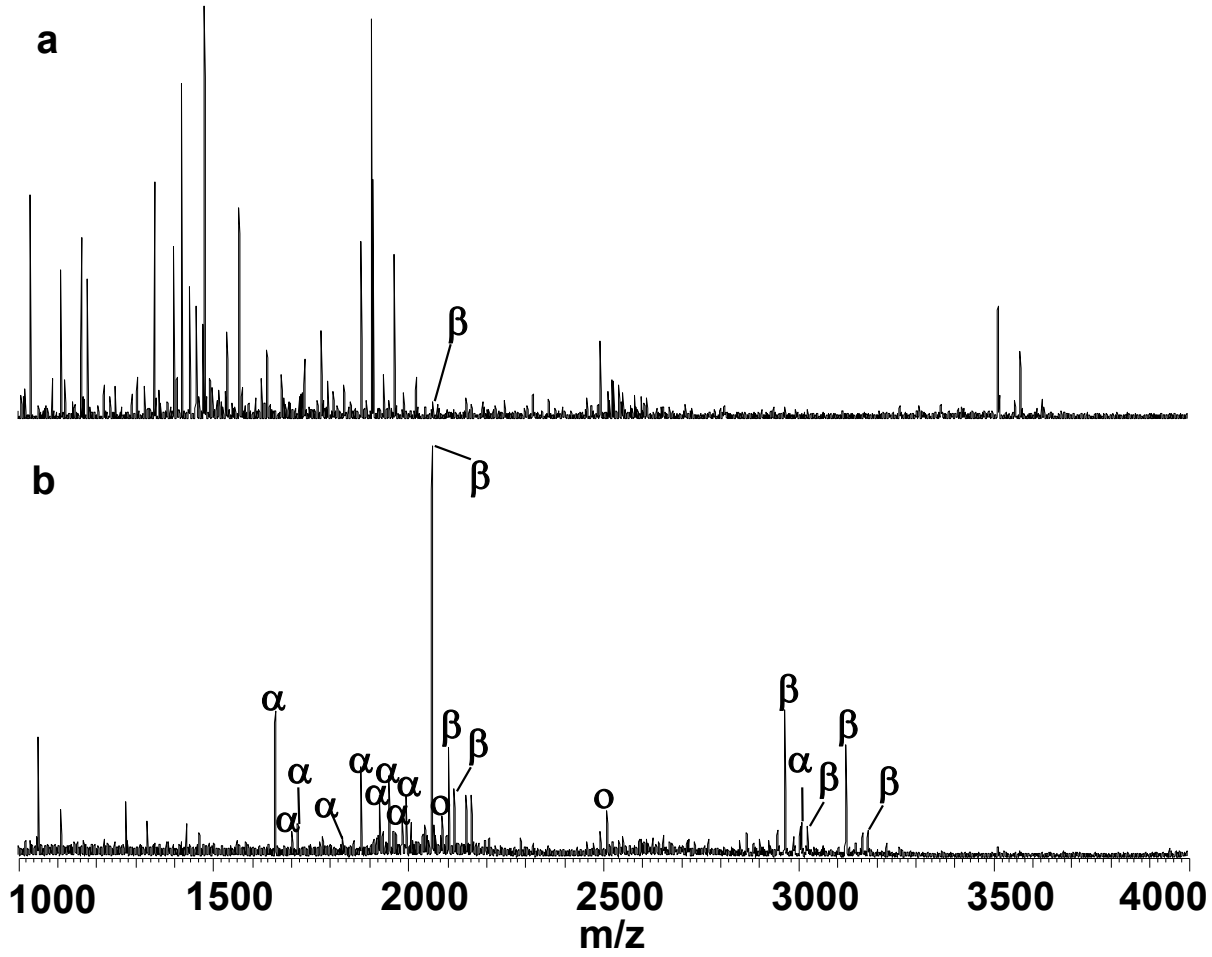

Figure 2.11. (a) MALDI mass spectrum of 1 μL of a loading solution containing 30 fmol (each) of digested α-casein, β-casein and ovalbumin and 3 pmol of BSA in 260 mM urea. (b) Mass spectrum of the phosphopeptides enriched from 500 μL of the above loading solution by adsorption on a $(PSS/TiO_2)_2$-modified nylon membrane, rinsing with 3 mL washing buffer II, and recovery with 10 μL of elution buffer. One μL of the eluate was spotted on the MALDI plate prior to addition of matrix.

Table 2.1. Phosphopeptides identified from the mass spectrum (Figure 2.11) of the membrane-enriched peptides from tryptic digests of α-casein, β-casein, and ovalbumin in loading buffer II. The loading solution contained a 100-fold excess of BSA. The m/z values, source proteins, peptide sequences and S/N are listed.

m/z	protein	Peptide sequence	S/N
1660.64	α-casein	K.VPQLEIVPN**pS**AEER.L	23
1703.64	α-casein	K.VPQLEIVPN**pS**AEER.L Carbamyl (N-term)	4
1717.64	α-casein	K.VPQLEIVPN**pS**AEER.L Carbamidomethyl (E)	6
1832.55	α-casein	YLGEYLIVPN**pS**AEER	3
1879.45	α-casein	YLGEYLIVPN**pS**AEER Carbamyl (N-term)	15
1927.36	α-casein	K.DIG**pS**E**pS**TEDQAMEDIK.Q	11
1952.64	α-casein	K.YKVPQLEIVPNpSAEER.L	13
1985.45	α-casein	K.DIG**pS**E**pS**TEDQAMEDIK.Q Carbamidomethyl (D)	7
1995.73	α-casein	K.YKVPQLEIVPNpSAEER.L Carbamyl (N-term)	11
2062.55	β-casein	K.FQ**pS**EEQQQTEDELQDK.I	50
2089.55	Ovalbumin	R.EVVG**pS**AEAGVDAASVSEEFR.A	5
2105.55	β-casein	K.FQ**pS**EEQQQTEDELQDK.I Carbamyl (N-term)	14
2119.55	β-casein	K.FQ**pS**EEQQQTEDELQDK.I Carbamidomethyl (E)	10
2511.73	ovalbumin	K.LPGFGD**pS**IEAQCGTSVNVHSSLR.D	9
2966.73	β-casein	R.ELEELNVPGEIVE**pS**L**pSpSpS**EESITR.I	24
3009.73	α-casein	R.NANEEEYSIG**pSpSpS**EE**pS**AEVATEEVK.I	6
3024.82	β-casein	A.RELEELNVPGEIVE**pS**L**pSpSpS**EESITR.I ($-H_3PO_4$)	5
3122.82	β-casein	A.RELEELNVPGEIVE**pS**L**pSpSpS**EESITR.I	19
3179.91	β-casein	A.RELEELNVPGEIVE**pS**L**pSpSpS**EESITR.I Carbamidomethyl (E)	3

2.4 Conclusions

Layer-by-layer modification of porous substrates with PSS/TiO_2 nanoparticle films is a convenient method for rapidly producing membranes that enrich phosphopeptides from small-volume samples. The TiO_2-modified membranes have a binding capacity of 540 nmol phosphoangiotensin/membrane for a 22-mm diameter disc, and a capacity of 3 nmol in membranes designed to handle small-volume (10's of μL) samples. Under sufficiently acidic conditions (2% TFA), the membranes selectively enrich phosphopeptides from a digest containing a 1:100 molar ratio of phosphoprotein to unphosphorylated protein. Thus, the membranes may prove useful in enriching phosphopeptides from modestly complex mixtures such as fusion proteins or immunoprecipitates.

2.5 Acknowledgement

We are grateful to the U.S. National Institutes of Health (GM 080511 to M.B.) for funding this work. I would like to thank Dr. Weihan Wang for help in the early stage and Dr. Amanda Palumbo for providing the D_5 and H_5 peptides.

REFERRENCE

2.6 References

1. Lee, M.; Goodbourn, S., Signalling from the Cell Surface to the Nucleus. In *Regulation of Gene Expression*, Portland Press Ltd: London, 2001; Vol. 37, pp 71-85

2. Cohen, P., The Regulation of Protein Function by Multisite Phosphorylation - a 25 Year Update. *Trends Biochem. Sci* **2000,** *25* (12), 596-601.

3. Graves, J. D.; Krebs, E. G., Protein Phosphorylation and Signal Transduction. *Pharmacol. Ther.* **1999,** *82* (2-3), 111-121.

4. Hunter, T., Signaling - 2000 and Beyond. *Cell* **2000,** *100* (1), 113-127.

5. Aebersold, R.; Mann, M., Mass Spectrometry-Based Proteomics. *Nature* **2003,** *422* (6928), 198-207.

6. Olsen, J. V.; Blagoev, B.; Gnad, F.; Macek, B.; Kumar, C.; Mortensen, P.; Mann, M., Global, in vivo, and Site-Specific Phosphorylation Dynamics in Signaling Networks. *Cell* **2006,** *127* (3), 635-648.

7. Thingholm, T. E.; Jensen, O. N.; Larsen, M. R., Analytical Strategies for Phosphoproteomics. *Proteomics* **2009,** *9* (6), 1451-1468.

8. Witze, E. S.; Old, W. M.; Resing, K. A.; Ahn, N. G., Mapping Protein Post-Translational Modifications with Mass Spectrometry. *Nat. Methods* **2007,** *4* (10), 798-806.

9. Pinkse, M. W. H.; Uitto, P. M.; Hilhorst, M. J.; Ooms, B.; Heck, A. J. R., Selective Isolation at the Femtomole Level of Phosphopeptides from Proteolytic Digests Using 2d-NanoLC-ESI-MS/MS and Titanium Oxide Precolumns. *Anal. Chem.* **2004,** *76* (14), 3935-3943.

10. Cantin, G. T.; Shock, T. R.; Park, S. K.; Madhani, H. D.; Yates, J. R., Optimizing TiO2-Based Phosphopeptide Enrichment for Automated Multidimensional Liquid Chromatography Coupled to Tandem Mass Spectrometry. *Anal. Chem.* **2007,** *79* (12), 4666-4673.

11. Thingholm, T. E.; Larsen, M. R.; Ingrell, C. R.; Kassem, M.; Jensen, O. N., TiO2-Based Phosphoproteomic Analysis of the Plasma Membrane and the Effects of Phosphatase Inhibitor Treatment. *J. Proteome Res.* **2008,** *7* (8), 3304-3313.

12. Pinkse, M. W. H.; Mohammed, S.; Gouw, L. W.; van Breukelen, B.; Vos, H. R.; Heck, A. J. R., Highly Robust, Automated, and Sensitive on Line TiO2-Based Phosphoproteomics Applied to Study Endogenous Phosphorylation in Drosophila Melanogaster. *J. Proteome Res.* **2008,** *7* (2), 687-697.

13. Li, Y.; Xu, X. Q.; Qi, D. W.; Deng, C. H.; Yang, P. Y.; Zhang, X. M., Novel Fe3O4@TiO2 Core-Shell Microspheres for Selective Enrichment of Phosphopeptides in Phosphoproteome Analysis. *J. Proteome Res.* **2008,** *7* (6), 2526-2538.

14. Wang, H.; Duan, J.; Cheng, Q., Photocatalytically Patterned TiO2 Arrays for on-Plate Selective Enrichment of Phosphopeptides and Direct MALDI MS Analysis. *Anal. Chem.* **2011,** *83* (5), 1624-1631.

15. Paradela, A.; Albar, J. P., Advances in the Analysis of Protein Phosphorylation. *J. Proteome Res.* **2008,** *7* (5), 1809-1818.

16. Reinders, J.; Sickmann, A., State-of-the-Art in Phosphoproteomics. *Proteomics* **2005,** *5* (16), 4052-4061.

17. Leitner, A., Phosphopeptide Enrichment Using Metal Oxide Affinity Chromatography. *Trac-Trend Anal. Chem.* **2010,** *29* (2), 177-185.

18. Han, G. H.; Ye, M. L.; Zou, H. F., Development of Phosphopeptide Enrichment Techniques for Phosphoproteome Analysis. *Analyst* **2008,** *133* (9), 1128-1138.

19. Tichy, A.; Salovska, B.; Rehulka, P.; Klimentova, J.; Vavrova, J.; Stulik, J.; Hernychova, L., Phosphoproteomics: Searching for a Needle in a Haystack. *J. Proteome* **2011,** *74* (12), 2786-2797.

20. Kweon, H. K.; Håkansson, K., Metal Oxide-Based Enrichment Combined with Gas-Phase Ion-Electron Reactions for Improved Mass Spectrometric Characterization of Protein Phosphorylation. *J. Proteome Res.* **2008,** *7* (2), 749-755.

21. Carrascal, M.; Ovefletro, D.; Casas, V.; Gay, M.; Ablan, J., Phosphorylation Analysis of Primary Human T Lymphocytes Using Sequential IMAC and Titanium Oxide Enrichment. *J. Proteome Res.* **2008,** *7* (12), 5167-5176.

22. Dunn, D. J.; Reid, E. G.; Bruening, L. M., Techniques for Phosphopeptide Enrichment Prior to Analysis by Mass Spectrometry. *Mass Spectrom. Rev.* **2010,** *29* (1), 29-54.

23. Connor, P. A.; McQuillan, A. J., Phosphate Adsorption onto TiO_2 from Aqueous Solutions: An in Situ Internal Reflection Infrared Spectroscopic Study. *Langmuir* **1999,** *15* (8), 2916-2921.

24. Larsen, M. R.; Thingholm, T. E.; Jensen, O. N.; Roepstorff, P.; Jorgensen, T. J. D., Highly Selective Enrichment of Phosphorylated Peptides from Peptide Mixtures Using Titanium Dioxide Microcolumns. *Mol. Cell. Proteomics* **2005,** *4* (7), 873-886.

25. Tsai, C. F.; Wang, Y. T.; Chen, Y. R.; Lai, C. Y.; Lin, P. Y.; Pan, K. T.; Chen, J. Y.; Khoo, K. H.; Chen, Y. J., Immobilized Metal Affinity Chromatography Revisited: pH/Acid Control toward High Selectivity in Phosphoproteomics. *J. Proteome Res.* **2008,** *7* (9), 4058-4069.

26. Dotzauer, D. M.; Dai, J. H.; Sun, L.; Bruening, M. L., Catalytic Membranes Prepared Using Layer-by-Layer Adsorption of Polyelectrolyte/Metal Nanoparticle Films in Porous Supports. *Nano Lett.* **2006,** *6* (10), 2268-2272.

27. Dunn, J. D.; Igrisan, E. A.; Palumbo, A. M.; Reid, G. E.; Bruening, M. L., Phosphopeptide Enrichment Using MALDI Plates Modified with High-Capacity Polymer Brushes. *Anal. Chem.* **2008,** *80* (15), 5727-5735.

28. Choi, W. Y.; Termin, A.; Hoffmann, M. R., The Role of Metal-Ion Dopants in Quantum-Sized TiO_2 - Correlation between Photoreactivity and Charge-Carrier Recombination Dynamics. *J. Phys. Chem.* **1994,** *98* (51), 13669-13679.

29. Lin, B.; Li, T.; Zhao, Y.; Huang, F. K.; Guo, L.; Feng, Y. Q., Preparation of a TiO_2 Nanoparticle-Deposited Capillary Column by Liquid Phase Deposition and Its Application in Phosphopeptide Analysis. *J. Chromatogr.* **2008,** *1192* (1), 95-102.

30. Liang, S. S.; Makamba, H.; Huang, S. Y.; Chen, S. H., Nano-Titanium Dioxide Composites for the Enrichment of Phosphopeptides. *J. Chromatogr.* **2006,** *1116* (1-2), 38-45.

31. Hsieh, H. C.; Sheu, C.; Shi, F. K.; Li, D. T., Development of a Titanium Dioxide Nanoparticle Pipette-Tip for the Selective Enrichment of Phosphorylated Peptides. *J. Chromatogr.* **2007,** *1165* (1-2), 128-135.

32. Lewis, S. R.; Datta, S.; Gui, M.; Coker, E. L.; Huggins, F. E.; Daunert, S.; Bachas, L.; Bhattacharyya, D., Reactive Nanostructured Membranes for Water Purification. *Proc. Natl. Acad. Sci. U. S. A.* **2011,** *108* (21), 8577-8582.

33. Thingholm, T. E.; Jorgensen, T. J. D.; Jensen, O. N.; Larsen, M. R., Highly Selective Enrichment of Phosphorylated Peptides Using Titanium Dioxide. *Nat. Protoc.* **2006,** *1* (4), 1929-1935.

Chapter 3. Investigation of Phosphorylation in Tau Protein and the Nuclear Factor Kappa B (NF-κB) Pathway using Phosphopeptide Enrichment with TiO_2-modified Membranes

(Work on phosphorylation of Tau was submitted as part of an article in *Analytical Chemistry*)

Chapter 2 describes the fabrication of TiO_2-modified nylon membranes and demonstrates their enrichment performance with model phosphoprotein digests. This chapter presents initial applications of these membranes for investigating phosphorylation of biologically important proteins, including immunoprecipitated species and proteins phosphorylated in vitro and in vivo. The goal is to demonstrate the strengths and limitations of the membranes in phosphopeptide enrichment with biologically relevant mixtures.

3.1 Introduction

Phosphopeptide enrichment is a prerequisite step for bottom up studies of protein phosphorylation because the sample complexity and low abundance of the target phosphopeptides impede their identification with MS analysis.[1-5] As described in the previous chapter, TiO_2-modifed nylon membranes (22-mm diameter disk) have a binding capacity of 540 nmol of phosphopeptides and enrich phosphopeptides from a 100-fold excess of non-phosphorylated, digested protein. These properties should enable TiO_2-modified membranes to effectively enrich phosphopeptides from modestly complex biological mixtures such as digests of fusion proteins, multi-protein complexes, or immunoprecipitates.

In contrast to global phosphoproteomics strategies that use SCX fractionation, MOAC/IMAC enrichment, and HPLC-MS,[6-7] our interests focus on investigating phosphorylation in proteins associated with a specific pathway or pathology, for instance the role of tau protein phosphorylation in Alzheimer's disease.[8-9] To demonstrate the utility of TiO_2-modified membranes, we examine phosphopeptide enrichment from a digest of tau protein that is phosphorylated by glycogen synthase kinase-3β (GSK-3β). The enrichment and analysis requires only 8 μg of protein, and the membrane eluent is amenable to analysis by both MALDI-MS and ESI-MS to identify the number and location of phosphorylation sites. The combination of membrane enrichment with tandem mass spectrometry reveals seven phosphorylation sites from *in vivo* phosphorylated tau (p-tau) protein, which is associated with Alzheimer's disease.

The NF-κB pathway employs a series of protein complexes to alter DNA transcription in almost all animal cells (Figure 3.1).[10] The signal transduction of NF-κB facilitates the cellular response to various stimuli, such as cytokines, environmental stress, UV-irradiation, radicals, antigens and bacterial infection.[11-12] Malfunction of the NF-κB pathway may lead to inflammation or immune disease, and even cancer.[13-14] Studies of phosphorylation related to the key transcriptional factor p65 (RelA) under the stimulation of tumor necrosis factor (TNF-α) will provide insight to further understand the NF-κB pathway.[15] In this chapter, the combination of membrane enrichment with MALDI MS/MS reveals eight phosphopeptides from p65-associated proteins immunoprecipitated from human acute monocytic leukemia (THP-1) cell nuclear extracts.

The inhibitor of kappa-B-alpha (IκBα) is also an important protein in the NF-κB pathway, as IκBα conserves and inhibits transcriptional factors p65 and p50 in the cytoplasm.[16] In addition to the well-known Inhibitor of kappa-B kinase beta (IKKβ), some studies suggest that

the G-protein coupled receptor kinase-5 (GRK5) also mediates the activation of the NF-κB pathway.[17-18] Even without enrichment, our LC-MS/MS analysis reveals two phosphorylation sites (Ser32 and 36) from a digest of IκBα that is *in vitro* phosphorylated by GRK5.

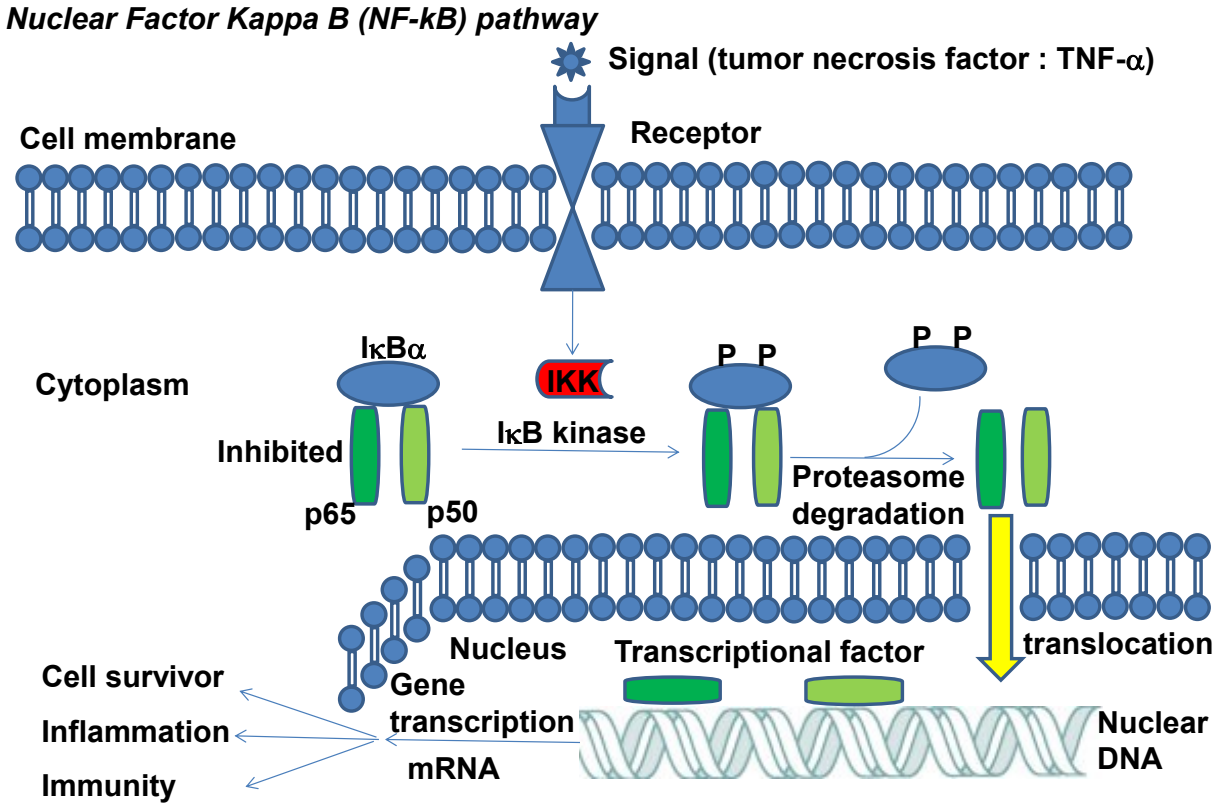

Figure 3.1. Cartoon of the NF-κB pathway under the stimulation of TNF-α. After the receptor outside the cellular membrane receives a signal (such as the cytokine TNF-α), the released IKK will phosphorylate the inhibited IκBα-p65/p50 complex in the cytoplasm. The phosphorylated IκBα-p65/p50 complex tends to undergo proteasome degradation and release the two transcriptional factors p65 and p50. The free transcriptional factors translocate into the nucleus and bind to the nuclear DNA to create different transcriptional mRNA. The normal NF-κB pathway would provide the right response for cell survival/apoptosis and immune response to outside stimulation.

3.2 Experimental

3.2.1 Materials and solutions, membranes and holders, membrane modification and protein digestion

See chapter 2 for details in this area.

3.2.2 Purification of p-tau

Protein expression and purification were performed by Dr. Dexin Sui from Prof. Min-Hao Kuo's group. Tau protein was overexpressed in *E. Coli*. A single plasmid contained genes for His_6FosGSK3β and Juntau fusion proteins. Bacterial cells in buffer (20 mM Tris, 100 mM NaCl and 2 mM orthovanadate, pH 8, production of a 0.1 g bacterial pellet requires 8 mL buffer) were sonicated, and the sample supernatant was saved after centrifuging at 13000 rpm for 30 min at 4 ºC. The supernatant was loaded on a Ni-NTA column and washed with buffer prior to elution with a 30 - 300 mM imidazole gradient. Eluate fractions were combined and concentrated in a 30 kDa spin column to a volume of 6 - 10 mL. One mL of the concentrated sample was loaded onto a size exclusion column (Superdex 200 10/300 GL) coupled to an fast protein liquid chromatography (FPLC) system (Amersham pharmacy biotech AKTA P-920). The eluent was 20 mM Tris and 100 mM NaCl at 0.4 mL/min. Fractions were collected every 1 mL and monitored by their absorbance at 280 nm. UV-absorbing fractions for a given peak were combined and concentrated with a 30 kDa spin column at 4000 rpm at 4 ºC. The final protein concentration was estimated from the UV absorbance at 280 nm, and these samples were digested and employed in MS studies.

3.2.3 Enrichment of phosphopeptides from digested p-tau

After in-solution digestion of 100 μg of purified protein using the protocol in Chapter 2 (page 65), 160 pmol of p-tau digest was dissolved in 200 μL of loading buffer II (2 % TFA in 1:1 water:ACN) and passed through a small-scale TiO_2-modified membrane at 10 μL/min. The membrane was washed with 200 μL of washing buffer II (2 % TFA in 1:1 water:ACN) at the same flow rate, and phosphopeptides were eluted with 50 μL of elution buffer (1 % NH_4OH in 1:1 water:ACN) at 5 μL/min.

3.2.4 Immunoprecipitation of p65 from THP-1 cells

The THP-Cells (from ATCC, Manassas, VA) were cultured in RPMI medium 1640 (Invitrogen) at 37 ºC with 5% CO_2 and ambient O_2 until reaching a concentration of 9.6 x 10^5/mL in flow cytometry. The cells were treated with TNF-α at a final concentration of 10 ng/mL for 30 min before harvest. The cell suspension was centrifuged (500g) for 5 min at 4 ºC, and after rinsing with 10 mL ice-cold phosphate buffered saline (PBS), the suspension was centrifuged again and the cells were lysed with 1.5 mL lysis buffer (10 mM HEPES pH=8.0, 1.5 mM $MgCl_2$ and 10 mM KCl) for 30 min on ice. The pellet from subsequent centrifugation was further extracted with 60 μL nuclear extraction buffer (20 mM HEPES pH=8.0, 1.5 mM $MgCl_2$, 0.42 M NaCl, 0.2 mM EDTA and 25 % glycerol) on a shaker (2500 rpm) for 30 min at 4 ºC. The final total protein concentration was ~6 μg/μL according to a Bradford assay. The phosphorylation of p65 was confirmed by Western blotting (WB) using a primary p65 polyclonal antibody (C-20 from Santa Cruz Biotechnology). Twenty plates of cells were treated in parallel, and 1000 μg of total cell extract was pooled into 800 μL PBS buffer and mixed with 30 μL covalently cross-

linked p65 antibody agorose (C20 from Santa Cruz Biotechnology) in 200 μL nuclear extraction buffer. The IP efficiency was probed using WB with a p65 antibody (C22B4 from Cell Signaling Technology, Boston, MA). Protein on the 30-μL antibody beads was digested according to the protocol for digesting 100 μg BSA (chapter 2, page 65), starting with the addition of the beads to the urea solution. This overall procedure was initially developed by Dr. Amanda Palumbo.[19]

3.2.5 Enrichment of on-bead digests of immunoprecipitated p65 and associated proteins

Sixteen μL of the p65 on-bead digest was dissolved in 200 μL of loading buffer I (0.1 % TFA in 1:1 water:ACN), and 5 pmol of ovalbumin digest was added to the solution. The sample was passed through the small membrane (0.02 cm^2) at a flow rate of 10 μL/min, and the membrane was rinsed with 200 μL washing buffer I (0.1 % TFA in 1:1 water:ACN) at the same flow rate. Finally 10 μL of (1 % H_3PO_4 in 1:1 water:ACN), was used to elute the phosphopeptide from the membrane at a flow rate of 2 μL/min.

3.2.6 *In vitro* phosphorylation of IκBα by GRK5 and IKKβ

The IκBα and protein kinases were kindly provided by Prof. Parameswaran. The 20 μL reaction system contained 2.6 μL of 0.049 μg/μL IκBα, 0.5 μL of 10 mM ATP, 0.25 μL of 0.22 μg/μL IKKβ or 0.26 μL of 0.17 μg/μL GRK5 (from Cell Signaling Technology, Boston, MA), 2.5 μL kinase buffer (from Cell Signaling Technology, Boston, MA) and H_2O (bring up to 20 μL). The *in vitro* phosphorylation was carried for 30 min at room temperature and stopped by addition of 5 μL of 2% SDS buffer. The IκBα phosphorylation by GRK5 and IKKβ was

confirmed by WB analysis. The system was scaled up to 5 μg of IκBα for the LC-MS/MS analysis. Five μg of IκBα with and without phosphorylation by GRK5 was digested in solution prior to the LC-MS/MS analysis.

3.2.7 Mass Spectrometry and Data Analysis

3.2.7.1 MS method for p-tau phosphorylation study

The MALDI analysis was the same as described in Chapter 2. For ESI-MS analyses, 40 μL samples in 1% acetic acid, 49% H_2O and 50% methanol were loaded into a Whatman multichem 96-well plate (Sigma Aldrich, St. Louis, MO) and sealed with Teflon Ultra Thin Sealing Tape (Analytical Sales and Services, Prompton Plains, NJ). Then, using an Advion Triversa Nanomate nano-electrospray ionization (nESI) source (Advion Ithaca, NY) with a spray voltage of 1.4 kV and a gas pressure of 1.0 psi, samples were introduced into a high resolution accurate mass LTQ Orbitrap Velos mass spectrometer (Thermo Fisher Scientific, San Jose, CA) equipped with a dual pressure ion trap, Higher-Energy Collisional Dissociation (HCD) cell and Electron Transfer Dissociation (ETD). The ion source interface settings (inlet temperature of 200 ^{o}C and S-Lens value of 60 %) were optimized to maximize the sensitivity of the precursor ions while minimizing 'in-source' fragmentation. High resolution mass spectra, as well as all ion trap CID-, HCD- and ETD-MS/MS and -MS^n spectra, were acquired in positive ionization mode using the FT analyzer operating at 100,000 resolving power. Spectra were typically signal averaged for 30-100 scans. Peptide precursor ions were mass-selected using an isolation width of 5 Da. CID was performed using default activation parameters (q=0.25, activation time 10 msec) with a normalized collision energy of 30. HCD was performed using default activation parameters, with a collision energy of 20-40 and a low mass cutoff of 100. For ETD, the

automatic gain control value and the maximum injection time of the reagent ion (fluoranthene anion) were set as 1.0×10^5 and 100 ms respectively, and the reaction time was optimized as 50 ms for +3 charge state. Assignment of peptides resulting from protein digestion was performed manually by mass fingerprinting or by MS/MS. Phosphorylation sites were manually assigned by matching MS/MS product ions with *in silico* peptide fragments generated using ProteinProspector (http://prospector.ucsf.edu).

3.2.7.2 MS method for p65 phosphorylation study

To increase the amount of material spotted on the MALDI plate, 5 μL of eluate (in 1 μL increments that were allowed to dry) was spotted onto the same well prior to addition of 1μL of 2,5-DHB matrix. The additional spotting gives stronger signal intensity and more precursor ions for MS/MS than the traditional 1μL spotting method. Ion trap CID-MS/MS was performed on mass-selected precursor ions, and MS/MS spectra shown were typically collected for about 1 hour to average 3000 scans. MS/MS spectra were transformed to DTA files by Bioworks 3.3 (Thermo Fisher Scientific), and searched using the Mascot algorithm (Matrix Science) under the NCBInr data base with taxonomy as homo sapiens (human) for p65 IP proteins. The identifications and determined phosphorylation sites were also confirmed manually.

3.2.7.3 MS method for IκBα phosphorylation study

These analyses were performed by Dr. Xiao Zhou from Prof. Gavin E. Reid's group. Five μL of digested IκBα at a concentration of 0.2 pmol/μL in 3% acetic acid/5% ACN was loaded from a Paradigm AS1 autosampler (from Michrom Bioresources, CA) onto a peptide CapTrap (from Michrom Bioresources, CA) at a flow rate of 15 μL/min using loading buffer 0.1% TFA/ 2%

ACN. After 5 min of loading, the peptides concentrated on the CapTrap were eluted onto a 200 μm id × 50 mm fused silica column packed with Magic C18AQ (3 μm particle, from Michrom Bioresources, CA) at a flow rate of 2 μL/min using a linear 45 min gradient from 95% solvent A (0.1% FA in H_2O) to 50% solvent B (0.1% FA in ACN). After gradient separation, the system was cleaned with 80% solvent B for 5 min followed by equilibrium with 95% solvent A for 5 min.

The mass spectrometer was programmed to operate in a data-dependent acquisition mode. In the full scan analysis, the five most intense ion signals (the signal threshold was set at 1.0×10^4 counts) from the survey MS scan were isolated with an isolation window of 2.0 m/z. During CID-MS/MS, when an AGC target value of 1.0×10^4 was reached within 100 ms maximum injection time in the ion trap, the isolated ions were fragmented with 35 normalized collision energy using a 10 ms activation time and an activation *q* value of 0.25.

3.3 Results and discussion

3.3.1 Enrichment of p-tau digests

The studies in the previous chapter suggest that TiO_2-modified membranes are attractive for enriching phosphopeptides from modestly complex samples such as digests of complexes containing fusion proteins. To test the membranes with a phosphoprotein with more direct relevance to biology, we enrich phosphopeptides from a digest of hyperphosphorylated tau (p-tau). Abundant in neurons, tau is a very soluble microtubule-associated protein that along with tubulin assembles and stabilizes the microtubule cytoskeleton.[20] In many neurodegenerative conditions such as Alzheimer's disease, hyperphosphorylated tau dissociates from the

microtubule and aggregates into paired helical filaments and neurofibrillary tangles,[8] whose abundance correlates well with the severity of neurodegeneration of Alzheimer's disease patients. Thus, compounds that block or reverse tau aggregation may have therapeutic value in treating Alzheimer's disease. Development of such potential drugs will benefit from a better understanding of the sites of p-tau phosphorylation.

One of the candidate kinases for tau hyperphosphorylation in Alzheimer's disease is GSK-3β. *In vitro*, GSK-3β catalyzes tau phosphorylation that facilitates the formation of tangle-like aggregates.[9, 21-23] To prepare the p-tau subjects for digestion and our TiO_2 enrichment, Prof. Kuo and Dr. Sui employed a protein interaction module-assisted catalysis technique in which GSK-3β and tau are expressed as His_6-FosB and JunD fusion proteins, respectively (Figure 3.2). The formation of a stable FosB-JunD leucine zipper complex in *E. coli* leads to high-efficiency phosphorylation of tau. Subsequently, affinity-trapping of the His-tag with a Ni-NTA column enables isolation of the complex, which in this study was further purified through size-exclusion FPLC. Selected FPLC fractions containing GSK-3β, p-tau and a small number of bacterial proteins were pooled for MS. It should be noted that the complexity of these samples is similar to our model solution containing phosphoproteins in excess BSA.

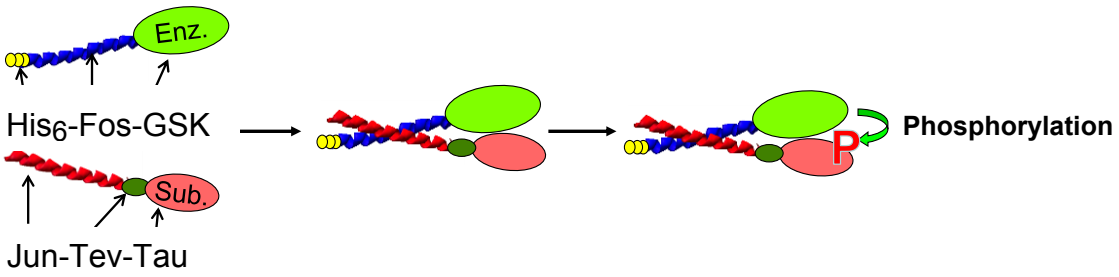

Figure 3.2. Scheme of the protein interaction module-assisted phosphorylation. The leucine zipper Fos and Jun bring the enzyme and substrate together after they are co-produced in cells, and phosphorylation occurs in vivo.

Figure 3.3a shows the MALDI mass spectrum of a digested FPLC fraction that contained p-tau. The peptide signals stem from GSK-3β, p-tau, and unknown proteins that co-purify with the complex. The sample also contains 0.12 M urea and 10 mM NaCl, which decrease the S/N, so the highest S/N is 20 for a peptide from GSK-3β. Overall, the spectrum reveals 63 peptides whose signals are above 10 % of the highest signal, but none of these are phosphopeptides.

Using the TiO_2-modified membranes with loading buffer II, we capture the phosphopeptides from 200 μL of the same digested FPLC fraction and then recover these peptides in 50 μL of elution buffer. The mass spectrum of 1 μL of the eluate spotted on a MALDI plate (Figure 3.3b) shows a much simpler pattern than in Figure 3.3a, and the S/N is as high as 100 for a phosphopeptide from p-tau. The TiO_2-modified nylon membrane isolates, concentrates (4-fold) and desalts the phosphopeptides to enable their detection. We identify seven phosphorylation sites from three phosphopeptides, P_1, P_3, and P_4 (P_2 results from in-source loss of 98 Da from P_3.) Even the strongest phosphopeptide signal, P_3 at 2455.00 m/z, is not present in the mass spectrum of the membrane-loading solution, presumably because of suppression. The enriched mixture also shows signals from four unphosphorylated peptides (labeled as n in spectrum b). These signals are also present in Figure 5a, but they do not stem from either p-tau or GSK-3β. A control experiment with tau digests without GSK-3β stimulation (Figure 3.4) shows no detectable phosphopeptides after enrichment.

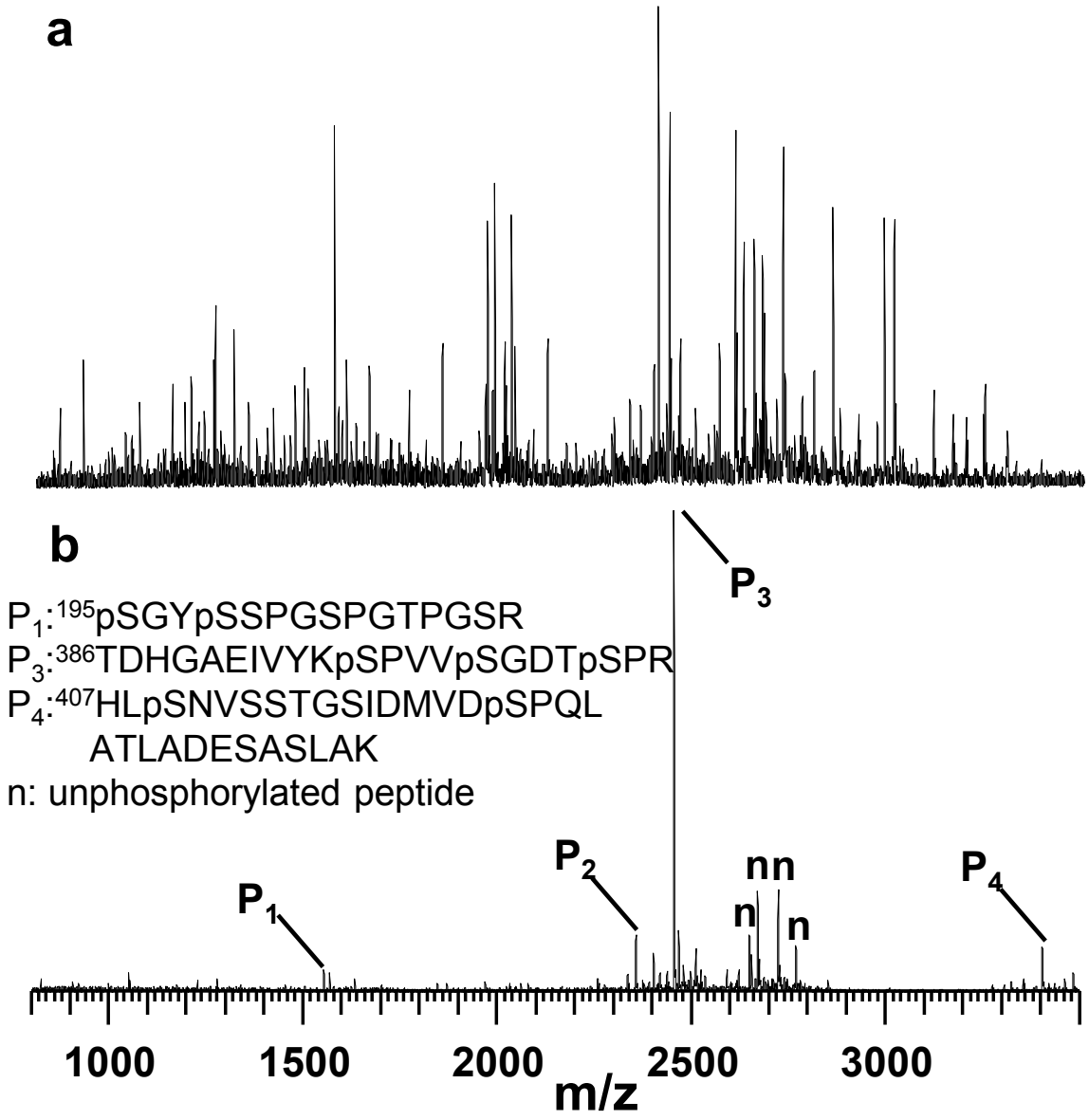

Figure 3.3**.** (a) MALDI mass spectrum of a digested FPLC fraction that contained approximately 800 fmol of GSK-3β-p-tau complex along with associated proteins; (b) The corresponding mass spectrum of peptides enriched from the above solution by adsorption on a TiO_2-modified nylon membrane and subsequent elution. The figure shows the sequences of 4 phosphopeptides, one of which, P_2, results from in-source P_3 dephosphorylation. Four major unphosphorylated peptides are labeled with n.

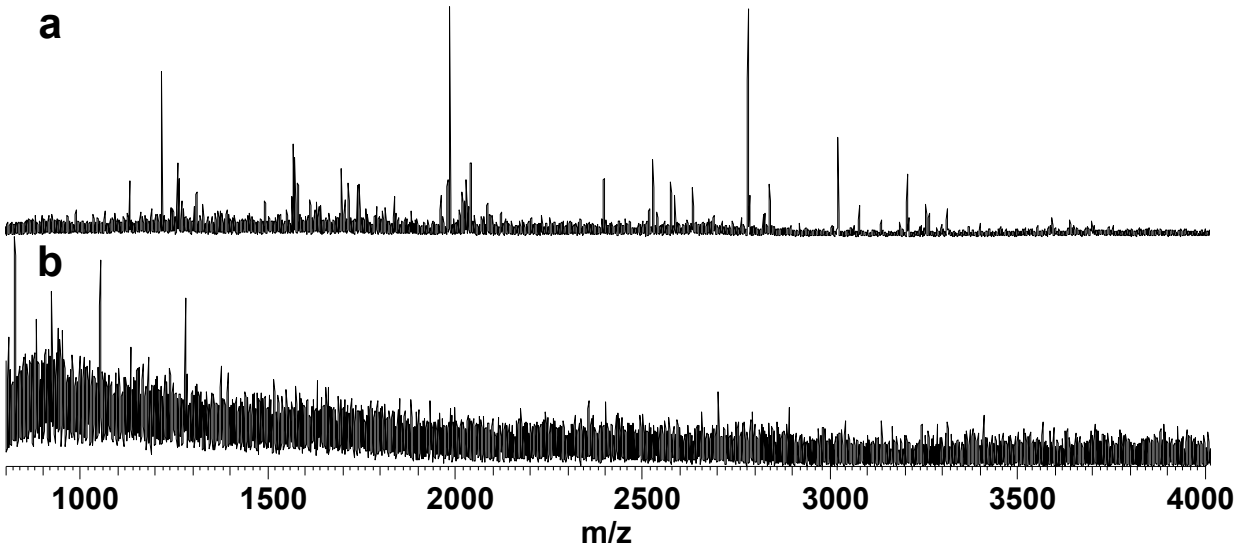

Figure 3.4. (a) MALDI mass spectrum of an FPLC fraction containing approximately 800 fmol of digested tau protein and associated proteins. (b) The corresponding mass spectrum of phosphopeptides enriched from the above solution by adsorption on a TiO_2-modified nylon membrane and elution. The spectra reveal no phosphopeptides, confirming that tau protein is not phosphorylated without GSK3 catalysis.

To identify the phosphorylation sites on p-tau, we employed ESI-Orbitrap-MS coupled with CID-, HCD-, or ETD-MS/MS and/or MS^n fragmentation. In CID-MS^n (Figure 3.5) the dominant sequential loss of phosphate under consecutive CID fragmentations confirms that ^{386}TDHGAEIVYK**pS**PVV**pS**GDT**pS**PR has three phosphate groups. The CID MS/MS spectrum gives 87 fragment ions resulting from breaking of 17 out of 20 peptide bonds. The HCD MS/MS spectrum shows 93 fragment ions from the breakage of 18 out of 20 peptide bonds (Figure 3.6). The higher energy causes more internal fragmentation, leading to additional small fragments at a low mass range compared to CID analysis. Both techniques provide high confidence for peptide

identification. However, the potential for competing losses of 98 Da (either directly as H_3PO_4 from a phosphorylated Serine or Threonine residue, or as the combined losses of 80 Da (HPO_3) from a phosphorylated Serine or Threonine residue and 18 Da (H_2O) from a non-phosphorylated Serine or Threonine residue) from either the precursor ion or from the b- and y-type product ions may result in ambiguity in assigning the sites of phosphorylation within the peptide sequence.[24] In contrast, retention of phosphate groups during ETD [25-26] allows confident assignment of phosphorylation sites (Figure 3.7). Two other phosphopeptides were identified using HCD analysis and the phosphate groups were assigned as ^{195}**pS**GY**pS**SPGSPGTPGSR and ^{407}HL**pS**NVSSTGSIDMVD**pS**PQLATLADESASLAK (see mass spectra in Figure 3.8). Overall, we identified 7 phosphorylation sites (S195, S198, S396, S400, S404 S409 and S422) using MS analysis following enrichment with the TiO_2-modified nylon membrane.

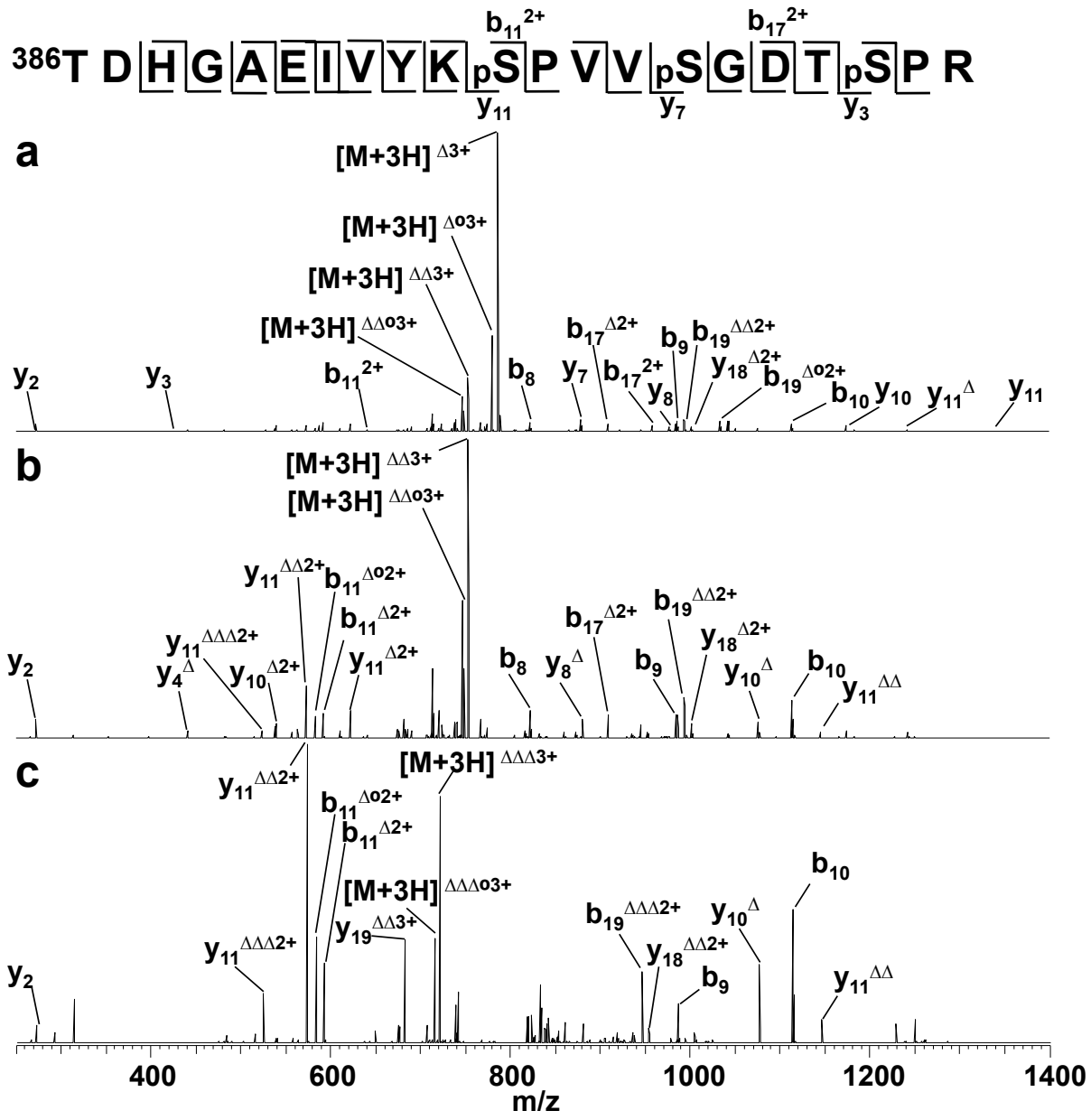

Figure 3.5. ESI-Orbitrap multistage CID-MS^n of the $[M+3H]^{3+}$ precursor ion of ^{386}TDHGAEIVYK**pS**PVV**pS**GDT**pS**PR (m/z 819.34). (a) CID-MS/MS, (b) CID-MS^3 of the -98 Da product ion from panel A (m/z 786.48), (c) CID-MS^4 of the -98 Da product ion (m/z 753.98) from panel B. The sequences show cleavage sites for formation of b and y ions. （Δ=-98 Da, o=-18 Da）

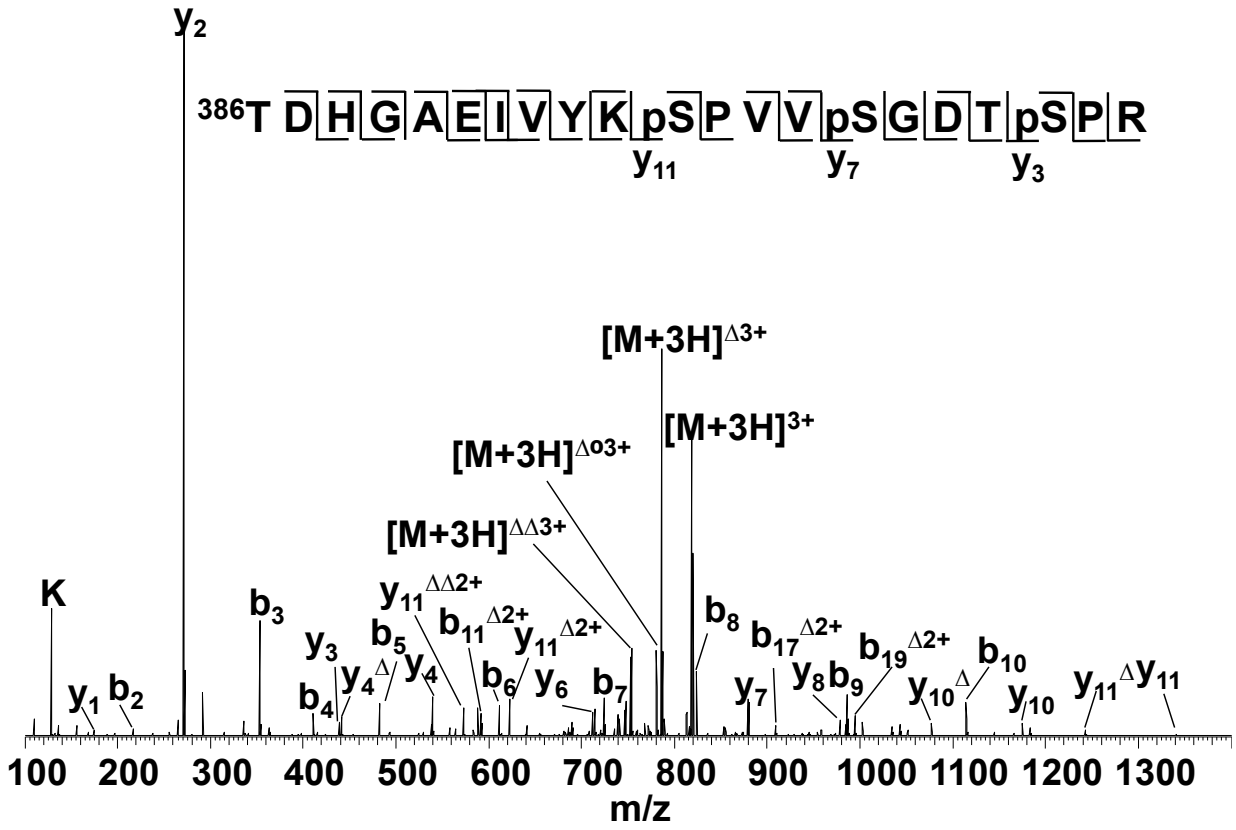

Figure 3.6. ESI-Orbitrap HCD-MS/MS spectra of the $[M+3H]^{3+}$ precursor ion of ^{386}TDHGAEIVYK**pS**PVV**pS**GDT**pS**PR (m/z 819.34). The sequences show cleavage sites for formation of b and y ions. （Δ=-98 Da, o=-18 Da）

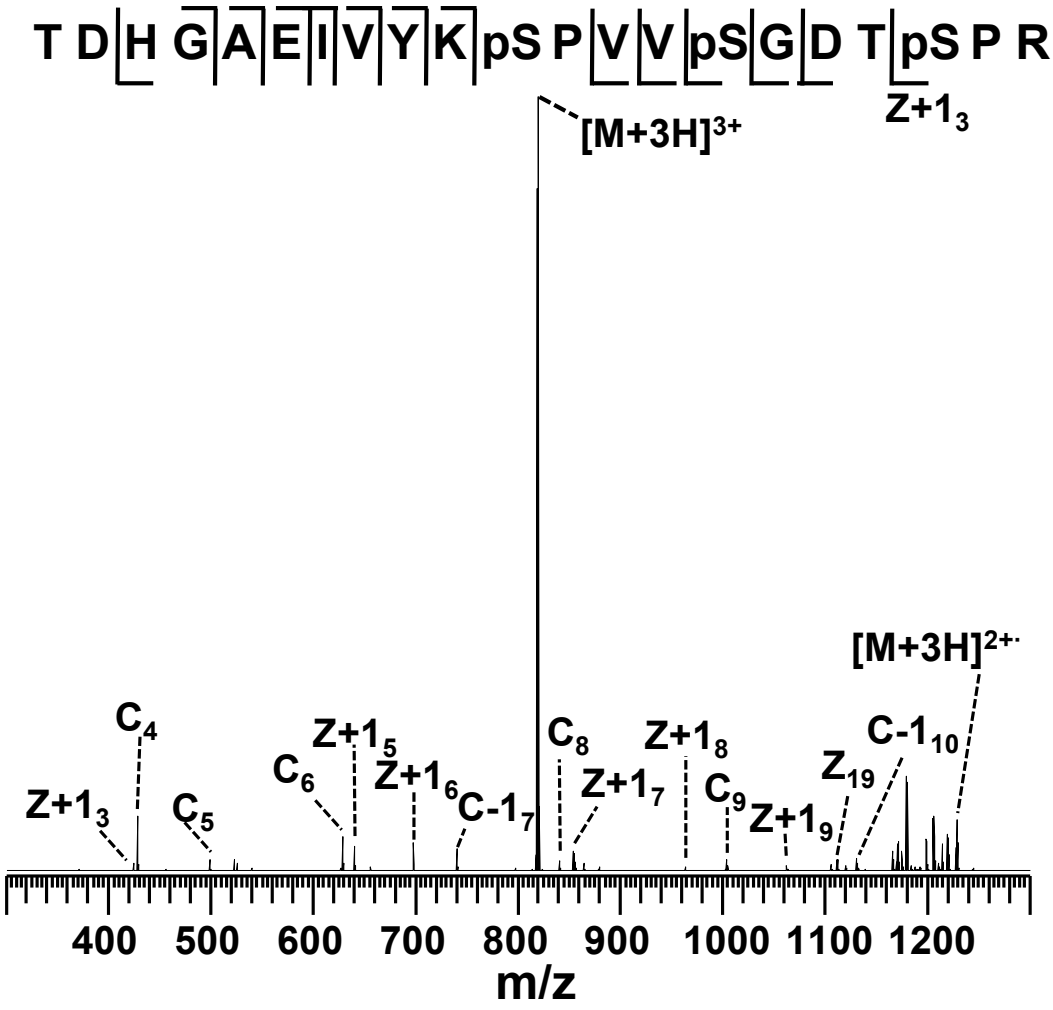

Figure 3.7. ESI-Orbitrap ETD-MS/MS spectrum of the $[M+3H]^{3+}$ precursor ion of ^{386}TDHGAEIVYK**pS**PVV**pS**GDT**pS**PR (m/z 819.34). The sequence shows cleavage sites for formation of c and z ions.

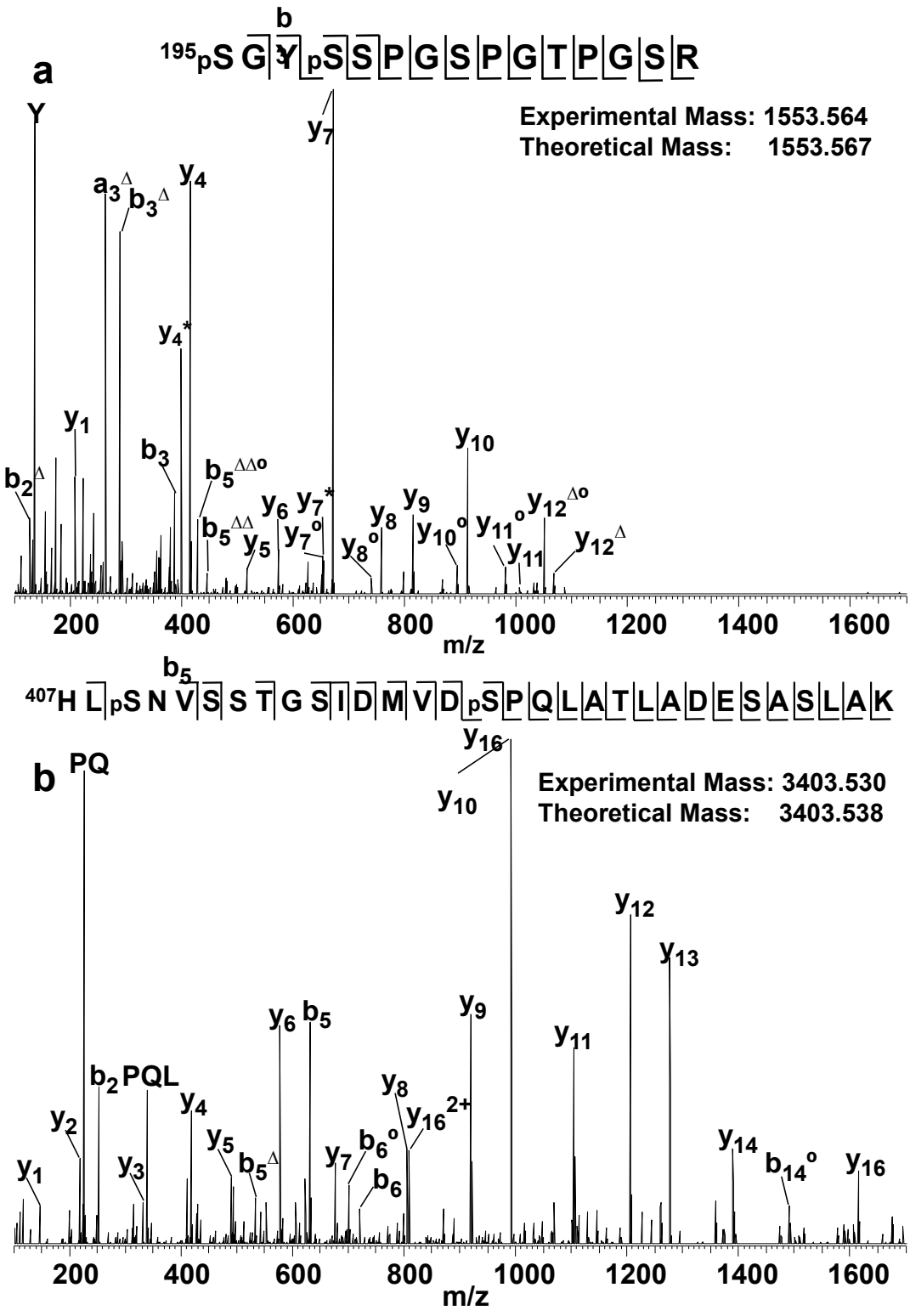

Figure 3.8. ESI-Orbitrap HCD-MS/MS of (a) the $[M+2H]^{2+}$ precursor ion of ^{195}**pS**GY**pS**SPGSPGTPGSR (m/z 778.00) and (b) the $[M+3H]^{3+}$ precursor ion of

^{407}HL**pS**NVSSTGSIDMVD**pS**PQLATLADESASLAK (m/z 1136.00). The figure lists the experimental and theoretical masses of the peptides, and the assigned sequences and phosphorylation sites. （Δ=-98 Da, o=-18 Da and *=-17 Da）

Multiple approaches such as MS, WB, and Edman degradation have previously revealed more than 40 phosphorylation sites in different tau isoforms,[27] making it particularly challenging to map all phosphorylation sites of a given p-tau species. However, as Figure 3.3b shows, the signal from the ^{386}TDHGAEIVYK**pS**PVV**pS**GDT**pS**PR (S396, S400 and S404) peptide dominates the spectrum of the enriched peptides. There are three possible reasons for this dominance. First, the peptide has a particularly high ionization efficiency. Given the presence of 3 phosphates, this seems unlikely for analysis in the positive ion mode. Second, the membrane selectively enriches the tri-phosphorylated peptide. However, TiO_2 usually shows a bias toward mono-phosphorylated peptides.[19, 28] Third, and the most likely of the three, the stoichiometry of ^{386}TDHGAEIVYK**pS**PVV**pS**GDT**pS**PR phosphorylation may surpass all other tryptic phosphopeptides of p-tau. Using traditional methods of preparing p-tau with a commercial GSK-3β, the Gamblin group phosphorylated tau with 3 moles of phosphate incorporated per mole of tau. Similarly, the Reynolds group reports 2-4 moles phosphate/mole of Tau.[22, 29] They also find a S396-S400-S404 tri-phosphorylated peptide. We thus suspect that these three residues are the most preferred targets for GSK-3β. This phenomenon is also consistent with the observation that GSK-3β activity can be enhanced by pre-existing, priming phosphorylation that lies 4 residues C-terminal to the next phosphorylation site.[30] On the other hand, whether any of these three phosphorylation sites plays a key role in Alzheimer's disease remains to be assessed. Further refinement of the phosphorylation, sample preparation, and enrichment procedures will likely yield more comprehensive mapping of GSK-3β-phosphorylated residues in p-tau.

Identification of the most dominant and other sub-stoichiometric phosphorylation sites may prove useful in designing drugs to prevent the pathological hyperphosphorylation of tau and even the appearance of the neurofibrillary tangles.[28]

3.3.2 Phosphopeptide enrichment from on-bead digests of immunoprecipitated p65 and associated proteins

Immunoprecipitated proteins are somewhat similar in complexity to the fusion proteins described above. In addition to peptides from the specific antigen protein, tryptic digests of immunoprecipitates contain peptides from associated proteins, the antibody, and nonspecifically adsorbed proteins. We examined enrichment of immunoprecipitated p65 and its associated proteins. The heterodimeric p65-p50 complex is the most abundant member of the NF-κB family of transcription factors present in almost all animal cell types.[31] These factors help regulate many biological processes such as inflammation, immunity and tumor genesis,[32-35] and the NF-κB pathway is mainly controlled by PTMs, especially phosphorylation.[36-37] Thus, we hope to identify phosphorylated p65 or p65-associated proteins in the nuclear extract of cells treated with a stimulating agent, TNF-α.

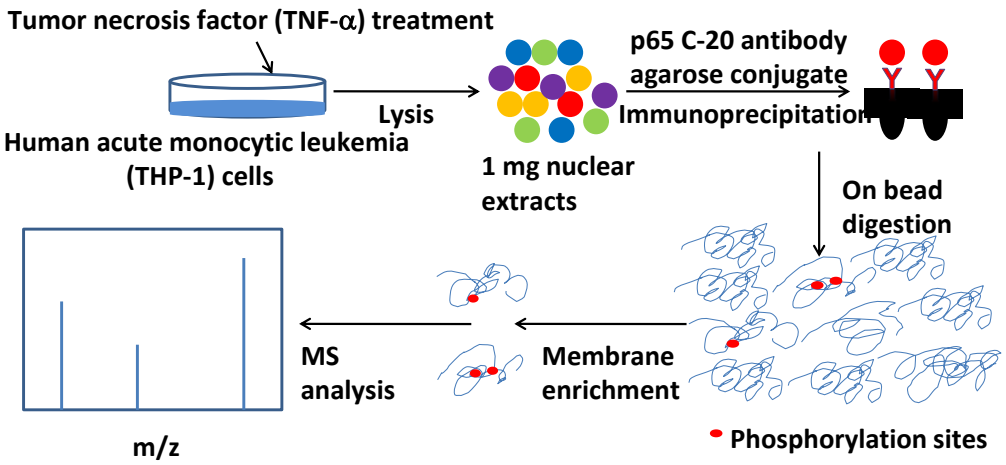

Scheme 3.1 Workflow of the p65 phosphorylation study. The THP-1 cells were treated by TNF-α, and 1 mg (based on a Bradford assay) of nuclear-extract proteins obtained from cell lysis was immunoprecipitated by a p65 C-20 antibody-agarose conjugate. After on bead digestion, the phosphopeptides were enriched by a TiO_2-modifed membrane, followed by MS-analysis.

The p65 and associated proteins were initially immunoprecipitated from a nuclear extract of TNF-α stimulated THP-1 cells (Scheme 3.1). Although WB clearly shows the presence of p65 in the treated cells and confirms the efficiency of IP, (Figure 3.9) we do not know how much p65 or associated phosphoprotein is present in the immunoprecipitated protein. Tryptic digestion was performed with the proteins still attached to the affinity beads, and 16 μL of digest was dried and dissolved in 200 μL of loading buffer I. To assess whether the membrane enriches phosphopeptides from this specific sample, we also add 5 pmol digested ovalbumin into the 200-μL solution prior to the enrichment procedure, which includes passing the digest through the membrane, rinsing, and elution with 10 μL of 1% H_3PO_4 in 1:1 water:ACN. We observed that when the sample amount is low, the NH_4OH elution leads to matrix cluster ions at a low mass

range in MALDI-MS. To avoid these cluster ions, we switched to an H_3PO_4 eluent that provides high elution efficient and alleviates the cluster problem.

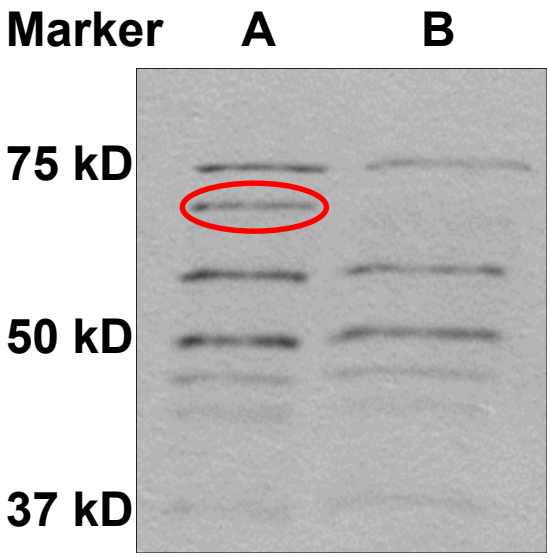

Figure 3.9. The WB analysis of p65 using primary polyclonal p65 antibody (C22B4). Lane A is the 25 μg nuclear extracts before IP, and lane B is the 25 nuclear extracts after IP. The red circle highlights the p65.

The MALDI mass spectrum of the digested and enriched IP contains an ovalbumin phosphopeptide signal at m/z 2089 (Figure 3.10), and 8 other phosphopeptide signals due to the p65 digest. A neutral loss of 98 Da in CID MS/MS spectra serves as the diagnostic marker for phosphopeptides.[38]

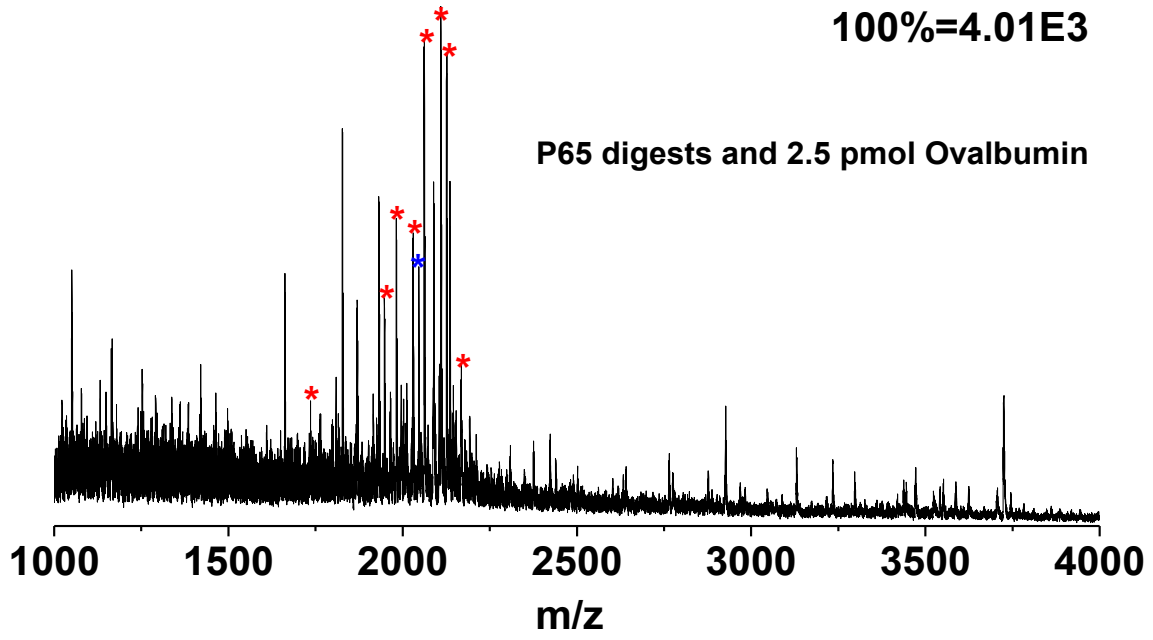

Figure 3.10. MALDI mass spectrum of a membrane-enriched digest of immunoprecipitated p65 and associated proteins. Sixteen μL of p65 on-bead dried digest and 5 pmol ovalbumin digest were dissolved in 200 μL loading buffer I, then passed through the TiO_2-modified membrane, and phosphopeptides were eluted in 10 μL of 1% H_3PO_4 in 1:1 water:ACN. Five μL of eluent was spotted on the same sample well prior to MALDI-MS. The red stars represent the phosphopeptides and the blue star is the phosphopeptide from the ovalbumin digest.

Interestingly, none of the phosphopeptides come from p65 itself. This most likely occurs because digestion of p65 does not produce phosphopeptides in the mass range we employ (*m*/*z* 1000-4000). Using the ProteinProspector MS-Digest Program (with no missed cleavages), we generate the potential p65 tryptic peptides that contain known phosphorylation sites. Unfortunately, only one of these peptides has a mass between 800-4000 Da, and we cannot be

sure that this particular peptide is phosphorylated in our samples.[39] In retrospect, p65 is not the best choice for verifying this technique.

The immunoprecipitates do contain eight phosphopeptides from the P1 or P2 isoform of the 60S acidic ribosomal protein (Ribosomal), which is likely associated with p65. Table 3.1 shows the m/z values and corresponding sequences of each peptide. The peptide at m/z 2029 is the mono-phosphopeptide (KEESEE**pS**DDDMGFGLFD), while the peptide at m/z 2109 is the diphosphopeptide with same sequence (KEE**pS**EE**pS**DDDMGFGLFD). Figures 3.11a and 3.11b show the MS/MS spectra of these peptides. The other phosphopeptides listed in Table 3.1 are peptides sharing the same sequence (KEESEESDDDMGFGLFD) but with modifications on methionine (Met) during alkylation.[40-42] The peptide at m/z 1734 is truncated from the peptide at m/z 2166, which may result from non-specific cleavage by trypsin, chymotrypsin proteolysis or proteolytic processing during sample preparation. We are unable to obtain a sequence for the peptide at m/z 1947, but the CID MS/MS spectrum gives a predominant neutral loss of 98 Da, which is an indication of a phosphopeptide ion. Additionally, at the low mass range, the CID MS/MS of this peptide contains some product ions identical to those resulting from the peptides with m/z 2029 and 1981. Thus, the peptide with m/z 1947 may share some of the sequence of the other peptides and contain a modification that we did not discover.

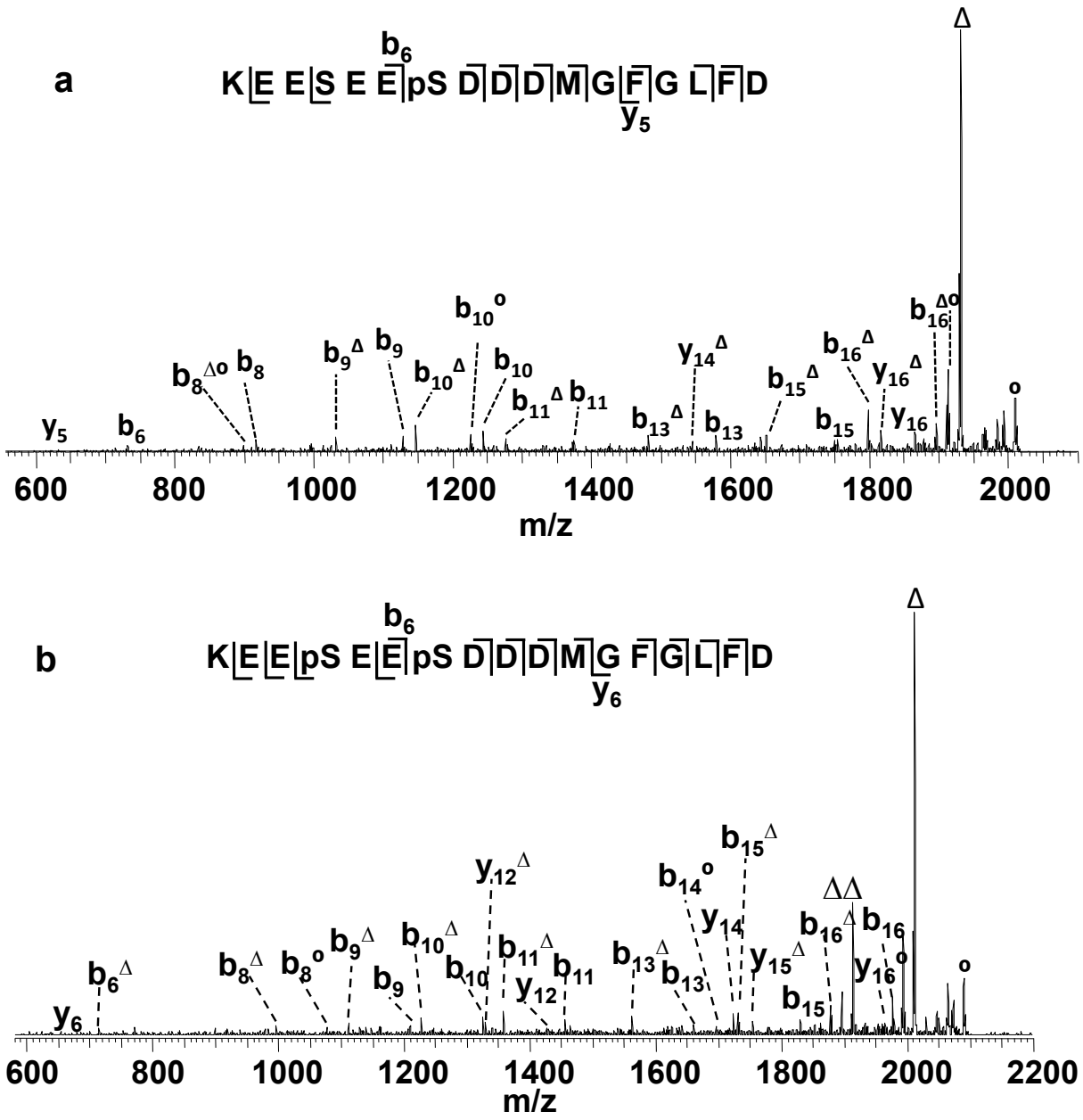

Figure 3.11. MALDI CID-MS/MS product-ion spectra of (a) the $[M+H]^+$ precursor ion of KEESEE**pS**DDDMGFGLFD (m/z 2029) and (b) the $[M+H]^+$ precursor ion of KEE**pS**EE**pS**DDDMGFGLFD (m/z 2109). The sequences show cleavage sites for formation of b and y ions. （Δ=-98 Da, o=-18 Da）

Table 3.1. Phosphopeptides identified from membrane-enriched tryptic digests of the nuclear extracts from TNF-α-treated THP-1 cells. The m/z value, peptide sequence and source are listed.

m/z $[M+H]^+$	Peptide sequence	Source
1734.8	KEE**pS**EE**pS**DDDMGF (1677.5+57: S-carbamidomethylmethionine)	Ribosomal
1947.5	Not sequenced	
1981.6	KEESEE**pS**DDDMGFGLFD (2029-48: loss of 2-(methylthio)acetamide)	Ribosomal
2029.6	KEESEE**pS**DDDMGFGLFD	Ribosomal
2061.6	KEEpSEE**pS**DDDMGFGLFD (2109-48: loss of 2-(methylthio)acetamide)	Ribosomal
2109.5	KEE**pS**EE**pS**DDDMGFGLFD	Ribosomal
2125.6	KEE**pS**EE**pS**DDDMGFGLFD (2109.5+16:Oxidation of methionine)	Ribosomal
2166.8	KEE**pS**EE**pS**DDDMGFGLFD (2109.5+57: S-carbamidomethylmethionine)	Ribosomal

These results suggest that the ribosomal protein associates with p65, although it is possible that it non-specifically interacts with the antibody beads. Ribosomal protein is involved in translational processes, and a study by Bouwmeester and coworkers indicates that nine ribosomal proteins and four other proteins are involved in ribosomal function with p65.[43-44] Thus it is highly likely that the Ribosomal protein associates with p65 during the IP process.

3.3.3 Analysis of *in vitro* phosphorylation of IκBα by GRK5

Recent studies by the Parameswaran group at Michigan State University suggest that similar to IKKβ, GRK5 can also mediate the activation of the NF-κB pathway via phosphorylation of IκBα.[17-18] The mutation of Ser 32 and 36, which are sites for IKKβ phosphorylation, alleviates but does not prevent the NF-κB activation. This fact suggests

that other potential phosphorylation sites co-conduct the signal transduction via NF-κB . Identification and localization of these sites will help in understanding the NF-κB pathway. We studied the phosphorylation of IκBα by GRK5 using HPLC-MS with and without enrichment (scheme 3.2)

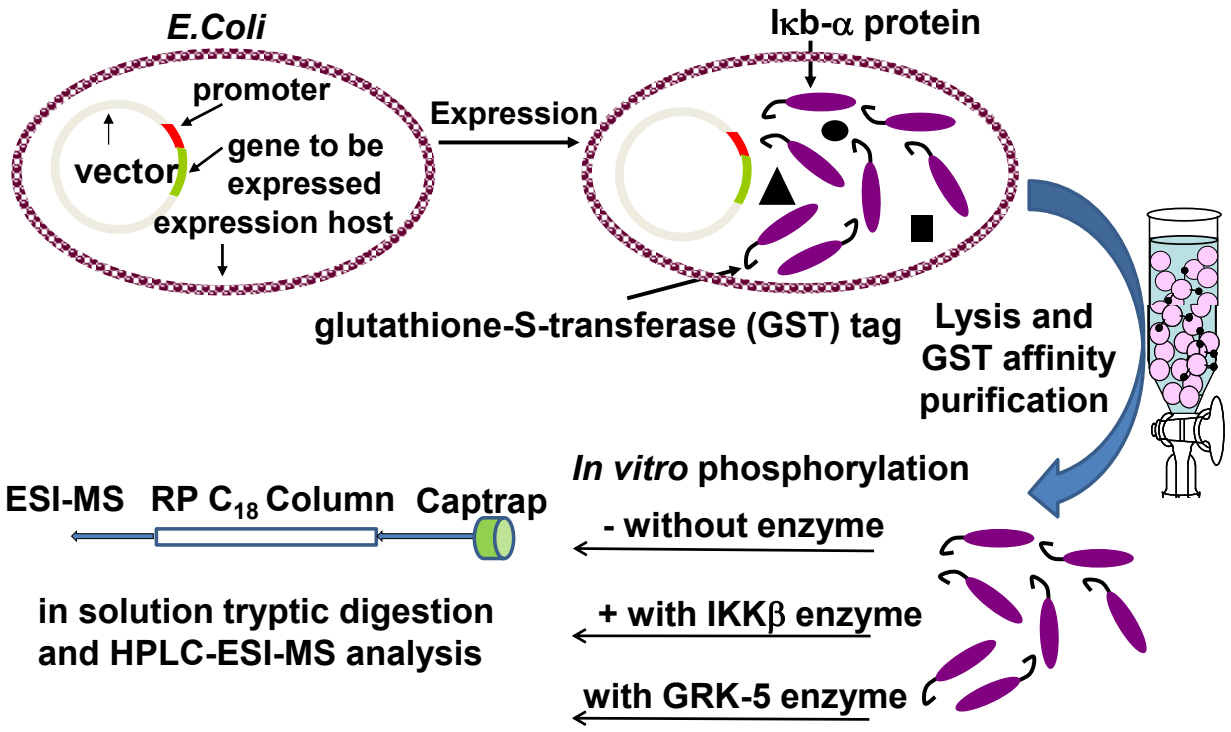

Scheme 3.2. Workflow for the investigation of phosphorylation of IκBα catalyzed by IKKβ and GRK5. The GST-IκBα protein is expressed in *E.Coli* and purified with a GST affinity column. The purified protein undergoes *in vitro* phosphorylation with no enzyme, with IKKβ or with GRK5. Each sample is later digested in solution by trypsin and the tryptic digest is analyzed by HPLC-ESI-MS. The protein expression and purification was performed by Ms. Wen Qin from Prof. Narayanan Parameswaran's group.

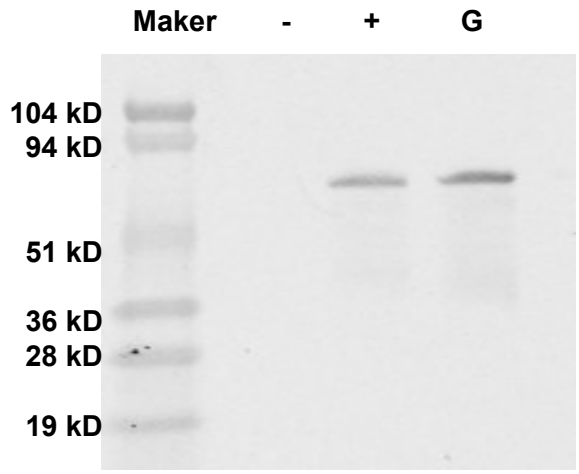

Figure 3.12. WB probe of phosphorylation of IκBα using phosphor- IκBα antibody from Cell Signaling Technology.

-: 0.12 μg Iκbα protein without any enzyme

+: 0.12 μg Iκbα protein with IKKβ enzyme

G: 0.12 μg Iκbα protein with GRK5 enzyme

After the *in vitro* phosphorylation, WB analysis confirmed the phosphorylation on IκBα by IKKβ and GRK5 (Figure 3.12). One pmol of digests of GST-IκBα and phosphorylated GST-IκBα (by GRK5) were submitted for LC-ESI-MS/MS analysis. Figure 3.13a shows the total ion current (TIC) chromatogram of the peptides eluted from the HPLC. Each peak may correspond to one or more peptides with multiple charge states. Figure 3.13b gives the full-MS scan at a retention time of 18.71 min, and the spectrum contains one dominant peptide signal and tens of small signals. At a given retention time, the peptides with the top five intensities are automatically selected for tandem MS spectra. Figure 3.13c reveals the CID-MS/MS spectrum of the $[M+3H]^{3+}$ precursor ion at m/z 768.23, which is a phosphopeptide with two phosphorylation sites (^{30}HD**pS**GLD**pS**MKDEEEQMVK). This result confirms that Ser32 and Ser36 are phosphorylated by GRK5.

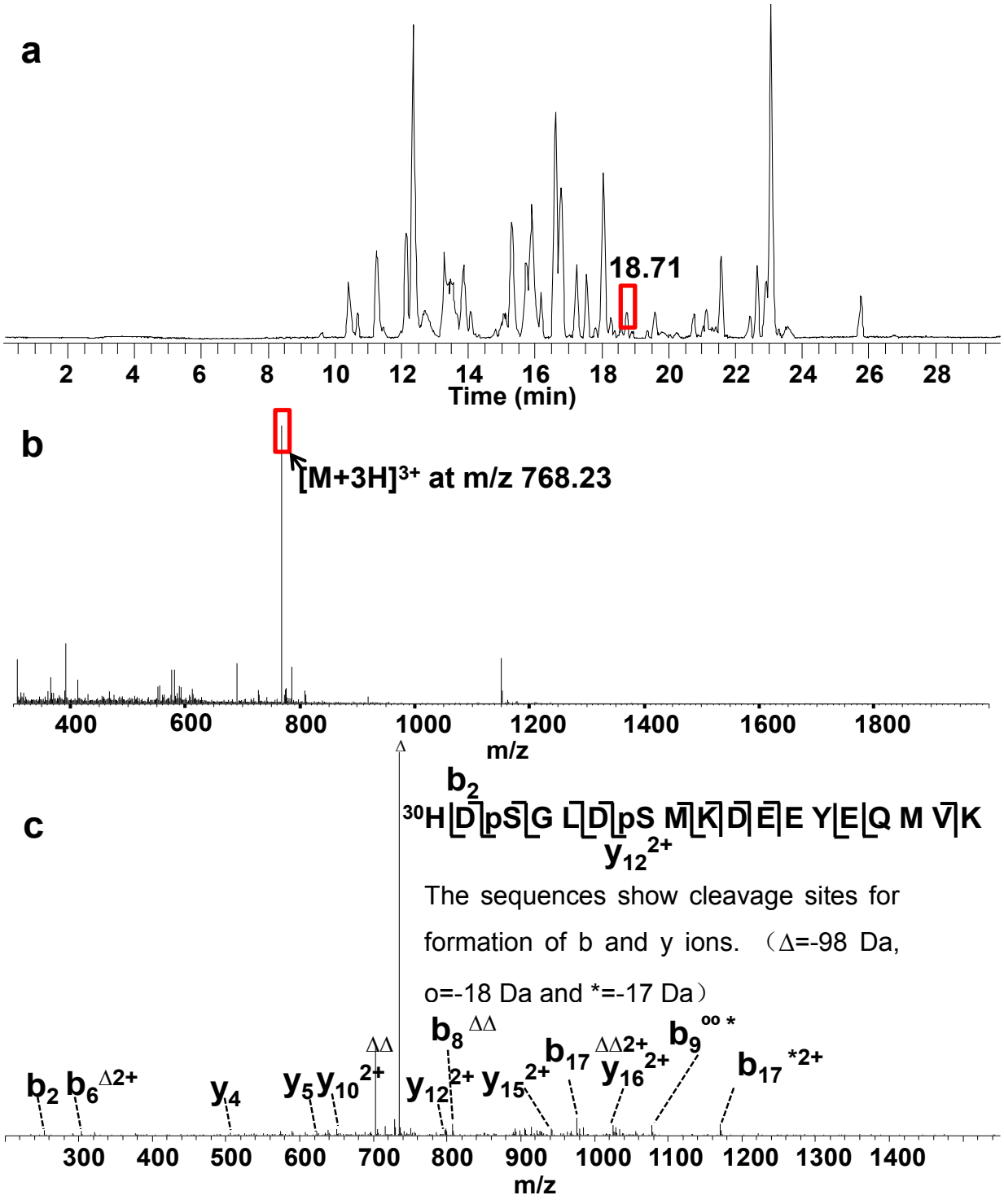

Figure 3.13 (a) TIC chromatogram of 1 pmol of a phosphorylated (by GRK5) IκBα digest (b) The full-MS scan of peptides eluted at 18.71 min in (a), and (c) CID-MS/MS spectrum of the $[M+3H]^{3+}$ precursor ion at m/z 768.23 in (b).

Table 3.2 lists all the peptides identified from 1 pmol of control GST-IκBα digests, and no phosphopeptides appear. Table 3.3 lists the peptides identified from the 1 pmol of GST-IκBα digests phosphorylated by GRK5. Among those peptides, three phosphopeptides stem from IκBα and two phosphopeptides stem from GRK5. Interestingly, the three phosphopeptides from IκBα have the same sequence (^{30}HDSGLDSMKDEEYEQMVK) but different modifications, including peptides eluting at 14.77 (pSer 32 and Carbamidomethyl (cam) on Met 37), 18.25 (pSer 32), and 18.71 (pSer 32 and 36) min. Furthermore signals for their two non-phosphorylated counterparts also appear at 14.06 and 17.51 min; one has cam on Met 37 and the other has no modification.

We estimate the phosphorylation efficiency using the ratio of the intensity sum of the three phosphopeptides to the intensity sum from all five peptides with the sequence ^{30}HDSGLDSMKDEEYEQMVK. The ratio suggests that 30-min *in vitro* phosphorylation of IκBα by GRK5 (enzyme/substrate mole ratio 1/3) yields ~40 % phosphorylation on ^{30}HDSGLDSMKDEEYEQMVK. The GRK5 also shows auto-phosphorylation reflected by DLVDIEQF**pSpT**VK or DLVDIEQF**pS**TVK sequences. We found no IκBα phosphorylation sites besides Ser 32 and 36, but this could be due to the low stoichiometry of the other phosphorylations, low sequence coverage from digestion or peptide loss during HPLC.

Phosphopeptide enrichment might enhance the phosphopeptide identification. Unfortunately, however, using the TiO_2-modified membrane enrichment does not reveal any phosphorylation sites. The presence of SDS or ATP may hinder the enrichment performance, and methods to remove the 0.4% SDS and 0.25 mM ATP from 0.08 μM proteins could lead to loss of protein. The ATP is essential for phosphorylation, but it may well compete with phosphopeptides

for binding sites. Further refinements in methods for ATP and SDS removal may lead to effective enrichment.

Table 3.2. Peptides identified using HPLC-ESI-MS/MS of 1 pmol of GST-IκBα digest. The retention time, peptide mass, sequence and origin protein are listed.

Retention Time	Peptide Mass	Peptide sequence	Origin Protein
9.7	631.62	LLDDR	IκBα
9.91	1661.44	YIADKHNM(cam)LGGC(cam)PK	GST
10.55	770.86	GLVQPTR	GST
10.84	1089.22	LTQSM(cam)AIIR	GST
11.42	703.72	GSEPWK	IκBα
12.18	1012.48	IKGLVQPTR	GST
12.56	967.84	LEPQEVPR	IκBα
12.97	2868.2	LLDDRHDSGLDSM(cam)KDEEYEQM(cam)VK	IκBα
13.05	1605.16	YIADKHNMLGGC(CAR)PK	GST
13.71	666.88	LVC(cam)FK	GST
13.9	2198.8	HDSGLDSM(cam)KDEEYEQMVK	IκBα
14.08	752.76	DEFTLK	GST
14.26	2198.8	HDSGLDSM(cam)KDEEYEQMVK	IκBα
14.53	2025.92	YEEHLYERDEGDKWR	GST
15.52	708.78	VDFISK	GST
15.93	1183.02	RIEAIPQIDK	GST
16.09	730.22	LPEMLK	GST
16.76	1033.06	LTQSMAIIR	GST
16.9	1027.08	IEAIPQIDK	GST
17.39	1077.34	VTYQGYSPY	IκBα
17.6	2158.06	HDSGLDSM(oxidation)KDEEYEQMVK	IκBα
18.21	932.96	ALTMEVIR	IκBα
18.65	1151.86	M(cam)SPILGYWK	GST
18.84	2754.92	LLDDRHDSGLDSMKDEEYEQMVK	IκBα
21.19	1859.59	ERAEISM(cam)LEGAVLDIR	GST
21.29	2261.29	VTYQGYSPYQLTWGRPSTR	IκBα
21.72	1574.35	AEISM(cam)LEGAVLDIR	GST
23.29	2324.44	QQLTEDGDSFLHLAIIHEEK	IκBα
23.66	2005.76	IAYSKDFETLKVDFLSK	GST
23.92	1442.08	DFETLKVDFLSK	GST
25.06	3156.3	LLLEYLEEKYEEHLYERDEGDKWR	GST
25.33	2688.55	HLAVITNQPEIAEALLGAGC(cam)DPELR	IκBα

Table 3.2 (cont'd)

25.69	1803.13	ERAEISMLEGAVLDIR	GST
26.05	2270.47	LLLEYLEEKYEEHLYER	GST
26.27	3865.4	HDSGLDSMC(cam)KDEEYEQM(DE)VK ELQEIQEIRLEPQEVPR	IκBα
26.53	1517.68	AEISMLEGAVLDIR	GST
26.98	2327.77	YIAWPLQGWQATFGGGDHPPK	GST
28.16	2358.01	KFELGLEPPNLPYYIDGDVK	GST
28.27	1933.9	GDLAFLNFQNNLQQTPL	IκBα
29.1	2174.38	TALHLAVDLQNPDLVSLLLK	IκBα
30.03	2230.54	FELGLEFPNLPYYIDGDVK	GST

Table 3.3. Peptides identified using HPLC-ESI-MS/MS of 1 pmol of GST-IκBα digest phosphorylated by GRK5. The retention time, peptide mass, sequence and origin protein are listed.

Retention time	Peptide mass	Peptide sequence	Origin protein
10.37	771	GLVQPTR	GST
10.63	1090.26	LTQSM(cam)AIIR	GST
11.2	787.56	LPEM(cam)LK	GST
12.3	968.12	LEPQEVPR	IκBα
13.82	753.2	DEFTLK	GST
14.06	2199.64	HDSGLDSM(cam)KDEEYEQMVK	IκBα
14.77	2279.6	HD**pS**GLDSM(cam)KDEEYEQMVK	IκBα
15.27	708.98	VDFISK	GST
15.71	1183.28	RIEAIPQIDK	GST
15.87	730.98	LPEMLK	GST
16.31	1627.24	GVNLDHTDDDFYSK	GRK5
16.58	1033.22	LTQSMAIIR	GST
16.75	1027.32	IEAIPQIDK	GST
17.21	916.18	ISDLGLAVK	GRK5
17.51	2142.67	HDSGLDSMKDEEYEQMVK	IκBα
18	933.26	ALTMEVIR	IκBα
18.25	2222.53	HD**pS**GLDSMKDEEYEQMVK	IκBα
18.55	1152.42	M(cam)SPILGYWK	GST
18.71	2302.48	HD**pS**GLD**pS**MKDEEYEQMVK	IκBα
19.57	1748.44	VGTVGYMAPEVLNNQR	GRK5
21.12	2262.01	VTYQGYSPYQLTWGRPSTR	IκBα

Table 3.3 (cont'd)

21.26	1575.44	AEISM(cam)LEGAVLDIR	GST
22.63	1912.54	DLKPENILLDDYGHIR	GRK5
22.71	1554.14	DLVDIEQF**pSpT**VK	GRK5
22.77	1474.26	DLVDIEQF**pS**TVK	GRK5
22.92	1095.22	MSPILGYWK	GST
23.06	1150.42	LLLEYLEEK	GST
25.74	2076.98	SPVFIAQVGQDLVSQTEEK	GRK5

3.4 Conclusions

The TiO_2-modified membrane effectively facilitated enrichment of the phosphopeptides from an *in vivo* phosphorylated fusion protein, Jun-Tev-tau. MS analysis of the enriched eluate revealed 7 phosphorylation sites on p-tau, three of which seem dominant. Identification of such sites might aid the design of therapeutic drugs that inhibit phosphorylation.[45-46] In phosphopeptide enrichment of an IP of p65, we find 8 phosphorylated peptides that correspond to only 2 unique phosphorylation sites from the p65-associated ribosomal protein. Membrane-based enrichment is rapid and facilitates simple identification of phosphopeptides. However, enrichment of *in vitro* phosphorylated IκBα does not reveal any phosphopeptides, perhaps because ATP or SDS interferes with binding. HPLC-MS, though more time consuming than membrane-based enrichment and direct MS, is sufficiently sensitive to reveal phosphorylation of IκBα at ser32 and ser36. The coupling of on-line membrane enrichment to HPLC-MS is worth trying in the future, but issues of solvent compatibility, membrane stability (preventing leaching of TiO_2, polyelectrolyte and substrate compounds), and compatibility of enrichment with compounds in the sample must be addressed. Overall, membrane-based enrichment is attractive for identifying phosphorylation in modestly complex samples such as fusion proteins.

3.5 Acknowledgement

Many thanks to Dr. Dexin Sui and Prof. Min-Hao Kuo for their collaboration in the p-tau study and Ms. Li Cui for useful discussion, to Dr. Amanda Palumbo, Dr. Teri Lansdell and Prof. Jetze J. Tepe for their collaboration in the p65 study, to Dr. Xiao Zhou, Ms. Wen Qin, and Prof. Narayanan Parameswaran for their collaboration in the IκBα Study. We are grateful to the U.S. National Institutes of Health (GM 080511, Bruening and AG039768, Kuo) for funding this work.

REFERENCES

3.6 References

1. Aebersold, R.; Mann, M., Mass Spectrometry-Based Proteomics. *Nature* **2003,** *422* (6928), 198-207.

2. Olsen, J. V.; Blagoev, B.; Gnad, F.; Macek, B.; Kumar, C.; Mortensen, P.; Mann, M., Global, in vivo, and Site-Specific Phosphorylation Dynamics in Signaling Networks. *Cell* **2006,** *127* (3), 635-648.

3. Thingholm, T. E.; Jensen, O. N.; Larsen, M. R., Analytical Strategies for Phosphoproteomics. *Proteomics* **2009,** *9* (6), 1451-1468.

4. Witze, E. S.; Old, W. M.; Resing, K. A.; Ahn, N. G., Mapping Protein Post-Translational Modifications with Mass Spectrometry. *Nat. Methods* **2007,** *4* (10), 798-806.

5. Han, X.; Aslanian, A.; Yates III, J. R., Mass Spectrometry for Proteomics. *Curr. Opin. Chem. Biol.* **2008,** *12* (5), 483-490.

6. Zhou, H.; Low, T. Y.; Hennrich, M. L.; van der Toorn, H.; Schwend, T.; Zou, H.; Mohammed, S.; Heck, A. J. R., Enhancing the Identification of Phosphopeptides from Putative Basophilic Kinase Substrates Using Ti (IV) Based IMAC Enrichment. *Mol. Cell. Proteomics* **2011,** *10* (10).

7. Leitner, A., Phosphopeptide Enrichment Using Metal Oxide Affinity Chromatography. *Trac-Trend Anal. Chem.* **2010,** *29* (2), 177-185.

8. Sergeant, N.; Delacourte, A.; Buee, L., Tau Protein as a Differential Biomarker of Tauopathies. *Biochim. Biophys. Acta, Mol. Basis Dis.* **2005,** *1739* (2-3), 179-197.

9. Wang, J. Z.; Wu, Q. L.; Smith, A.; Grundke-Iqbal, I.; Iqbal, K., Tau Is Phosphorylated by GSK-3 at Several Sites Found in Alzheimer Disease and Its Biological Activity Markedly Inhibited Only after It Is Prephosphorylated by a-Kinase. *FEBS Lett.* **1998,** *436* (1), 28-34.

10. Gilmore, T. D., Introduction to NF-[Kappa]B: Players, Pathways, Perspectives. *Oncogene* **2006,** *25* (51), 6680-6684.

11. Brasier, A., The NF-Kb Regulatory Network. *Cardiovasc. Toxicol.* **2006,** *6* (2), 111-130.

12. Perkins, N. D., Integrating Cell-Signalling Pathways with NF-[Kappa]B and IKK Function. *Nat Rev Mol Cell Biol* **2007,** *8* (1), 49-62.

13. Meffert, M. K.; Chang, J. M.; Wiltgen, B. J.; Fanselow, M. S.; Baltimore, D., NF-[Kappa]B Functions in Synaptic Signaling and Behavior. *Nat. Neurosci.* **2003,** *6* (10), 1072-1078.

14. Tian, B.; Brasier, A. R., Identification of a Nuclear Factor Kappa B-Dependent Gene Network. *Recent Prog. Horm. Res.* **2003,** *58* (1), 95-130.

15. Albensi, B. C.; Mattson, M. P., Evidence for the Involvement of TNF and NF-Kb in Hippocampal Synaptic Plasticity. *Synapse* **2000,** *35* (2), 151-159.

16. Vallabhapurapu, S.; Karin, M., Regulation and Function of NF-Kb Transcription Factors in the Immune System. *Annu. Rev. Immunol.* **2009,** *27* (1), 693-733.

17. Patial, S.; Luo, J.; Porter, K. J.; Benovic, J. L.; Parameswaran, N., G-Protein-Coupled-Receptor Kinases Mediate TNFα-Induced NF-Kb Signalling Via Direct Interaction with and Phosphorylation of IκBα. *Biochem. J* **2009,** *425* (1), 169-178.

18. Patial, S.; Shahi, S.; Saini, Y.; Lee, T.; Packiriswamy, N.; Appledorn, D. M.; LaPres, J. J.; Amalfitano, A.; Parameswaran, N., G-Protein Coupled Receptor Kinase 5 Mediates Lipopolysaccharide-Induced NFκB Activation in Primary Macrophages and Modulates Inflammation in vivo in Mice. *J. Cell. Physiol.* **2011,** *226* (5), 1323-1333.

19. Wang, W.-H.; Palumbo, A. M.; Tan, Y.-J.; Reid, G. E.; Tepe, J. J.; Bruening, M. L., Identification of P65-Associated Phosphoproteins by Mass Spectrometry after on-Plate Phosphopeptide Enrichment Using Polymer-Oxotitanium Films. *J. Proteome Res.* **2010,** *9* (6), 3005-3015.

20. Wagner, U.; Utton, M.; Gallo, J. M.; Miller, C. C. J., Cellular Phosphorylation of Tau by GSK-3 Beta Influences Tau Binding to Microtubules and Microtubule Organisation. *J. Cell Sci.* **1996,** *109*, 1537-1543.

21. Hanger, D. P.; Noble, W., Functional Implications of Glycogen Synthase Kinase-3-Mediated Tau Phosphorylation. *Int. J. Alzheimers Dis.* **2011,** *2011*, 352805.

22. Rankin, C.; Sun, Q.; Gamblin, T., Tau Phosphorylation by GSK-3β Promotes Tangle-Like Filament Morphology. BioMed Central: 2007.

23. Smet-Nocca, C.; Broncel, M.; Wieruszeski, J.-M.; Tokarski, C.; Hanoulle, X.; Leroy, A.; Landrieu, I.; Rolando, C.; Lippens, G.; Hackenberger, C. P. R., Identification of O-Glcnac Sites within Peptides of the Tau Protein and Their Impact on Phosphorylation. *Mol. Biosyst.* **2011,** *7* (5), 1420-1429.

24. Palumbo, A. M.; Reid, G. E., Evaluation of Gas-Phase Rearrangement and Competing Fragmentation Reactions on Protein Phosphorylation Site Assignment Using Collision Induced Dissociation-MS/MS and MS(3). *Anal. Chem.* **2008,** *80* (24), 9735-9747.

25. Palumbo, A. M.; Smith, S. A.; Kalcic, C. L.; Dantus, M.; Stemmer, P. M.; Reid, G. E., Tandem Mass Spectrometry Strategies for Phosphoproteome Analysis. *Mass Spectrom. Rev.* **2011,** *30* (4), 600-625.

26. Kim, M.-S.; Zhong, J.; Kandasamy, K.; Delanghe, B.; Pandey, A., Systematic Evaluation of Alternating Cid and Etd Fragmentation for Phosphorylated Peptides. *Proteomics* **2011,** *11* (12), 2568-2572.

27. Hanger, D. P.; Anderton, B. H.; Noble, W., Tau Phosphorylation: The Therapeutic Challenge for Neurodegenerative Disease. *Trends Mol. Med.* **2009,** *15* (3), 112-119.

28. Thingholm, T. E.; Jensen, O. N.; Robinson, P. J.; Larsen, M. R., Simac (Sequential Elution from IMAC), a Phosphoproteomics Strategy for the Rapid Separation of Monophosphorylated from Multiply Phosphorylated Peptides. *Mol. Cell. Proteomics* **2008,** *7* (4), 661-671.

29. Reynolds, C. H.; Betts, J. C.; Blackstock, W. P.; Nebreda, A. R.; Anderton, B. H., Phosphorylation Sites on Tau Identified by Nanoelectrospray Mass Spectrometry. *J. Neurochem.* **2000,** *74* (4), 1587-1595.

30. Cohen, P.; Frame, S., The Renaissance of GSK3. *Nat Rev Mol Cell Biol* **2001,** *2* (10), 769-776.

31. Hoffmann, A.; Baltimore, D., Circuitry of Nuclear Factor Kappa B Signaling. *Immunol. Rev.* **2006,** *210*, 171-186.

32. Karin, M.; Lin, A., NF-Kappa B at the Crossroads of Life and Death. *Nat. Immunol.* **2002,** *3* (3), 221-227.

33. Sen, R.; Baltimore, D., Multiple Nuclear Factors Interact with the Immunoglobulin Enhancer Sequences. *Cell* **1986,** *46* (5), 705-716.

34. Vallabhapurapu, S.; Karin, M., Regulation and Function of NF-Kappa B Transcription Factors in the Immune System. *Annu. Rev. Immunol.* **2009,** *27*, 693-733.

35. Bonizzi, G.; Karin, M., The Two NF-Kappa B Activation Pathways and Their Role in Innate and Adaptive Immunity. *Trends Immunol.* **2004,** *25* (6), 280-288.

36. O'Shea, J. M.; Perkins, N. D., Regulation of the Reia (P65) Transactivation Domain. *Biochem. Soc. Trans.* **2008,** *36*, 603-608.

37. Perkins, N. D., Post-Translational Modifications Regulating the Activity and Function of the Nuclear Factor Kappa B Pathway. *Oncogene* **2006,** *25* (51), 6717-6730.

38. Mann, M.; Ong, S. E.; Gronborg, M.; Steen, H.; Jensen, O. N.; Pandey, A., Analysis of Protein Phosphorylation Using Mass Spectrometry: Deciphering the Phosphoproteome. *Trends Biotechnol.* **2002,** *20* (6), 261-268.

39. Ryo, A.; Suizu, F.; Yoshida, Y.; Perrem, K.; Liou, Y. C.; Wulf, G.; Rottapel, R.; Yamaoka, S.; Lu, K. P., Regulation of NF-Kappa B Signaling by Pin1-Dependent Prolyl Isomerization and Ubiquitin-Mediated Proteolysis of P65/Rela. *Mol. Cell* **2003,** *12* (6), 1413-1426.

40. Lapko, V. N.; Smith, D. L.; Smith, J. B., Identification of an Artifact in the Mass Spectrometry of Proteins Derivatized with Iodoacetamide. *J. Mass Spectrom.* **2000,** *35* (4), 572-575.

41. Kruger, R.; Hung, C. W.; Edelson-Averbukh, M.; Lehmann, W. D., Iodoacetamide-Alkylated Methionine Can Mimic Neutral Loss of Phosphoric Acid from Phosphopeptides as Exemplified by Nano-Electrospray Ionization Quadrupole Time-of-Flight Parent Ion Scanning. *Rapid Commun. Mass Spectrom.* **2005,** *19* (12), 1709-1716.

42. Reid, G. E.; Roberts, K. D.; Simpson, R. J.; O'Hair, R. A. J., Selective Identification and Quantitative Analysis of Methionine Containing Peptides by Charge Derivatization and Tandem Mass Spectrometry. *J. Am. Soc. Mass Spectrom.* **2005,** *16* (7), 1131-1150.

43. Wool, I. G., Extraribosomal Functions of Ribosomal Proteins. *Trends Biochem. Sci* **1996,** *21* (5), 164-165.

44. Lindstrom, M. S., Emerging Functions of Ribosomal Proteins in Gene-Specific Transcription and Translation. *Biochem. Biophys. Res. Commun.* **2009,** *379* (2), 167-170.

45. Hong, M.; Chen, D. C. R.; Klein, P. S.; Lee, V. M. Y., Lithium Reduces Tau Phosphorylation by Inhibition of Glycogen Synthase Kinase-3. *J. Biol. Chem.* **1997,** *272* (40), 25326-25332.

46. Mazanetz, M. P.; Fischer, P. M., Untangling Tau Hyperphosphorylation in Drug Design for Neurodegenerative Diseases. *Nat. Rev. Drug Discovery* **2007,** *6* (6), 464-479.

Chapter 4. Limited Proteolysis Via msec-Digestions in Protease-Modified Membranes

(This chapter was submitted for publication as part of an article in *Analytical Chemistry*)

Sequential adsorption of poly(styrene sulfonate) (PSS) and proteases in porous nylon yields enzymatic membrane reactors for limited protein digestion. Although a high local enzyme density (~30 mg/cm^3) and small pore diameters in the membrane lead to digestion in < 1 sec, the low membrane thickness (170 μm) affords control over residence times at the ms level to limit digestion. Apomyoglobin digestion demonstrates that peptide lengths increase as the residence time in the membrane decreases. Moreover, electron transfer dissociation (ETD) tandem mass spectrometry (MS/MS) on a large myoglobin proteolytic peptide (8 kD) provides a resolution of 1-2 amino acids. Under denaturing conditions, limited membrane digestion of bovine serum albumin (BSA) and subsequent ESI-Orbitrap MS analysis reveal large peptides (3-10 kD) that increase the sequence coverage from 53 % (2-s digestion) to 82 % (0.05-s digestion).

4.1 Introduction

Proteolysis is a vital initial step in most analyses of proteins by MS. Traditional in-solution digestion employs a dilute protease solution to avoid sample contamination and self-digestion of the enzyme, but the low protease concentration leads to extended digestion times. To increase throughput and facilitate online MS analysis, a number of research groups now employ immobilized enzymes for proteolysis.[1-3] Immobilization greatly reduces self-digestion even at high local enzyme density (e.g. 30 mg/cm^3),[4-6] and such high densities allow protein

digestion in as little as a few seconds. In addition, adsorption stabilizes the enzyme in many cases.[1] Protease immobilization can occur via covalent,[7] hydrophobic[4, 6] or electrostatic interactions,[8] and supports for these enzymes include resins,[9] monoliths,[5] polymeric microfluidic channels[4, 10] and membranes.[6] All of these substrates provide relatively high surface areas for protease binding. However, porous membranes are unique in that their minimal thickness (typically 10-170 μm) should afford fine control over proteolysis time in flow-through digestion. When coupled with simple syringe pumps, membranes provide digestion times ranging from a few milliseconds to several seconds.

This chapter exploits short residence times in enzyme-modified membranes to perform limited proteolysis of BSA and apomyoglobin. We hypothesize that decreasing membrane residence times will lead to longer peptides with more charge (Figure 4.1), and this is particularly the case for pepsin-modified membranes. Unlike solution digestion, where partially digested peptides continuously compete with intact proteins for enzyme sites that catalyze additional proteolysis, convective flow in membranes rapidly separates digested peptides from immobilized enzymes. Large proteolytic peptides often contain more basic residues than small tryptic peptides and are particularly amenable to ETD MS/MS analyses with high amino acid resolution, which is important for studies of hydrogen/deuterium exchange (HDX) to determine amino acid accessibility.[11-12] Current methods for creating large proteolytic peptides employ expensive enzymes such as Asp-N and Glu-C that cut proteins only before or after one type of amino acid.[13] However, these methods work only for a few proteins that contain a limited number of cleavable sites. Limited digestion in membranes should be applicable to a wide range of proteins because generation of long peptides relies on rapid convection of partially digested peptides away from the protease.

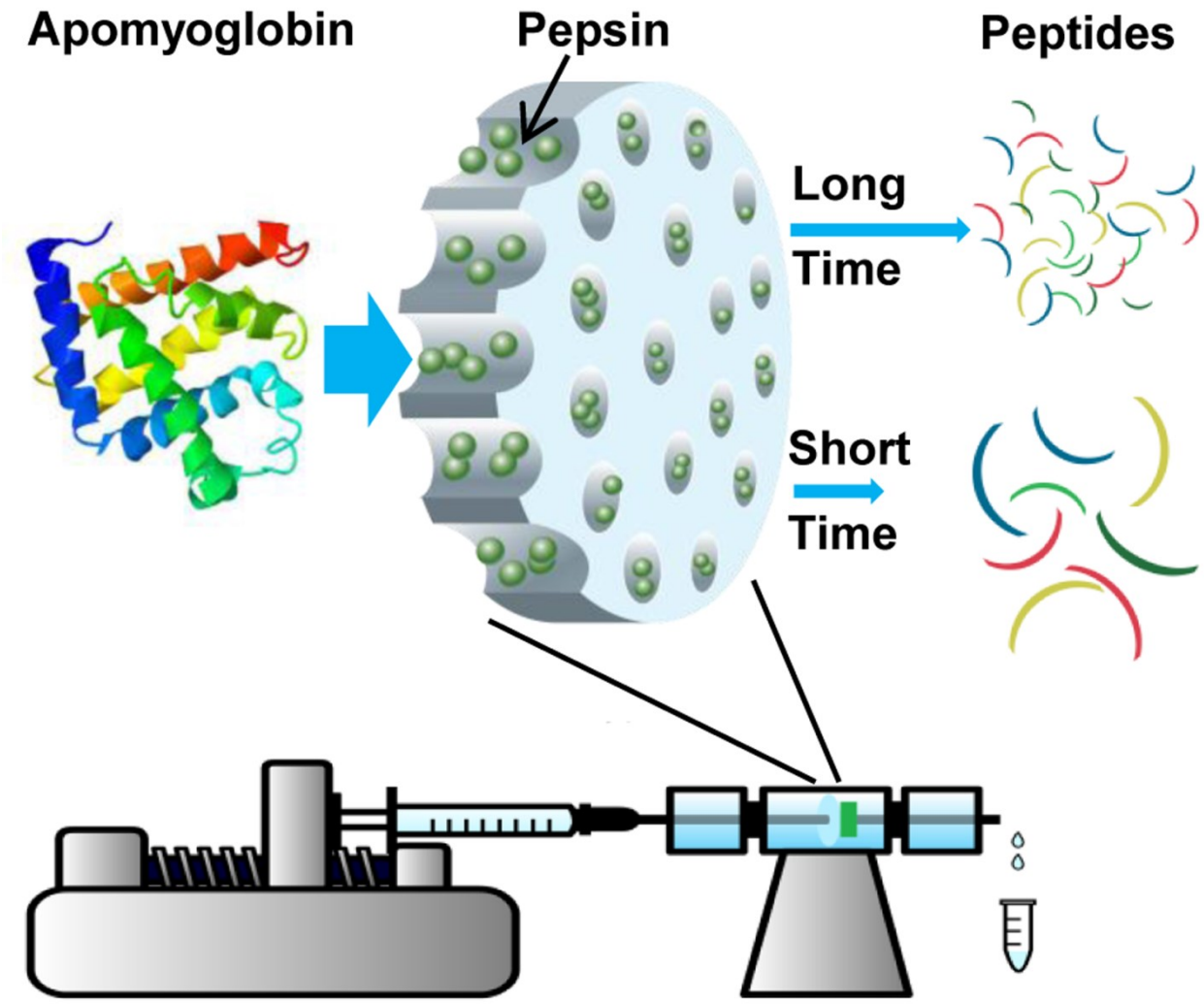

Figure 4.1. Cartoon of controlled digestion using a membrane containing immobilized pepsin and a miniaturized holder with a syringe pump. (The apomyoglobin structure was generated from PDB 1MBN.）

4.2 Experimental

4.2.1 Materials

Pepsin from porcine gastric mucosa (lyophilized powder, 3200-4500 units/mg protein), trypsin from bovine pancreas (type I, 12200 units/mg solid), α-chymotrypsin from bovine pancreas (L-1-tosylamide-2-phenylethyl chloromethyl ketone treated to inactivate residual trypsin activity, type VII, salt-free lyophilized power), apomyoglobin (protein sequencing grade from horse skeletal muscle, salt-free lyophilized powder), PSS (average molecular weight ~70,000), and bovine serum albumin (BSA) were purchased from Sigma-Aldrich. Important chemicals for digestion and analysis included Tris-HCl (Invitrogen), urea (J.T.Baker), 1,4-dithio-DL-threitol (DTT) (BioChemika), iodoacetamide (Sigma), ammonium bicarbonate (Columbus Chemical), 2,5-dihydroxybenzoic acid (DHB, Sigma), tris(2-carboxyethyl) phosphine hydrochloride (TCEP, >98%, Fluka), Progenta^{TM} non-ionic acid labile surfactant (NALS, Protabio), and formic acid (FA, > 96%, Spectrum) .

4.2.2 Membrane and holder

The unmodified nylon membranes (25 mm-diameter, 0.45 μm nominal pore size) were obtained from Millipore (HNWP02500). Membrane modification employed an Amicon cell (model 8010, Millipore) that exposed a membrane area of 3.8 cm^2. A peristaltic pump pulled solutions through the membrane. For experiments with small sample volumes (<1 mL), a 6 mm-diameter piece of membrane was placed in a flangeless fitting system (A-424, Upchurch Scientific) connected to 1/16 inch OD tubing via ferrules. The membrane was supported by a frit in the holder. The membrane area exposed to sample was 0.02 cm^2, and sample injection

occurred via a syringe pump (Cole-Parmer 74900 series) using a 1-mL or 5-mL disposable syringe.

4.2.3 Modification of membranes with proteases

Modification of UV/ozone-cleaned (10 min) nylon membranes with trypsin was reported previously, but I increased the trypsin concentration in the adsorption solution from 0.6 to 1.0 mg/mL.[8] For modification with pepsin, the procedure was similar and also occurred through consecutive adsorption of PSS and proteases. Ten mL of a 0.02 M PSS, 0.5 M NaCl solution (pH=2.3) was first passed through the membrane at 2 mL/min, followed by 30 mL of deionized water at the same flow rate. Subsequently, 4 mL of 2 mg/mL pepsin in 5% v/v FA was circulated through the membrane at 1 mL/min for one hour. After protease deposition, the membrane was rinsed with 30 mL of 5% v/v FA. Modified membranes were dried and stored in a desiccator. Using a Bradford assay with calibration curves, the amount of pepsin in the membrane was determined from the decrease in pepsin concentration in the loading solution after circulation through the membrane. The amounts of trypsin immobilized in membranes were similarly determined from direct UV absorbance at 280 nm using a Nanodrop^{TM} UV/Vis Spectrometer (Thermo).

4.2.4 Controlled apomyoglobin digestion with a pepsin-modified membrane

Without urea denaturation or reduction, 100 μg of apomyoglobin was dissolved in 1 mL of 5% v/v FA, and this solution was passed through a small membrane (Figure 4.1) at flow rates from 0.1 to 30 mL/h. We calculated the residence time by dividing the membrane pore volume (estimated assuming 50% porosity, a 170-μm thickness, and for the small holder 0.02 cm^2 of

external area) by the flow rate. Consequently, the residence times for 0.1 and 30 mL/h flow rates were 6 s and 0.02 s, respectively. Fifty μL of each digest was collected, dried with a Speed-Vac and reconstituted in 50 μL of 1% acetic acid/49% H_2O/50% methanol. The same experiments were also carried out with a trypsin-modified membrane, except that the apomyoglobin buffer was 10 mM NH_4HCO_3. For in-solution peptic digestion, 100 μg of apomyoglobin in 200 μL 5% v/v FA was mixed with 5 μg of pepsin and incubated at 37 ºC for 5 min or 20 s. Two hundred μL of acetonitrile was added to stop the reaction, and the solution was immediately frozen with liquid nitrogen and lyophilized with a Speed-Vac.

4.2.5 Controlled BSA digestion with a pepsin-modified membrane

BSA was digested with urea denaturation and TCEP reduction. Thus, 100 μg of BSA was dissolved in 10 μL of 6 M urea and mixed with 1 μL of 0.5 M TCEP for 30 min at 56 ºC. To make a 0.1 mg/mL BSA solution, 989 μL of 5% v/v FA was added to the above 11 μL samples. This solution was passed through a small membrane at 0.3, 1.5, 3, 6 and 12 mL/h (the 5-mL syringe was used for the last two flow rates). Two hundred μL of each digest was collected, dried with a Speed-Vac and reconstituted in 200 μL of 1% acetic acid/49% H_2O/50% methanol. A similar experiment occurred with a trypsin-modified membrane, except that we applied a NALS as the denaturation agent following the manufacture's protocol with slight modification: 100 μg of BSA was dissolved in 20 μL of 0.1 % NALS at pH 7.8 (50 mM NH_4HCO_3), reduced with 5 μL of 10 mM DTT for 30 min at 56 ºC and allowed to react with 10 μL of 100 mM iodoacetamide in the dark for 30 min.

4.2.6 Mass spectrometry and data analysis

An LTQ XL ion trap mass spectrometer equipped with a vMALDI source (Thermo Fisher) was used to perform MALDI-MS and CID-MS/MS analyses. Typically, 1 μL of sample solution was spotted onto the stainless steel MALDI plate, followed by addition of 1 μL of matrix solution (40 mg/mL of 2,5 DHB in 1% TFA, 49% H_2O, 50% ACN) and drying. MALDI-MS spectra were acquired using a laser power of 10 μJ across the m/z range 300-2000 (normal mass range) or 800-4000 (high mass range). Spectra were the average of 30-100 scans.

For ESI-MS analyses, 40 μL of samples in 1% acetic acid, 49% H_2O and 50% methanol were loaded into a Whatman multichem 96-well plate (Sigma Aldrich) and sealed with Teflon Ultra Thin Sealing Tape (Analytical Sales and Services, Prompton Plains, NJ). Then, using an Advion Triversa Nanomate nano-electrospray ionization (nESI) source (Advion, Ithaca, NY) with a spray voltage of 1.4 kV and a gas pressure of 1.0 psi, samples were introduced into a high resolution accurate mass LTQ Orbitrap Velos mass spectrometer (Thermo Fisher) equipped with a dual pressure ion trap, Higher-Energy Collisional Dissociation (HCD) cell and ETD. The ion source interface settings (inlet temperature of 200 ^{o}C and S-Lens value of 60 %) were optimized to maximize the sensitivity of the precursor ions while minimizing 'in-source' fragmentation. High resolution mass spectra, as well as all ETD-MS/MS spectra, were acquired in positive ionization mode using the FT analyzer operating at 100,000 resolving power. Spectra were typically signal averaged for 30-300 scans, and peptide precursor ions were mass-selected using an isolation width of 5 Da. In ETD-MS/MS, fragmentation of isolated ions was performed when an automatic gain control (AGC) target value of 5.0×10^4 was reached within a 100 ms maximum injection time in the ion trap. The AGC value and maximum injection time of the

reagent ion (fluoranthene anion) were set as 1.0×10^5 and 100 ms, respectively, and the reaction time was optimized as 15 ms for the +10 charge state.

Peptides in Tables 4.1 and 4.2 were identified using peptide mass fingerprinting. If the monoisotopic peak (m/z=a) could be found, then the monoisotopic peptide mass was calculated by using the equation, M+H= (a*z-(z-1)*1.0078). The calculated mass was matched with a mass from *in silico* digestion of the target protein with ProteinProspector (http://prospector.ucsf.edu). For ESI-Orbitrap data, the mass tolerance was 5 ppm. If the monoisotopic peak could not be located, the mass of the highest peak served as an estimate of the average mass of the target peptide. The simulated spectrum of the potential peptide match was then compared with the experimental spectrum, and the peptide was assigned if specific isotopic signals in the two spectra matched within 5 ppm. For MALDI-LTQ data, the mass tolerance was 100 ppm.

4.3 Results and discussion

4.3.1 Membrane modification with protease

We previously showed that alternating adsorption of PSS and trypsin effectively immobilizes trypsin in nylon membranes.[8] In 2.7 mM HCl, the protonated trypsin (isoelectric point, pI, of 10.2) adsorbs to negatively charged PSS.[8, 14-15] Pepsin has a much lower pI (2.8), so we both adsorb this protease and perform peptic digestion using solutions containing 5% v/v FA (pH=2). Based on analyses of protease adsorption solutions, the protease/PSS-modified nylon membranes contain ~30 mg of trypsin/cm^3 of pores, and ~60 mg pepsin/cm^3 (Figure 4.2). These values assume a membrane porosity of 50%. Control experiments show that pepsin and trypsin do not adsorb to the bare membrane without PSS. The high local protease density in

modified membranes, compared to 0.025 mg/cm^3 for in-solution digestion, leads to membrane-based protein digestion in times ranging from milliseconds to seconds, depending on the protein.

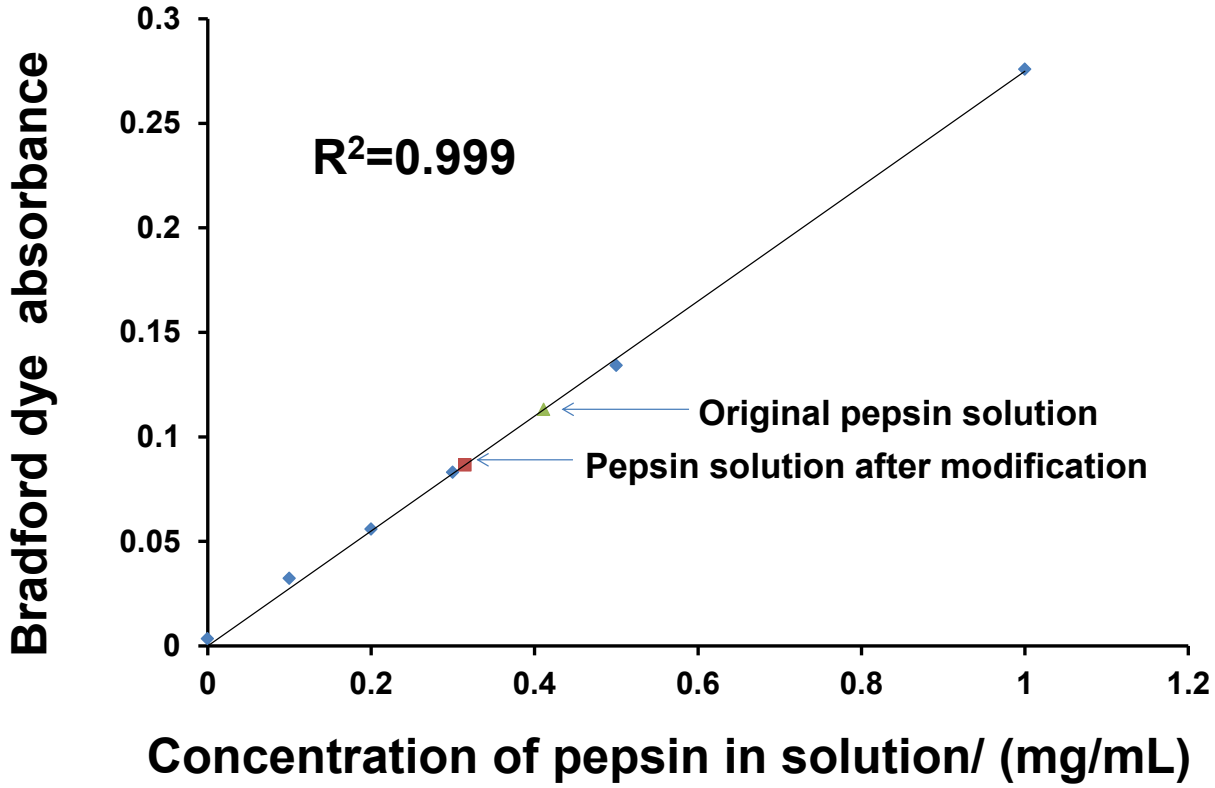

Figure 4.2**.** Bradford assay calibration curve for pepsin, and the absorbance of a pepsin solution (0.4 mg/mL after a 5-fold dilution) before and after circulating through the membrane. By subtraction, we estimate that 1.8 mg of pepsin adsorbed to the PSS-modified nylon membrane. This corresponds to a local density of 60 mg pepsin per cm^3 of pore.

4.3.2 Apomyoglobin digestion with different membrane residence times

Due to its simple secondary structure and high purity, apomyoglobin served as the first model protein to test our hypothesis that decreasing the membrane residence time will give longer proteolytic peptides. Figure 4.3 shows manually deconvoluted ESI-Orbitrap mass spectra

of myoglobin digested by passing solutions through pepsin-modified membranes at flow rates of 0.1, 1, 10 and 30 mL/h, which correspond to residence times of 6, 0.6, 0.06 and 0.02 s, respectively. As the residence time decreases, large peptides emerge and the strongest signals shift to a higher m/z region. (Figure 4.4 shows the original spectra, and Table 4.1 lists peptides identified from the spectra along with their monoisotopic masses, amino acid positions and cleavage sites). With the 6-s residence time, all detected peptides have masses less than 5 kD, suggesting a relatively complete digestion. In-solution digestion for 5 min or 20 s and membrane digestion for 6 s give similar mass spectra that yield 100 % sequence coverage with a minimum of 5 peptides (**2**, **7**, **8**, **11** and **13**) (Figure 4.5). For the 0.6 and 0.06-s membrane-based digestions, covering the entire 153 amino acid sequence requires 4 peptides (**2**, **7**, **8**, and **16**) and only 3 peptides (**7**, **15** and **16**), respectively. As the residence time decreases, the signal for peptide **16** replaces the signals for peptides **11** and **13** due to missed cleavage. Similarly, signals for peptides **2** and **8** decrease in absolute intensity and the signal for peptide **15** (the combination of peptides **2** and **8**) grows. For the 0.02-s digestion, signals for the intact protein (**20**) and peptide **19** (amino acids 30-153) dominate the spectrum, indicating incomplete digestion.

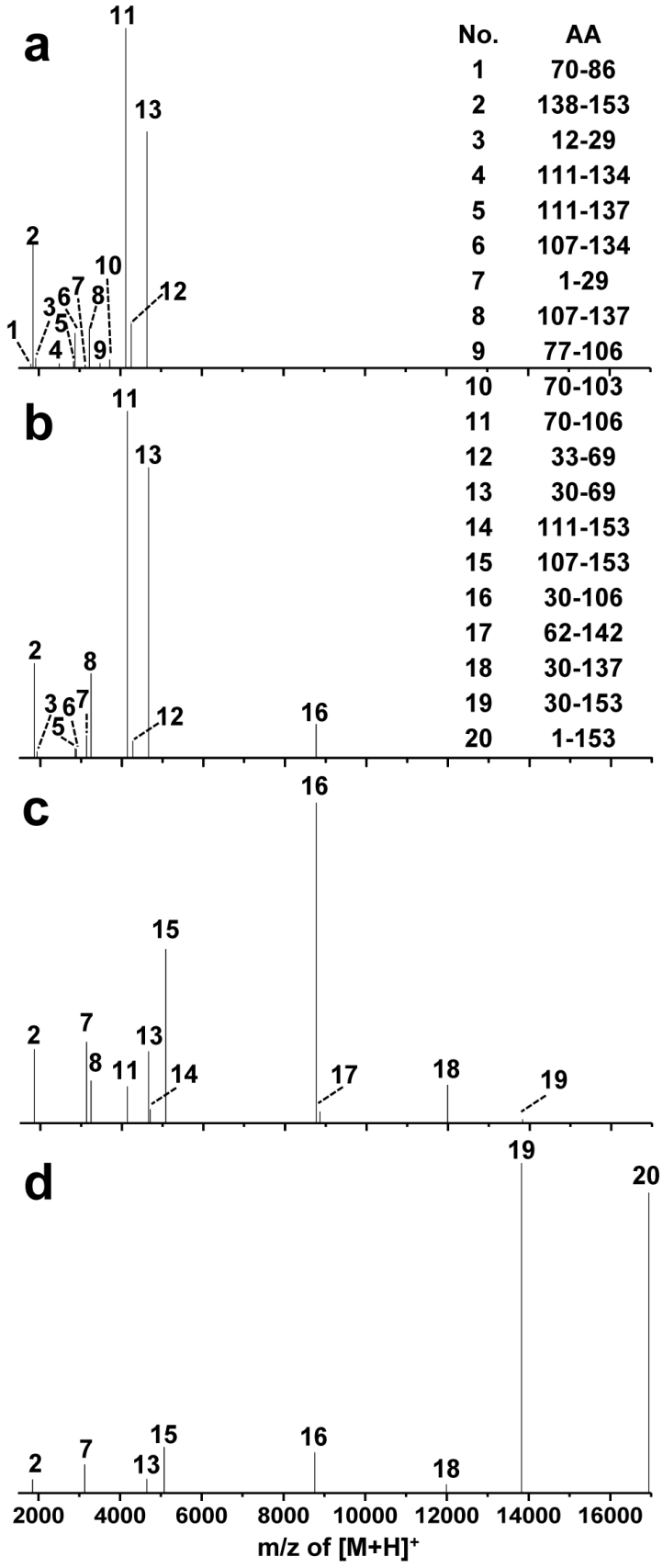

Figure 4.3. Manually deconvoluted ESI-Orbitrap mass spectra of 0.1 mg/mL (6 μM) apomyoglobin digested with residence times of (a) 6, (b) 0.6, (c) 0.06 and (d) 0.02 s in a pepsin-modified membrane. Signals with intensities above 1% of the highest signal are assigned to the specific peptides if possible and converted to the m/z value for the +1 charge state. The normalized intensities in the spectra are the sum of signal intensities for all detected charge states of a given peptide. The inset table lists all peptides identified in the four spectra (AA represents the amino acid sequences).

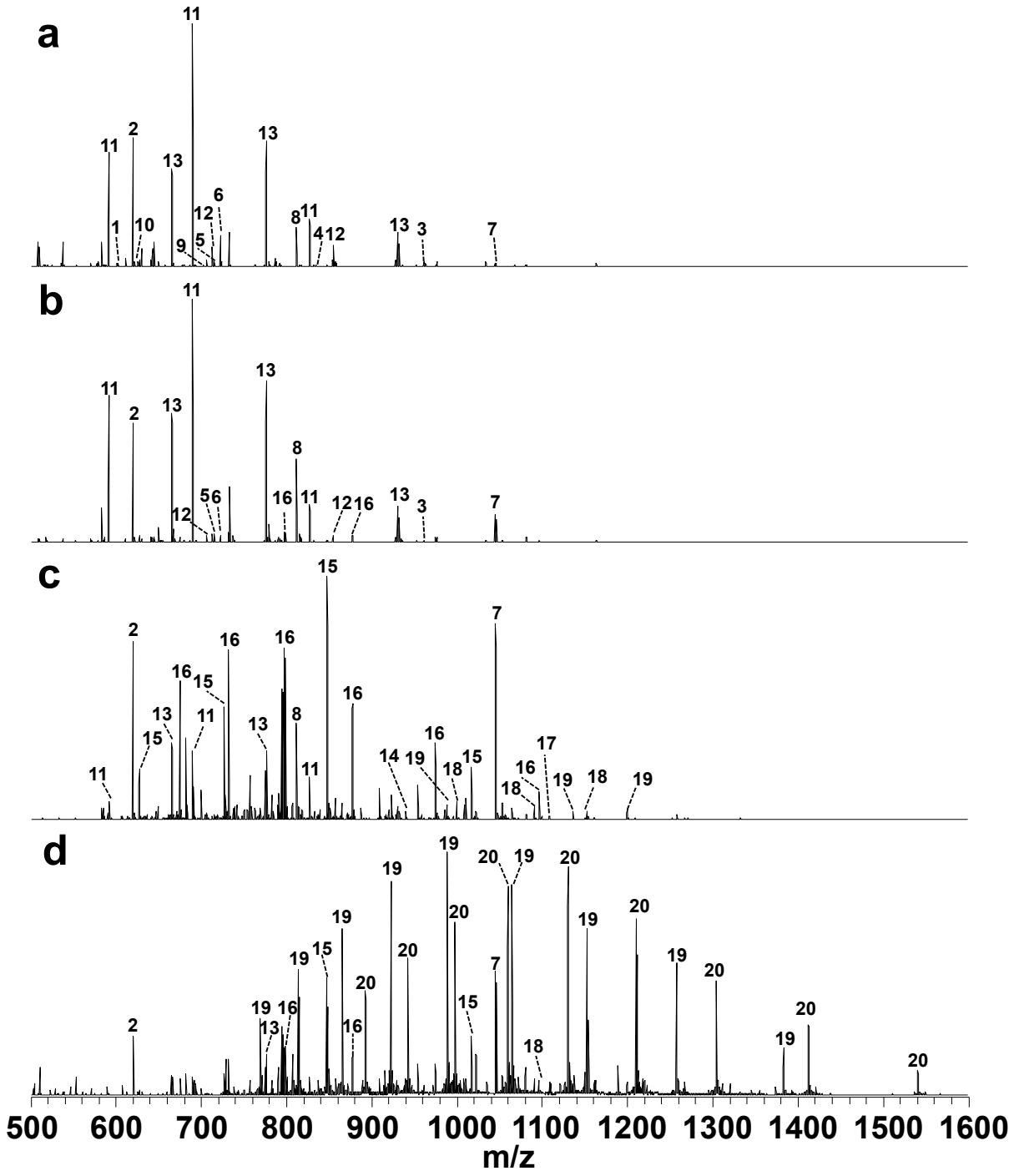

Figure 4.4**.** ESI-Orbitrap mass spectra of 0.1 mg/mL (6 μM) apomyoglobin digested by a pepsin-modified membrane in (a) 6, (b) 0.6, (c) 0.06 and (d) 0.02 s. Labels refer to the peptide list in Table 4.1

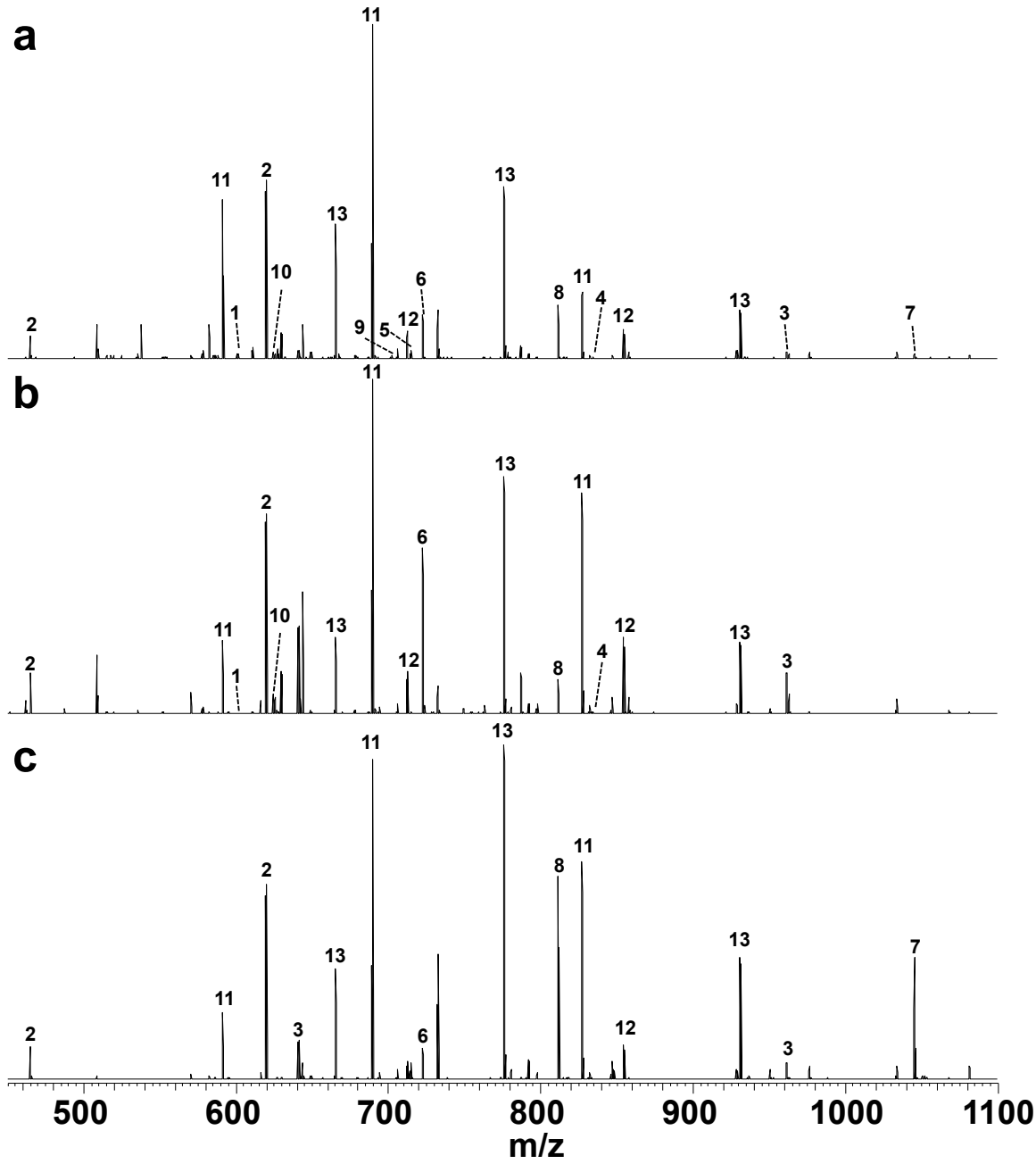

Figure 4.5. ESI-Orbitrap mass spectra of (a) 0.1 mg/mL (6 μM) apomyoglobin digested by a pepsin-modified membrane for 6 s and (b, c) 100 μg apomyoglobin digested by 5 μg pepsin in 0.2 mL of 5% v/v FA. Digestion times are 5 min and 20 s for (b) and (c), respectively. Both solution digests are diluted to 0.1 mg/mL (6 μM) before MS analysis. The labels refer to the peptide list in Table 4.1.

Table 4.1. Apomyoglobin peptides identified from ESI-Orbitrap mass spectra of protein digested in a pepsin-modified membrane. Peak number, monoisotopic mass, amino acids, cleavage sites and missed cleavage sites are listed.

Peak Number	Peptide Monoisotopic Mass	Amino Acids	Cleavage Sites	Missed Cleavage Sites
1	1802.03	70-86	L, L	2A, 2L, I
2	1856.97	138-153	L, End	2A, I, L,Y, 2F
3	1921.98	12-29	L, L	2A, 2L
4	2501.27	111-134	A, A	4A, 2I, L
5	2856.48	111-137	A, L	4A, 3L, 2I
6	2887.45	107-134	F, A	5A, 3I, L
7	3134.55	1-29	L	2A, 2L, I, 2W
8	3242.67	107-137	F, L	5A, 3I, 3L
9	3506.97	77-106	L, F	3A, 3L, 2I, Y
10	3743.16	70-103	L, Y	4A, 4L, 3I
11	4132.35	70-106	L, F	5L, 4A, 3I, Y
12	4269.24	33-69	L, L	3F, 3L, 2A
13	4651.51	30-69	L, L	4L, 3F, 2A, I
14	4694.43	111-153	A, End	7A, 3I, 3L, 3F, Y
15	5080.61	107-153	F, End	6A, 4L, 3I, 3F, Y
16	8764.84	30-106	L, F	10L, 6A, 4I, 3F, Y
17	8863.86	62-142	L, I	9L, 9A, 6I, 3F, Y
18	11988.49	30-137	L, L	12L, 11A,7I, 5F, Y
19	13826.44	30-153	L, End	14L, 13A, 8I, 7F, 2Y
20	16941.97	1-153	End	17L, 15A, 9I, 7F, 2Y, 2W

Apomyoglobin Sequence:

[1]GLSDGEWQQVLNVWGKVEADIAGHGQEVLIRLFTGHPETLEKFDKFKHLKTEAE MKASEDLKKHGTVVLTALGGILKKKGHHEAELKPLAQSHATKHKIPIKYLEFISDA IIHVLHSKHPGDFGADAQGAMTKALELFRNDIAAKYKELGFQG

We also explored residence time-dependent digestion of apomyoglobin using trypsin/PSS -modified membranes and observed large tryptic peptides at faster flow rates. However, a high level of intact apomyoglobin co-exists with these peptides (data not shown). The presence of intact protein confirms that convection rapidly removes protein from the membrane, in contrast to a previous study that employed trapping in nanopores to enhance digestion.[16] In conventional in-solution digestion with several proteases, apomyoglobin undergoes slow proteolysis at pH 7-8.[17] Apomyoglobin denaturation at pH 2 might explain why at low residence times peptic digestion is more efficient than tryptic digestion for this protein. Thus, pepsin is superior to trypsin for creating large proteolytic peptides from apomyoglobin.

4.3.3 ESI-Orbitrap ETD-MS/MS analysis of a large apomyoglobin peptide

Figure 4.6 summarizes the results of apomyoglobin digestion in pepsin-modified membranes in terms of number of peptides, average peptide length and average charge state. Overall, shorter residence times generate larger peptides with more charge. ETD analysis of peptide sequences requires multiple charges to generate abundant fragments,[18] and Coon and coworkers suggest that a low residues/charge ratio and three or more charges are the ideal conditions for effective ETD MS/MS.[19] Short membrane digestion (0.06 s) gives a myoglobin peptide (**16**, amino acids 30-106) with a mass of 8764.93 Da and a +10 charge state, and Figure 4.7 shows the ETD MS/MS spectrum for this peptide. We identified 46 c ions and 52 z ions, which represent cleavage of 61 out of 76 total amino acid junctions. The average spatial resolution is less than two amino acid residues, equivalent to the results carried out by more complex instrumentation in Top-Down FT-ICR ECD analysis.[20]

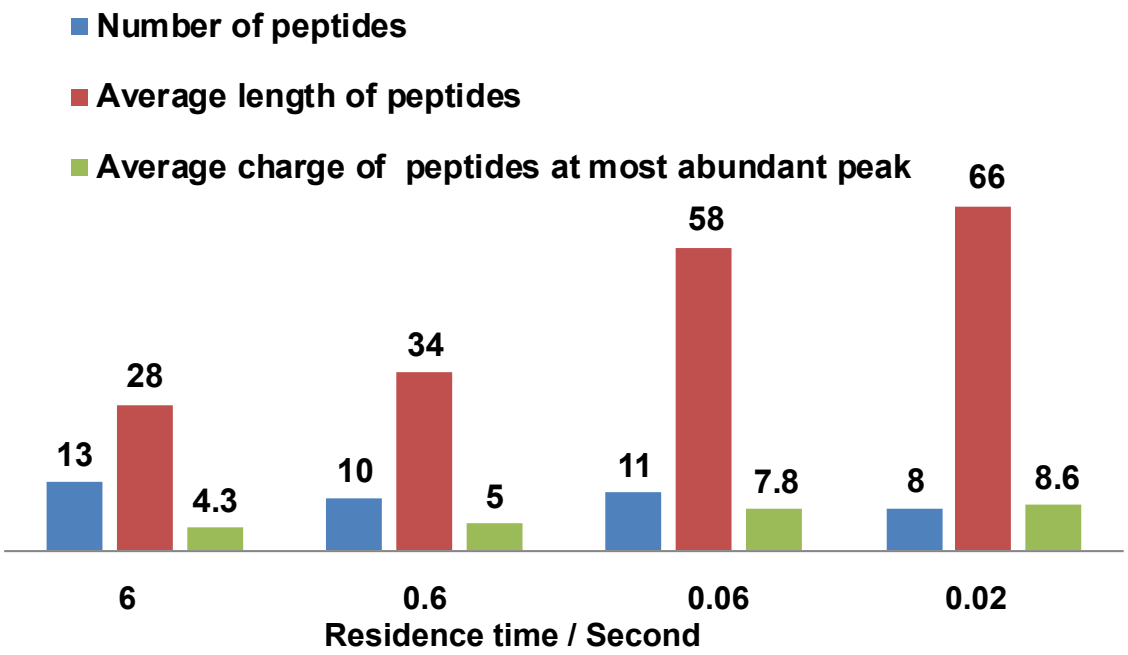

Figure 4.6. Number (blue), average length (red), and average charge of peptides at the most abundant peak (green) in ESI-Orbitrap mass spectra of 0.1 mg/mL apomyoglobin digested in a membrane for 6 s, 0.6 s, 0.06 s and 0.02 s.

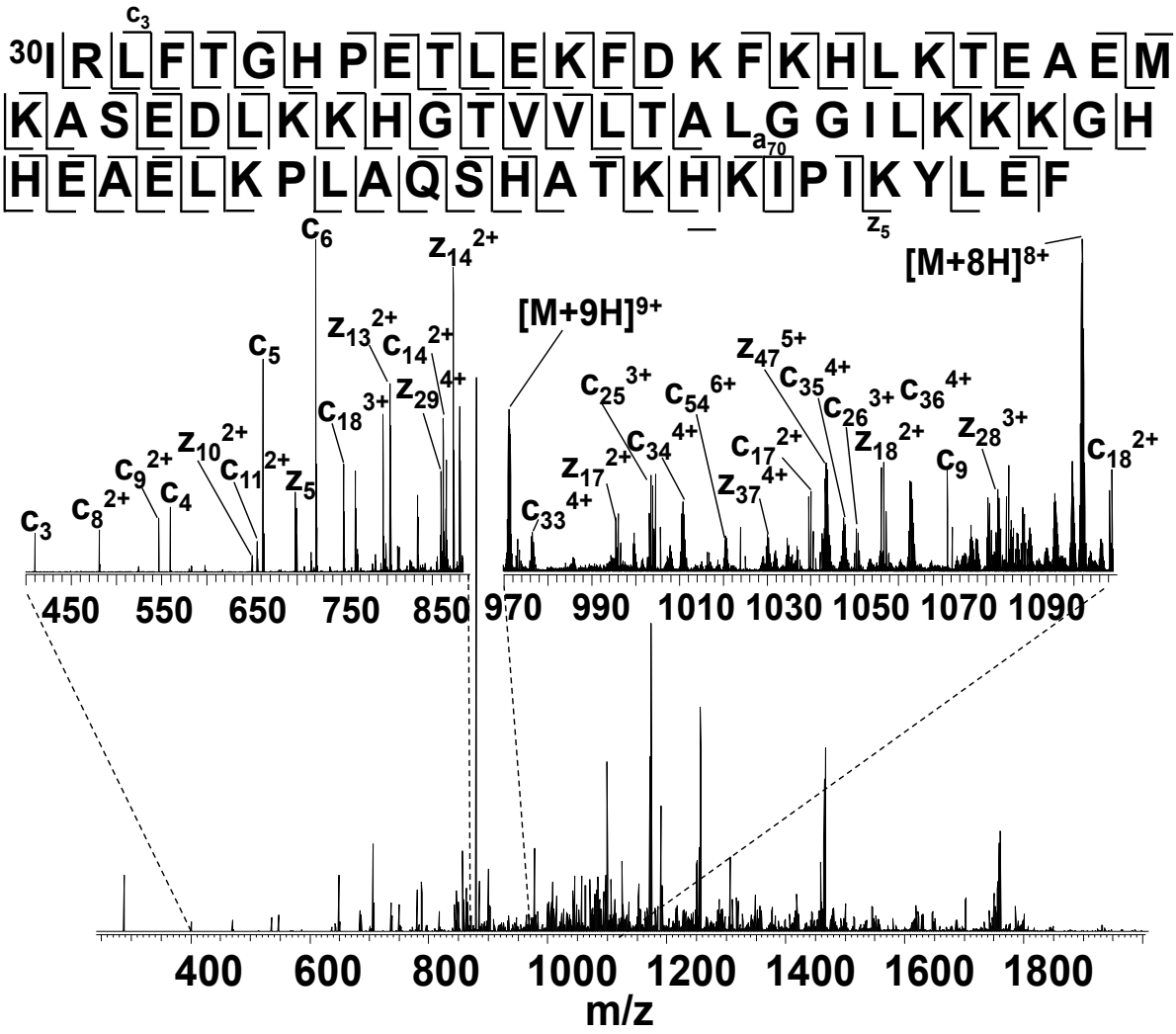

Figure 4.7. ESI-Orbitrap ETD-MS/MS spectrum of the $[M+10H]^{10+}$ precursor ion at 878.00. The sequence shows cleavages site for formation of major c and z ions.

This high spatial resolution coupled with rapid, acidic peptic digestion may be particularly attractive for HDX studies that provide structural information.[11-12] Short, acidic digestion should reduce either back-exchange or over-exchange in HDX, and high spatial resolution will increase the confidence in exchange site localization. Additionally, acidic digestion might facilitate characterization of membrane proteins that are insoluble at neutral pH.

4.3.4 In-membrane BSA digestion under denaturing conditions

Sequence coverage is a critical parameter for MS-based protein characterization, particularly for comprehensive examination of posttranslational modifications. With a molecular mass of 66 kD (583 amino acids) and 17 disulfide bonds, BSA is a reasonable model for examining how membrane-based digestion time affects sequence coverage for a medium-sized, denatured protein. The 17 disulfide bonds make denaturation and reduction prerequisites for membrane digestion.

Figure 4.8 shows the ESI-Orbitrap MS spectra (m/z 540-1440) of BSA digested in membranes using flow rates of 12 and 0.3 mL/h, or residence times of 0.05 and 2 s, respectively. The 0.05-s residence time represents limited digestion, and the 2-s residence time usually provides nearly complete digestion. Peak labels indicate identified BSA peptides in order of increasing mass of $(M+H)^+$ from 628.414 for peptide **1** to 9204.38 for peptide **52**. Comparing the 2-s (Figure 4.8a) and 0.05-s (Figure 4.8b) digestions, the shorter time reveals more peptides at a high m/z range. Figure 4.9 presents the peptide size distributions in the two digestions. Remarkably, short digestion yields 10 peptides with masses >5 kD, whereas the 2-s digestion shows only 1 peptide with a mass greater than 3 kD. With 0.05-s digestion, 12 peptides (**17**, **21**, **33**, **35**, **39**, **44**, **45**, **46**, **48**, **50**, **51** and **52**) cover 82 % of the 583 amino acids, while the 2-s membrane digestion needs 19 peptides (**1**, **2**, **8**, **9**, **10**, **11**, **17**, **18**, **20**, **22**, **26**, **27**, **28**, **29**, **30**, **31**, **32**, **33** and **36**) to cover just 53 % of the sequence. (The inclusion of other identified peptides does not increase sequence coverage, and we included only peptides with signals >1.5% of the highest signal in the spectrum.) The low ionization efficiency of some small peptides may contribute to the low sequence coverage with the 2-s digestion time, whereas longer peptides

with more basic residues (Lys and Arg) provide higher ionization efficiency in positive-ion mode.[21]

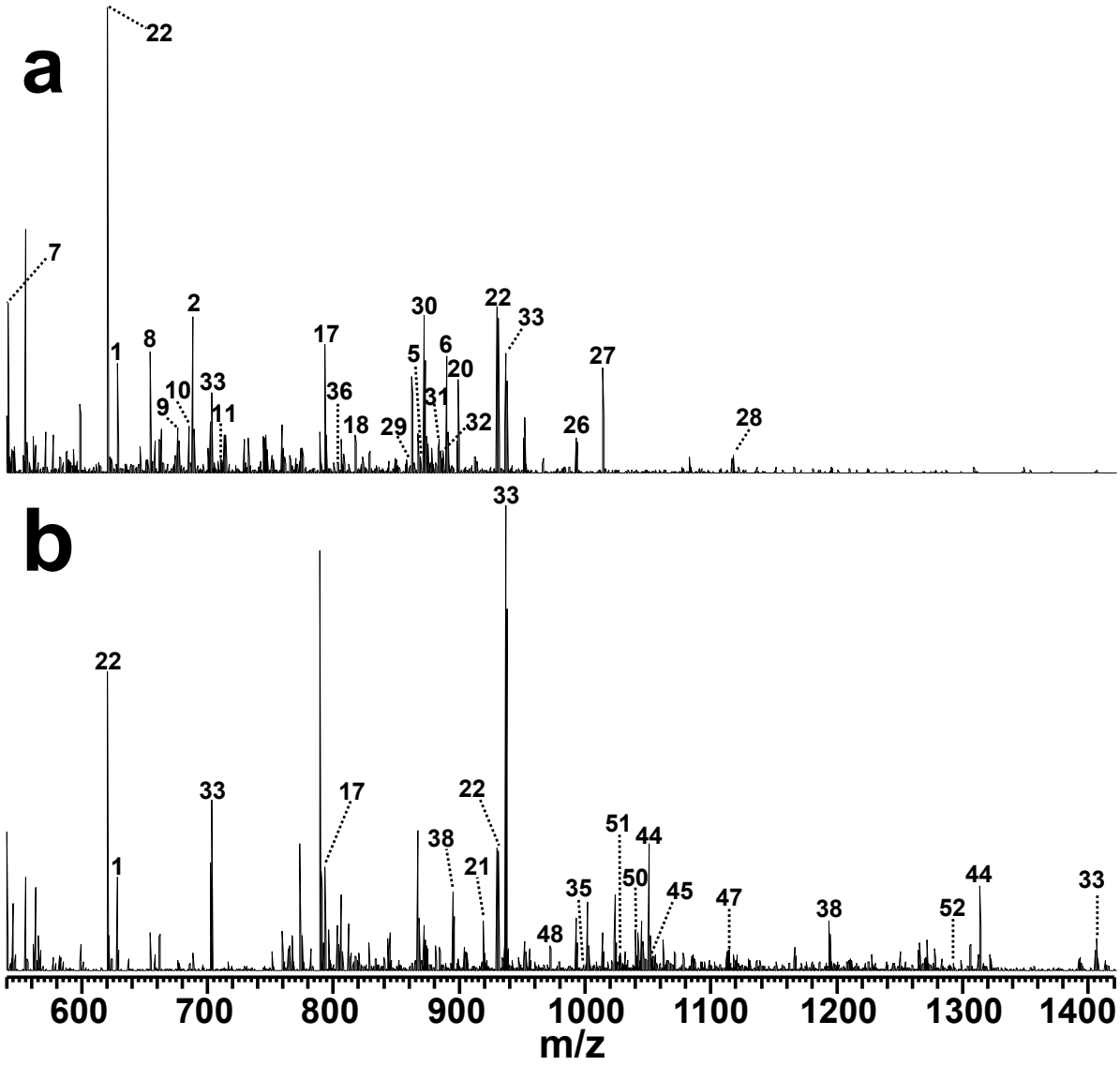

Figure 4.8. ESI-Orbitrap mass spectra of 0.1 mg/mL BSA (1.5 μM in 0.06 M urea) digested in a pepsin-modified membrane using (a) 2-s and (b) 0.05-s residence times. The numbers refer to the identified BSA peptides where m/z values increase with the peptide number. (Table 4.2 lists all peptides along with their monoisotopic masses and sequences.)

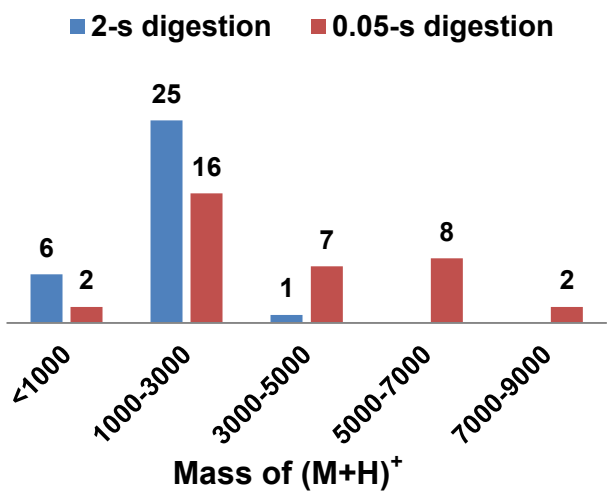

Figure 4.9. Peptides size distributions in ESI-Orbitrap mass spectra of 0.1 mg/mL BSA digested in a pepsin-modified membrane for 2-s (blue, 32 peptides) and 0.05-s (red, 35 peptides).

Table 4.2. BSA peptides identified from ESI-Orbitrap mass spectra of protein digested in a pepsin-modified membrane. Peak number, monoisotopic mass, amino acids, cleavage sites and missed cleavage sites are listed.

Peak Number	Peptide Monoisotopic Mass	Amino Acids	Cleavage Site	Missed Cleavage Sites
1	628.414	455-459	L, L	I, L
2	688.424	228-233	F, L	NONE
3	713.419	568-574	F, L	A
4	731.42	213-218	A, L	W, A
5	868.423	544-550	L, F	NONE
6	889.499	573-583	L, END	A, L
7	1081.57	219-227	L, F	A, F
8	1306.74	346-356	L, L	2A, 2L, Y
9	1351.67	154-164	L, F	3Y, L, A
10	1368.68	395-406	F, L	L, Y, F, A
11	1414.81	179-190	L, A	I, L
12	1421.81	532-543	L, L	L, A
13	1499.84	516-528	L, L	I, A
14	1517.6	554-567	F, F	3A
15	1538.77	488-501	F, F	2A, L, Y
16	1548.84	374-386	F, L	2L

Table 4.2 (cont'd)

17	1583.9	568-583	F, END	2A, 2L
18	1632.86	142-154	I, L	2A, 2Y, L, F
19	1763.01	529-543	L, L	2L, A
20	1793.97	213-227	A, F	2A, L, F, W
21	1834.78	551-567	F, F	4A, F
22	1858.09	407-422	L, L	I, Y
23	1868.93	331-345	L, L	3Y, A
24	1971.18	406-422	A, L	L, I, Y
25	1982.01	330-345	F, L	3Y, L, A
26	1983.05	370-386	Y, L	2L, F
27	2024.02	488-505	F, L	2A, L, Y, F
28	2230.17	103-122	F, L	3L
29	2568.19	302-324	L, A	3A, L, F, Y
30	2612.41	529-550	L, F	3L, A
31	2648.38	506-528	L, L	2F, 2A, 2I, L
32	2655.4	327-348	L, L	3L, 3Y, F, A
33	2806.46	1-24	L	2F, 2L, I, A
34	2929.59	529-553	L, F	3L, 2A, F
35	2998.47	25-49	L, F	3L, 2F, A, I, Y
36	3206.59	460-487	L, F	2L
37	3269.73	330-356	F, L	4L, 4Y, 3A
38	3573.72	423-454	L, L	2L, Y
39	3616.74	226-257	A, A	4L, F, A
40	3799.88	423-456	L, L	3L, Y, I
41	3815.99	455-487	L, F	4L, I
42	4510.23	104-141	L, I	4L, 2F, 2Y, A, W
43	5211.6	460-505	L, L	3L, 2F, 2A, Y
44	5241.77	506-550	L, F	5L, 3A, 2F, 2I
45	5254.58	155-200	L, A	5A, 4L, 3Y, F, I
46	5412.79	407-454	L, L	3L, 2Y, I
47	5558.94	506-553	L, F	5L, 4A, 3F, 2I
48	5820.99	455-505	L, L	5L, 2A, 2F, Y, I
49	6124.03	103-153	F, L	5L, 4Y, 3F, 3A ,W ,I
50	6237.16	103-154	F, L	6L, 4Y, 3F, 3A, W, I
51	7174.47	346-407	L, I	8L, 5A, 3Y, 3F, I
52	9024.38	283-361	L, A	9L, 9A, 5Y, 3F, 2I

BSA sequence:

[1]DTHKSEIAHRFKDLGEEHFKGLVLIAFSQYLQQCPFDEHVKLVNELTEFAKTCVA

DESHAGCEKSLHTLFGDELCKVASLRETYGDMADCCEKQEPERNECFLSHKDDSP

DLPKLKPDPNTLCDEFKADEKKFWGKYLYEIARRHPYFYAPELLYYANKYNGVFQ

ECCQAEDKGACLLPKIETMREKVLASSARQRLRCASIQKFGERALKAWSVARLSQ

KFPKAEFVEVTKLVTDLTKVHKECCHGDLLECADDRADLAKYICDNQDTISSKLKE

CCDKPLLEKSHCIAEVEKDAIPENLPPLTADFAEDKDVCKNYQEAKDAFLGSFLYE

YSRRHPEYAVSVLLRLAKEYEATLEECCAKDDPHACYSTVFDKLKHLVDEPQNLIK

QNCDQFEKLGEYGFQNALIVRYTRKVPQVSTPTLVEVSRSLGKVGTRCCTKPESER

MPCTEDYLSLILNRLCVLHEKTPVSEKVTKCCTESLVNRRPCFSALTPDETYVPKAF

DEKLFTFHADICTLPDTEKQIKKQTALVELLKHKPKATEEQLKTVMENFVAFVDK

CCAADDKEACFAVEGPKLVVSTQTALA

We also employed trypsin/PSS-modified membranes to digest BSA denatured with a NALS, but there is no obvious trend in peptide size with residence time. With a ~0.05-s digestion, the sequence coverage is 90%, even higher than for short-time peptic digestion. The relatively high sequence coverage with the tryptic digest may stem from a denaturing procedure that, in contrast to the denaturation for peptic digestion, included alkylation and no urea. However, out of 65 tryptic peptides, 63 have masses less than 5 kD and the remaining 2 peptides have masses between 5 and 6 kD. Large peptides are important for correlating neighboring posttranslational modifications.[22-23] Unfortunately, with the simple syringe pump system we could not achieve accurate flow control at higher rates where larger tryptic peptides might appear.

Although pepsin provides large peptides more easily than trypsin, low specificity is a drawback of pepsin. In our database searching, we assume peptic cleavage occurs at the C-

terminus side of A, F, I, L, W and Y. For apomyoglobin digestion in pepsin-modified membranes, we observe at least some cleavage at 2/15 A, 1/7 F, 1/9 I, 9/17 L, 0/2 W and 0/2 Y residues. With BSA, the values are 8/47 A, 12/27 F, 2/14 I, 28/61 L, 0/2 W and 1/20 Y residues. In both cases pepsin cleavage occurs preferentially after L, and with BSA, peptic cleavage after F also occurs at nearly 50% of the sites. These data are consistent with a previous statistical analysis of the specificity of immobilized pepsin in the digestion of 39 proteins (13766 amino acids residuals). That study shows that F and L have a cleavage probability larger than 40 %, whereas cleavage is less than 20% at A, I, W, and Y sites. [24] One particular challenge in working with pepsin is that other cleavage sites or N-terminus cleavage of A, L, I, F, W or Y could lead to unassigned peptide signals, but tandem mass spectrometry can potentially overcome this problem.[25]

4.4 Conclusions

Immobilizing common proteases (trypsin and pepsin) in nylon membranes at high enzyme density (30-60 mg/cm^3) conveniently creates membrane-based enzymatic reactors. These reactors catalyze limited proteolysis in <1 s. More importantly, tuning the flow rate through the membrane affords control over the size of proteolytic peptides. For apomyoglobin digestion by pepsin, shorter residence times yield longer peptides with more charge. A large peptide (8kD) with a +10 charge state provides a spatial resolution of <2 amino acid residues in ETD MS/MS analysis. Similarly, in membrane-based peptic digestion of denatured BSA, limited digestion yields many missed cleavages and creates long peptides that increase the sequence coverage from 53% to 82% on going from 2-s to 0.05-s digestion. Future work will focus on

limited digestion of proteins with multiple posttranslational modifications to study correlations between different modifications.

4.5 Acknowledgement

We are grateful to the U.S. National Institutes of Health (GM 080511 to M.B.) for funding this work. I would like to thank Ms. Li Cui from Prof. Gavin Reid's group for the initial help of using the Orbitrap Velos instrument.

REFERENCES

4.6 References

1. Ma, J.; Zhang, L.; Liang, Z.; Shan, Y.; Zhang, Y., Immobilized Enzyme Reactors in Proteomics. *TrAC, Trends Anal. Chem.* **2011,** *30* (5), 691-702.

2. Ma, J.; Hou, C.; Sun, L.; Tao, D.; Zhang, Y.; Shan, Y.; Liang, Z.; Zhang, L.; Yang, L.; Zhang, Y., Coupling Formic Acid Assisted Solubilization and Online Immobilized Pepsin Digestion with Strong Cation Exchange and Microflow Reversed-Phase Liquid Chromatography with Electrospray Ionization Tandem Mass Spectrometry for Integral Membrane Proteome Analysis. *Anal. Chem.* **2010,** *82* (23), 9622-9625.

3. Rey, M.; Man, P.; Brandolin, G.; Forest, E.; Pelosi, L., Recombinant Immobilized Rhizopuspepsin as a New Tool for Protein Digestion in Hydrogen/Deuterium Exchange Mass Spectrometry. *Rapid Commun. Mass Spectrom.* **2009,** *23* (21), 3431-3438.

4. Gao, J.; Xu, J.; Locascio, L. E.; Lee, C. S., Integrated Microfluidic System Enabling Protein Digestion, Peptide Separation, and Protein Identification. *Anal. Chem.* **2001,** *73* (11), 2648-2655.

5. Krenkova, J.; Lacher, N. A.; Svec, F., Highly Efficient Enzyme Reactors Containing Trypsin and Endoproteinase LysC Immobilized on Porous Polymer Monolith Coupled to MS Suitable for Analysis of Antibodies. *Anal. Chem.* **2009,** *81* (5), 2004-2012.

6. Cooper, J. W.; Chen, J.; Li, Y.; Lee, C. S., Membrane-Based Nanoscale Proteolytic Reactor Enabling Protein Digestion, Peptide Separation, and Protein Identification Using Mass Spectrometry. *Anal. Chem.* **2003,** *75* (5), 1067-1074.

7. Dulay, M. T.; Baca, Q. J.; Zare, R. N., Enhanced Proteolytic Activity of Covalently Bound Enzymes in Photopolymerized Sol Gel. *Anal. Chem.* **2005,** *77* (14), 4604-4610.

8. Xu, F.; Wang, W. H.; Tan, Y. J.; Bruening, M. L., Facile Trypsin Immobilization in Polymeric Membranes for Rapid, Efficient Protein Digestion. *Anal. Chem.* **2010,** *82* (24), 10045-10051.

9. Walter, B., Characterization of Agarose-Bound Trypsin. *Biochim. Biophys. Acta* **1976,** *429* (3), 950-953.

10. Liuni, P.; Rob, T.; Wilson, D. J., A Microfluidic Reactor for Rapid, Low-Pressure Proteolysis with On-Chip Electrospray Ionization. *Rapid Commun. Mass Spectrom.* **2010,** *24* (3), 315-320.

11. Engen, J. R., Analysis of Protein Conformation and Dynamics by Hydrogen/Deuterium Exchange MS. *Anal. Chem.* **2009,** *81* (19), 7870-7875.

12. Konermann, L.; Pan, J.; Liu, Y.-H., Hydrogen Exchange Mass Spectrometry for Studying Protein Structure and Dynamics. *Chem. Soc. Rev.* **2011,** *40* (3), 1224-1234.

13. Ge, Y.; Rybakova, I. N.; Xu, Q.; Moss, R. L., Top-down High-resolution Mass Spectrometry of Cardiac Myosin Binding Protein C Revealed that Truncation Alters Protein Phosphorylation State. *Proc. Natl. Acad. Sci. U. S. A.* **2009,** *106* (31), 12658-12663.

14. Liu, G.; Dotzauer, D. M.; Bruening, M. L., Ion-Exchange Membranes Prepared using Layer-by-Layer Polyelectrolyte Deposition. *J. Membr. Sci.* **2010,** *354* (1–2), 198-205.

15. Bhattacharjee, S.; Dong, J.; Ma, Y.; Hovde, S.; Geiger, J. H.; Baker, G. L.; Bruening, M. L., Formation of High-Capacity Protein-Adsorbing Membranes through Simple Adsorption of Poly(acrylic acid)-Containing Films at Low pH. *Langmuir* **2012,** *28* (17), 6885-6892.

16. Bi, H.; Qiao, L.; Busnel, J.-M.; Liu, B.; Girault, H. H., Kinetics of Proteolytic Reactions in Nanoporous Materials. *J. Proteome Res.* **2009,** *8* (10), 4685-4692.

17. Fontana, A.; Zambonin, M.; Polverino de Laureto, P.; De Filippis, V.; Clementi, A.; Scaramella, E., Probing the Conformational State of Apomyoglobin by Limited Proteolysis. *J. Mol. Biol.* **1997,** *266* (2), 223-230.

18. Syka, J. E. P.; Coon, J. J.; Schroeder, M. J.; Shabanowitz, J.; Hunt, D. F., Peptide and Protein Sequence Analysis by Electron Transfer Dissociation Mass Spectrometry. *Proc. Natl. Acad. Sci. U. S. A.* **2004,** *101* (26), 9528-9533.

19. Good, D. M.; Wirtala, M.; McAlister, G. C.; Coon, J. J., Performance Characteristics of Electron Transfer Dissociation Mass Spectrometry. *Mol. Cell. Proteomics* **2007,** *6* (11), 1942-1951.

20. Pan, J.; Han, J.; Borchers, C. H.; Konermann, L., Hydrogen/Deuterium Exchange Mass Spectrometry with Top-Down Electron Capture Dissociation for Characterizing Structural Transitions of a 17 kDa Protein. *J. Am. Chem. Soc.* **2009,** *131* (35), 12801-12808.

21. Wu, S.-L.; Kim, J.; Hancock, W. S.; Karger, B., Extended Range Proteomic Analysis (ERPA): A New and Sensitive LC−MS Platform for High Sequence Coverage of Complex Proteins with Extensive Post-translational ModificationsComprehensive Analysis of Beta-Casein and Epidermal Growth Factor Receptor (EGFR)†. *J. Proteome Res.* **2005,** *4* (4), 1155-1170.

22. Kellie, J. F.; Tran, J. C.; Lee, J. E.; Ahlf, D. R.; Thomas, H. M.; Ntai, I.; Catherman, A. D.; Durbin, K. R.; Zamdborg, L.; Vellaichamy, A.; Thomas, P. M.; Kelleher, N. L., The Emerging Process of Top Down Mass Spectrometry for Protein Analysis: Biomarkers, Protein-Therapeutics, and Achieving High Throughput. *Mol. Biosyst.* **2010,** *6* (9), 1532-1539.

23. Siuti, N.; Kelleher, N. L., Decoding Protein Modifications using Top-Down Mass Spectrometry. *Nat. Methods* **2007,** *4* (10), 817-821.

24. Hamuro, Y.; Coales, S. J.; Molnar, K. S.; Tuske, S. J.; Morrow, J. A., Specificity of Immobilized Porcine Pepsin in H/D Exchange Compatible Conditions. *Rapid Commun. Mass Spectrom.* **2008,** *22* (7), 1041-1046.

25. Nelson, D. L.; Lehninger, A. L.; Cox, M. M., *Lehninger Principles of Biochemistry*. W.H. Freeman: New York, 2008.

Chapter 5. Protease-Modified Membranes for Studies of Protein Structure: Limited Proteolysis and Rapid Digestion for HDX

(The work on RHD3 is part of a manuscript submitted to *Analytical Chemistry*)

Chapter 4 introduced protease-modified membranes whose low thickness (170 μm) enables limited digestion with msec residence times. This chapter explores the use of protease-modified membranes as part of two techniques for investigating protein structure, HDX and limited digestion of proteins without denaturation. After HDX, rapid peptic digestion in membranes facilitates MS analysis of the mass increase on deuterium-containing peptides. In contrast, limited proteolysis of a large Arabidopsis GTPase, ROOT HAIR DEFECTIVE 3 (RHD3), shows suitable probing for labile regions near the C-terminus to suggest what protein reconstruction might make RHD3 more suitable for crystallization.

5.1 Introduction

Complementary to NMR and X-ray crystallography, HDX followed by MS is an emerging method in the study of protein structure and dynamics.[1] The sites of deuterium exchange on a protein after exposure to D_2O often indicate which regions of a protein or protein complex are accessible to water and have weak hydrogen bonding. Moreover, the kinetics of exchange can also suggest the time-frame of protein dynamics.[2] After a specified time of protein exposure to D_2O, quenching of HDX occurs via acidification and a decrease in temperature. Moreover, the low pH (pH=2.5) and temperature (0 ºC) are also important for

preventing back-exchange during digestion and analysis.[1, 3] Due to the need for low pH, pepsin is the ideal protease for HDX applications.[4] In this chapter, after exposure to D_2O for 5 min we digest apomyoglobin in pepsin-modified membranes (1-s residence time) at pH 2.5 and subject the resulting peptides to ESI-MS analysis (Figure 5.1). Comparison of the spectra from digests of deuterium-exchanged and control proteins shows the mass increase due to the replacement of amide hydrogen by deuterium at different regions. (The technique must take into account exchange on the side chains of labile residues.)

Limited digestion can also provide low-resolution structural information when digesting proteins in their native configuration. In this case proteolysis only occurs in target protein regions that are readily accessible to the enzyme. Traditional limited protein digestion employs a solution-based approach, which includes varying the incubation time, enzyme to substrate ratio, or reaction temperature to control the extent of proteolysis. This approach is laborious and sometimes difficult to reproduce.[5-6] With protease-containing membranes, similar experiments can be performed by simply varying the flow rate of a protein solution through the membrane. This method can greatly decrease the experimental time (~15 min) and sample consumption (~100 μg) in limited digestion studies, and fine control of the flow rate using a syringe pump may increase reproducibility. We demonstrate this concept by investigating which regions of recombinant RHD3 are flexible and susceptible to hydrolysis. Based on sodium dodecyl sulfate polyacrylamide gel electrophoresis (SDS-PAGE) and MS data, we find four readily accessible regions at the protein C-terminus and suggest that truncation of the most labile site may increase the likelihood of RHD3 crystallization.

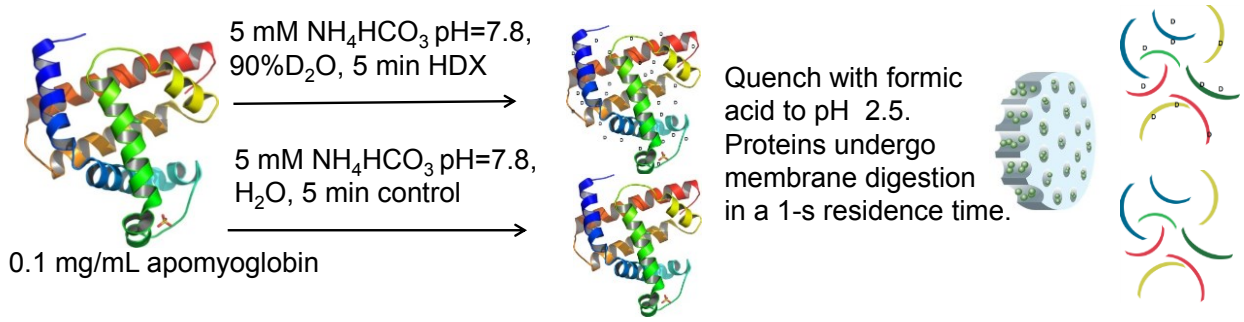

Figure 5.1. The workflow of HDX and membrane digestion. The 0.1 mg/mL apomyoglobin is exchanged in 90% D_2O (or 100% H_2O) for 5 min (5 mM NH_4HCO_3, pH=7.8). The reaction is quenched by lowering the pH to 2.5 via addition of FA, and the deuterium protein or control protein (no exchange) immediately undergoes membrane digestion to generate peptides with or without deuterium.

5.2 Experimental

5.2.1 Materials, membranes and membrane holders

See chapter 4 for details in this area.

5.2.2 Membrane modification with protease

The modification of membranes with pepsin and trypsin was the same as described in chapter 4. An α-chymotrypsin-modified membrane was also used in the RHD3 study. For α-chymotrypsin immobilization, ten mL of a 0.02 M PSS, 0.5 M NaCl solution (pH=2.3) was first passed through the membrane at 2 mL/min, followed by 30 mL of deionized water at the same flow rate. Subsequently, 5 mL of 1 mg/mL α-chymotrypsin in 2.7 mM HCl, 2 mM $CaCl_2$ was circulated through the membrane at 1 mL/min for one hour. After protease deposition, the membrane was rinsed with 30 mL of 1 mM HCl. Modified membranes were dried and stored in a

desiccator. The amounts of α-chymotrypsin immobilized in membranes were determined from direct UV absorbance at 280 nm using a Nanodrop^{TM} UV/Vis Spectrometer (Thermo).

5.2.3 Apomyoglobin HDX and membrane-digestion procedure

One mg of apomyoglobin was dissolved in one mL of 50 mM NH_4CO_3 to make a stock solution. One hundred μL of stock solution was diluted with D_2O or H_2O (control) at a 1:9 ratio, and the mixture was left for 5 min at room temperature. The reaction was quenched by addition of 50 μL of formic acid (FA), and 100 μL of the quenched sample (0.095 mg/mL or 6 μM apomyoglobin) was immediately passed through the pepsin-modified membrane at a flow rate of 0.6 mL/h (1 s residence time), and this process took 10 min. The 100 μL of digested sample was mixed with 100 μL acetonitrile and frozen quickly with liquid nitrogen prior to lyophilization with a Speed-Vac. The lyophilization took 20 min, during which the mixture was frozen. The dried digest was dissolved in 100 μL of MS buffer (3% FA, 47% H_2O and 50% methanol, pH=2.5, precooled on ice), and 40 μL of this sample was infused into ESI-MS. The time from dissolving to injection was 3 min.

5.2.4 RHD3 expression and purification

The RHD3(1-676)-HIS6 was cloned by Dr. Giovanni Stefano from Prof. Federica Brandizzi's group, and the protein expression and purification was performed by Dr. Yi Zheng from Prof. R. Michael Garavito's group. The Production of RHD3(1-676)-HIS_6 subcloned in pET28b vector was induced in *Escherichia coli* (BL21 λDE3). The bacteria were cultured at 37 °C in LB medium containing 100 μg/ml of kanamycin until reaching an optical density of 1.0 at 600 nm. Protein production was induced by addition of 1 mM isopropyl 1-thio-β-D-

galactopyranoside for 5 h at 30 °C. Harvested cells from 1 L of cell culture were suspended in 50 mL of buffer A (30 mM Tris-HCl, pH 8.0, 200 mM NaCl, 4 mM $MgCl_2$, 2 mM β-mercaptoethanol and 1 mM phenylmethanesulfonyl fluoride) and lysed with 4 min of sonication at an output of 48 watts with 10 s pulses (Sonicator Misonix 3000). Following a centrifugation step at 20,000 x g (4 °C) for 20 min, the clarified lysate was applied to a 7-mL Ni-NTA (Qiagen) gravity flow column, which was pre-equilibrated in buffer A containing 25 mM imidazole. After extensive washing with buffer A, fractions were eluted over 2 column volumes using buffer A containing 150 mM imidazole. Fractions containing RHD3 (as shown by UV absorbance at 280 nm) were pooled and concentrated to about 1 mL, and 500 µL volumes were applied at 0.4 ml/min to a Superose 6 10/300 GE gel filtration column (GE Healthcare), which was pre-equilibrated with buffer B (30 mM Tris-HCl, pH 8.0, 200 mM NaCl, 4 mM $MgCl_2$, 1 mM EDTA, and 1 mM DTT). Peak fractions containing target proteins were concentrated using a spin column (30 kD molecular weight cutoff) to ~15 mg/mL based on UV/Vis absorbance at 280 nm. Analytical gel filtration chromatography was also used to estimate the molecular size of purified RHD3, which eluted at a position corresponding to a homo dimer with a molecular weight of 150 kD.

5.2.5 Limited proteolysis of RHD 3 with either trypsin- or α-chymotrypsin-modified membranes

The gel filtration-purified RHD3 was diluted with 10 mM NH_4HCO_3 to make 1 mL of 0.1 mg/mL RHD3, and this solution was passed through a small trypsin- or α-chymotrypsin-modified membrane at 0.6, 3 and 13 mL/h. The digests were analyzed by MALDI-MS and ESI-

MS, and 3 μg of each digested protein and intact protein were also analyzed by SDS-PAGE with Coomassie Blue staining.

5.2.6 Mass spectrometry and data analysis

See chapter 4 for details in this area.

5.3 Results and discussion

5.3.1 Preliminary study of HDX on apomyoglobin using digestion in a pepsin-modified membrane

In HDX, digestion of the deuterium-exchanged protein should be rapid to prevent back exchange in H_2O matrix, or in our case to prevent over-exchange in a D_2O matrix. Highly active pepsin-containing reactors can catalyze the digestion in a short time. Moreover the immobilized-pepsin reactor keeps the enzyme away from the peptic digest after proteolysis to decrease MS interferences from self-digested enzyme.[1, 4] Pepsin-modified membranes may be especially effective reactors to digest deuterium-exchanged proteins because of the short radial diffusion distances in membrane pores. We performed membrane digestion of deuterium-exchanged apomyoglobin using 1-s residence times and analyzed the peptic digests using ESI-MS. Figures 5.2a and 5.2b show the spectra of 6 μM peptic digests of deuterium-exchanged apomyoglobin and control (non-exchanged) apomyoglobin, respectively. They demonstrate very similar digestion, so it is easy to compare the two spectra. As expected, the isotopic distributions of peptide signals in 5.2a are wider than in 5.2b, and dominant signals shift to a slightly higher m/z value. The deuterium exchange not only increases a peptide's mass but variable exchange also complicates the isotopic mass distribution. Figures 5.2c and d are expanded (x-axis) views

of signals from a peptide selected (red rectangle) from a and b, respectively. The peptides have the same sequence (amino acids 1-29 of apomyoglobin) and both show a monoisotopic mass at m/z 1045.53 (+3 charge state). We use the difference between the centroid masses (shown in Figure 5.2d) to estimate the amount of exchanged deuterium. (The centroid mass is calculated as the peak height-weighted averaged mass of all isotopic peaks.) The 2.24 Da difference between the centroid masses indicts an average 6.72 Da mass increase (based on the +3 charge state) due to D exchange. The mass increases occur to different extent with different peptides. The above data suggest the success of HDX and the peptic membrane digestion, but localization of deuterium exchange to more specific amino acid regions needs further investigation. This will require either ETD fragmentation or digestion into smaller, overlapping peptides.

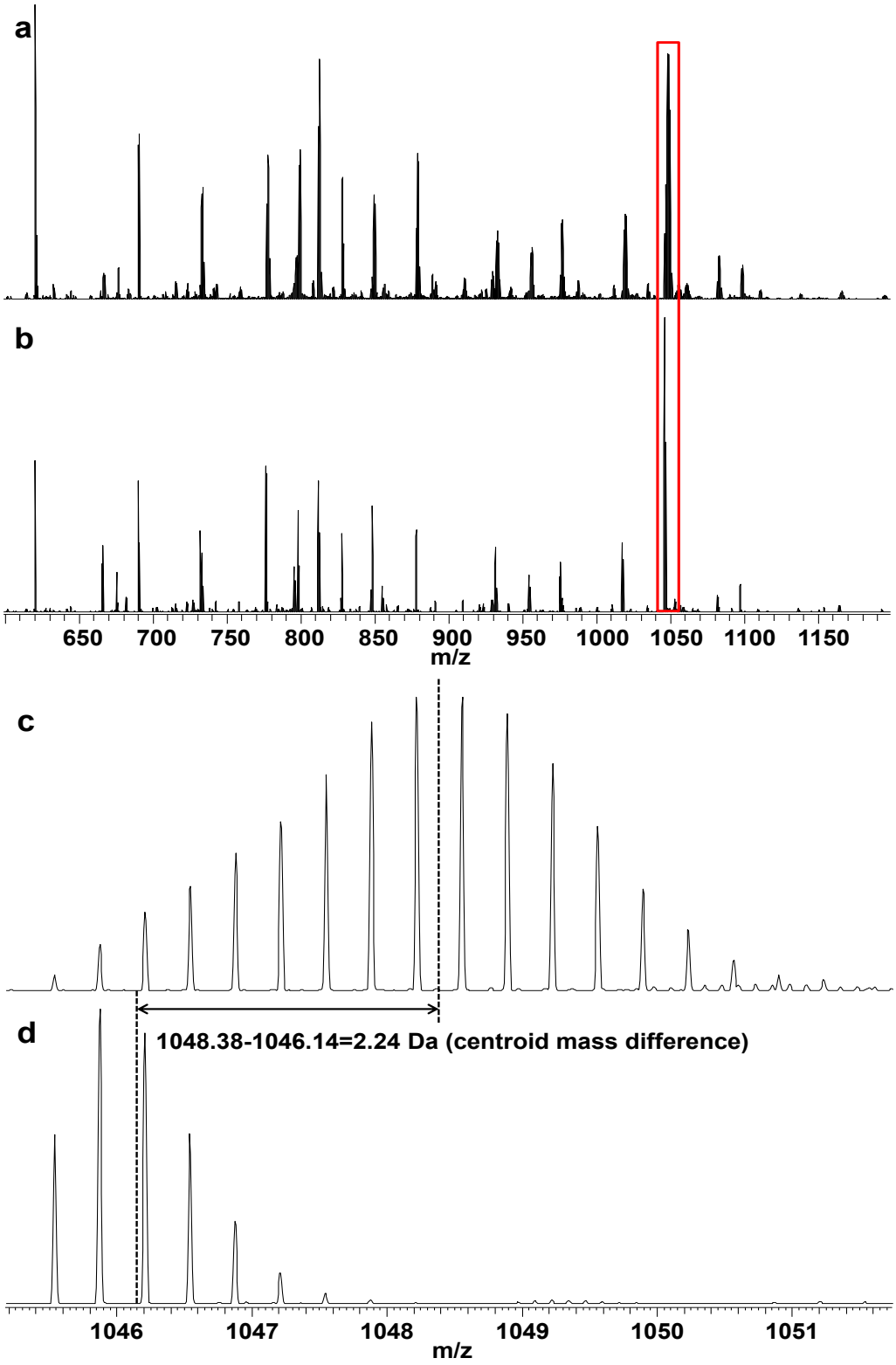

Figure 5.2. ESI-Orbitrap mass spectra of 6 μM (a) deuterium-exchanged or (b) control apomyoglobin digested by a pepsin-modified membrane (1-s residence time). (c) and (d) are

enlarged (x-axis) views of the selected peaks (red rectangles) from (a) and (b), respectively. The centroid masses of (c) and (d) are labeled by the dash line, and the difference is given.

5.3.2 Limited membrane proteolysis of RHD3 for structural information

In a simpler method for investigating protein structure with low resolution, we suggest which regions of a protein are highly accessible to enzymes by observing where limited digestion occurs. RHD3 serves as our initial example. Homologous to human atlastins, RHD3 is one of the largest membrane-bound GTPases in *Arabidopsis thaliana*.[7] This protein participates in the modeling of the endoplasmic reticulum and contains a GTPase domain, a helix bundle, two trans-membrane helices and one cytosolic tail.[8] Human atlastin may be involved in homotypic fusion of the membrane of the endoplasmic reticulum, and much of the information in the mechanisms that could underpin such a fusion has been gathered from crystallographic analyses of the soluble domain (cytosolic) of atlastin.[7] The biological role of RHD3 is unknown,[9] and a crystal structure of this protein would most likely offer valuable insights into RHD3's role in plant cells.

This work aims to use limited membrane-based proteolysis to map flexible protein regions that may restrict crystallization (Scheme 5.1).[10-11] Flexible regions should contain digestion sites that are much more accessible to proteolysis than similar sites in the globular region of the protein. Subsequently, proteins expressed without the flexible regions would be more stable and compact, and consequently have a much higher probability of crystallization.[5-6, 10, 12] Because the globular regions of the protein resist digestion, we could employ trypsin and α-chymotrypsin in limited proteolysis. These enzymes are more specific than pepsin and operate at a non-denaturing pH (NH_4HCO_3 buffer, pH 7.5), which is vital for structural studies.

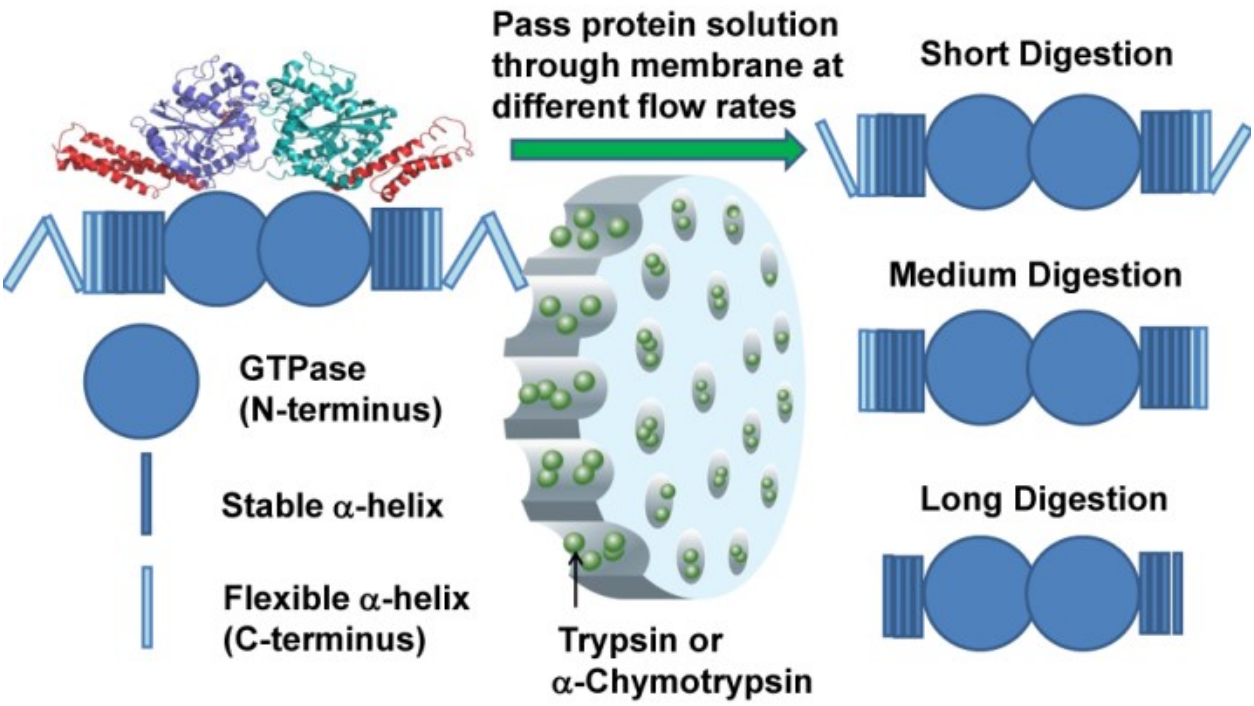

Scheme 5.1. Strategy for limited RHD3 digestion in membranes containing trypsin and α-chymotrypsin. The protein picture (top left) is that for a human atlastin dimer (made from PDB 3QOF and 3QNU using Pymol), which has a similar domain configuration to RHD3 but with less α-helix. The drawings represent RHD3 dimers (one GTPase domain and 9 α-helices on each monomer).

To obtain different digestion patterns, we selectively pass the RHD3 solutions through either trypsin- or α-chymotrypsin-modified membranes at 0.6, 3 and 13 mL/h. Figure 5.3 shows the SDS-PAGE analysis of the proteolytic digests. In both images, lane 1 is the protein ladder, lane 2 is the intact protein, and lanes 3-5 are the digests at the different flow rates, which correspond to residence times of 0.045, 0.2 and 1 s, respectively. After tryptic digestion, three major protein bands appear with molecular masses around 70, 65, and 60 kD. We performed the α-chymotrypsin membrane digestion one week after the trypsin membrane digestion, and the protein itself degraded slightly, presumably because of trace protease not removed during the

purification process. The SDS-PAGE after chymotrypsin digestion reveals a dominant intermediate protein with a molecular weight around 65 kD.

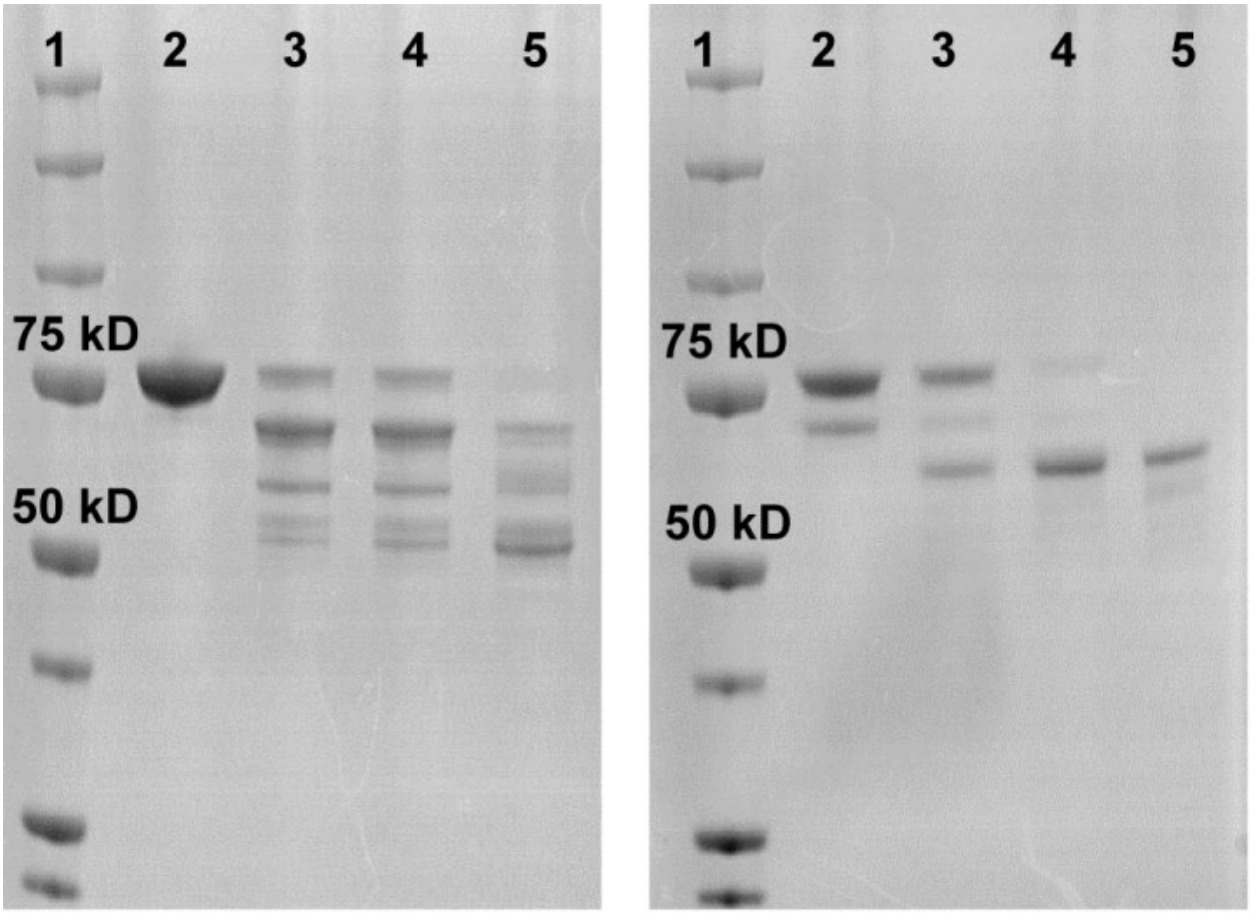

Figure 5.3**.** SDS-PAGE analysis of limited RHD3 digestions in a trypsin-modified membrane (left) and an α-chymotrypsin-modified membrane (right). Three μg of either protein or digests were loaded onto each column, and Lanes 1-5 are protein ladder, intact protein, digests at 13 mL/h (residence time of 0.045 s), digests at 3 mL/h (residence time of 0.2 s) and digests at 0.6 mL/h (residence time of 1 s), respectively.

We applied both MALDI-LTQ MS and ESI-Orbitrap MS to investigate the most abundant peptides in the RHD3 digests. Figures 5.4a, b and c show the MALDI mass spectra of RHD3 digested in a trypsin-modified membrane for different residence times. Peak labels show peptide sequences determined from comparison of masses with theoretical masses obtained from

in silico digestion. The recombinant RHD3 protein has 691 amino acids including its polyhistidine tag, and the most intense peak at the shortest digestion time corresponds to the peptide with amino acids 673-691, suggesting a flexible polyhistidine tag region. The mass spectra also indicate cleavage after amino acids R542, R560, R569, K600, K617, K632, K637, K646 and R650. α-Chymotrypsin also shows cleavage sites in these regions (Table 5.1). In the predicted secondary structure, all of these peptides lie within the last 4 α-helices or regions between them. Comparison of the three spectra in Figure 5.4 suggests that cleavage is most rapid at R672, as relative to the peptide 673-691, signals for other peptides typically increase with increasing digestion time. This suggests that longer digestion times result in digestion deeper into the protein, which is consistent with the SDS-PAGE results.

The ESI-Orbitrap mass spectrum (Figure 5.4d) confirms MALDI-MS results and shows dominant cleavage sites after R576, K617, R650, and R672. The signal for peptide 673-691 is especially strong. Overall, the mass spectra suggest there are 4 highly accessible regions around R576, K617, R650, and R672. Because ESI gives multiple charge states, we see larger peptides than with MALDI. Figure 5.5 (ESI mass spectra of RHD3 digested in a trypsin-modified membrane for different residence times) shows that peptide 618-691 is present primarily at low digestion times, suggesting that the K617 site is more accessible than R650. This Figure also reveals a small signal for peptide 1-71 from the N-terminus, showing limited access to this part of the protein. Table 5.1 lists the most abundant peptides in limited trypsin and α-chymotrypsin digests. In Figures 5.4a, b and c there is a signal that seems to correspond to peptide 251-263. This peptide is in the globular region of the protein where the GTPase domain and helical region connect, and this linker region may be also accessible to the enzyme.

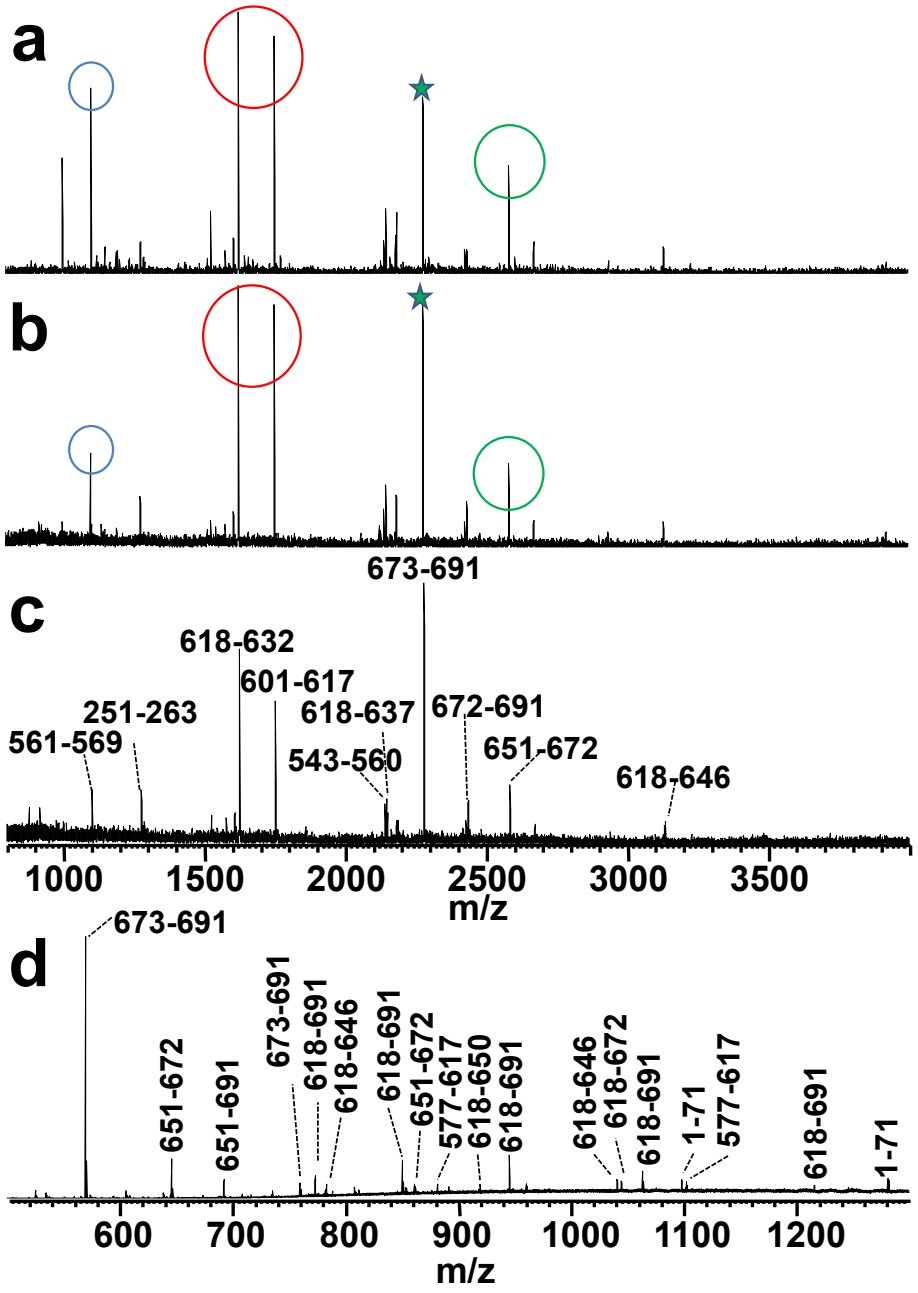

Figure 5.4**.** MALDI mass spectra of 0.1 mg/mL (1.3 μM) RHD 3 digested in residence times of (a) 1 sec, (b) 0.2 sec and (c) 0.045 s by a trypsin-modified membrane, and (d) ESI mass spectrum of the same sample as (c). Signals were assigned to peptides by mass fingerprinting and are labeled with the amino acid position of these peptides (protein full length 1-691). Compared to the C-terminus peptide (673-691, stars), the relative intensities of the smaller peptides cleaved

after amino acids K600, K617 (red circles), R650 (green circle) or R560 (blue circles) increase as the residence time increases from (c) to (b) to (a), suggesting that longer digestion times result in deeper access into the protein.

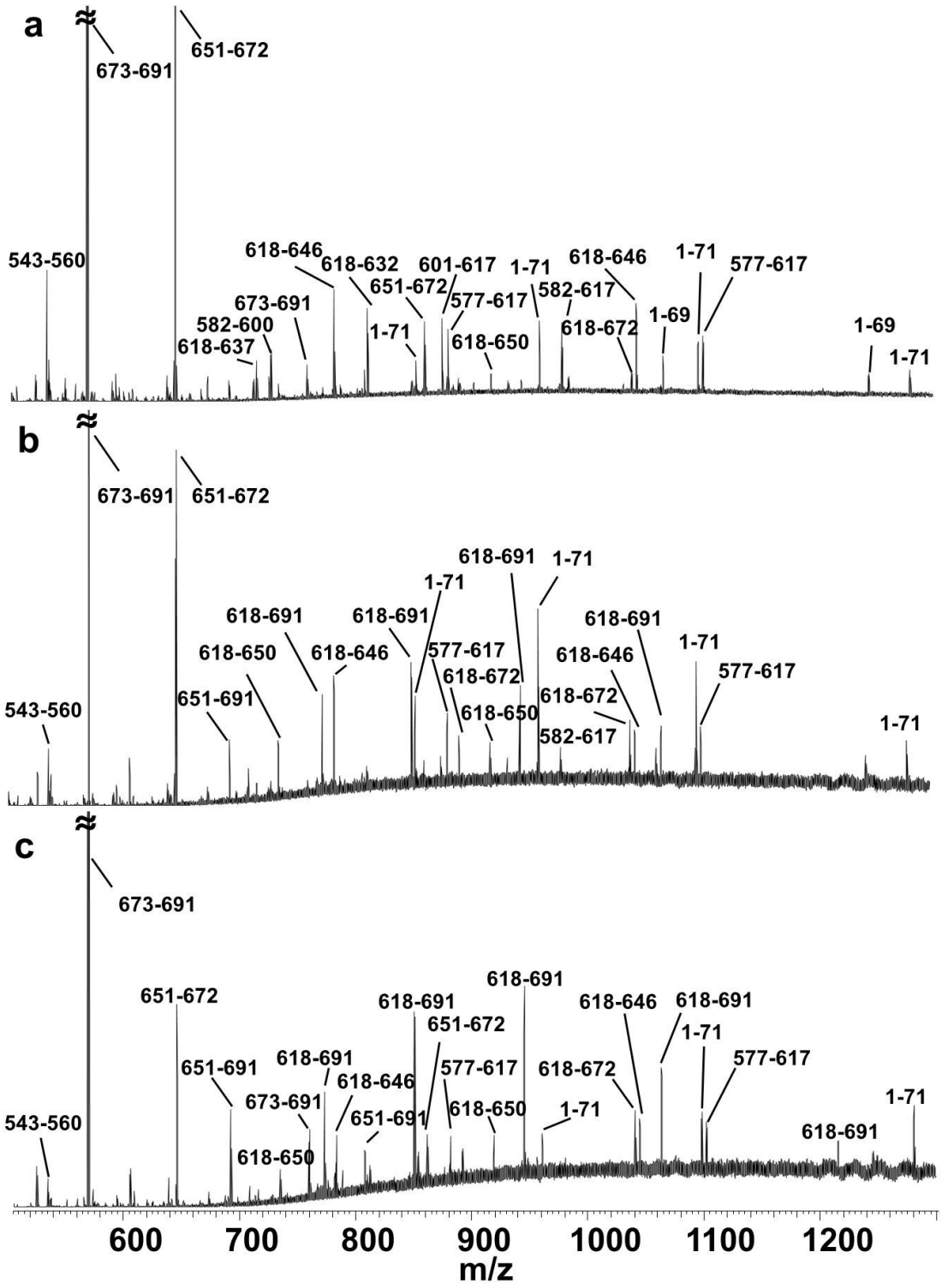

Figure 5.5**.** ESI-Orbitrap mass spectra of 0.1 mg/mL (1.3 μM) RHD 3 digested in residence times of (a) 1, (b) 0.2 and (c) 0.045 s by a trypsin-modified membrane. The peptides are labeled with

their amino acid positions. The dominant peak at m/z 570.78 suggests that the most labile cleavage site is after K672, and the presence of other major peptides in (c) cleaved after amino acids R650, K617 and R576 is consistent with the MALDI mass spectra in Figure 7a, b and c. The y axis is limited to 30% of the signal at m/z 570.78.

Table 5.1**.** RHD3 peptides identified from MALDI and ESI-Orbitrap mass spectra obtained after digestion in trypsin-modified and α-chymotrypsin-modified membranes.

Trypsin-modified membrane digestion			
Peptide Monoisotopic Mass	**Peptide sequence**	**Amino Acids**	**MS Instrument**
2280.09	**(R)NNNWVDKLAAALEHHHHHH(-)**	**673-691**	**MALDI/ESI**
2436.19	**(R)RNNNWVDKLAAALEHHHHHH(-)**	**672-691**	**MALDI/ESI**
2584.28	**(R)QFKNETEYTVTQAISAQEANRR(N)**	**651-672**	**MALDI/ESI**
4845.35	**(R)QFKNETEYTVTQAISAQEANRRNNNWVDKLAAALEHHHHHH(-)**	**651-691**	**ESI**
1624.81	**(K)SISTIDSLASSTWEK(V)**	**618-632**	**MALDI/ESI**
2149.10	**(K)SISTIDSLASSTWEKVAPEK(T)**	**618-637**	**MALDI/ESI**
3132.65	**(K)SISTIDSLASSTWEKVAPEKTLITPVQCK(S)**	**618-646**	**MALDI/ESI**
3674.95	**(K)SISTIDSLASSTWEKVAPEKTLITPVQCKSLWR(Q)**	**618-650**	**ESI**
6240.20	**(K)SISTIDSLASSTWEKVAPEKTLITPVQCKSLWRQFKNETEYTVTQAISAQEANRR(N)**	**618-672**	**ESI**
8501.28	**(K)SISTIDSLASSTWEKVAPEKTLITPVQCKSLWRQFKNETEYTVTQAISAQEANRRNNNWVDKLAAALEHHHHHH(-)**	**618-691**	**ESI**
1752.91	**(K)TLTLALFNSTGNNATSK(S)**	**601-617**	**MALDI/ESI**
4406.35	**(R)SASLKLLSVMAVIRLDDELDNIEKTLTLALFNSTGNNATSK(S)**	**577-617**	**ESI**
1103.58	**(R)VWTGKEDIR(A)**	**561-569**	**MALDI**
2140.99	**(R)MKDRFATIFSHDSDSMPR(V)**	**543-560**	**MALDI/ESI**
1278.68	**(R)GVVPANAFAFSAK(Q)**	**252-263**	**MALDI**
7680.71	**MDAACSTQLIDGDGVFNVSGVDHFIKEVKLDECGLSYAVVSIMGPQSSGKSTLLNHLFGTNFREMDAFRGR(S)**	**1-71**	**ESI**

Table 5.1 (cont'd)

α-chymotrypsin-modified membrane digestion			
Peptide Monoisotopic Mass	**Peptide sequence**	**Amino Acids**	**MS Instrument**
3805.89	**(Y)TVTQAISAQEANRRNNNWVDKLAA ALEHHHHHH(-)**	**659-691**	**MALDI/ESI**
1214.58	**(W)RQFKNETEY(T)**	**650-658**	**MALDI/ESI**
2170.19	**(W)EKVAPEKTLITPVQCKSLW(R)**	**631-649**	**MALDI/ESI**
2342.11	**(F)NSTGNNATSKSISTIDSLASSTW(E)**	**608-630**	**MALDI/ESI**
1362.74	**(W)TGKEDIRAITKM(A)**	**563-574**	**MALDI/ESI**
1316.57	**(F)SHDSDSMPRVW(T)**	**552-562**	**MALDI/ESI**
1284.27	**(M)RMKDRFATIF(S)**	**542-551**	**MALDI/ESI**
2582.24	**(M)RMKDRFATIFSHDSDSMPRVW(T)**	**542-562**	**MALDI/ESI**

RHD3 sequence:

[1]MDAACSTQLIDGDGVFNVSGVDHFIKEVKLDECGLSYAVVSIMGPQSSGKSTLLNH LFGTNFREMDAFRGRSQTTKGIWIARCAGIEPCTVVMDLEGTDGRERGEDDTAFE KQSALFALAVSDIVLINMWCHDIGREQAANKPLLKTVFQVMMRLFSPRKTTLMFVI RDKTRTPLENLEPVLREDIQKIWDSVPKPQAHKETPLSDFFNVEVVALSSYEEKEEQ FKEQVYNLRQRFFQSVAPGGLAGDRRGVVPANAFAFSAKQMWQVIKDNKDLDLPA HKVMVATVRCEEIANEKFSSFIANENWRELEEAVQSGPVSGFGRKLSSILQASLSEY DTEATYFEESVRSSKRQQLQEKLLQLVQPTFQDVLGHLRAGALENFKNAFEKALD AGEGFSSSAKSCAQSCISKFDKGCEEAVIEQAKWDTSKTREKLERDIEAHISSVRTAK LAELTTLYESKLNVALSGPVEALLDGANDETWPAIRKLLRREGELAVYGLSNALSGF EMDEETRSKMLADLENYARGIVETKAKEEAGRAMMRMKDRFATIFSHDSDSMPRV WTGKEDIRAITKMARSASLKLLSVMAVIRLDDELDNIEKTLTLALFNSTGNNATSKSI STIDSLASSTWEKVAPEKTLITPVQCKSLWRQFKNETEYTVTQAISAQEANRRNNN WVDKLAAALEHHHHHH

Overall, these data suggest that the region around R672 is highly flexible and that truncating the protein at R672 may increase the probability of crystallization. (Notably, we do not detect the cleavage at K679). In fact a new construct up to R672 shows no degradation over several weeks, but we have not yet successfully crystallized this protein. Compared to in-solution limited digestion methods to suggest truncated protein sequences, the membrane method is rapid and convenient and provides finer control over the digestion time.

5.4 Conclusions

The pepsin-modified membrane successfully generates peptides from deuterium-exchanged apomyoglobin, and ESI-MS detects the mass increases for peptic digests. However, more experiments needs to be done to improve resolution. The localization of deuterium exchange could be achieved by ETD-MS/MS analysis of large peptides,[13] the overlapping of small peptides from longer digest times,[4] or a combination of the two methods. Probing the structure of BSA using HDX-MS coupled to membrane digestion might be an interesting and challenging future work, and the comparison of the obtained HDX data with simulation data or data from other methods would increase the impact of this work in the area of studying large proteins with HDX.

Limited, membrane-based proteolysis shows which regions of a protein are readily accessible to enzymes. For RHD3, digestion in a membrane-based enzymatic reactor reveals rapid digestion at K672 and suggests that truncation of the protein at this amino acid will stabilize RHD3. Future studies with other proteins will further demonstrate the value of limited digestion in protease-modified membranes.

5.5 Acknowledgement

Many thanks to Dr. Giovanni Stefano, Prof. Federica Brandizzi (F.B.), Dr. Yi Zheng and Prof. R. Michael Garavito (R.M.G) for their collaboration in the RHD3 study. We are grateful to the U.S. National Institutes of Health (GM 080511, Bruening), the Chemical Sciences, Geosciences and Biosciences Division, Office of Basic Energy Sciences, Office of Science, U.S. Department of Energy (DE-FG02-91ER20021, F.B.), the National Science Foundation (MCB 0841594, F.B), and the MSU-REF Center Program (REF03-016, R.M.G) for funding portions of this work.

REFERENCES

5.6 References

1. Engen, J. R., Analysis of Protein Conformation and Dynamics by Hydrogen/Deuterium Exchange MS. *Anal. Chem.* **2009,** *81* (19), 7870-7875.

2. Konermann, L.; Pan, J.; Liu, Y.-H., Hydrogen Exchange Mass Spectrometry for Studying Protein Structure and Dynamics. *Chem. Soc. Rev.* **2011,** *40* (3), 1224-1234.

3. Morgan, C. R.; Engen, J. R., Investigating Solution-Phase Protein Structure and Dynamics by Hydrogen Exchange Mass Spectrometry. In *Current Protocols in Protein Science*, John Wiley & Sons, Inc.: 2009.

4. Rey, M.; Man, P.; Brandolin, G.; Forest, E.; Pelosi, L., Recombinant Immobilized Rhizopuspepsin as a New Tool for Protein Digestion in Hydrogen/Deuterium Exchange Mass Spectrometry. *Rapid Commun. Mass Spectrom.* **2009,** *23* (21), 3431-3438.

5. Gao, X.; Bain, K.; Bonanno, J.; Buchanan, M.; Henderson, D.; Lorimer, D.; Marsh, C.; Reynes, J.; Sauder, J.; Schwinn, K.; Thai, C.; Burley, S., High-Throughput Limited Proteolysis/Mass Spectrometry for Protein Domain Elucidation. *J. Struct. Funct. Genomics.* **2005,** *6* (2), 129-134.

6. Dong, A.; Xu, X.; Edwards, A. M., In Situ Proteolysis for Protein Crystallization and Structure Determination. *Nat. Methods* **2007,** *4* (12), 1019-1021.

7. Bian, X.; Klemm, R. W.; Liu, T. Y.; Zhang, M.; Sun, S.; Sui, X.; Liu, X.; Rapoport, T. A.; Hu, J., Structures of the Atlastin Gtpase Provide Insight into Homotypic Fusion of Endoplasmic Reticulum Membranes. *Proc. Natl. Acad. Sci. U. S. A.* **2011,** *108* (10), 3976-3981.

8. Chen, J.; Stefano, G.; Brandizzi, F.; Zheng, H., Arabidopsis RHD3 Mediates the Generation of the Tubular ER Network and Is Required for Golgi Distribution and Motility in Plant Cells. *J. Cell Sci.* **2011**.

9. Hu, J.; Prinz, William A.; Rapoport, Tom A., Weaving the Web of ER Tubules. *Cell* **2011,** *147* (6), 1226-1231.

10. Cohen, S. L.; Chait, B. T.; Ferré-D'Amaré, A. R.; Burley, S. K., Probing the Solution Structure of the DNA-Binding Protein Max by a Combination of Proteolysis and Mass Spectrometry. *Protein Sci.* **1995,** *4* (6), 1088-1099.

11. Cohen, S. L.; Chait, B. T., Mass Spectrometry as a Tool for Protein Crystallography. *Annu. Rev. Biophys. Biomol. Struct.* **2001,** *30* (1), 67-85.

12. Zhang, G.; Liu, Y.; Qin, J.; Vo, B.; Tang, W.-J.; Ruoho, A. E.; Hurley, J. H., Characterization and Crystallization of a Minimal Catalytic Core Domain from Mammalian Type II Adenylyl Cyclase. *Protein Sci.* **1997,** *6* (4), 903-908.

13. Pan, J.; Han, J.; Borchers, C. H.; Konermann, L., Hydrogen/Deuterium Exchange Mass Spectrometry with Top-Down Electron Capture Dissociation for Characterizing Structural Transitions of a 17 Kda Protein. *J. Am. Chem. Soc.* **2009,** *131* (35), 12801-12808.

Chapter 6. Summary and Future Work

6.1 Research summary

This dissertation describes the development of functional nylon membranes containing TiO_2 nanoparticles or proteases and their applications in phosphopeptide enrichment and limited protein digestion prior to MS analysis, respectively. Chapters 2 and 3 describe research with TiO_2-modified nylon membranes in phosphopeptide enrichment, and chapters 4 and 5 discuss applications of protease-containing membranes in limited digestion.

Chapter 2 focuses on the characterization of TiO_2-modified nylon membranes and enrichment of model phosphopeptides and digested phosphoproteins. Alternating adsorption of PSS and TiO_2 allows rapid modification of nylon membranes. The size of aggregated TiO_2 particles is about 50 nm as measured by TEM, and SEM-EDX analyses show that TiO_2 adsorbs uniformly across the membrane. Based on phosphoangiotensin breakthrough curves during membrane loading, the TiO_2-modified membranes have a binding capacity of 540 nmols of phosphopeptide in a 22-mm diameter disc. These membranes selectively isolate the phosphopeptides from α-casein, β-casein and ovalbumin digests, and even in a 100-fold excess of non-phosphorylated BSA digests, the membrane still captures phosphopeptides from the three model phosphoproteins digests when using 2% TFA in 1:1 H_2O/acetonitrile as a loading and washing buffer. The selectivity of the TiO_2-modified membrane is sufficient for capturing the phosphopeptides from modestly complex mixtures.

Chapter 3 describes the use of the TiO_2-modified membranes in phosphopeptide enrichment from immunoprecipitates and *in vivo* phosphorylated proteins including fusion proteins. Enrichment with the modified membranes is vital for identifying phosphopeptides from a digest of a tau protein, which is *in vivo* phosphorylated by glycogen synthase kinase-3β (GSK-3β). The MALDI-MS and ESI-MS analyses of enriched p-tau phosphopeptides reveal seven phosphorylation sites, three of which seem dominant. Comprehensive CID-, HCD- and ETD-MS/MS studies localize and confirm the seven sites. In analyses of phosphopeptides from an immunoprecipitate of p65 (from the nuclear extract of human acute monocytic leukemia cells stimulated with tumor necrosis factor), membrane enrichment combined with MALDI-MS/MS reveals eight phosphopeptides from the p65-associated 60S acidic ribosomal protein. Unfortunately, none of the phosphopeptides originate from p65 and the eight peptides contain only two unique phosphorylation sites because the peptides share a similar sequence with different modifications from the alkylation process. In a complementary study, HPLC-ESI-MS/MS analysis confirms the phosphorylation of Ser 32 and 36 on the inhibitor of kappa-B-alpha protein (IκBα), which is *in vitro* phosphorylated by G-protein coupled receptor kinase-5, and the ratio of phosphopeptide signals to their non-phosphorylated counterparts suggests ~40% efficiency for this phosphorylation event. However, the membrane enrichment pretreatment did not reveal any phosphorylation sites, presumably because the matrix interfered with adsorption.

Although these studies show the effectiveness of membrane enrichment, both the protein composition and the sample matrix are important issues. For example, digestion of p65 may only give large phosphopeptides that are not detectable in our MALDI-MS instrument. Moreover, the large excess of ATP in studies of IκBα may prevent capture of phosphopeptides,

and detergent could also interfere with phosphopeptide adsorption. Future studies of membrane stability will also be important for potential online applications.

Chapter 4 applies a similar adsorption procedure for creating protease-modified membranes for protein digestion. Based on the work of Dr. Fei Xu and Dr. Wei-Han Wang with trypsin-containing membranes, I expand the types of proteases adsorbed in membranes. The protease-modified membranes have an enzyme density of 30 mg/cm^3 (trypsin and α-chymotrypsin) and 60 mg/cm^3 (pepsin), and this enables the membrane to catalyze digestion even in <1 s. The digestion occurs in membrane pores via simply passing the protein solution through the membrane with a syringe pump. Most importantly in this work, the protease-containing membrane affords control of peptides sizes by altering the flow rate. Even though digestion is rapid, because the membranes are only 170 μm thick, the residence time can be as low as a few msec to limit the extent of digestion. For digestion with pepsin-modified membranes, ESI-MS analysis demonstrates that the sizes of peptic peptides increase as the residence time decreases for both BSA and apomyoglobin. In the case of BSA membrane digestion, the sequence coverage increases from 53% (2-s digestion) to 82% (0.05-s digestion). Additionally the ETD-MS/MS analysis of a large apomyoglobin peptide (8 kD) provides a 1-2 amino acid resolution, which suggests that this protease-modified membrane might find its application in hydrogen-deuterium exchange (HDX) or middle-down proteomics studies.

Chapter 5 explores applications of the protease-modified membranes for probing protein structure, both from the perspective of limited proteolysis to reveal accessible protein regions or rapid peptic digestion for HDX studies. Using trypsin- and α-chymotrypsin-modified membranes, the limited proteolysis of a large Arabidopsis GTPase, ROOT HAIR DEFECTIVE 3 (RHD3), shows suitable probing for labile regions near the C-terminus to suggest the protein

reconstruction. Truncation of a protein construct at the most labile digestion site, K672, gives a protein that is stable in solution for a few weeks without observable degradation. This, along with the absence of a flexible region should increase the likelihood of the crystallization of this target protein.

Preliminary ESI-MS analysis of digests of deuterium-exchanged apomyoglobin suggests the success of deuterium exchange on apomyoglobin and the following digestion on the pepsin-modified membrane. However we have not yet investigated localization of the deuterium exchange, and we need to validate whether there is over-exchange or back-exchange occurring during the workflow. There are two options to increase the resolution, and one is based on the ETD-MS/MS analysis of the large peptides from limited digestion. However, some portions of the sequence are only represented by small peptides that are not amenable to ETD. Another option to enhance amino acid resolution is to increase the digestion efficiency and generate many small peptides with overlapping sequences. The overlapped deuterium exchange states from MS can help to increase the resolution. Slower digestion in membranes combined with multiple enzymes might successfully yield the small overlapping peptides. Additionally, limited digestion and ETD may be more attractive for large (>50 kD) proteins.

6.2 Future work

6.2.1 Study of the correlation of multiple phosphorylation events on p-tau and α-synuclein using membrane enrichment combined with limited digestion or intact protein analysis

The investigation of p-tau phosphorylation in chapter 3 reveals seven phosphorylation sites after enrichment, and three sites (S396, S400 and S404) seem to dominate the GSK-

3β phosphorylation events in our study. There are 23 phosphorylation sites reported in various studies of p-tau phosphorylated by GSK-3β.[1] The full phosphorylation mapping may prove important in understanding p-tau behavior in Alzheimer's disease. Nevertheless, the correlation between the phosphorylation of tau and its aggregation into paired helical filaments and neurofibrillary tangles is still hard to assess. Mutation of the vital site which triggers or accelerates the aggregation process may abolish or alleviate the aggregation. However among all the phosphorylation sites, only a few may play vital roles in aggregation. We suspect that the sites with higher phosphorylation stoichiometry are more likely to serve as the key factors in aggregation. Thus proving that the three phosphorylation sites (S396, S400 and S404) are indeed those with the highest stoichiometry may have relevance to understanding p-tau aggregation.

Measurement of the exact mass of intact p-tau can potentially demonstrate the average number of phosphorylation sites per protein. Presuming this number is 3, it would be consistent with S396, S400 and S404 being the dominant sites of phosphorylation. However, the isotopic resolution for intact protein (>50 kD) is still challenging for our current ESI-Orbitrap instrument, especially when the protein is not homogenous (various modifications). Adequate starting material, careful sample desalting and optimization of mass spectrometer settings are prerequisites to get an accurate mass increase due to phosphorylation. In a complementary method based on the strategy of middle-down proteomics, a large peptide covering multiple posttranslational modification (PTMs) sites will provide the correlation information for these PTMs.[2-3] For this particular study, the peptide ^{386}TDHGAEIVYK**pS**PVV**pS**GDT**pS**PR and ^{407}HL**pS**NVSSTGSIDMVD**pS**PQLATLADESASLAK happen to be successive in the p-tau and separated due to the cleavage at R406. Assuming that the limited proteolysis on the trypsin membrane would possibly miss the R406 site, we expect to observe less

^{386}TDHGAEIVYK**pS**PVV**pS**GDT**pS**PRHL**pS**NVSSTGSIDMVD**pS**PQLATLADESASLAK(5P) and more ^{386}TDHGAEIVYK**pS**PVV**pS**GDT**pS**PRHL**S**NVSSTGSIDMVD**S**PQLATLADESASLAK(3P) if the S396, S400 and S404 are major phosphorylation sites while the S409 and S422 are minor.

Preliminary data suggest the possibility of limited digestion for looking at the abundance of phosphorylation events. Figure 6.1 shows the MALDI mass spectra of 2 pmol of p-tau digested for (a) 0.05 s in a trypsin-modified membrane and (b) 16 h in solution. The spectra show some similar peptides, but new peptides also emerge from the limited digestion, suggesting missed cleavages. Unfortunately, the mass range does not show peptides large than 4 kD. The use of enrichment combined with ESI-MS will reveal more information from the limited digests of p-tau. Besides p-tau, α-synuclein, another important protein associated with neurological diseases is also available from our collaborator Prof. Min-Hao Kuo. This protein has a molecular weight of 14 kD and three potential phosphorylation sites (Figure 6.2). Future work will focus on correlating phosphorylation events on p-tau and α-synuclein using intact protein analysis and limited digestion with phosphopeptide enrichment.

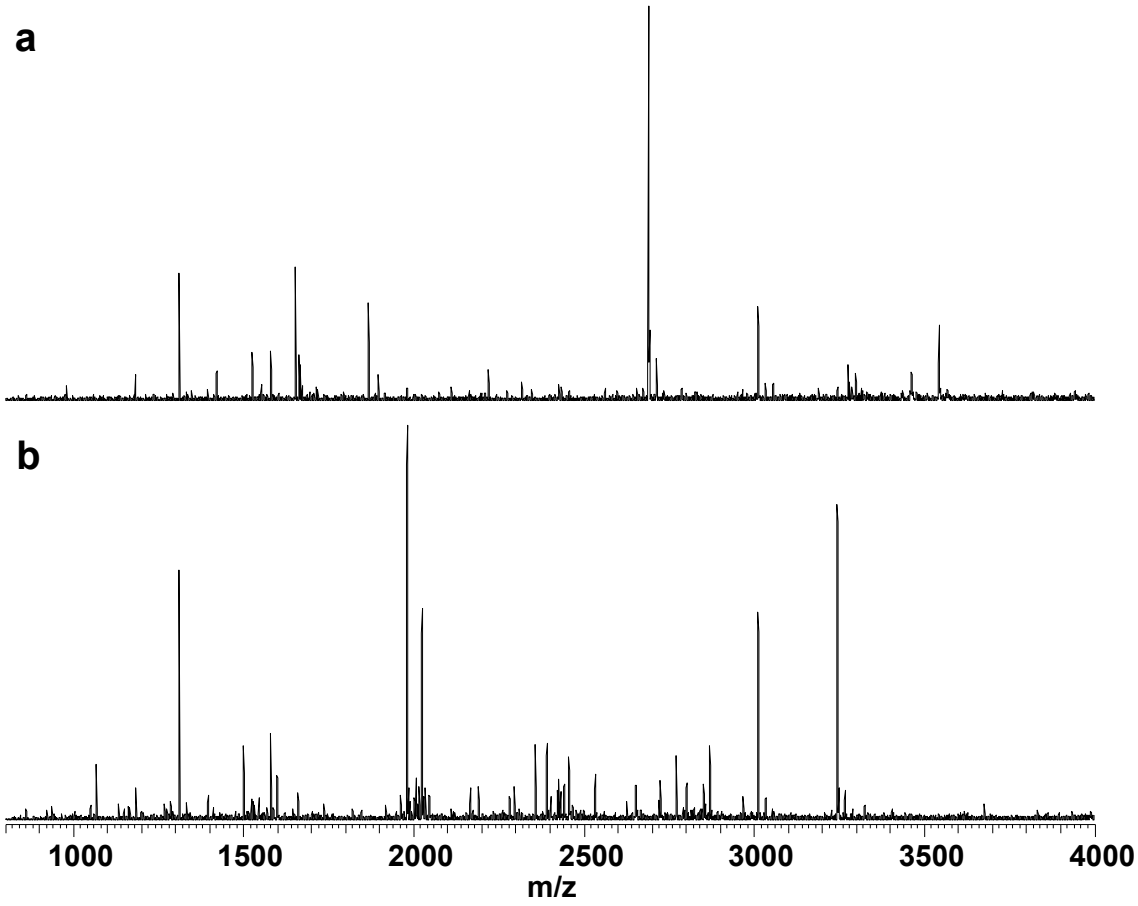

Figure 6.1. MALDI mass spectra of 2 pmol of p-tau digested for (a) 0.05 s in a trypsin-modified membrane and (b) 16 h in solution.

Alpha-Synuclein, associated with Parkinson's disease

Size: 140 Amino Acids MW: 14460 Da

Potential phosphorylation sites: S87, Y125, S129

```
        10         20         30         40         50         60
MDVFMKGLSK AKEGVVAAAE KTKQGVAEAA GKTKEGVLYV GSKTKEGVVH GVATVAEKTK
        70         80         90        100        110        120
EQVTNVGGAV VTGVTAVAQK TVEGAGSIAA ATGFVKKDQL GKNEEGAPQE GILEDMPVDP
       130        140
DNEAYEMPSE EGYQDYEPEA
```

Figure 6.2. Properties of α-synuclein.

6.2.2 Phosphorylation mapping in tau isomers and multiple kinase events

To date, multiple approaches such as MS, western blotting, and Edman degradation have revealed more than 40 phosphorylation sites in tau protein associated with Alzheimer's disease, resulting from *in vitro* phosphorylation of tau isomers by four kinases.[1] The four pathological kinases in humans are GSK-3β, cyclin-dependent kinase-5, casein kinase 1 and cyclic adenosine monophosphate-dependent protein kinase, and tau isomers in humans are differentiated into six (0N3R, 0N4R, 1N3R, 1N4R, 2N3R, 2N4R) variations based on the presence or absence of specific exons at the C-terminus or N-terminus.[4] To examine phosphorylation in *in vivo* studies, our collaborator Prof. Kuo employs the protein interaction module-assisted catalysis technique (Figure 6.3). In chapter 3 we studied p-tau (1N4R) phosphorylation by GSK-3β, however the enzyme and substrate can be replaced by any of the other candidates to reveal other phosphorylation sites. In addition to the enzyme/substrate replacement, the affinity zipper Jun-Fos can also change to small ubiquitin-like modifier (SUMO)-N and SUMO-C, another affinity pair. Multiple affinity zipper tests can reduce the conformational bias of the phosphorylation bought about by the zipper in this design. Using our newly developed enrichment and analysis techniques, we can investigate all the phosphorylated protein samples and pool the data together, hoping to reveal specific trends in phosphorylation that will be beneficial for the design and development of therapeutic drugs that inhibit or reverse the phosphorylation on Alzheimer tau. [5-6]

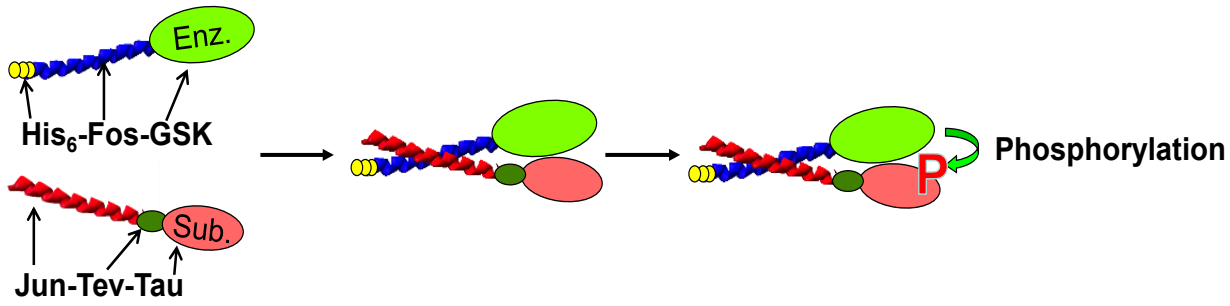

Figure 6.3. Scheme of the protein interaction module-assisted phosphorylation. The leucine zipper Fos and Jun bring the enzyme and substrate together after they are co-produced in cells, and phosphorylation occurs in vivo.

6.2.3 De novo sequencing of monoclonal antibodies using limited proteolysis and a middle-down approach

De novo monoclonal antibody sequencing is drawing great interest from many companies because the obtained sequence can be directly used for recombinant protein production. High resolution MS instrumentation with top-down strategies make *de novo* approaches possible.[7] However, direct, efficient fragmentation of a protein larger than 150 kD is not sufficient enough to resolve single amino acid residues.[8] The common strategy is to cut the protein then analyze the parts, and finally map the information together. Papain is frequently used to cut antibodies because it separates the fragment antigen-binding (Fab) of immunoglobulin G (IgG) from the fragment crystallizable region (Fc). Another method to cut the antibody is to dissociate the heavy chains from the light chains by breaking the disulfide bonds linking them.[9] Furthermore, size exclusion chromatography (SEC) can separate the heavy and light chains.[10] According to Prof. Gavin Reid's suggestion, membrane digestion of purified antibody light chain using different residence times combined with *de novo* sequencing of the large peptides may provide comprehensive sequence information. Subsequent mapping and integration of those data should

reveal the light chain sequence. Research in this area could begin with commercially available IgG from Sigma to optimize the reduction (breaking the disulfide bonds between heavy and light chains) efficiency and separation conditions for SEC in terms of elution buffer, flow rate and the amount of starting material. Such research will benefit from collaboration with a group equipped with a fast protein liquid chromatography system to perform the separation. Some preliminary trials of IgG reduction and separation suggest that the superdex 200 10/300 GL column from GE Healthcare separates proteins with masses similar to heavy and light chains. Denaturing or disulfide bond reforming during the separation will influence the separation, so the elution buffer also must be optimized. Similarly, membrane digestion with MS-analysis requires optimization with the model IgG protein. Success in *de novo* antibody sequencing using the limited membrane digestion approach will greatly increase the impact of protease-modified membranes.

6.2.4 Functional membranes for removal of affinity tags

Recombinant proteins often incorporate affinity tags at a terminus to enhance the protein solubility in some cases and also facilitate the detection and purification of the protein.[11] Invented by Roche Corporation, the polyhistidine-tag (His-tag) is the most common tag for purifying a target protein from a whole cell lysate.[12] After the protein purification, the His-tag is often removed to avoid its potential influence in down streaming analysis or protein usage. In many cases, the His-tag is attached to a protein via a cleavable linkage of artificial sequence or protein, and removed by tobacco etch virus (TEV), thrombin or SUMO proteases. Specifically, the Tev protease recognizes a seven amino acid sequence (Glu-Asn-Leu-Tyr-Phe-Gln-Gly) and cleaves between Gln-Gly; the thrombin recognizes the sequence (Leu-Val-Pro-Arg-Gly-Ser) and cleaves between Arg and Gly; and the SUMO protease directly recognizes the tertiary structure of SUMO protein and removes the SUMO. Removal of these linkers also removes the His-

tag.[13] Our group has extensive experience in protein purification using Ni-nitrilotriacetic acid (NTA)-containing membranes,[14] as well as immobilization of proteases for efficient digestion.[15] Thus, we should be able to immobilize the TEV, Thrombin or SUMO proteases onto a membrane for tag removal, and flow of the cleaved mixture through a second membrane can capture the cleaved tag to yield purified protein. Although the traditional protocol is widely used in many labs (Scheme 6.1), the high enzyme density in a membrane may increases the digestion efficiency and decreases the time, and the immobilization could stabilize the protease and allow its reuse.

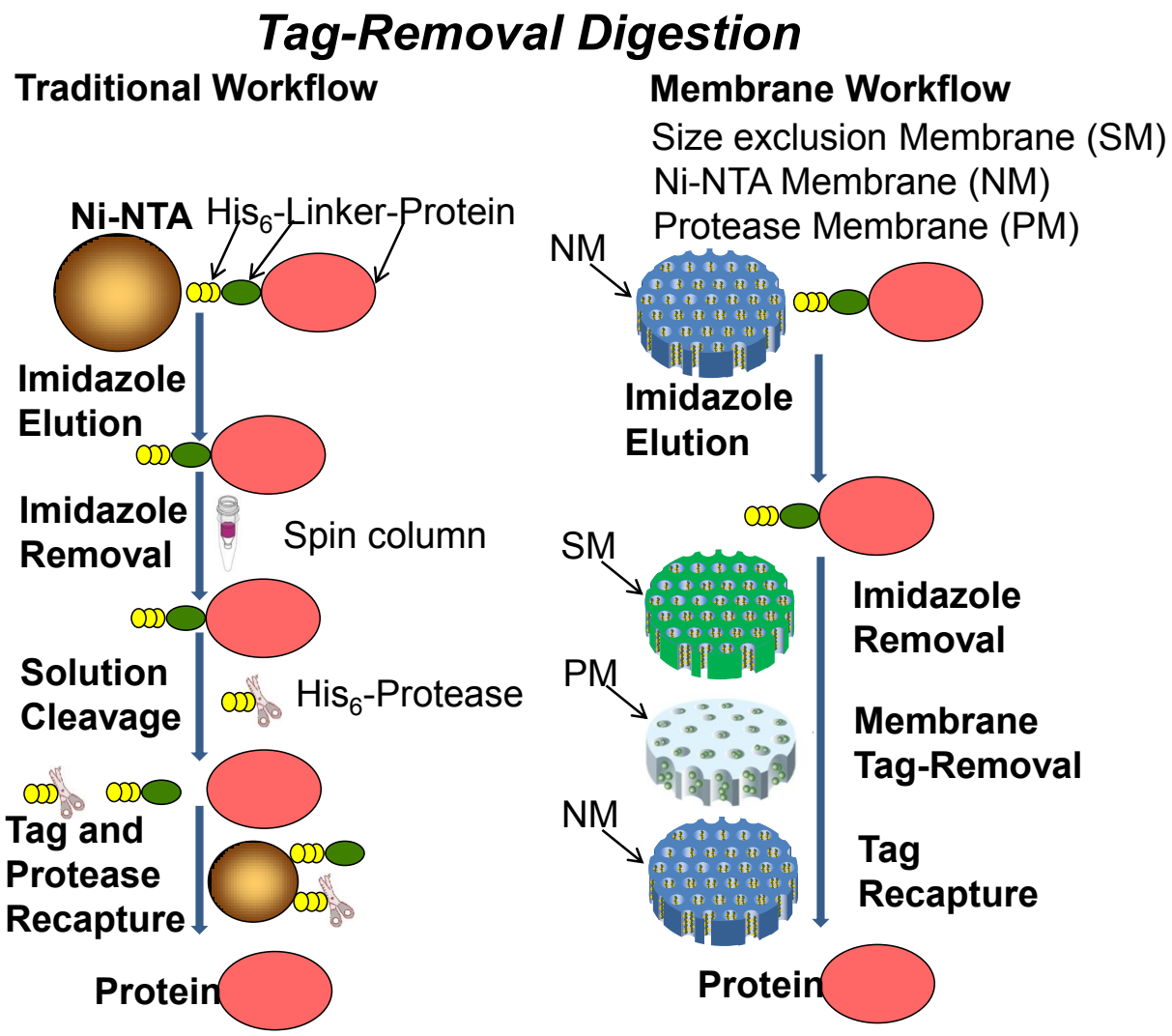

Scheme 6.1. Comparison of enzymatic tag-removal in traditional and membrane-based work flows. In the traditional workflow, imidazole is applied to elute the fusion protein from the Ni-NTA beads, and before the in-solution tag cleavage, the imidazole is removed via spin column to facilitate the later tag recapture step. The Ni-NTA beads recapture the His_6 tag and His_6-protease and leave the pure target protein. In contrast, the proteins are eluted from Ni-NTA membrane, and size-exclusion membrane is used to capture the imidazole. Then the protein will undergo membrane digestion to remove the His_6-tag, which will be recaptured by another Ni-NTA membrane. Pure proteins will be in the last flow-through.

6.3 Summary of Future Work

The proposed future work has three directions. The first is the use of TiO_2-modifed membranes combined with limited digestion and intact protein analysis for tau phosphorylation mapping. This should provide both phosphorylation sites and stoichiometry information to correlate with biological consequences. The second direction is *de novo* monoclonal antibody sequencing using membrane digestion combined with MS analysis. If successful this approach would provide a routine method for *de novo* antibody sequencing, an extremely attractive but unrealized area. The last direction is the development of membrane-based methods to remove the affinity tag from a recombinant protein. Compared to traditional in-solution cleavage, the membrane tag removal could provide an alternative method with higher efficiency and less digestion time.

6.4 Acknowledgement

We are grateful to the U.S. National Institutes of Health (CHE-1152762 to M.B.) for funding this work.

REFERENCES

6.5 References

1. Hanger, D. P.; Noble, W., Functional Implications of Glycogen Synthase Kinase-3-Mediated Tau Phosphorylation. *Int. J. Alzheimers Dis.* **2011**, *2011*, 352805.

2. Kellie, J. F.; Tran, J. C.; Lee, J. E.; Ahlf, D. R.; Thomas, H. M.; Ntai, I.; Catherman, A. D.; Durbin, K. R.; Zamdborg, L.; Vellaichamy, A.; Thomas, P. M.; Kelleher, N. L., The Emerging Process of Top Down Mass Spectrometry for Protein Analysis: Biomarkers, Protein-Therapeutics, and Achieving High Throughput. *Mol. Biosyst.* **2010**, *6* (9), 1532-1539.

3. Siuti, N.; Kelleher, N. L., Decoding Protein Modifications Using Top-Down Mass Spectrometry. *Nat. Methods* **2007**, *4* (10), 817-821.

4. Voss, K.; Gamblin, T. C., GSK-3beta Phosphorylation of Functionally Distinct Tau Isoforms Has Differential, but Mild Effects. *Mol. Neurodegener.* **2009**, *4* (1), 18.

5. Hong, M.; Chen, D. C. R.; Klein, P. S.; Lee, V. M. Y., Lithium Reduces Tau Phosphorylation by Inhibition of Glycogen Synthase Kinase-3. *J. Biol. Chem.* **1997**, *272* (40), 25326-25332.

6. Mazanetz, M. P.; Fischer, P. M., Untangling Tau Hyperphosphorylation in Drug Design for Neurodegenerative Diseases. *Nat. Rev. Drug Discovery* **2007**, *6* (6), 464-479.

7. Resemann, A.; Wunderlich, D.; Rothbauer, U.; Warscheid, B.; Leonhardt, H.; Fuchser, J.; Kuhlmann, K.; Suckau, D., Top-Down De Novo Protein Sequencing of a 13.6 Kda Camelid Single Heavy Chain Antibody by Matrix-Assisted Laser Desorption Ionization-Time-of-Flight/Time-of-Flight Mass Spectrometry. *Anal. Chem.* **2010**, *82* (8), 3283-3292.

8. Bondarenko, P. V.; Second, T. P.; Zabrouskov, V.; Makarov, A. A.; Zhang, Z., Mass Measurement and Top-Down HPLC/MS Analysis of Intact Monoclonal Antibodies on a Hybrid Linear Quadrupole Ion Trap–Orbitrap Mass Spectrometer. *J. Am. Soc. Mass Spectrom.* **2009**, *20* (8), 1415-1424.

9. Gagnon, P.; Rodriquez, G.; Zaidi, S., Dissociation and Fractionation of Heavy and Light Chains from Igg Monoclonal Antibodies. *J. Chromatogr.* **2011**, *1218* (17), 2402-2404.

10. Liu, H.; Gaza-Bulseco, G.; Chumsae, C., Analysis of Reduced Monoclonal Antibodies Using Size Exclusion Chromatography Coupled with Mass Spectrometry. *J. Am. Soc. Mass Spectrom.* **2009**, *20* (12), 2258-2264.

11. Waugh, D. S., An Overview of Enzymatic Reagents for the Removal of Affinity Tags. *Protein Expr. Purif.* **2011**, *80* (2), 283-293.

12. Hochuli, E.; Bannwarth, W.; Dobeli, H.; Gentz, R.; Stuber, D., Genetic Approach to Facilitate Purification of Recombinant Proteins with a Novel Metal Chelate Adsorbent. *Nat. Biotechnol.* **1988**, *6* (11), 1321-1325.

13. Arnau, J.; Lauritzen, C.; Petersen, G. E.; Pedersen, J., Current Strategies for the Use of Affinity Tags and Tag Removal for the Purification of Recombinant Proteins. *Protein Expr. Purif.* **2006**, *48* (1), 1-13.

14. Jain, P.; Vyas, M. K.; Geiger, J. H.; Baker, G. L.; Bruening, M. L., Protein Purification with Polymeric Affinity Membranes Containing Functionalized Poly(Acid) Brushes. *Biomacromolecules* **2010**, *11* (4), 1019-1026.

15. Xu, F.; Wang, W. H.; Tan, Y. J.; Bruening, M. L., Facile Trypsin Immobilization in Polymeric Membranes for Rapid, Efficient Protein Digestion. *Anal. Chem.* **2010**, *82* (24), 10045-10051.